frontiers | Research Topics

Innovative medical technology based on artificial cells, including its different configurations

Edited by
Thomas Ming Swi Chang and Binglan Yu

Published in
Frontiers in Medical Technology
Frontiers in Oncology
Frontiers in Bioengineering and Biotechnology
Frontiers in Medicine
Frontiers in Molecular Biosciences

ISSN 1664-8714
ISBN 978-2-8325-4002-2
DOI 10.3389/978-2-8325-4002-2

About Frontiers

Frontiers is more than just an open access publisher of scholarly articles: it is a pioneering approach to the world of academia, radically improving the way scholarly research is managed. The grand vision of Frontiers is a world where all people have an equal opportunity to seek, share and generate knowledge. Frontiers provides immediate and permanent online open access to all its publications, but this alone is not enough to realize our grand goals.

Frontiers journal series

The Frontiers journal series is a multi-tier and interdisciplinary set of open-access, online journals, promising a paradigm shift from the current review, selection and dissemination processes in academic publishing. All Frontiers journals are driven by researchers for researchers; therefore, they constitute a service to the scholarly community. At the same time, the *Frontiers journal series* operates on a revolutionary invention, the tiered publishing system, initially addressing specific communities of scholars, and gradually climbing up to broader public understanding, thus serving the interests of the lay society, too.

Dedication to quality

Each Frontiers article is a landmark of the highest quality, thanks to genuinely collaborative interactions between authors and review editors, who include some of the world's best academicians. Research must be certified by peers before entering a stream of knowledge that may eventually reach the public - and shape society; therefore, Frontiers only applies the most rigorous and unbiased reviews. Frontiers revolutionizes research publishing by freely delivering the most outstanding research, evaluated with no bias from both the academic and social point of view. By applying the most advanced information technologies, Frontiers is catapulting scholarly publishing into a new generation.

What are Frontiers Research Topics?

Frontiers Research Topics are very popular trademarks of the *Frontiers journals series*: they are collections of at least ten articles, all centered on a particular subject. With their unique mix of varied contributions from Original Research to Review Articles, Frontiers Research Topics unify the most influential researchers, the latest key findings and historical advances in a hot research area.

Find out more on how to host your own Frontiers Research Topic or contribute to one as an author by contacting the Frontiers editorial office: frontiersin.org/about/contact

Innovative medical technology based on artificial cells, including its different configurations

Topic editors

Thomas Ming Swi Chang — McGill University, Canada

Binglan Yu — Massachusetts General Hospital, Harvard Medical School, United States

Citation

Chang, T. M. S., Yu, B., eds. (2023). *Innovative medical technology based on artificial cells, including its different configurations*. Lausanne: Frontiers Media SA. doi: 10.3389/978-2-8325-4002-2

Table of contents

frontiers | Frontiers in Medical Technology

TYPE Editorial
PUBLISHED 10 November 2023
DOI 10.3389/fmedt.2023.1306419

OPEN ACCESS

EDITED AND REVIEWED BY
Sarah Harriet Cartmell,
The University of Manchester, United Kingdom

*CORRESPONDENCE
Thomas M. Chang
artcell.med@mcgill.ca

RECEIVED 03 October 2023
ACCEPTED 30 October 2023
PUBLISHED 10 November 2023

CITATION
Chang TMS (2023) Editorial: Innovative medical technology based on artificial cells, including its different configurations.
Front. Med. Technol. 5:1306419.
doi: 10.3389/fmedt.2023.1306419

Editorial: Innovative medical technology based on artificial cells, including its different configurations

Thomas Ming Swi Chang*

Artificial Cells & Organs Research Centre, Department of Physiology, Medicine and Biomedical Engineering, Faculty of Medicine and Health Sciences, McGill University, Montreal, QC, Canada

KEYWORDS

artificial cells, hemoglobin, antioxidant, carbonic anhydrase, nanobiotherapeutic, regeneration, enzyme therapy, COVID-19

Editorial on the Research Topic
Innovative medical technology based on artificial cells, including its different configurations

1. Introduction

Artificial cell is a highly interdisciplinary area involving medicine, chemistry, bioengineering, biotechnology, biochemistry, and other areas. The highly interdisciplinary approach is such that this Research Topic includes the following participating Frontiers journals: Frontiers in Medical Technology, Frontiers in Bioengineering and Biotechnology, Frontiers in Medicine, Frontiers in Oncology, Frontiers in Molecular Biosciences, and Frontiers in Pediatrics.

Red blood cells (rbc) are one of the most important cells since without them, our organs, tissues and cells cannot survive. The first artificial cell prepared is artificial rbc (1, 2). (**Figure 1**). By going outside the box, we and others are able to extend this to prepare artificial cells of unlimited configurations and contents (2–6). (**Figure 1**) resulting in large areas of applications (2–6) (**Figure 1**).

Many of the ideas of artificial cells are being extensively applied and extended by us and by researchers worldwide, resulting in exciting progress and applications (**Figure 1**). Artificial cell is too large an area to be covered under this journal Research Topic. Artificial red blood cells or blood substitute alone already require a >1,000-page multi-author books (7). Many other areas of artificial cells are in development or routine clinical use. For this Research Topic we shall concentrate on artificial red blood cells as the basis for novel and innovative medical technology and showing how outside the box approaches can lead to innovation application.

2. Artificial red blood cell (blood substitutes)

Red blood cells have 3 major functions: 1. Oxygen Carrier 2. Antioxidant functions and 3. transport of carbon dioxide. There was no initial public interest to develop artificial rbc

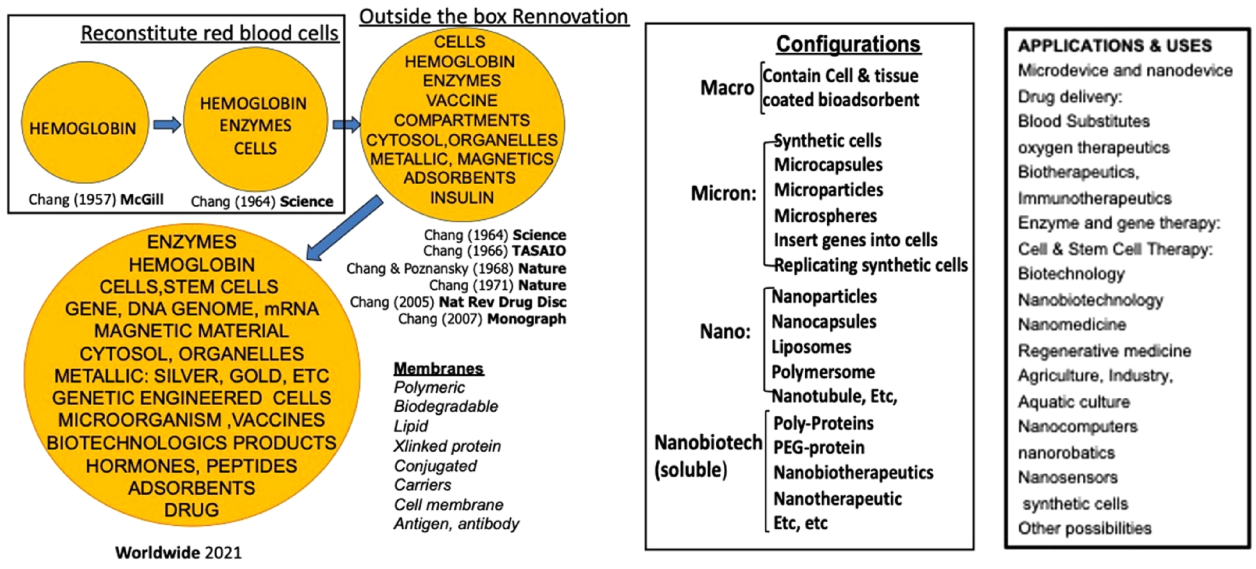

FIGURE 1
Left: the basic idea of artificial cells evolved into "out of the box variation in contents and membrane materials." middle: the basic idea of artificial cells extended into different configurations. Right: Examples of uses of artificial cells [Figure from Chang (5) with written copyright permission from the publisher Taylor and Frances].

when it was published in 1964 (2). It was the 1980s HIV contamination of donor blood that led to the belated effort to develop a suitable blood substitute.

2.1. Oxygen carrier

The urgency was such that researchers concentrated on just an oxygen carrier. In the form of hemoglobin-based oxygen carriers (7). Hemoglobin, a tetramer, is an excellent oxygen carrier. However, in the body it is converted into toxic dimers. Chang used diacid (2) or glutaraldehyde (8) to crosslink hemoglobin into polyhemoglobin (PolyHb) and prevent its breakdown into toxic dimers. This has been developed and tested in clinical trials. A glutaraldehyde crosslinked bovine polyhemoglobin has been approved for routine clinical use for surgical procedures in South Africa and Russia to avoid the use of HIV contaminated donor blood (9). Thus, the original aim has been reached as described in Jahr's article on *Blood substitutes: Basic science, translational studies and clinical trials*.

Polyhemoglobins do not have blood group. Moore et al. reported their clinical trials with glutaraldehyde crosslinked human PolyHb. They showed that this could be given right In the ambulance for patients with hemorrhagic shock without the need for cross matching. This was more effective than the saline control group. They reported a very slight increase in non-fatal myocardial ischemia (10). This could be due to a number of reasons as discussed by Alayash in their article *Oxidation reactions of cellular and acellular hemoglobins: Implications for human health* and Williams et al. in their article *Renal glomerular and tubular responses to glutaraldehyde- polymerized human hemoglobin*.

2.2. Oxygen carrier with antioxidant functions

For those conditions with ischemia-reperfusion, one would need an oxygen carrier with antioxidant properties. Thus, our approach of polyhemoglobin-catalase-superoxide dismutase (PolyHb-CAT-SOD) prevents cerebral edema in hemorrhagic shock with cerebral ischemia (11, 12). Another oxygen carrier with antioxidant showed similar results. This is reported by Jun Wang et al.'s group in *Polynitroxylated PEGylated hemoglobin protects pig brain neocortical gray and white matter after traumatic brain injury and hemorrhagic shock*.

2.3. Oxygen carrier with antioxidant property and CO2 transport

Another possible problem is an increase in intracellular pCO2 in severe hemorrhagic shock (13, 14). We therefore added an enhanced level of carbonic anhydrase (CA) to prepare a PolyHb-CAT-SOD-CA. The result is an oxygen carrier with enhanced Carbonic Anhydrase for CO2 transport and enhanced Catalase and Superoxide Dismutase for antioxidant functions (15). This is reported by Bian and Chang in this Research Topic. Hoq and Chang used more stable chemical CAT, SOD and CA instead of biological enzymes for certain uses as reported in the Research Topic article *Preliminary feasibility study using a solution of synthetic enzymes to replace the natural enzymes in polyhemoglobin-catalase-superoxide dismutase-carbonic anhydrase: effect on warm ischemic hepatocyte cell culture*.

2.4. Other approaches

Many other approaches are being explored (7). This Research Topic shows two examples. One is Kettisen et al.'s group in *Structural and oxidative investigation of a recombinant high-yielding fetal hemoglobin mutant*. Another is Sakai et al.'s group in *Research of storable and ready-to-use artificial red blood cells (hemoglobin vesicles) for emergency medicine and other clinical applications*. Biodegradable polymeric membrane nano-rbc is also possible (16).

2.5. Preservation of pretransplant cells and organs: regenerative medicine

A very promising and exciting area is the use of blood substitute in the preservation of cells and organs for transplantation. Zal's murine HEMARINA has been approved in the EU for the pretransplant preservation of human kidneys (17).

Active research continues in this exciting application. A number of years ago we show that oxygen carrier with antioxidants is effective for the preservation of rat small intestine and hepatocytes (18). Andrijevic et al. reported their detailed study in Nature (2022) (19). In this Research Topic, Li et al. describe their work in *Application of polymerized porcine hemoglobin in the ex vivo normothermic machine perfusion of rat livers* alongside Shen et al. in *The role of normothermic machine perfusion (NMP) in the preservation of ex-vivo liver before transplantation: A review*.

3. Other areas

Artificial rbc or blood substitutes is but a very small area of artificial cells. Much larger areas of uses have been reviewed elsewhere (**Figure 1**) (4, 5). A very brief summary of some of these follows.

1. Hemoperfusion: Artificial cells containing bioactive material for hemoperfusion (20–22). One example is the. routine clinical use of artificial cells containing adsorbent for the removal of waste metaboletes and drug poisoning (21,22) and in cytokine storm of severe COVID-19 (23). It also has other uses like the treatment for immunological disease as reported in this Research Topic in *The development of immunosorbents for the treatment of systemic lupus erythematosus via hemoperfusion* by Yu and Ou.
2. Delivery system: Artificial cells in different configurations have used successfully as drug carriers (4, 5, 24, 25). A recent report is Dhasmana et al.'s *Fabrication and evaluation of herbal beads to slow cell ageing*.
3. Artificial Cells in the fight against COVID: The potential of artificial cells as carrier for vaccine has been proposed many years ago (24, 26, 27). Artificial cells prevent mRNA from inactivation by body enzymes and allow it to carry out its function as COVID-19 vaccine (26, 28). Artificial cells based hemoperfusion has also been used to lower the elevated toxic level of cytokines in patients with severe COVID-19 (23, 26).
4. Hereditary enzyme deficiency: We first show that catalase artificial cells can replace the deficient enzyme in hereditary catalase deficient mice (29). Use in patients only became possible when stable simple enzymes became available for artificial cells. This allowed us to treat a patient with Lesch Nyhan disease using artificial cells contain xanthine oxidase (30, 31). We also use artificial cells containing Phenylalanine ammonia lyase (PAL) to treat rats with Phenylketonuria (32). A company collaborated with us to prepared less expensive recombinant PAL which was used by another company to prepare PEG-PAL that has been approved by FDA for adult PKU patients (33).
5. Cancer therapy: We first reported the use of artificial cells containing asparaginase for the suppression of lymphosarcoma in mice (35). This is now being used in patients in the form of PEG-asparaginase. We are using artificial cell containing polyHb-tyrosinase in mice with melanoma (37, 38) Soltys et al.'s group reports in this Research topic in *Inhibition of metastatic brain cancer in Sonic Hedgehog medulloblastoma using caged nitric oxide albumin nanoparticles*.
6. Other areas: Other areas of uses include cell/stem cell therapy and regenerative medicine (39–43), encapsulated microbe (44–46) industry, agriculture, aquatic culture (4, 5, 49), synthetic cells (47), nanomedicine, biotherapeutics, gene therapy, nano-robotics and others (**Figure 1**) (4, 5, 49).

Summary

Artificial cells can be prepared with extensive variations in terms of their contents, membranes, dimensions, and configurations. This allows for an array of promising and innovative medical applications. In this Research Topic, we will start with a detailed discussion of the current status and future prospects of artificial red blood cells. Notable developments in this area include hemoglobin-based oxygen carriers, which have been approved for use in surgical patients by two countries. Additionally, researchers are using natural and synthetic enzymes to form oxygen carriers with antioxidant properties or those with CO2 transport and antioxidant properties. Other approaches include bioengineered hemoglobin and hemoglobin vesicles. Another active area of research centers on the preservation of tissues and cells, with Hemarina having received approval in the EU for the pretransplant preservation of human kidneys. Brief discussion of other notable innovative applications of artificial cells encompasses hemoperfusion, delivery systems, COVID-19 vaccines, cancer therapy, and hereditary enzyme defects. The possibilities extend beyond these, as listed in **Figure 1**, encompassing nanomedicine, biotherapeutics, gene therapy, regenerative medicine, cell and stem cell therapies, and nanorobotics.

Author contributions

TC: Conceptualization, Data curation, Formal analysis, Investigation, Methodology, Project administration, Resources, Supervision, Validation, Writing – original draft, Writing – review & editing, Funding acquisition.

Funding

The author(s) declare that no financial support was received for the research, authorship, and/or publication of this article.

Conflict of interest

The author declare that the research was conducted in the absence of any commercial or financial relationships that could be construed as a potential conflict of interest.

Publisher's note

References

1. Chang TMS. (1957) 1957 Report on "method for preparing artificial hemoglobin corpuscles". *BSc thesis*. McGill University: Montreal, QC. Available at: http://www.medicine.mcgill.ca/artcell/514.pdf

2. Chang TMS. Semipermeable microcapsules. *Science*. (1964) 146:524–5. doi: 10.1126/science.146.3643.524

3. Chang TMS. *Artificial cells*. Springfield, IL: Charles C Thomas Publisher. (1972). p. 1–207. Available at: www.artcell.mcgill.ca/1972bookcovercr.pdf

4. Chang TMS. *Monograph on "ARTIFICIAL CELLS: Biotechnology, nanotechnology, blood substitutes, regenerative medicine, bioencapsulation, cell/stem cell therapy"* Singapore/London: World Scientific Publisher/Imperial College Press (2007). p. 435. Available at: http://www.medicine.mcgill.ca/artcell/2007%20ebook%20artcell%20web.pdf

5. Chang TMS. ARTIFICIAL CELL evolves into nanomedicine, biotherapeutics, blood substitutes, drug delivery, enzyme/gene theraphy, cancer therapy, cell/stem cell therapy, nanoparticles, liposomes, bioencapsulation, replicating synthetic cells, cell encapsulation/scaffold, biosorbent/immunosorbent haemoperfusion/plasmapheresis, regenerative medicine, encapsulated microbe, nanobiotechnology, nanotechnology. *Artif Cells Nanomed Biotechnol*. (2019) 47(1):997–1013. doi: 10.1080/21691401.2019.1577885

6. Abuchowski A, Kazo GM, Jr VC, Van Es T, Kafkewitz D, Nucci ML, et al. Cancer therapy with chemically modified enzymes. I. antitumor properties of polyethylene glycol-asparaginase conjugates. *Cancer Biochem Biophys*. (1984) 7(2):175–86.

7. Chang TMS, Bulow L, Jahr J, Sakai H, Yang CM. (editors) *Nanobiotherapeutic based blood substitutes*. World Scientific Publisher/Imperial College (2021). p. 1040 doi: 10.1142/12054

8. Chang TMS. Stabilisation of enzymes by microencapsulation with a concentrated protein solution or by microencapsulation followed by cross-linking. *BBRC*. (1971) 44 (6):1531–36. doi: 10.1016/S0006-291X(71)80260-7

9. Mer M, Hodgson E, Wallis L, Jacobson B, Levien L, Snyman J, et al. Hemoglobin glutamer-250 (bovine) in South Africa: consensus usage guidelines from clinician experts who have treated patients. *Transfusion*. (2016) 56(10):2631–6. doi: 10.1111/trf.13726

10. Moore EE, Moore FA, Fabian TC, Bernard AC, Fulda GJ, Hoyt DB, et al. Human polymerized hemoglobin for the treatment of hemorrhagic shock when blood is unavailable: the USA multicenter trial. *J Am Coll Surg*. (2009) 208(1):1–13. doi: 10.1016/j.jamcollsurg.2008.09.023

11. D'Agnillo F, Chang TM. Polyhemoglobin-superoxide dismutase-catalase as a blood substitute with antioxidant properties. *Nat Biotechnol*. (1998) 16(7):667–71. doi: 10.1038/nbt0798-667

12. Powanda DD, Chang TM. Cross-linked polyhemoglobin-superoxide dismutase-catalase supplies oxygen without causing blood-brain barrier disruption or brain edema in a rat model of transient global brain ischemia-reperfusion. *Artif Cells Blood Substit Immobil Biotechnol*. (2002) 30(1):23–37. doi: 10.1081/bio-120002725

13. Sims C, Seigne P, Menconi M, Monarca J, Barlow C, Pettit J, et al. Skeletal muscle acidosis correlates with the severity of blood volume loss during shock and resuscitation. *J Trauma*. (2001) 51(6):1137–45. doi: 10.1097/00005373-200112000-00020

14. Tronstad C, Pischke SE, Holhjem L, Tønnessen TI, Martinsen OG, Grimnes S. Early detection of cardiac ischemia using a conductometric pCO(2) sensor: real-time drift correction and parameterization. *Physiol Meas*. (2010) 31(9):1241–55. doi: 10.1088/0967-3334/31/9/013

15. Bian Y, Chang TMS. A novel nanobiotherapeutical poly-[hemoglobin-superoxide dismutase-catalase-carbonic anhydrase] with no cardiac toxicity for the resuscitation of a 90 min sustained severe hemorrhagic shock rat model with 2/3 blood volume loss. *Artif Cells Nanomedicine and Biotechnology*. (2015) 43(1):1–9. doi: 10.1142/9789811228698_0025

16. Chang TM, Powanda D, Yu WP. Analysis of polyethylene-glycol-polylactide nano-dimension artificial red blood cells in maintaining systemic hemoglobin levels and prevention of methemoglobin formation. *Artif Cells Blood Substit Immobil Biotechnol*. (2003) 31(3):231–47. doi: 10.1081/bio-120023155

17. Atlanpole Biotherapies and Zal F. (2022) The biotechnology company HEMARINA obtains the CE mark for its HEMO2life® technology. Available at: https://www.atlanpolebiotherapies.eu/news/the-biotechnology-company-hemarina-obtains-the-ce-mark-for-its-hemo2life-technology/

18. Chang TMS, Razack S, Jiang W, D'Agnillo F. Nanobiotherapeutics as preservation fluids for organs and cells. In: Chang TMS, Jiang W, Razack S, editors. *Nanobiotherapeutic based blood substitutes*. Singapore/London: World Science Publisher (2021). p. 959–76. doi: 10.1142/9789811228698_0044

19. Andrijevic D, Vrselja Z, Lysyy T, Zhang S, Skarica M, Spajic A, et al. Cellular recovery after prolonged warm ischaemia of the whole body. *Nature*. (2022) 608 (7922):405–12. doi: 10.1038/s41586-022-05016-1

20. Chang TMS. Semipermeable aqueous microcapsules ("artificial cells"): with emphasis on experiments in an extracorporeal shunt system. *Trans Am Soc Artif Intern Organs*. (1966) 12:13–9.

21. Chang TMS, Coffey JF, Barre P, Gonda A, Dirk J, Levy M, et al. Microcapsule artificial kidney:treatment of patients with acute drug intoxication. *Can Med Assoc J*. (1973) 108:429–33.

22. Chang TMS, Endo Y, Nicolaev VG, Tani T, Zheng Y, editors. Hemoperfusion and plasma-perfusion and other clinical uses of general, biospecific, immune and leucocyte adsorbents. *Regenerative medicine, artificial cells and nanomedicine chapter 1*. World Scientific Publisher/Imperial College Press (2017). p. 1004. Available at: www.medicine.mcgill.ca/artcell/HPBk_Ch1.pdf

23. Zhou F, Yu T, Du R, Fan G, Liu Y, Liu Z, et al. Clinical course and risk factors for mortality of adult inpatients with COVID-19 in Wuhan, China: a retrospective cohort study. *Lancet*. (2020) 395(10229):1054–62. doi: 10.1016/S0140-6736(20)30566-3

24. Chang TM. Biodegradable semipermeable microcapsules containing enzymes, hormones, vaccines, and other biologicals. *J Bioeng*. (1976) 1(1):25–32.

25. Torchilin VP. Recent advances with liposomes as pharmaceutical carriers. *Nat Rev Drug Discov*. (2005) 4(2):145–60. doi: 10.1038/nrd1632

26. Chang TMS. The role of artificial cells in the fight against COVID-19: deliver vaccine, hemoperfusion removes toxic cytokines, nanobiotherapeutics lower free radicals and pCO2 and replenish blood supply. *Artif Cells Nanomed Biotechnol*. (2022) 50(1):240–51. doi: 10.1080/21691401.2022.2126491

27. Chang TMS. The one-shot vaccine. In: HEDEN C-G, editors. *"Socio-Economic and ethical implications of enzyme engineering"*, Stockholm, Sweden: International Federation of Institutes for Advanced Studies (1975). p. 17–8.

28. Kulkarni JA, Witzigmann D, Thomson SB, Chen S, Leavitt BR, Cullis PR, et al. The current landscape of nucleic acid therapeutics. *Nat Nanotechnol*. (2021) 16 (6):630–43. doi: 10.1038/s41565-021-00898-0

29. Chang TM, Poznansky MJ. Semipermeable microcapsules containing catalase for enzyme replacement in acatalasaemic mice. *Nature*. (1968) 218(5138):243–5. doi: 10.1038/218243a0

30. Chang TM. Preparation and characterisation of xanthine oxidase immobilised by microencapsulation in artificial cells for the removal of hypoxanthine. *Biomater Artif Cells Artif Organs*. (1989) 17(5):611–6. doi: 10.3109/10731198909117640

31. Palmour RM, Goodyer P, Reade T, Chang TM. Microencapsulated xanthine oxidase as experimental therapy in lesch-nyhan disease. *Lancet*. (1989) 2 (8664):687–8. doi: 10.1016/s0140-6736(89)90939-2

32. Bourget L, Chang TM. Phenylalanine ammonia-lyase immobilized in microcapsules for the depletion of phenylalanine in plasma in phenylketonuric rat model. *Biochim Biophys Acta*. (1986) 883(3):432–8. doi: 10.1016/0304-4165(86)90281-3

33. U.S. Food and Drug Administration. *FDA approves a new treatment for PKU, a rare and serious genetic disease* (2018). Available at: https://www.fda.gov/news-events/press-announcements/fda-approves-new-treatment-pku-rare-and-serious-genetic-disease

34. Mahan KC, Gandhi MA, Anand S. Pegvaliase: a novel treatment option for adults with phenylketonuria. *Curr Med Res Opin*. (2019) 35(4):647–51. doi: 10.1080/03007995.2018.1528215

35. Chang TM. The in vivo effects of semipermeable microcapsules containing L-asparaginase on 6C3HED lymphosarcoma. *Nature*. (1971) 229(5280):117–8. doi: 10.1038/229117a0

36. Wetzler M, Sanford BL, Kurtzberg J, DeOliveira D, Frankel SR, Powell BL, et al. Effective asparagine depletion with pegylated asparaginase results in improved outcomes in adult acute lymphoblastic leukemia: cancer and leukemia group B study 9511. *Blood*. (2007) 109(10):4164–7. doi: 10.1182/blood-2006-09-045351

37. Yu B, Swi Chang TM. In vitro and in vivo effects of polyhaemoglobin-tyrosinase on murine B16F10 melanoma. *Melanoma Res*. (2004) 14(3):197–202. doi: 10.1097/01.cmr.0000131013.71638.c0

38. Wang Y, Chang TMS. A polymer–lipid membrane artificial cell nanocarrier containing enzyme–oxygen biotherapeutic inhibits the growth of B16F10 melanoma in 3D culture and in a mouse model. *Artificial Cells, Nanomedicine & Biotechnology*. (2021) 49:461–70. doi: 10.1080/21691401.2021.1918134

39. Lim F, Sun AM. Microencapsulated islets as bioartificial endocrine pancreas. *Science*. (1980) 210(4472):908–10. doi: 10.1126/science.6776628

40. Wong H, Chang TM. Bioartificial liver: implanted artificial cells microencapsulated living hepatocytes increases survival of liver failure rats. *Int J Artif Organs*. (1986) 9(5):335–6. doi: 10.1177/039139888600900515

41. Liu ZC, Chang TM. Transdifferentiation of bioencapsulated bone marrow cells into hepatocyte-like cells in the 90% hepatectomized rat model. *Liver Transpl*. (2006) 12(4):566–72. doi: 10.1002/lt.20635

42. Liu ZC, Chang TMS. Intrasplenic transplantation of bioencapsulated mesenchymal stem cells enhances the regeneration of remnant livers and improves the recovery rates of 90% partial hepatectomized rats. *Stem Cells Int*. (2012) 12:697094. doi: 10.1155/2012/697094

43. Grant R, Hay D, Callanan A. From scaffold to structure: the synthetic production of cell derived extracellular matrix for liver tissue engineering. *Biomed Phys Eng Express*. (2018) 4(6):065015. doi: 10.1088/2057-1976/aacbe1

44. Prakash S, Chang TM. Microencapsulated genetically engineered live E. coli DH5 cells administered orally to maintain normal plasma urea level in uremic rats. *Nat Med*. (1996) 2(8):883–7. doi: 10.1038/nm0896-883

45. Chow KM, Liu ZC, Prakash S, Chang TM. Free and microencapsulated Lactobacillus and effects of metabolic induction on urea removal. *Artif Cells Blood Substit Immobil Biotechnol*. (2003) 31(4):425–34. doi: 10.1081/bio-120025412

46. Iqbal U, Westfall S, Prakash S. Novel microencapsulated probiotic blend for use in metabolic syndrome: design and in-vivo analysis. *Artificial Cells Nanomedicine and Biotechnology*. (2018) 46(1):1–9.

47. Hutchison CA 3rd, Chuang RY, Noskov VN, Assad-Garcia N, Deerinck TJ, Ellisman MH, et al. Design and synthesis of a minimal bacterial genome. *Science*. (2016) 351(6280):aad6253. doi: 10.1126/science.aad6253

48. Poncelet D, Neufeld R. *Bioencapsulation Research Group on industrial and agricultural applications*. Available at: http://bioencapsulation.net

49. Chang TMS (2023) *Artificial Cells, Blood Substitutes and Nanomedicine website containing reviews and monographs for free online viewing or download*: Available at: www.medicine.mcgill.ca/artcell

frontiers | Frontiers in Medical Technology

TYPE Opinion
PUBLISHED 18 August 2022
DOI 10.3389/fmedt.2022.989829

OPEN ACCESS

EDITED BY
Binglan Yu,
Massachusetts General Hospital and Harvard Medical School, United States

REVIEWED BY
Leif Bulow,
Lund University, Sweden
Hongli Zhu,
Northwest University, China

*CORRESPONDENCE
Jonathan S. Jahr
j.s.jahr@ucla.edu

SPECIALTY SECTION
This article was submitted to Regenerative Technologies, a section of the journal Frontiers in Medical Technology

RECEIVED 08 July 2022
ACCEPTED 28 July 2022
PUBLISHED 18 August 2022

CITATION
Jahr JS (2022) Blood substitutes: Basic science, translational studies and clinical trials.
Front. Med. Technol. 4:989829.
doi: 10.3389/fmedt.2022.989829

Blood substitutes: Basic science, translational studies and clinical trials

Jonathan S. Jahr*

Department of Anesthesiology and Perioperative Medicine, David Geffen School of Medicine, University of California, Los Angeles, Los Angeles, CA, United States

KEYWORDS

blood substitutes, artificial oxygen carriers, Hemopure, HBOC-201, hemoglobin

Introduction

According to recent reports, the yearly mortality rate is 1.9 million worldwide from hemorrhage (1). This stunning statistic has been slightly improved from the estimated 5 million deaths worldwide each year from earlier reports (2); however, compared with COVID-19, this extreme death rate is continuing, yet relatively little research and productivity has been seen over the last 5 decades regarding improving survival, as the treatment of acute anemia is relatively simple as compared with deriving new vaccines, etc. for a pandemic.

Setting the stage for need of blood substitutes

This work will describe the nature of the problem, hemorrhage, work that has been performed for almost 50 years to ameliorate hemorrhage and acute anemia, with treatments other than transfusion of erythrocytes. There follows a brief history of hemoglobin-based oxygen carriers (HBOCs); erythrocytes may not be available in emergency situations and where patients refuse transfusion and where blood is not an option (3). Studies performed in this area will be documented in three sections: Basic Science, Translational Studies and Clinical Trials.

Hemorrhage

When accident victims are bleeding to death, there have been few medical treatment options to save their lives until they can be rescued and transported to a hospital, despite new campaigns, including use of tranexamic acid as an antifbrinolytic (4).

Therefore, work that proposes to develop a new type of fluid, with multiple medical effects, that is designed to improve survival from first-aid treatment by a healthcare professional is warranted. It will include fluids, oxygenating capability (like erythrocytes), blood clotting capability and other essential factors to improve survival—a revolutionary concept for the improvement of current hemorrhagic trauma medical care.

Transfusion medicine and current standard of care

Blood transfusion, including use of erythrocytes, plasma, and platelets, is currently the most effective therapy for hemorrhage but often not immediately available during out of-hospital settings where most traumatic injuries occur (remote sites of injury or battlefields). Current standard prehospital therapy for hemorrhage is infusion of isotonic crystalloid solutions (less commonly, colloids and, rarely in civilian and military trauma, blood, and blood products) (5). However, the large volumes of crystalloids often required to maintain BP in these patients may cause fluid overload and dilution of red cells (anemia), hemostatic and other beneficial mediators in blood. In addition, crystalloid volume expanders neither carry the oxygen that is essential to maintain vital organ functions nor the coagulation factors that prevent further blood loss.

A recent Cochrane project (6) outlines a protocol whose objective is to assess the effects and safety of blood product transfusion strategies started during the first day post injury for trauma patients of all ages with major bleeding. Clearly, the need to understand and improve the standard of care is warranted, possibly including blood substitutes and/or oxygen carriers.

All recent iterations of guidelines for resuscitation following hemorrhage and trauma acknowledge the challenge of providing oxygen carrying capacity early on in the injury and that later coagulation concerns become paramount to resolution for survival to occur (7).

NICE Pathways have been constructed for hemorrhage in the hospital setting[1], which also indicate that the need for rapid oxygen carrying delivery is key to survival and later coagulation concerns are vital. However, without a blood substitute/oxygen therapeutic, such delivery to ischemic tissues is difficult and sometimes impossible without ECMO or cardiopulmonary bypass, given the need to have pulsatile blood flow in order for erythrocytes to offload oxygen in the capillaries. It is conceivable that oxygen therapeutics, depending on design, may deliver oxygen in non-pulsatile situations, such as cardiopulmonary arrest with resuscitation and even chest compressions.

Recent trials, such as PAMPER, have attempted to improve this but only with currently available blood products (5). Therefore, development of a "blood substitute? that is efficacious and without risk for management of hemorrhage, including coagulopathy, has been a long-standing goal which remains unfulfilled (3).

1 https://pathways.nice.org.uk/pathways/trauma (accessed January 15, 2021).

Traumatic hemorrhagic shock

Traumatic hemorrhagic shock (THS), as compared with surgical hemorrhage, is a high mortality, multiple pathophysiology condition, including hypovolemic anemia, coagulopathy, inflammation, and infection due to open wounds and damaged blood vessels. Erythrocyte, plasma, and platelet administration is currently the most effective therapy for traumatic hemorrhagic shock, but it is rarely available for out-of-hospital settings where most traumatic injuries occur. Current standard prehospital treatment for THS is infusion of isotonic crystalloid solution administered by the first responder healthcare professionals. Therefore, crystalloids formulated as hypertonic solutions (3–7%) have been proposed to be more effective in the resuscitation of hemorrhagic patients as they may permit "small volume" resuscitation thus preventing fluid overload and secondary hemorrhage that may occur with conventional isotonic resuscitation that typically requires 2–3 times the volume (8). In addition, small volume hypertonic solutions may provide anti-inflammatory effects; however, recent trials have suggested that these are ineffective (8). Although crystalloids may be effective in blood volume expansion, they do not transport the oxygen critical for vital organ function and survival. In addition, trauma victims often present with coagulopathy that causes uncontrollable bleeding. Intravenous use of recombinant human coagulation factor VIIa in hospitalized trauma patients have been studied and appears efficacious in soldiers wounded in the battlefield during the Iraq war (9). In the Iraq war experience, early use of factor VIIa reduced blood transfusions by 20%. Other trials have indicated promise, though no better outcomes (10).

Brief history of hemoglobin-based oxygen carriers (HBOC)

The recent review on the topic is used as a reference (3). It reviews the science to date as of its composition and highlights 11 of my significant publications in this area (11–21).

Additionally, it provides the reader with an update on the newest of products currently under study. Additionally, the review sheds light on the worldwide need for these products when blood is either unavailable or not an option, whether for personal reasons, unavailability or for incompatibility.

Hemoglobin-based oxygen carriers were created as early as 1934, when Amberson purified bovine hemoglobin and infused it into study feline models and summarized in 1949, when he described purified human hemoglobin being infused into anemic parturients with hemorrhage after childbirth (22). Development continued when the US Army manufactured a tetrameric cross-linked hemoglobin (α-α

cross-linked hemoglobin) which later was produced by the Baxter Corporation (Deerfield, IL), as 2,3-diaspirin cross-linked hemoglobin (HemAssist) (23). However, it failed in human studies because of decreased cellular perfusion and increased morbidity and mortality (3). During a resurgence of activity in the mid-1980s, manufacturers developed second-generation HBOCs, including Biopure Corp. (Cambridge, MA) with HBOC-200 (Oxyglobin, approved by the FDA and the European Union for canine anemia in 1997 and 1998, respectively); Hemoglobin-glutamer-201 (Hemopure, approved in South Africa for treatment of human anemia in 2001 and Russia in 2006); PolyHeme by Northfield Laboratories (Evanston, IL); Hemolink by Hemosol, Inc. (Mississauga, ON, Canada) (24). Several studies critically evaluated these products both in animal studies and human trials, documenting successful outcomes being met in Phase I, II and III trials (25, 26).

Allogeneic blood transfusion risks

Blood transfusions are amongst the most common hospital procedures and have been in practice since 1795. Despite their prevalence, risks that are related to blood transfusions are most commonly: iron overload, TRALI (transfusion related acute lung injury) and resultant death in significant proportions (27). Other risks which, thanks to updated practice, have been mitigated, include transmitted disease (Chagas disease, HIV, Hepatitis C, malaria etc.), compatibility complications and TRALI (28). Blood product ease of access including the risks have directed the requirement for an oxygen carrier that is both safe and effective. A suitable blood substitute would eliminate the need for cross matching, reduce risk of pathogen transmission, increase availability in remote regions and be storable for longer periods of time. Much work has been done to create blood substitutes. The first involved removing the erythrocyte (RBC) coat and infusing stroma-free hemoglobin (SFH). However, infusion of SFH imitates extreme hemolysis, leading to jaundice, renal failure and death (11). To increase stability and avoid hemolysis, hemoglobin-based oxygen carriers (HBOC) use purified human, animal, or recombinant hemoglobin (Hb) in a cell-free preparation (11). Early generation HBOCs had adverse events, including renal failure, scavenging of nitric oxide (NO) causing vasoconstriction and oxidation causing methemoglobinemia (29).

These adverse effects are due to tetramers of hemoglobin being cleaved into dimers. Alleviating the adverse effects, specifically decreasing the severity of vasoconstriction, has led to several modifications such as cross-linkage, polymerization and encapsulation with polyethylene glycol (PEGylation), which will all be discussed (30).

Advances in second generation HBOCs and beyond

Stroma-free hemoglobin were produced by either ultrafiltration or crystallization. The ultrafiltration method yielded SFH free of vasocontraction and contractility-depressant effects when tested on an *ex vivo* perfused heart (31). Although the adverse effects described above prevented use of SFH, results were useful in showing ultrafiltration should be the preferred method of production. Improving upon SFH, it was hypothesized that crosslinking might help in reducing the adverse effects. The concepts were evaluated with diaspirin-crosslinked Hb (DCLHb), known as HemAssist. Due to increased mortality, the studies on this product were terminated. The patients experienced major vasoconstrictive adverse events (23).

Following the failure of HemAssist, a second generation of HBOCs was created. The first was Hemolink, (24). Hemolink is a raffinose crosslinked HBOC prepared from outdated human erythrocytes (24).

The next HBOC, Polyheme, was a glutaraldehyde polymerized human Hb from outdated RBCs and is primarily used as a resuscitation fluid (25). The product was discontinued after Phase III following negative results of imbalance in mortality (32). It is unclear if the poor outcomes resulted from the product or protocol of the trials. There were also some ethical issues raised in the conduct of trauma trials having to do with lack of subject consent and community assent issues (33).

The final product of the second generation of HBOCs was Hemopure (HBOC-201) and made from purified bovine hemoglobin cross-linked and then polymerized with glutaraldehyde. Hemopure does not contain any cell blood membrane antigens, so may be tolerated by all blood types (16). Its benefit arises from its ability to maintain O 2 delivery to ischemic tissues during anemia or low blood flow.

Following the setbacks of the second generation HBOCs, researchers focused on a product that would avoid the toxic chemical and biophysical effects demonstrated by the crosslinked/polymerized HBOCs. Instead of producing a substitute for blood transfusions, researchers began developing a product for situations in which blood is not available for transfusion or in situations in which a blood transfusion is not possible due to health or religious objections, for example, Jehovah's Witness. Further work showed that an oxygen-binding agent may be more valuable in preventing or treating ischemia-related morbidity, thereby reducing mortality (34).

The first product to come from this new, shifted thinking was Hemospan/MP4 (Sangart, San Diego, CA). Hemoglobin derived from outdated human blood was modified with Maleimide-Polyethylene Glycol and regarded as a plasma expander due to its purported vasodilatory effects, which was in stark contrast to its vasoconstrictive predecessors.

MP4 showed promise in its Phase I study when, upon administration to healthy patients, it did not induce hypertension or cause any gastrointestinal side effects, unlike other HBOCs (35). However, in further Phase II trials, MP4 administration did cause vasoconstriction due to release of un-crosslinked free hemoglobin and, therefore, was not successful in alleviating issues from earlier HBOCs (3).

Update on newer/newest products that have been studied in humans

Current development with new concepts in products which change former generations HBOC characteristics of lowered hemoglobin (from 10–13 g/dL to 4–6 g/dL) and oxyhemoglobin dissociation shifting the curve to the left from the right (p50 30–40 mmHg to 6 mmHg) (OxyVita and MP4) (3, 17). These strategies for improved function remain to be validated and verified independently. The newest generation HBOCs to be evaluated in human trials, Saguinate (Prolong Pharmaceuticals, Piscataway, NJ) has similar pharmacologic profiles, and some successful trials have been published (3). A marine worm derived HBOC, from Hemarina (Morlaix, Brittany, France) has also been evaluated in a few human trials and also for use in pulmonary failure related to COVID-19 (3, 36).

Clinical trials

Multiple clinical trials have been executed on HBOCs, to evaluate their safety and efficacy in various disease states. The area most studied has been as oxygen carriers to facilitate transport to hypoxemic and ischemic tissues and hopefully resume homeostasis within the organism and protect survival. The following two studies are examples of clinical trials that exemplify the urgency for the need for approval of blood substitutes, with one pivotal trial that compared the only HBOC still available for human use, to erythrocytes.

While no product or trial is perfect, both studies that follow make serious attempts to address issues that had been unaddressed to date and, with hopeful regulatory approval in more countries, many lives may be able to be saved as a result of hemorrhage and surgical bleeding where blood is not an option or available.

Consort abstract

As a landmark study was published just prior to the time CONSORT provided guidelines for structured abstracts[2], the study abstract has been expanded and retrofitted to enable easier understanding with modern terminology (see Supplementary Table 1).

Summary

The HEM-0115 Phase III prospective, randomized, single-blind trial included 688 subjects planned for orthopedic elective surgery, who were randomized at firsttransfusion decision to Hemopure (13 g/dL hemoglobin in 250 ml) or erythrocytes to treat surgery-related anemia (14). Hemopure has a p50 of 40 mm Hg compared to adult corpuscular hemoglobin of 27 mm Hg, so the oxyhemoglobin curve is shifted to the right to facilitate easier onloading and offloading of oxygen to the tissues.

Transfusion thresholds included [THb] of <10.5 g/dL and a patient exhibiting at least one of the clinical signs: heart rate 100 bmp; SBP <90 mm Hg or <70% of preoperative screening value; electrocardiogram evidence of myocardial ischemia; metabolic acidosis (Base Deficit −4 or worse); acute blood loss >7 mL/kg within 2 h or less. oliguria with urine output <0.5 mL/kg/h ongoing for 2 h or more. The threshold would be considered high by today's care but was standard of care at the time the trial was undertaken (3). Additionally, transfusion thresholds included [THb] of 7 mL/kg within 2 h or less as an inclusion criterion, automatically (14).

Three hundred and fifty patients were randomized to a Hemopure infusion and 338 patients randomized to erythrocytes. Based on the cumulative clinical trial material units administered, the majority of Hemopure subjects received 5 or fewer 250 ml infusions with 18.7% receiving 6–10,250 ml infusions; one patient received 330 g or 11 infusions. By contrast, the erythrocyte subjects received 243 ± 9 g Hb on average, with 78.4% receiving ≥2 units (14).

Once treatment was initiated with a 2-unit (500 ml) loading dose of Hemopure, additional treatment was permitted for up to 6 days for a maximum of 10 units Hemopure (130 g hemoglobin) using the same criteria as for enrolment. The need for continuing oxygen transport beyond 10 units of Hemopure was met by crossing over Hemopure randomized subjects to erythrocytes. Transfusion avoidance was the primary outcome including a blinded assessment of safety. The designs of this Phase III study required that limits be placed regarding the volume of Hemopure infused. In severe hemorrhage, after limits of Hemopure infusions were met, patients were crossed over to receive erythrocytes. The clinical trial scenarios simulated circumstances where Hemopure was used until erythrocytes became available to replace moderate (≤3 units erythrocytes) blood loss for elective surgery (14).

Primary outcome

Among 350 HBOC-201 patients in the HEM-0115 trial, 96% avoided erythrocyte transfusion at Day 1, 70% at Day

2 http://www.consort-statement.org/extensions/overview/abstracts (accessed January 16, 2021).

7 and 59% at 6 weeks after surgery (the 95% confidence intervals were not presented). Low total Hb in combination with restricted subject activity was the reason most often documented for the first transfusion decision followed by tachycardia (100 beats/min). Achievement of the primary efficacy outcome, with subjects in this group receiving Hemopure, 59%, did not receive erythrocyte transfusions throughout the entire 6-week study period. Considering the intent to replace up to 6 units of erythrocytes by up to 10 units of HBOC-201, the actual rate of full blood avoidance was even higher since 317 (94%) of subjects in erythrocyte arm received 6 or less units. Administration of Hemopure resulted in an expected hematocrit reduction related to the acellular Hemopure solution infusions through treatment Day 5; in both cohorts, hematocrit values returned to normal at 6 weeks. An infusion of the loading dose of two units of Hemopure produced a 1.44 ± 0.03 g/dL increase in plasma hemoglobin and a 0.39 ± 0.06 g/dL increase in [THb]. Analysis of the total hemoglobin concentrations [THb] as a function of how many infusions received, revealed that subjects needing continuing Hemopure infusions, revealed a lower [THb] (p < 10.5 g/dL) at a hemoglobin level of 8.85 ± 0.07 g/dL throughout the treatment period, excepting the loading 2-unit dose post-Hemopure total hemoglobin. HEM-0115 study subjects (n = 139), whose oxygen transport requirements were unmet by 10 units Hemopure, by protocol, were transfused erythrocytes (14).

Secondary outcomes

Examining the laboratory studies in the HEM-0115 study, the following laboratory values were not different between cohorts: albumin, alkaline phosphatase, total bilirubin, glucose, glutamyl transferase, lactate dehydrogenase and acid base-values. However, at follow up, an elevated total protein in the Hemopure group was noted, including an increase in aspartate aminotransferase and alanine aminotransferase. Lipase was increased in the Hemopure group in 5–11% of patients vs. 1–2% of patients in the erythrocyte group. Creatinine was increased 25% over baseline in 12 subjects (6%) from the Hemopure group compared with 3 subjects (2%) from the packed red blood cell group (14).

A summary of overall medical risk assessment for the intent to treat mandated by protocol, determined by blinded review of patient medical records and adverse events by treatment group, demonstrated the overall odds ratio for adverse events was 1.41–1.43 between groups (the 95% confidence intervals were not presented). Deaths were reported in10 subjects randomized to Hemopure and six in the patients randomized to PRBC (p =0.450). No deaths in either treatment group were categorized as associated with either treatment (14).

Discussion and context

As discussed in Section Advances in second generation HBOCs and beyond, development of Hemopure started in the late 1980s and by mid-1990s had completed multiple clinical trials, under the FDA Phase I and II designation (12). My participation in the Phase II Cardiac trial of Hemopure (15), that was designed as a double-blind protocol and proved extremely difficult to blind the investigators (and subjects) as to which cohort they had been randomized into, helped dictate the single-blind protocol that was eventually designed and utilized for the Phase III.

This study and many to follow on Hemopure (16) have led to use in South Africa indicated for anemia and if blood is not an option or available and, in the US, and EU for Expanded Use/Compassionate use (3). Additional uses currently include preparation to conduct a trauma trial in South Africa, funded by the US Military[3] as a perfusate in organ donor perfusion systems to lengthen the down time for organ transplants between harvest and implantation (37) and other novel indications (3).

The US FDA and EU regulatory authorities have yet to approve Hemopure for routine use as an oxygen therapeutic and may do so with positive results of the planned trauma trial. Niche uses will also likely be approved, especially when blood is not an option or available.

Discussion of these research findings by other investigators has highlighted that the imbalance in adverse events and serious adverse events are not the result of toxicity of the product but were likely a mix of subject pre-existing conditions, how management of clinical issues differed amongst practitioners and possible inadequate volumes of Hemopure infusions, in the face of continuing bleeding and low hemoglobin concentrations and hypoxemic tissues on one side of the equation and possible over infusion of Hemopure with congestive heart dysfunction on the other (38–40). Mackenzie et al. highlighted the challenges of conducting research in urgent/ emergency settings, leading to incomplete data, one of the challenges faced in this trial (41). Others highlight the benefits of blood substitutes as they are extensively scrubbed to remove infectious agents (including bovine encephalitis) and may be administered immediately when required in the field or ambulance avoiding the need of blood type and crossmatch procedures (42). As this trial was designed more than 20 years ago and was completed with enrolment in 2001, there are some significant shortcomings that may have been avoided had the CONSORT guidelines been published and adopted (see text footnote 2).

The first weakness is that attempting to compare an HBOC with a circulating plasma half-life of no longer than 24 h, with erythrocytes, depending on how fresh they are, which may

3 https://www.dvidshub.net/news/printable/311421 (accessed January 16, 2021).

circulate up to 30 days. However, this was the only head-to-head study against red blood cells as there is no comparator (crystalloids, colloids, plasma) that exists that is approved, due to lack of oxygen carrying capacity. This study did, in fact, demonstrate savings of erythrocytes, especially in the cohort of under 80-year-old subjects and patients in whom a hematinic effect could be demonstrated, with high reticulocyte counts and regeneration of autologous erythrocytes (43). Hemopure's breakdown is like any other hemoglobin and is, ultimately, turned to bilirubin but, in the process, there is a huge usable iron load released as well as globin proteins, often when the body may be starved due to medical therapy. This hematinic effect has been challenging to document yet, if it exists, might prove one of the most valuable attributes of a product as this.

Additionally, the transfusion thresholds or triggers for transfusion have been modified to around 7 g/dL (44) and not the 9–10 g/dL that were used in the trial. This could mean that the infusions of Hemopure were either unnecessary or provided other benefits as indicated above. Moreover, there may be some value in higher hemoglobin (and plasma and platelets) early in trauma or a surgical blood loss and may improve outcomes (45). Either way, the importance of the study is somewhat diminished by this and, were it to be repeated, it would need to be infused at hemoglobin concentrations <7 g/dL.

A comparison of [THb] and serious adverse events (SAEs) among HEM-0115 subjects given 10 units Hemopure ($n = 211$) and those given Hemopure plus erythrocytes showed that [THb] was significantly lower (<10 Hemopure 250 ml infusions were identical to those receiving $\leq$3 units erythrocytes). Five deaths in the Hemopure arm occurred in patients older than 80 years compared with 1 in the erythrocyte group.

There was an equal number of deaths ($n = 5$) among patients under 80 years of age receiving either treatment. The HEM-0115 trial demonstrated that Hemopure with a hemoglobin concentration of 13 g/dL in comparison with erythrocytes provided management of hemorrhage of up to 3 units for elective orthopedic surgery without the use of erythrocytes or significant differences in mortality or serious adverse events. Weaknesses in this study could have been mitigated, had it been performed after the CONSORT guidelines (see text footnote 2) were promulgated. It would likely have questioned the direct comparison against erythrocytes and focused more on oxygen delivery, especially to the microcirculation, where the effect of oxygen delivery is required. Evaluating macrocirculatory issues, such as blood pressure and heart rate, amongst others, may be primitive, in terms of understanding the efficacy of an oxygen therapeutic, albeit important for resuscitation and survival. Also, the discrepancy between the Intent to Treat and those actually treated, which was due to situations where Hemopure was administered, did not yet meet inclusion criteria for Hemopure infusion as a protocol violation, would have been prevented from entering the trial from the start of infusion, not post hoc during data tabulation and analysis.

These findings demonstrate that Hemopure may be useful in the prehospital phase of trauma patient management when blood is unavailable. Also, Hemopure with hemoglobin concentration equivalent to whole blood may be infused safely to avoid up to 3 units of erythrocytes for elective surgery. Ensuring adequate oxygen delivery and coagulation factors are present are important considerations when administering Hemopure.

Significance

This multicenter, single-blind, randomized, multinational study was one of the two largest clinical trials ever conducted with HBOC products (close to 700 subjects). The purpose of the study was whether use of Hemopure would reduce allogeneic red blood cells (PRBC) in orthopedic patients requiring blood transfusion. In subjects with moderate transfusion needs, Hemopure was shown to significantly reduce PRBC use without increase in adverse effects. However, in patients with higher transfusion needs, Hemopure failed to correct the anemic condition due, in part, to unbalanced study design and inherent limitations of Hemopure. Considering the relatively more dilute Hb concentration, HBOC would inherently require more volume than erythrocytes. Therefore, in high demand subjects for comparable effect, larger volumes of HBOC were required that might have led to volume overload and higher incidences of adverse effects. This study taught the PI a critically important lesson regarding fluid resuscitation and risk of volume overload, a key need for formulating a small volume, multifunctional, resuscitation fluid.

Conclusion of trial

Despite its successful ability to decrease the likelihood of transfusion in nearly 50% of the subjects studied, the FDA has not yet approved Hemopure; however, the FDA has allowed its use under expanded access and compassionate use (3). It may be used in situations in which all other options have been exhausted and the patient is experiencing severe and dangerous anemia and is approved for human use if blood is unavailable or not an option in South Africa and other countries.

Summary of review

This review has attempted to describe a major morbidity and mortality of hemorrhagic shock, that is either inadequately treated or unable to be treated at the site of injury due to blood not being available or not an option and, in the perioperative setting, where expected blood loss is managed with erythrocytes

and clotting factors but due to the inherent risks of allogeneic blood, may worsen outcomes.

Hemoglobin-based oxygen carriers may offer a solution to acute anemia, whatever the etiology and provide rapid onset oxygenation to tissues even without pulsatile blood flow. Doing so may improve the statistics of mortality of hemorrhage, which may account for between 1.9 and 5 million lives annually, dwarfing even devastating deaths due to the pandemic with COVID-19.

Therefore, continued work on HBOCs is warranted and, despite multiple setbacks with trials and products, it makes sense that further work be funded and continued, on the most promising products. The question of whether or not to create HBOCs with high or low p50's has been raised, and while Hemopure has shifted the oxyhemoglobin curve to the right, a number of newer products have been developed with lower p50's, analogous to fetal hemoglobin (p50 = 19 mm Hg), and even lower, with the concept being that only severely hypoxemic hemoglobin will load and offload oxygen, providing only to tissues severely depleted; however, no comparative studies have been performed to demonstrate which is more effective (46).

Hemopure may be one of those HBOCs, given its approval for human use since 2001 in South Africa and multiple trials in humans and continued use that demonstrate reasonable safety and efficacy. To compare this, or any product for that matter, against blood, which has never undergone safety or efficacy trials, may be meaningless; far more important is to find those niches where survival is improved while maintaining safety. This work has attempted to do just that: demonstrate reasonable safety and efficacy despite adverse events that all pharmacotherapies have and accept those with the understanding that no drug is side-effect free which would be an unlikely expectation. The challenge is to accept the side-effect profile and modify usage and indication so that benefits may outweigh risks, the challenge upon which all life is predicated.

Author contributions

The author confirms being the sole contributor of this work and has approved it for publication.

Conflict of interest

The author declares that the research was conducted in the absence of any commercial or financial relationships that could be construed as a potential conflict of interest.

Publisher's note

Supplementary material

The Supplementary Material for this article can be found online at: https://www.frontiersin.org/articles/10.3389/fmedt.2022.989829/full#supplementary-material

References

1. Chambers JA, Seastedt K, Krell R, Caterson E, Levy M, Turner Nt. Stop the bleed: a US military installation and model for implementation of a rapid hemorrhage. *Mil Med.* (2019) 184:67–71. doi: 10.1093/milmed/usy185

2. Kauvar DS, Lefering R, Wade CE. Impact of hemorrhage on trauma outcome: an overview of epidemiology, clinical presentations, and therapeutic considerations. *J Trauma.* (2006) 60:S3–11. doi: 10.1097/01.ta.0000199961.02677.19

3. Jahr JS, Guinn NR, Lowery DR, Shore-Lesserson L, Shander A. Blood substitutes and oxygen therapeutics: a review. (2019). *Anesth Analg.* (2021) 132:119–29. doi: 10.1213/ANE.0000000000003957

4. Morrison JJ, Dubose JJ, Rasmussen TE, Midwinger MJ. Military application of tranexamic acid in trauma emergency resuscitation (MATTERs) study. *Arch Surg.* (2012) 147:113–9. doi: 10.1001/archsurg.2011.287

5. Sperry JL, Guyette FX, Brown JB, Yazer MH, Triulzi DJ, Early-Young BJ, et al. Prehospital plasma during air medical transport in trauma patients at risk for hemorrhagic shock. *N Engl J Med.* (2018) 379:315–26. doi: 10.1056/NEJMoa1802345

6. Wong H, Pottle J, Curry N, Stanwroth SJ, Brunskill SJ, Davenpoint R, et al. Strategies for use of blood products for major bleeding in trauma. *Cochrane Database Syst Rev.* (2017) (4):CD012635. doi: 10.1002/14651858.CD012635

7. Spahn DR, Bouillon B, Cerny V, Duranteau J, Filpescu D, Hunt BJ, et al. The European guidelines on management of major bleeding and coagulopathy following trauma: fifth edition. *Crit Care.* (2019) 23:98. doi: 10.1186/s13054-019-2347-3

8. Pfortmueller CA, Kindler M, Schenk N, Messmer AS, Hess B, Jakob L, et al. Hypertonic saline for fluid resuscitation in ICU patients post-cardiac surgery (HERACLES): a double-blind randomized controlled clinical trial. *Intensive Care Med.* (2020) 46:1683–95. doi: 10.1007/s00134-020-06132-0

9. Perkins JG, Schreiber MA, Wade CE, Holcomb JB. Early versus late recombinant factor viia in combat trauma patients requiring massive transfusion. *J Trauma.* (2007) 62:1095–9. doi: 10.1097/TA.0b013e31804798a4

10. Hauser CJ, Boffard K, Dutton R, Bernard GR, Croce MA, Holcomb JB, et al. Results of the CONTROL trial: efficacy and safety of recombinant activated factor VII in the management of refractory traumatic hemorrhage. *J Trauma.* (2010) 69:489–500. doi: 10.1097/TA.0b013e3181edf36e

11. Jahr JS, Sadighi Akha A, Holtby R. Crosslinked, polymerized, and pegylated hemoglobin-based oxygen carriers: clinical safety and efficacy of recent and current products. *Curr Drug Discov Technol.* (2012) 9:158–65. doi: 10.2174/157016312802650742

12. Mackenzie CF, Pitman AN, Hodgson E, Sussman MJ, Levien LJ, Jahr JS, et al. Are hemoglobin-based oxygen carriers being withheld because of regulatory

requirement for equivalence to packed red blood cells? *Am J Ther*. (2015) 22:e115–e121. doi: 10.1097/MJT.0000000000000009

13. Driessen B, Jahr JS, Lurie F, Gunther RA. Inadequacy of low-volume resuscitation with hemoglobin-based oxygen carrier, hemoglobin glutamer-200 (bovine) in canine hypovolemia. *J Vet Pharmacol Ther*. (2001) 24:61–72. doi: 10.1046/j.1365-2885.2001.00307.x

14. Jahr JS, Mackenzie C, Pearce B, Pitman A, Greenburg AG. HBOC-201 as an alternative to blood transfusion: efficacy and safety evaluation in a multicenter phase III trial in elective orthopedic surgery. *J Trauma-Injury Infection Crit Care*. (2008) 64:1484–97. doi: 10.1097/TA.0b013e318173a93f

15. Levy JH, Goodnough LT, Greilich PE, Parr GVS, Stewart RW, Gratz I, et al. Polymerized bovine hemoglobin solution as a replacement for allogeneic red blood cell transfusion after cardiac surgery: results of a randomized, double- blind trial. *J Thorac Cardiovasc Surg*. (2002) 124:35–42. doi: 10.1067/mtc.2002.121505

16. Mer M, Hodgson E, Wallis L, Jacobson B, Levien L, Snyman J, et al. Hemoglobin glutamer-250 (bovine) in South Africa: consensus usage guidelines from clinician experts who have treated patients. *Transfusion*. (2016) 56:2631–6. doi: 10.1111/trf.13726

17. Jahr JS, Weeks DL, Desai P, Lim JC, Butch AW, Gunther R, et al. Does OxyVita, a new generation hemoglobin-based oxygen carrier, or oxyglobin acutely interfere with coagulation compared with normal saline or 6% hetastarch? An ex vivo thrombelastography study. *J Cardiothorac Vasc Anesth*. (2008) 22:34–9. doi: 10.1053/j.jvca.2007.02.016

18. Jahr JS, Lurie F, Driessen B, Davis JA, Gosselin R, Gunther RA. The HemoCue®, a point of care B-hemoglobin photometer, accurately measures hemoglobin levels when mixed in vitro with canine plasma and three hemoglobin-based oxygen carriers (HBOC). *Can j Anesth*. (2002) 49:243–8. doi: 10.1007/BF03020522

19. Jahr JS, Lurie F, Xi S, Golkaryeh MS, Kuznetsova OA, Kullar RK, et al. Novel approach to measuring circulating blood volume: use of a hemoglobin-based oxygen carrier (HBOC) in a rabbit model. *Anesth Analg*. (2001) 92:609–14. doi: 10.1213/00000539-200103000-00010

20. Jahr JS, Osgood S, Rothenberg SJ Li Q-L, Butch AW, Gunther RA, et al. Lactate interference by hemoglobin-based oxygen carriers (oxyglobin, hemopure and hemolink). *Anesth Analg*. (2005) 100:431–6. doi: 10.1213/01.ANE.0000142116.42938.82

21. Jahr JS, Lurie F, Gosselin R, Lin JS, Wong L, Larkin E. Effects of a hemoglobin-based oxygen carrier (HBOC-201) on coagulation testing. *Am J Ther*. (2002) 9:431–6. doi: 10.1097/00045391-200209000-00011

22. Amberson WR, Jennings JJ, Rhode CM. Clinical experience with hemoglobin–saline solutions. *J. Appl Physiol*. (1949) 1:469–489. doi: 10.1152/jappl.1949.1.7.469

23. Sloan EP, Koenigsberg M, Gens D, Cipolle M, Runge J, Mallory MN, et al. Diaspirin cross-linked hemoglobin (DCLHb) in the treatment of severe traumatic hemorrhagic shock: a randomized controlled efficacy trial. *J Am Med Dir Assoc*. (1999) 282:1857–64. doi: 10.1001/jama.282.19.1857

24. Cheng DC, Mazer CD, Martineau R, Ralph-Edwards A, Karski J, Robblee J et al. A phase II dose-response study of hemoglobin raffimer (Hemolink) in elective coronary artery bypass surgery. *J Thorac Cardiovasc Surg*. (2004) 127:79–86. doi: 10.1016/j.jtcvs.2003.08.024

25. Moore EE, Moore FA, Fabian TC, Bernard AC, Fulda GJ, Hoyt DB, et al. PolyHeme Study Group. Human polymerized hemoglobin for the treatment of hemorrhagic shock when blood is unavailable: the USA multicenter trial. *J Am Coll Surg*. (2009) 208:1–13. doi: 10.1016/j.jamcollsurg.2008.09.023

26. Jahr JS, Sadighi Akha A, Doherty L, Li A, Kim HW. Chapter 22: Hemoglobin-based Oxygen Carriers: History, Limits, Brief Summary of the State of the Art, Including Clinical Trials. In: Mozzarelli A, Bettati S, editors. *Chemistry and Biochemistry of Oxygen Therapeutics: from Transfusion to Artificial Blood, First Edition*. London, England: John Wiley and Sons Ltd. (2011) p. 301–316. doi: 10.1002/9781119975427.ch22

27. Carson JL, Triulzi DJ, Ness PM. Indications for and adverse effects of red-cell transfusion. *N Engl J Med*. (2017) 377:1261–72. doi: 10.1056/NEJMra1612789

28. Vlaar APJ, Juffermans NP. Transfusion-related acute lung injury: a clinical review. *Lancet*. (2013) 382:984–94. doi: 10.1016/S0140-6736(12)62197-7

29. Moallempour M, Jahr JS, Lim JC, Weeks D, Butch A, Driessen B. Methaemoglobin effects on coagulation: a dose response study with HBOC-200 (Oxyglobin) in an ex vivo thrombelastogram Model. *J Cardiothorac Vasc Anesth*. (2009) 23:41–7. doi: 10.1053/j.jvca.2008.06.006

30. Roghani K, Holtby RJ, Jahr JS. Effects of hemoglobin-based oxygen carriers on blood coagulation. *J Funct Biomater*. (2014) 5:288–95. doi: 10.3390/jfb5040288

31. Schaer DJ, Buehler PW, Alayash AI, Belcher JD, Vercellotti GM. Hemolysis and free hemoglobin revisited: exploring hemoglobin and hemin scavengers as a novel class of therapeutic proteins. *Blood*. (2013) C121:1276–84. doi: 10.1182/blood-2012-11-451229

32. Jahr JS, Varma N. PolyHeme. *IDrugs*. (2004) 7:478–82.

33. Dickert N, Sugarman J. Getting the ethics right regarding research in the emergency setting: lessons from the polyheme study. *Kennedy Institute of Ethics J*. (2007). 17 (2):153-169. Project MUSE. doi: 10.1353/ken.2007.0010

34. Thuillier R, Delpy E, Matillon X, Kaminski J, Kasil A, Soussi D, et al. Preventing acute kidney injury during transplantation: the application of novel oxygen carriers. *Expert Opin Investig Drugs*. (2019) 28:643–57. doi: 10.1080/13543784.2019.1628217

35. Björkholm M, Fagrell B, Przybelski R, Winslow N, Young M, Winslow RM, et al. Phase I single blind clinical trial of a new oxygen transport agent (MP4), human hemoglobin modified with maleimide-activated polyethylene glycol. *Haematologica*. (2005) 90:505–15.

36. Lantieri L, Cholley B, Lemogne C, Guillemain R, Ortonne N, Grimbert P, et al. First human facial retransplantation: 30-month follow-up. *Lancet*. (2020) 396:1758–65. doi: 10.1016/S0140-6736(20)32438-7

37. Fontes P, Lopez R, van der Plaats A, Vodovotz Y, Minervini M, Scott V, et al. Liver preservation with machine perfusion and a newly developed cell-free oxygen carrier solution under subnormothermic conditions. *Am J Transplant*. (2015) 15:381–94. doi: 10.1111/ajt.12991

38. Silverman TA, Weiskopf RB. Hemoglobin-based oxygen carriers: current status and future directions. *Anesthesiology*. (2009) 111:946–63. doi: 10.1097/ALN.0b013e3181ba3c2c

39. Leal-Noval SR, Munoz M, Asuero M, Contreras E, Garcia-Erce JA, Llau JV, et al. Spanish consensus statement on alternatives to allogeneic blood transfusion: the 2013 update of the "seville document". *Blood Transfus*. (2013) 11:585–610. doi: 10.2450/2013.0029-13

40. Goodnough LT, Shander A. Current status of pharmacologic therapies in patient blood management. *Anesth Analg*. (2013) 116:15–34. doi: 10.1213/ANE.0b013e318273f4ae

41. Mackenzie CF, Moon-Massat PF, Shander A, Javidroozi M, Greenburg AG. when blood is not an option: factors affecting survival after the use of a hemoglobin-based oxygen carrier in 54 patients with life-threatening anemia. *Anesth Analg*. (2010) 110:685–93. doi: 10.1213/ANE.0b013e3181cd473b

42. Chang TMS. Blood replacement with nanobiotechnologically engineered hemoglobin and hemoglobin nanocapsules. Interdisciplinary Review. *Nanomedicine Nanobiotechnol*. (2010) 2:418–30. doi: 10.1002/wnan.95

43. Frielich D, Pearce BL, Pitman A, Greenburg G, Berzins M, Bebris L, et al. HBOC-201 Vasoactivity in a phase III clinical trial in orthopedic surgery subjects–extrapolation of potential risk for acute trauma trials. *J Trauma*. (2009) 66:365–76. doi: 10.1097/TA.0b013e3181820d5c

44. Mazer CD, Whitlock RP, Fergusson DA, Hall J, Belley-Cote E, Connolly K, et al. Restrictive or liberal red-cell transfusion for cardiac surgery. *N Engl J Med*. (2017) 377:2133–44. doi: 10.1056/NEJMoa1711818

45. Junco DJ, Holcomb JB. Fox EE, Brasel KJ, Phelan HA, Bulger EM, et al. Resuscitate early with plasma and platelets or balance blood products gradually: findings from the prospective, observational, multicentre, major trauma transfusion (PROMMTT) study. *J Trauma, Acute Care Surgery*. (2013) 75:S24–30. doi: 10.1097/TA.0b013e31828fa3b9

46. Storz JF. REVIEW: Hemoglobin–oxygen affinity in high-altitude vertebrates: is there evidence for an adaptive trend? *J Exp Biolog*. (2016) 219:3190–203 doi: 10.1242/jeb.127134

frontiers | Frontiers in Medical Technology

TYPE Mini Review
PUBLISHED 28 November 2022
DOI 10.3389/fmedt.2022.1068972

OPEN ACCESS

EDITED BY
Thomas Ming Swi Chang,
McGill University, Canada

REVIEWED BY
Jonathan JAHR,
UCLA Health System, United States

*CORRESPONDENCE
Abdu I. Alayash
abdu.alayash@fda.hhs.gov

†This article reflects the views of the author and should not be construed to represent FDA's views or policies.

SPECIALTY SECTION
This article was submitted to Regenerative Technologies, a section of the journal Frontiers in Medical Technology

RECEIVED 13 October 2022
ACCEPTED 31 October 2022
PUBLISHED 28 November 2022

CITATION
Alayash AI (2022) Oxidation reactions of cellular and acellular hemoglobins: Implications for human health.
Front. Med. Technol. 4:1068972.
doi: 10.3389/fmedt.2022.1068972

Oxidation reactions of cellular and acellular hemoglobins: Implications for human health

Abdu I. Alayash*†

Laboratory of Biochemistry and Vascular Biology (LBVB), Center for Biologics Evaluation and Research (CBER), Food and Drug Administration (FDA), Silver Spring, MD, United States

Oxygen reversibly binds to the redox active iron, a transition metal in human Hemoglobin (Hb), which subsequently undergoes oxidation in air. This process is akin to iron rusting in non-biological systems. This results in the formation of non-oxygen carrying methemoglobin (ferric) (Fe^{3+}) and reactive oxygen species (ROS). In circulating red blood cells (RBCs), Hb remains largely in the ferrous functional form (HbF^{2+}) throughout the RBC's lifespan due to the presence of effective enzymatic and non-enzymatic proteins that keep the levels of metHb to a minimum (1%–3%). In biological systems Hb is viewed as a Fenton reagent where oxidative toxicity is attributed to the formation of a highly reactive hydroxyl radical ($OH^{\bullet}$) generated by the reaction between Hb's iron (Fe^{2+}) and hydrogen peroxide (H_2O_2). However, recent research on both cellular and acellular Hbs revealed that the protein engages in enzymatic-like activity when challenged with H_2O_2, resulting in the formation of a highly reactive ferryl heme (Fe^{4+}) that can target other biological molecules before it self-destructs. Accumulating evidence from several *in vitro* and *in vivo* studies are summarized in this review to show that Hb's pseudoperoxidase activity is physiologically more dominant than the Fenton reaction and it plays a pivotal role in the pathophysiology of several blood disorders, storage lesions associated with old blood, and in the toxicity associated with the infusion of Hb-derived oxygen therapeutics.

KEYWORDS

hemoglobin, oxidation, blood substitutes, stored blood, ferryl heme species

Introduction

Oxidation reactions of hemoglobin

The primary function of Hb within the RBC is to transport oxygen from lungs to tissues and to facilitate the removal of carbon dioxide (CO_2) that accumulates in tissues due to active metabolism. The molecule is made up of four subunits: two α and two β (α with 141 amino acids and ß with 146 amino acids). The subunits are packed in pairs forming a tetramer. Each globin chain carries a heme prosthetic group surrounded by hydrophobic amino acids. The $\alpha 1ß2/\alpha 2\beta 1$ interface plays a crucial role in oxygen binding, as oxygen is released through a subunit rearrangement in the tetramer resulting in significant quaternary conformational changes during the binding of oxygen (1).

In biological systems, Hb's iron promotes the generation of ROS which involves a reduction of oxygen (O_2) by one electron, forming superoxide ($O_2^{\bullet -}$). This superoxide ion can be dismutated to yield H_2O_2 that, on subsequent reduction, forms hydroxyl radicals ($OH^{\bullet}$). This form of Hb oxidation is known as the Fenton reaction (2) and can be seen in Equation 1:

$$Fe^{2+} + H_2O_2 \rightarrow Fe^{3+} + OH^{\bullet} + OH^{-} \quad (1)$$

This hypothesis, however, was questioned as it was pointed out more recently that in the case of the Fenton reaction, H_2O_2 reacts directly with the free iron but not with iron that is still part of Hb's prosthetic group (3–5).

In recent years, oxidation reactions of Hb took a center stage as researchers and developers focused on cell-free Hb as a starting material for the manufacture of Hb-based oxygen carrier (HBOC) therapeutics. Proposed alternative pathways describing *in vitro* and *in vivo* Hb oxidation reactions fall into two categories. First, Hb in an oxygenated medium undergoes spontaneous oxidation of its ferrous iron to form the ferric-non oxygen carrying protein. This reaction is referred to as the autoxidation process of Hb and described by Equation 2:

$$HbFe^{2+}O_2 \rightarrow HbFe^{3+} + O^{\bullet -} \quad (2)$$

In this reaction an anion-induced autoxidation of Hb occurs in which nucleophilic anion displacement of molecular oxygen results in an intermediate ferrous heme/anion complex that acts as an electron donor to displaced oxygen (6).

In the presence of small quantities of H_2O_2, or when H_2O_2 is generated enzymatically by systems such as xanthine oxidase or glucose oxidase, Hb enters a vicious redox cycle that generates several damaging oxidative intermediates. This peroxidatic action is often termed as pseudoperoxidase activity. In general, the first product of the reaction of ferrous Hb with H_2O_2 is an oxo ferryl heme (Equation 3). The reaction of the ferric heme with H_2O_2 on the other hand leads to the production of a porphyrin radical cation (the protein radical cation $P^{\bullet +}$ deprotonates to yield the stable electron paramagnetic resonance [EPR] detectable $P^{\bullet}$) that can be damaging to the Hb itself as it migrates to cysteine-93 of the β chain and other "hotspot" amino acid targets (Equation 4) (7).

$$HbFe^{2+} + H_2O_2 \rightarrow HbFe^{4+} = O^{2-} + H_2O \quad (3)$$

$$HbFe^{3+} + H_2O_2 \rightarrow P^{\bullet +}HbFe^{4+} = O^{2-} + H_2O \quad (4)$$

In addition, a covalent heme-to-protein link has been detected by HPLC during the reaction of Hb and H_2O_2. This adduct has been recognized as a valuable biomarker for the peroxidatic activity of myoglobin and Hb (7, 8).

Oxidation reactions of acellular hemoglobin: the case of hemoglobin-based oxygen carriers

HBOCs manufacturing and developments

HBOCs have been developed as oxygen carrying solutions for a variety of clinical applications, most typically as a substitute for allogeneic RBC transfusion in settings where transfusion is indicated, but RBC are unavailable. This includes cases of major hemorrhage, whether traumatic or surgically induced; where compatible blood is unavailable; or where transfusion therapy is refused on religious grounds. Potential benefits include universal compatibility, immediate availability, and long-term storage. However, no HBOCs have been approved by the US FDA as if yet (9). Oxyglobin was approved by US FDA in 1997 for veterinary use only and in 1998 was approved in Europe.

Over the last three decades there has been an intense research and development effort in using acellular Hb as an oxygen carrying therapeutic in transfusion medicine. This led to increasing opportunities for researchers to work on Hb oxidation reactions in this unique and challenging environment, which led to the unraveling of several novel oxidative pathways (10).

HBOCs are derived from outdated human blood or in some cases from animal blood after extensive purification and filtration processes. The cell-free Hb, also known as stroma free Hb is used as a starting material for further processing to ensure the complete removal of RBC proteins and enzymes. In some cases, manufacturers applied further chromatographic procedures to produce a highly purified HbA (known as HbA_0) as starting material for subsequent chemical modifications (11). Chemical modifications have been widely used to generate variable size HBOCs, using polymerizing reagents such as glutaraldehyde and polyethylene glycol which result in inter- and intramolecular crosslinked stabilized tetramers or conjugated/polymerized molecules. These modifications are non-site specific and, in some cases, random modifications of the Hb molecule occur (12).

Genetically modified HBOCs have also been expressed in *E. coli* and have advanced to late-stage clinical trials in the case of some chemically modified Hbs. Because of the potential side effects of free Hb, crosslinking of Hb with antioxidative enzymes and/or encapsulation of the protein inside lipid vesicles with antioxidative enzymes have been investigated as an alternative model system mimicking RBCs (13, 14). Second-generation versions of these vesicles are now under active investigation (15).

Several newly developed third generation HBOCs, such as HEMO2life has recently been approved in Europe for kidney transplant donor perfusion. This is an extracellular Hb derived from see worms and it is a multicomponent molecule carrying

multiheme sites with a large oxygen-binding capacity (16). OxyVita is another newly developed HBOC produced by using a modified zero-linked polymerization process that employs chemical activators to incorporate cross-linked bovine Hb tetramers into "super-polymeric" macromolecules (17).

A first-in-human Phase 1 clinical trial assessing the safety and pharmacokinetics of Hb vesicles (HbV) in healthy male adult volunteers was recently reported from Japan (18). HbV infusion (with half-life of approximately 8 h) was well tolerated and all adverse events observed, including liposome-induced infusion reactions, were spontaneously resolved. Dose escalation studies are planned for a larger number of subjects in a Phase 2 clinical trial.

Because of the proprietary nature of the commercially manufactured HBOCs, it was not until recently that a very comprehensive comparative study of all HBOCs (tested in humans in late clinical trials) was published (19). Generally, HBOCs were found to be variable in their autoxidation rates, oxidative changes, and heme loss kinetics, in large part due to the varied and random nature of chemical modifications. When these HBOCs were challenged with H_2O_2, some underwent oxidative changes that were more exaggerated than others, leading to the accumulation of higher levels of oxidation intermediates (ferryl in particular) compared to the unmodified human or bovine forms (19).

Invitro and *in vivo* cardiovascular effects of HBOCs with a focus on oxidative pathways

Cardiovascular effects were one of the most frequently reported adverse events experienced by human volunteers infused with HBOCs. The development of cardiac lesions after infusion of some HBOCs in several animal models was used to illustrate the potential role of oxidative pathways in development of lesions in the heart. Myocardial lesions following administration of DCLHb in several animal models have been reported (20).

Due to their relatively long circulation time, acellular Hbs are exposed to oxidative changes and metHb accumulation. For example, rapid oxidation of some HBOCs in circulation has been reported reaching levels as high as 40%–60% metHb in humans after transfusion (21).

An isolated rat heart Langendorff perfusion system was recently used to monitor the recovery of left ventricular functions following hypoxic perfusion with ferrous and ferric forms of diaspirin crosslinked human Hb (DCLHb [also known as DBBF] developed by Baxter). Morphological and biochemical changes, including the development of heart lesions, were documented and changes in tissue marker oxidation (i.e., lipid peroxidation and heme oxygenase expression) were also observed. At the subcellular levels, ferric and possibly ferryl Hb induced impairment of mitochondrial function associated with the inhibition of state 3 respiration and cytochrome c oxidase activity as well as changes in the heart tissue proteome. Co-perfusion of hearts with ferrous DCLHb/DBBF and ascorbic acid (Asc) under normoxia led to a sharp decline in cardiac parameters. This trend continued with ferric Hb co-perfusion, but only at the higher concentration of Asc (22).

Hemodynamic changes in humans due to the scavenging of the blood vessel vasodilator nitric oxide (NO) became a serious impediment to the progress and clinical utility of HBOCs (23, 24). NO reacts avidly with infused HBOCs regardless of their molecular sizes or shapes, resulting in blood pressure elevation due to the vasoconstriction of blood vessels. Sodium nitrite ($NaNO_2$) was used as a mechanism to replace scavenged NO. One lesser-known attribute of HBOCs is that they exhibit some nitrite reductase activity; therefore, Hb can become a source of NO in the presence of $NaNO_2$ (24).

In a swine model of liver hemorrhage, Biopure's HBOC-201 was infused with or without concurrent $NaNO_2$ and moderation of vasoconstriction was indeed achieved. However, the highest incidence of adverse events, including pulmonary complications, were also recorded in a dose-dependent fashion (25). In a guinea pig model, known for its inability to synthesize Asc, infusion of nitrite with an HBOC (DCLHb/DBBF) potentiated renal oxidative stress and injury in these animals with large accumulation of metHb (26). Although no attempts were made to look at the ferryl fingerprints, nitrite is known to directly interact with βCys93 which may destabilize Hb (27).

To establish a role for Asc as an effective endogenous reducer of Hb oxidation intermediates, a glutaraldehyde polymerized bovine Hb, Oxyglobin™ (Biopure), was infused to rats and guinea pigs. Rats can endogenously synthesize Asc, but guinea pigs, like humans, lack the enzymatic machinery to produce it. This experiment demonstrated clearly that the ferric HBOC levels were 4-fold greater in the guinea pig compared to the rat. HPLC and mass spectrometric methods also showed oxidative instability of Oxyglobin™ following administration in the guinea pig but not in the rat (28).

To capture ferryl/ferryl radicals or endogenous defenses invoked against them such as plasma Asc, EPR was used in a rabbit model of 20% blood for HBOC (DCLHb/DBBF) exchange transfusion. Rabbits, unlike humans, maintain an effective Asc reducing system in their blood. In these experiments, it was noted that metHb levels in circulation were reduced to oxyHb by a slow process ($t_{1/2}$=1 h), with no globin-bound free radicals found in the plasma of these animals (29). It was noted, however, that endogenous Asc was able to effectively reduce plasma metHb, ferrylHb, and its associated globin radicals. The detection of ascorbyl free radicals by EPR was used to confirm that the intraerythrocytic Asc acted as the electron donor (29, 30).

Another study in humans that confirmed the role of Asc in controlling Hb oxidation involved a Jehovah Witness patient who lost a considerable amount of blood. This patient was

given large doses of Asc after transfusion with the human analog of Oxyglobin, Hemopure, which led to a considerable reduction in this patient's oxidized Hb levels (21). Therefore, in severe anemia or when HBOCs are infused antioxidants, such as ascorbic acid may be indicated as exogenous agents to control methemoglobinemia.

Oxidation reactions of cellular hemoglobin in health and in disease states

Oxidation reactions in Normal red blood cells

RBCs maintain very effective antioxidative enzyme systems that keep Hb in the ferrous functional form in circulation during its lifespan. However, as cells age, oxidation of Hb and oxidative side reactions intensify due to the weakening of these antioxidative defense mechanisms (31). The antioxidative defense enzymes in normal RBCs include superoxide dismutase, catalase, glutathione peroxidase, and glutathione reductase. Other low-molecular-weight antioxidants, such as glutathione, and vitamins E and C are also known to contribute to the overall control of Hb oxidation within cells. RBCs also maintain a plasma membrane redox system that transfers electrons from intracellular substrates to extracellular electron acceptors, which may be NAD+or vitamin C (32). Therefore, RBCs are uniquely designed to transport oxygen as well as providing enzymatic mechanisms to maintain Hb in a functional nontoxic state (33).

Band 3 and its associated proteins are an integral part of the RBC membrane and are responsible for maintaining acid balance, ion distribution (Cl^- and $HCO3^-$) across the RBC membrane exchange, and cell shape integrity and durability (34). More recently a role for band 3 in the overall maintenance of the redox balance in RBCs has been identified (see below).

Pathophysiology of oxidation reactions and the detection of ferryl hemoglobin *in vivo*

Recent experiments from our laboratory on blood from transgenic sickle cell disease (SCD) mice and from patients with SCD showed that Hb's higher oxidation state, ferrylHb, interacts directly with band 3 resulting in oxidative modifications of the band 3 network of proteins (35, 36). These experiments also confirmed that Hb mediated oxidation of band 3 triggers band 3 clustering and microparticle (MP) formation and release from mother cells. MPs are miniature RBCs containing almost all the elements of mature RBCs, including Hb (for review, see 37).

Photometric and proteomic analyses of the MP content from a Townes-sickle cell mice model showed the presence of considerable levels of Hb oxidation intermediates (ferric/ferryl). Moreover, it was also shown by mass spectrometry in these experiments that the degree of β-globin post-translational modifications (PTMs) in Hb within MPs, including irreversible oxidation of βCys93 and the ubiquitination of βLys96 and βLys145 (35), was very evident. A definitive follow-up experiment also revealed that ferryl Hb, but not hemichromes, was found to induce the complex formation with band 3 and RBC membrane proteins, consistent with early *in vitro* reports (38). When MPs obtained from Townes-SS mice that were fed a diet rich in hydroxyurea (HU), fewer PTM modifications were found on the Hb. *In vitro*, HU (an NO producing molecule) reduced the levels of ferryl Hb and shielded its target residue, βCys93, by a process of S-nitrosylation (35).

In a follow up clinical investigation using MPs from blood of SCD patients who were either on or off HU treatment was carried out recently (36). Proteomic analysis showed that band 3 and its interaction network were involved in MP formation. Samples from SS patients exhibited more extensive protein phosphorylation and ubiquitination in SCD patients than in samples from ethnic matched controls. Samples from patients who were treated with HU showed little or no oxidative PTMs like those samples from the control group (36).

Several studies in recent years focused on detecting the short-lived ferryl and its radical in human blood/tissues and animal models. An EPR study (39) detected a protein based radical at $\sim$1 μM concentration in human venous blood samples. This radical was identical in line-shape and power saturation characteristics to that generated from *in vitro* experiments through the reaction of ferric Hb with H_2O_2. In addition, characteristic EPR protein radical signal was detected, representing oxidative damage to the heme and by implication the oxoferryl species. Similar ferryl mediated-protein-heme modifications were reported in acute kidney dysfunction following rhabdomyolysis (8) and in cerebral spinal fluid following subarachnoid hemorrhage (40). Oxidized Hb intermediates and cross-linked globin chains were confirmed by another group using LC-MS/MS in atherosclerotic lesions of the human carotid artery and hemorrhagic cerebrospinal fluid from preterm infants (41). In a follow-up study, the same group used specific monoclonal anti-ferrylHb antibody and found that ferrylHb was localized extracellularly and internalized by macrophages in the human hemorrhagic complicated lesions (42).

Hb's pseudoperoxidase activity is best illustrated in sickle cell disease, a biologically more relevant model system for the investigation of Hb oxidation reactions in humans and animals. Sickle cell Hb (HbS) oxidizes faster and its ferryl persists longer in solutions than ferryl HbA (43). *In vivo* verification of the ferryl heme was therefore achievable. One of the early reports on the persistence of ferrylHb in SS RBCs infected with malarial parasites found that ferryl Hb inhibited actin

polymerization in RBCs-infected malaria, thereby preventing the malarial parasites from creating their own actin cytoskeleton within the host cell cytoplasm (44, 45). This also shed some light on the question of how HbS provides protection against malarial parasitic infection in SCD (46).

Pseudoperoxidative activity of Hb and its potential impact on the integrity and long-term stability of blood stored in cold temperatures for 42 days was recently discussed (47). These reactions are collectively known as "oxidative lesion" which may impact clinical outcomes associated with the use of stored blood or pathogen inactivated blood for therapeutic purposes (47).

Under standard storage conditions, Hb oxidation is seen due to a decrease in its antioxidant capacity. This results in the oxidation and deterioration of membrane lipids and proteins, which can ultimately lead to irreversible damage to the membrane.

Most used commercial methods for pathogen reduction and/or inactivation processes are largely based on exposing major blood components (RBCs, platelets, and plasma) to UV light and photosensitizer molecules. UV light radiation of blood contained in plastic bags may lead to the deterioration of RBCs (48). The participation of ROS may drive some of the observed biochemical changes that included cytosolic proteins (including Hb) and lipid proteins (49). Although very little experimental evidence is available that points to the involvement of Hb's pseudoperoxidase activity, storage conditions or inactivation processes under some circumstances may favor these reactions.

Summary and conclusion

Under oxidative stress conditions, the redox active protein Hb triggers a pseudoenzymatic cycle within RBCs. Outside the RBCs, such as in the case of Hb-based oxygen therapeutics or hemolytic conditions, this effect is amplified. The byproduct of this reaction and most active intermediate, ferryl Hb, has been detected in several *ex-vivo* and *in vivo* model systems, in atherosclerotic lesions of carotid arteries, in blood from mice and SCD patients, and in blood from SCD patients infected with malaria. Unique cellular, and in some instances subcellular, injuries have been attributed to the ferryl Hb's redox reactivity. These reactions are also suspected to be responsible for the oxidation lesions associated with stored blood or pathogen-inactived blood. The knowledge gained in the understanding of the underlying mechanisms of Hb oxidative pathways led to the rational design of several protective intervention strategies that will hopefully augment the safe use of blood for therapeutic purposes.

Author contributions

AIA is the sole author and approved the submitted version.

Funding

Internal FDA funding.

Acknowledgments

The author wishes to thank members of his laboratory at CBER/FDA for their contributions to this work and Matthew Williams for reading the manuscript.

Conflict of interest

The authors declare that the research was conducted in the absence of any commercial or financial relationships that could be construed as a potential conflict of interest.

Publisher's note

References

1. Dickerson RE, Gies I. *Hemoglobin: Structure, function, evolution, and pathology*. California: Benjamin/Cummings Publishing Company (1983).

2. Bystrom LM, Rivella S. Cancer cells with irons in the fire. *Free Radic Biol Med*. (2015) 79:337–42. doi: 10.1016/j.freeradbiomed.2014.04.035

3. Van Dyke BR, Saltman P. Hemoglobin: a mechanism for the generation of hydroxyl radicals. *Free Radic Biol Med*. (1996) 20:985–9. doi: 10.1016/0891-5849(95)02186-8

4. Puppo A, Halliwell B. Formation of hydroxyl radicals from hydrogen peroxide in the presence of iron. Is haemoglobin a biological fenton reagent? *Biochem J*. (1988) 249:185–90. doi: 10.1042/bj2490185

5. Gutterige JM. Iron promoters of the fenton reaction and lipid peroxidation can be released from haemoglobin by peroxides. *FEBS Lett*. (1986) 201:291–5. doi: 10.1016/0014-5793(86)80626-3

6. Balagopalakrishna C, Manoharan PT, Abugo O, Rifkind JM. Production of superoxide from hemoglobin-bound oxygen under hypoxic conditions. *Biochemistry* (1996) 35: 6393–8. doi: 10.1021/bi952875+

7. Jia Y, Buehler PW, Boykins RA, Venable RM, Alayash AI. Structural basis of peroxide-mediated changes in human hemoglobin: a novel oxidative pathway. *J Biol Chem*. (2007) 282:4894–907. doi: 10.1074/jbc.M609955200

8. Wilson MT, Reeder BJ. The peroxidatic activities of myoglobin and hemoglobin. Their pathological consequences and possible medical interventions. *Mol Asp Med*. (2022) 84:101045. doi: 10.1016/j.mam.2021.101045

9. Silverman TA, Weiskopf RB. Hemoglobin-based oxygen carriers: current status and future directions. *Transfusion*. (2009) 49:2495–515. doi: 10.1111/j.1537-2995.2009.02356.x

10. Alayash AI. Oxygen therapeutics: can we tame haemoglobin? *Nat Rev Drug Discov*. (2004) 3:152–9. doi: 10.1038/nrd1307

11. Privalle C, Talarico T, Keng T, DeAngelo J. Pyridoxalated hemoglobin polyoxyethylene: a nitric oxide scavenger with antioxidant activity for the treatment of nitric oxide-induced shock. *Free Radic Biol Med*. (2000) 28:1507–17. doi: 10.1016/S0891-5849(00)00260-4

12. Alayash AI. Mechanisms of toxicity and modulation of hemoglobin-based oxygen carriers. *Shock*. (2019) 52:41–9. doi: 10.1097/SHK.0000000000001044

13. D'Agnillo F, Chang TM. Polyhemoglobin-superoxide dismutase-catalase as a blood substitute with antioxidant properties. *Nat Biotechnol*. (1998) 16:667–71. doi: 10.1038/nbt0798-667

14. Sakai H, Kobayashi N, Kure T, Okuda C. Translational research of hemoglobin vesicles as a transfusion alternative. *Curr Med Chem*. (2022) 29:591–606. doi: 10.2174/0929867328666210412130035

15. Azuma H, Fujihara M, Sakai H. Biocompatibility of HbV: liposome-encapsulated hemoglobin molecules-liposome effects on immune function. *Funct Biomater*. (2017) 8(3):24. doi: 10.3390/jfb8030024

16. Le Meur Y, Badet L, Essig M, Thierry A, Büchler M, Drouin S. First-in-human use of a marine oxygen carrier (M101) for organ preservation: a safety and proof-of-principle study. *Am J Transplant*. (2020) 20:1729–38. doi: 10.1111/ajt.15798

17. Wollocko H, Wollocko BM, Wollocko J, Grzegorzewski W, Smyk L. Oxyvita®C, a next-generation haemoglobin-based oxygen carrier, with coagulation capacity (OVCCC). modified lyophilization/spray-drying process: proteins protection artif. *Cells Nanomed Biotechnol*. (2017) 45:1350–5. doi: 10.1080/21691401.2017.1339052

18. Azuma H, Amano T, Kamiyama N, Takehara N, Jingu M, Takagi H, et al. First-in-human phase 1 trial of artificial red blood cells and hemoglobin vesicles developed as a transfusion alternative. *Blood Adv*. (2022) 6(21):5711–5. doi: 10.1182/bloodadvances.2022007977

19. Meng F, Kassa T, Jana S, Wood F, Zhang X, Jia Y, et al. Comprehensive biochemical and biophysical characterization of hemoglobin-based oxygen carrier therapeutics: all HBOCs are not created equally. *Bioconjug Chem*. (2018) 29:1560–75. doi: 10.1021/acs.bioconjchem.8b00093

20. Estep TN. Issues in the development of hemoglobin-based oxygen carriers. *Semin Hematol*. (2019) 56(4):257–61. doi: 10.1053/j.seminhematol.2019.11.006

21. Fitzgerald MC, Chan JY, Ross AW, Liew SM, Butt WW, Baguley D, et al. A synthetic haemoglobin-based oxygen carrier and the reversal of cardiac hypoxia secondary to severe anaemia following trauma. *Med J Aust*. (2011) 194:471–3. doi: 10.5694/j.1326-5377.2011.tb03064.x

22. Edmondson M, Jana S, Meng F, Strader MB, Baek JH, Gao Y, et al. Redox states of hemoglobin determine left ventricle pressure recovery and activity of mitochondrial complex IV in hypoxic rat hearts. *Free Radic Biol Med*. (2019) 141:348–61. doi: 10.1016/j.freeradbiomed.2019.07.008

23. Olson JS, Foley EW, Rogge C, Tsai AL, Doyle MP, Lemon DD. NO Scavenging and the hypertensive effect of hemoglobin-based blood substitutes. *Free Radic Biol Med*. (2004) 36:685–97. doi: 10.1016/j.freeradbiomed.2003.11.030

24. Kim-Shapiro DB, Gladwin MT. Mechanisms of nitrite bioactivation. *Nitric Oxide*. (2014) 38:58–68. doi: 10.1016/j.niox.2013.11.002

25. Moon-Massat P, Scultetus A, Arnaud F, Brown A, Haque A, Saha B, et al. Effect of HBOC-201 and sodium nitrite resuscitation after uncontrolled haemorrhagic shock in swine. *Injury*. (2012) 43:638–47. doi: 10.1016/j.injury.2010.10.013

26. Baek JH, Zhang X, Williams MC, Hicks W, Buehler PW, D'Agnillo F. Sodium nitrite potentiates renal oxidative stress and injury in hemoglobin exposed Guinea pigs. *Toxicol*. (2015) 333:89–99. doi: 10.1016/j.tox.2015.04.007

27. Mansouri A. Non-equivalent behavior of alpha and beta subunits in methemoglobin reduction. *Biochim Biophys Acta*. (1979) 579:191–9. doi: 10.1016/0005-2795(79)90098-9

28. Buehler PW, D'Agnillo F, Hoffman V, Alayash AI. Effects of endogenous ascorbate on oxidation, oxygenation, and toxicokinetics of cell-free modified hemoglobin after exchange transfusion in rat and Guinea pig. *J Pharmacol Exp Ther*. (2007) 323:49–60. doi: 10.1124/jpet.107.126409

29. Dunne J, Caron A, Menu P, Alayash AI, Buehler PW, Wilson MT, et al. Ascorbate removes key precursors to oxidative damage by cell-free haemoglobin in vitro and in vivo. *Biochem J*. (2006) 399:513–24. doi: 10.1042/BJ20060341

30. Sibmooh N, Piknova B, Rizzatti F, Schechter AN. Oxidation of iron-nitrosyl-hemoglobin by dehydroascorbic acid releases nitric oxide to form nitrite in human erythrocytes. *Biochemistry*. (2008) 47:2989–96. doi: 10.1021/bi702158d

31. Nagababu E, Chrest EF, Rifkind JM. Hydrogen-peroxide-induced heme degradation in red blood cells: the protective roles of catalase and glutathione peroxidase. *Biochem Biophys Acta*. (2003) 1620:211–7. doi: 10.1016/S0304-4165(02)00537-8

32. Buehler PW, Alayash AI. Redox biology of blood revisited: the role of red blood cells in maintaining circulatory reductive capacity. *Antioxid Redox Signal*. (2003) 7:1755–60. doi: 10.1089/ars.2005.7.1755

33. Rizvi SI, Jha R, Maurya PK. Erythrocyte plasma membrane redox system in human aging. *Rejuvenation Res*. (2006) 9:470–4744. doi: 10.1089/rej.2006.9.470

34. Jay DG. Role of band 3 in homeostasis and cell shape. *Cell*. (1996) 86:853–4. doi: 10.1016/S0092-8674(00)80160-9

35. Jana S, Strader MB, Meng F, Hicks W, Kassa T, Tarandovskiy I, et al. Hemoglobin oxidation–dependent reactions promote interactions with band 3 and oxidative changes in sickle cell–derived microparticles. *J Clinic Investig Insight*. (2018) 3(21):e120451. doi: https://doi.org/10.1172/jci.insight.120451

36. Strader MB, Jana S, Meng F, Heaven MR, Shet AS, Thein S L, et al. Post-translational modification as a response to cellular stress induced by hemoglobin oxidation in sickle cell disease. *Sci Rep*. (2020) 10(1):14218. doi: 10.1038/s41598-020-71096-6

37. Georgatzatou HT, Fortis SP, Papageorgiou EG, Antonelou MH, Kriebardis AG. Blood cell-derived microvesicles in hematological diseases and beyond. *Biomolecules*. (2022) 12(6):803. doi: 10.3390/biom12060803

38. Welbourn EM, Wilson MT, Yusof A, Metodiev MV, Cooper CE. The mechanism of formation, structure, and physiological relevance of covalent hemoglobin attachment to the erythrocyte membrane. *Free Radic Biol Med*. (2017) 103:95–106. doi: 10.1016/j.freeradbiomed.2016.12.024

39. Svistunenko DA, Patel RP, Voloshchenko SV, Wilson MT. The globin-based free radical of ferryl hemoglobin is detected in Normal human blood. *J Biol Chem*. (1997) 272:7114–21. doi: 10.1074/jbc.272.11.7114

40. Reeder BJ, Sharpe MA, Kay AD, Kerr M, Moore K, Wilson MT. Toxicity of myoglobin and haemoglobin: oxidative stress in patients with rhabdomyolysis and subarachnoid haemorrhage. *Biochem Soc Trans*. (2002) 30:745–8. doi: 10.1042/bst0300745

41. Posta N, Csősz E, Oros M, Pethő D, Potor L, Kalló K, et al. Hemoglobin oxidation generates globin-derived peptides in atherosclerotic lesions and intraventricular hemorrhage of the brain, provoking endothelial dysfunction. *Lab Investig*. (2020) 100:986–1002. doi: 10.1038/s41374-020-0403-x

42. Potor L, Hendrik Z, Patsalos A, Katona E, Méhes G, Póliska S, et al. Oxidation of hemoglobin drives a proatherogenic polarization of macrophages in human atherosclerosis. *Antioxid Redox Signal*. (2021) 35:917–50. doi: 10.1089/ars.2020.8234

43. Kassa T, Jana S, Strader MB, Meng F, Jia Y, Wilson MT, et al. Sickle cell hemoglobin in the ferryl state promotes βCys-93 oxidation and mitochondrial dysfunction in epithelial lung cells (E10). *J Biol Chem*. (2015) 290 (46):27939–58. doi: 10.1074/jbc.M115.651257

44. Cyrklaff M, Sanchez CP, Kilian N, Bisseye C, Simpore J, Frischknecht F, et al. Hemoglobins S and C interfere with actin remodeling in plasmodium falciparum-infected erythrocytes. *Science*. (2011) 334:1283–6. doi: 10.1126/science.1213775

45. Alayash AI. Oxidative pathways in the sickle cell and beyond. *Blood Cells Mol Dis*. (2018) 70:78–86. doi: 10.1016/j.bcmd.2017.05.009

46. Band G, Leffler EM, Jallow M, Sisay-Joof F, Ndila CM, Macharia AW, et al. Malaria protection due to sickle haemoglobin depends on parasite genotype. *Nature*. (2022) 602:106–11. doi: 10.1038/s41586-021-04288-3

47. Alayash AI. Hemoglobin oxidation reactions in stored blood. *Antioxidants (Basel)*. (2022) 11(4):747. doi: 10.3390/antiox11040747

48. Remigante A, Morabito R, Marino A. Band 3 protein function and oxidative stress in erythrocytes. *J Cell Physiol*. (2021) 236:6225–34. doi: 10.1002/jcp.30322

49. Seghatchian J, Putter JS. Pathogen inactivation of whole blood and red cell components: an overview of concept, design, developments, criteria of acceptability and storage lesion. *Transfus Apher Sci*. (2013) 49:357–63. doi: 10.1016/j.transci.2013.07.023

frontiers | Frontiers in Bioengineering and Biotechnology

TYPE Original Research
PUBLISHED 01 December 2022
DOI 10.3389/fbioe.2022.1072950

OPEN ACCESS

EDITED BY
Thomas Ming Swi Chang,
McGill University, Canada

REVIEWED BY
Lian Zhao,
Academy of Military Medical Sciences (AMMS), China
Serena Del Turco,
National Research Council (CNR), Italy
Binglan Yu,
Massachusetts General Hospital and Harvard Medical School, United States

*CORRESPONDENCE
Hongli Zhu,
zhuyjw1971@nwu.edu.cn

†These authors have contributed equally to this work and share first authorship

SPECIALTY SECTION
This article was submitted to Tissue Engineering and Regenerative Medicine, a section of the journal Frontiers in Bioengineering and Biotechnology

RECEIVED 18 October 2022
ACCEPTED 22 November 2022
PUBLISHED 01 December 2022

CITATION
Li B, Zhang J, Shen C, Zong T, Zhao C, Zhao Y, Lu Y, Sun S and Zhu H (2022), Application of polymerized porcine hemoglobin in the *ex vivo* normothermic machine perfusion of rat livers.
Front. Bioeng. Biotechnol. 10:1072950.
doi: 10.3389/fbioe.2022.1072950

Application of polymerized porcine hemoglobin in the *ex vivo* normothermic machine perfusion of rat livers

Bin Li[1,2,3†], Jie Zhang[1†], Chuanyan Shen[1†], Tingting Zong[1], Cong Zhao[1], Yumin Zhao[1], Yunhua Lu[1], Siyue Sun[1] and Hongli Zhu[1,2,3*]

[1]The College of Life Sciences, Northwest University, Xi'an, Shaanxi, China, [2]National Engineering Research Center for Miniaturized Detection Systems, Northwest University, Xi'an, China, [3]Key Laboratory of Resource Biology and Biotechnology in Western China, Ministry of Education, School of Medicine, Northwest University, Xi'an, China

Background: In contrast to traditional static cold preservation of donor livers, normothermic machine perfusion (NMP) may reduce preservation injury, improve graft viability and potentially allows *ex vivo* assessment of graft viability before transplantation. The polymerized porcine hemoglobin is a kind of hemoglobin oxygen carrier prepared by crosslinking porcine hemoglobin by glutaraldehyde to form a polymer. The pPolyHb has been proved to have the ability of transporting oxygen which could repair the organ ischemia-reperfusion injury in rats.

Objective: In order to evaluate the effectiveness of rat liver perfusion *in vitro* based on pPolyHb, we established the NMP system, optimized the perfusate basic formula and explored the optimal proportion of pPolyHb and basal perfusate.

Methods: The liver was removed and perfused for 6 h at 37°C. We compared the efficacy of liver perfusion with different ratios of pPolyHb. Subsequently, compared the perfusion effect using Krebs Henseleit solution and pPolyHb perfusate of the optimal proportion, and compared with the liver preserved with UW solution. At 0 h, 1 h, 3 h and 6 h after perfusion, appropriate samples were collected for blood gas analysis and liver injury indexes detection. Some tissue samples were collected for H&E staining and TUNEL staining to observe the morphology and detect the apoptosis rate of liver cells. And we used Western Blot test to detect the expression of Bcl-2 and Bax in the tissues.

Results: According to the final results, the optimal addition ratio of pPolyHb was 24%. By comparing the values of Bcl-2/Bax, the apoptosis rate of pPolyHb group was significantly reduced. Under this ratio, the results of H&E staining and TUNEL staining showed that the liver morphology was well preserved without additional signs of hepatocyte ischemia, biliary tract injury, or hepatic sinusoid injury, and hepatocyte apoptosis was relatively mild.

Conclusion: Through the above-mentioned study we show that within 6 h of perfusion based on pPolyHb, liver physiological and biochemical activities may

essentially be maintained *in vitro*. This study demonstrates that a pPolyHb-based perfusate is feasible for NMP of rat livers. This opens up a prospect for further research on NMP.

KEYWORDS

organ preservation, liver transplantation, normothermic mechanical perfusion, pPolyHb, liver injury indexs

Introduction

Liver transplantation is the primary form of therapy for end-stage liver disease. The success rate and long-term survival rate of liver transplantation have significantly increased thanks to improvements in surgical technique, perioperative care, and the use of immunosuppressants. Although liver transplantation has successfully resolved the therapeutic conundrum for patients with liver illnesses, it has also brought new issues, such as the limited availability of transplantation owing to a shortage of organ donors. The number of people who require liver transplantation is far higher than the number of eligible liver donors, despite the fact that treatments for liver disorders are continually being improved. The increased use of extended standard donors has been encouraged by the demand for liver transplantation donors (Tullius and Rabb, 2018). The use of extended standard donors for liver transplantation, however, increases the risk of postoperative problems, such as early allograft dysfunction (EAD), primary non-functionality, or severe chronic sequelae. The liver from both donation after brain death (DBD)and donation after cardiac death (DCD) donors may sustain long-term thermal ischemia damage or a hypotension attack (Vogel et al., 2012). The optimization study on some marginal liver donors and elderly liver donors has also been more in-depth in recent years.

The most used technique for *in vitro* organ preservation in clinical practice is static cold storage (SCS) (Jing et al., 2018). The absence of metabolic substrates and the buildup of metabolites would nonetheless harm the donor liver since the low temperature (0–4°C) environment slows down but does not entirely cease organ metabolism (Clavien et al., 1992; Jaeschke, 1998). Normothermic machine perfusion of liver (NMP-L) is a technique for preserving the graft under near-physiological conditions (Vogel et al., 2017). The liver is quickly stripped out by vascular cannulation and removal of excess tissue, it is then connected to a heparinized circuit filled with warm, oxygenated blood and supplied with nutrients. Compared with static cold storage at low temperature, this technology is more in line with physiological characteristics. In contrast to SCS, Normothermic machine perfusion (NMP) is dynamic and it provides a continuous supply of oxygen and other metabolic precursors at physiological temperature. Liver transplantation studies in pigs have shown that NMP-preserved grafts, including those with significant warm ischemia injury before transplantation, which with good post-reperfusion function and survival compared with grafts preserved with SCS (Schön et al., 2001; Brockmann et al., 2009; Fondevila et al., 2011). In human clinical studies, NMP has been shown to lead to glycogen recruitment, which stores graft energy (Mergental et al., 2016). Given that the liver is fully metabolically active, NMP also provides the best opportunity to assess graft viability prior to reperfusion *in vivo* (Perk et al., 2011). The perfusate used for liver NMP usually consists of crystalline or colloidal solutions, oxygen carriers, calcium, broad-spectrum antibiotics, insulin, and heparin (Butler et al., 2002; op den Dries et al., 2013; Vogel et al., 2017; Liu et al., 2018). Depending on the duration of perfusion, metabolic substrates, including glucose or parenteral nutrition, trace elements and vitamins, may also be added. Given the high metabolic demands at 35–37°C, NMP requires the use of oxygenators and the addition of oxygen transporters to the perfusate to use sufficient oxygen carriers to deliver oxygen throughout the organs during perfusion. Red blood cell (RBC) is the most commonly used oxygen carrier for NMP in clinical practice, but it is easy to cause hemolysis due to red blood cell rupture during perfusion (Laing et al., 2017). Currently, hemoglobin-based cell-free solutions are also used for hepatic NMP (Fontes et al., 2015; Laing et al., 2017). In addition, non-cellular hemoglobin oxygen carriers such as HBOC-201 (Hemopure, HbO_2 Therapeutics LCC, Souderton, Pennsylvania, USA) can provide oxygen dissociation properties similar to those of red cell hemoglobin, allowing the use of NMP without changing the perfusate (de Vries et al., 2019).

Hemoglobin-based oxygen carriers (HBOCs) may now be mechanically perfused *in vitro* at room temperature, according to research. Using HBOCs to preserve organs *in vitro* may have the following potential advantages: effective preservation of cell metabolism and reduction of hypoxia-induced damage, the diameter is significantly smaller than that of red blood cells to more effectively carry oxygen, without immunological response, lengthy storage time and good stability, broad tolerance for temperature, readily available from a variety of sources (Cao et al., 2021). In this study, polymerized porcine hemoglobin (pPolyHb) was used as the oxygen carrier during NMP perfusion. Pig hemoglobin (pHb), which serves as the raw material, is chemically changed to form a novel type of polymeric hemoglobin oxygen carrier called polymerized porcine hemoglobin (pPolyHb) (Zhang et al., 2012). pPolyHb possesses the usual properties of

HBOCs.Furthermore, the raw material pHb is extremely similar to human hemoglobin (hHb), has abundant resources (Zhu et al., 2011a). In the previous study, our laboratory conducted systemic exchange transfusion and emergency transfusion of hemorrhagic shock animals. From the aspects of hemodynamics, acid-base balance metabolism, and oxygen delivery, pPolyHb has good capacity of expansion, oxygen carrying and release, and can be used for normal tissue perfusion and hemodynamic stability in experimental animals, reaching the standard of replacing red blood cells. In this study, we constructed a normothermic machine perfusion system for isolated rat liver, designed the perfusate based on pPolyHb which as oxygen carrier for the first time, in order to explored the optimal proportion of pPolyHb in the perfusate as oxygen carrier, and evaluated its effectiveness in the perfusion of isolated rat liver, thereby demonstrating the utility of liver preservation.

Materials

Animals

Male Sprague-Dawley rats weighing 240 ± 20 g were used in the study (n = 42). The animals were kept in standard temperature conditions (22 ± 1°C), relative humidity of 55%–58%, 12 h/12 h light and dark cycle, with free access to food and water. The experiments described in this study were performed in accordance with the guidelines of the National Institutes of Health on the use of experimental animals. Approval of the Animal Care Committee of Northwest University was obtained prior to initiating the experiments.

Solution used in the experiment

pPolyHb: 10.5 ± 0.5 g/dl pPolyHb, methemoglobin <5%, endotoxin <1.0 EU/mL, osmolality 300–330 mOsm, pH 7.4 ± 0.05, average molecular weight of pPolyHb 600 ± 50 kDa, 64 kDa tetramer <2%. Prepared in buffers composed of Na^+ 135–155 mmol/L, K^+ 3.0–5.0 mmol/L, Ca^{2+}1–3 mmol/L, and Cl^- 140–160 mmol/L, and stored in nitrogen at 4°C until use (Zhu et al., 2011b). Briefly, hemoglobin from fresh porcine blood was purified through specific steps, and then cross-linked by glutaraldehyde. Small molecules, including excess glutaraldehyde and tetramer-hemoglobin, were removed by ultrafiltration. Additional details regarding pPolyHb are currently being withheld because of pending patents. The P50 of pPolyHb is 20–28 mmHg.

Basal perfusate: Hydroxyethyl starch, 0.9% NaCl injection, $MgSO_4$, $CaCl_2$, KH_2PO_4, $NaHCO_3$, Compound Amino Acid Injection, Glucose, Insulin, L-glutamine, Penicillin, Dexamethasone, Heparin.

Krebs-Henseleit solution: Potassium 5 mmol/L, Sodium 150 mmol/L, Calcium 2 mmol/L, Magnesium 1.2 mmol/L, Chloride 131 mmol/L, Phosphate 1.25 mmol/L, Sulfate 1.2 mmol/L, Glucose 10 mmol/L, Osmolality 312 mOsm/L (Chien et al., 2000).

UW solution: Potassium 125 mmol/L, Sodium 30 mmol/L, Magnesium 5 mmol/L, Phosphate 25 mmol/L, Sulfate 5 mmol/L, Glutathione 3 mmol/L, Adenosine 5 mmol/L, Lactobionate 100 mmol/L, Raffinose 30 mmol/L, Allopurino l1 mmol/L, Dexamethasone 20.3 mmol/L, Hydroxyethyl starch 5 g/dl, Insulin 40 U/L, Osmolality 320 mOsm/L (Chien et al., 2000).

Perfusion system

The NMP device includes: blood transfusion pump, thermostatic water bath, small animal membrane oxygenator, filter, infusion connecting pipe, three-way valve, oxygen cylinder, flow pressure sensor (Figure 1).

Methods

Surgical procedures

The rats fasted 12 h before the experiment and could not refrain from water. Before laparotomy, the rats were weighed and anesthetized (2% pentobarbital sodium, 40 mg/kg for rat), and then fixed to the bench in supine position. Using scissors along the xiphoid process to the pubic bone opening in the midline, from the bladder above the incision to the left and right sides of the oblique upward until below the ribs, fixed, the abdominal cavity is fully exposed to view. A sterile and moist cotton swab was used to push the stomach, intestines and other organs or tissues of the rat to one side of the gauze, so that the liver was not covered and completely exposed to the field of vision. Sutures were applied to the proximal and distal ends of the inferior vena cava respectively and were treated during intubation. Renal vein and adrenal vein were layed, hepatic artery spare ring was layed, portal vein left and right branches were layed, and portal vein above the spare ring was layed. Ligate the distal hepatic end of the portal vein, intubate and fix it above the ligature. The hepatic artery and distal hepatic end of inferior vena cava were ligated, and the vessels above the distal hepatic end were cut. The liver was rinsed with a portal vein cannula. After rinsing, the inferior vena cava was lapped near the liver. Cut the septum and the ribs of the rat, and ligate the proximal end of the superior vena cava. A ring was inserted at the distal end, and an opening was made above it to intubate and fix it. Heparin was injected again through the portal vein to flush the liver, and the blood was drained through the superior vena cava. When the color gradually faded, the liver was removed and rinsed with normal saline, followed by immediate perfusion or preservation.

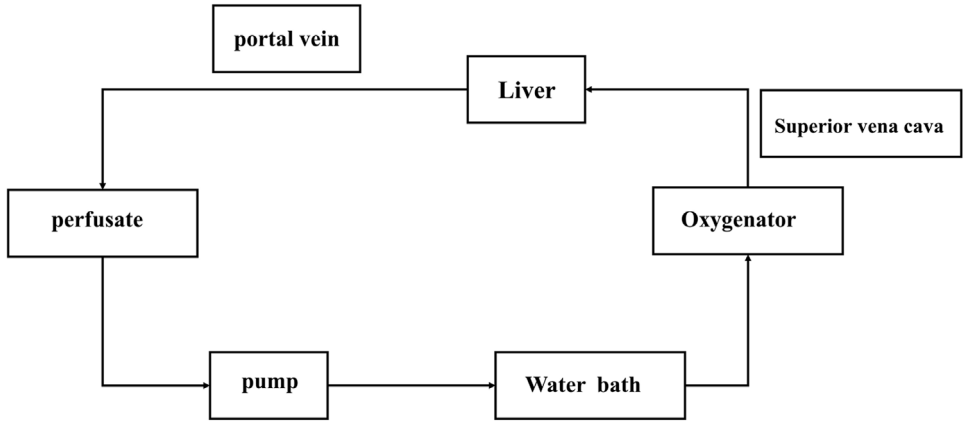

FIGURE 1
Normothermic machine perfusion system. The pump is the main switch of the system. After the corresponding parameters are set, the filling liquid starts to flow. After the perfusate flows through the pump (if has bubbles, they will be displayed here, and the perfusion will be stopped immediately), it will connect to the blood inlet end of the oxygenator, the bleeding end will be connected to the portal vein of the liver, and the perfusate will flow back to the infusion bottle from the superior vena cava end of the liver after flowing through the liver.

Experimental groups

SD rats were randomized ($n = 6$) and the livers were perfused or preserved with the following solution.

Experiment 1. To explore the optimal addition ratio of pPolyHb in perfusion solution (37°C)

Group 1: Basal perfusate.
Group 2: 12% pPolyHb + basal perfusate.
Group 3: 24% pPolyHb + basal perfusate.
Group 4: 36% pPolyHb + basal perfusate.

Experiment 2. Evaluation of the effectiveness of the infusion solution with the best proportion of pPolyHb

Group 1: 24% pPolyHb + basal perfusate (37°C).
Group 2: Krebs Henseleit perfusate (37°C).
Group 3: UW solution (4°C).

NMP process and sample collection

Open the water bath for heating in advance, set the temperature at 37°C, and input the gas composition as 95% O_2 + 5% CO_2. The liver is connected to the perfusion system and then open the transfusion pump and oxygenator. The perfusate flows into the liver through the superior vena cava and exits through the portal vein then circulates. After the beginning of perfusion, the perfusion fluid samples were collected from the portal vein at 0 h, 1 h, 3 h and 6 h, respectively.

UW solution storage and sample collection

After liver removal, it was stored in UW solution at 4°C, and samples of the preservation solution were collected at 0 h, 1 h, 3 h, and 6 h.

Assessment of liver function and injury

Detect the liver injury indicators alanine aminotransferase (ALT), aspartate aminotransferase (AST), lactate dehydrogenase (LDH), malonaldehyde (MDA)and monitor the changes of pH, pO2, pCO2, blood glucose (Glu), lactic acid (Lac) and other physiological indicators in real time. The pathological sections were stained with H&E staining and TUNEL staining to observe the morphological changes of liver tissue and the number of hepatocyte apoptosis. The expression of apoptosis protein Bcl-2 and Bax was detected by Western Blot.

Statistical analysis

Data were statistically analyzed and plotted using Graphpad Prism 8.0. Each experimental group was repeated more than three times, statistical differences between groups were determined using One-Way ANOVA, and data were reported as mean ± SD. A p value less than 0.05 was considered statistically significant. Western Blot analysis detection data were analyzed using image J.

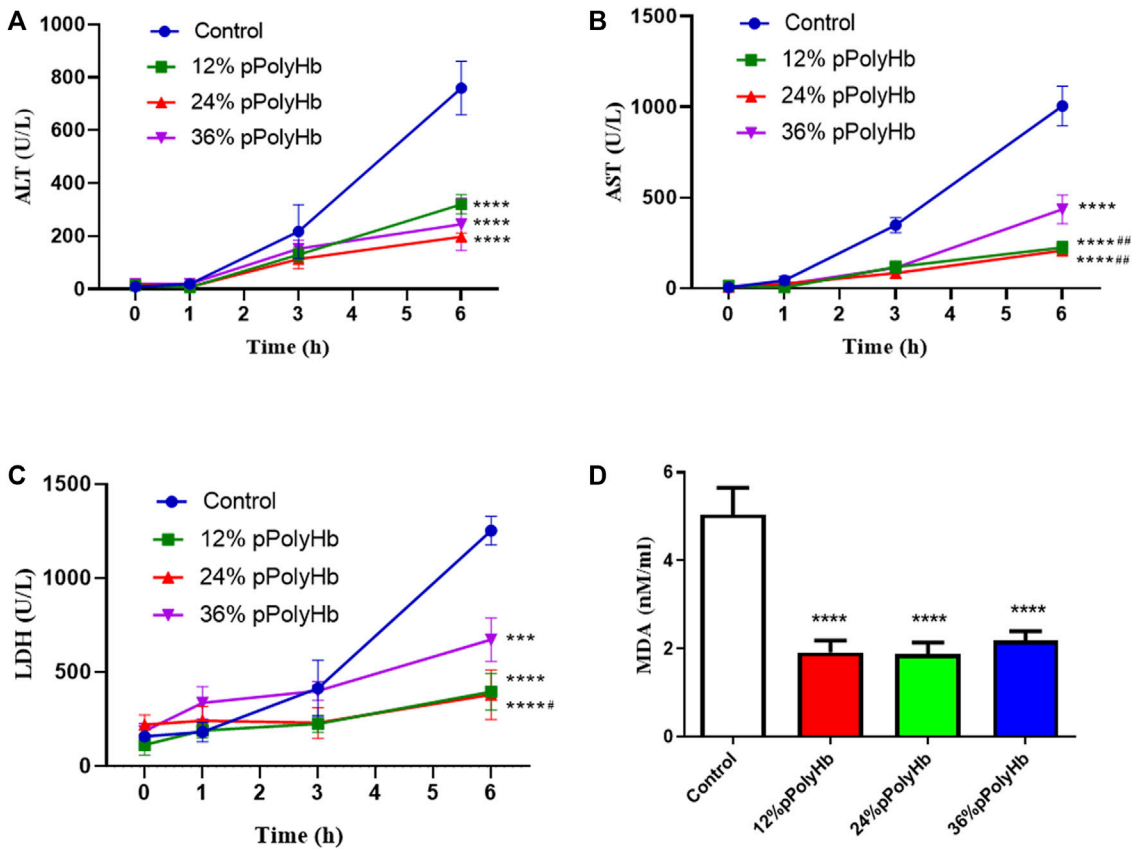

FIGURE 2
(A) After 1 h of perfusion, the levels of ALT in the three groups supplemented with pPolyHb were significantly lower than those in basal perfusate group (****$p < 0.0001$) and the lowest level was found in the 24%pPolyHb group **(B)** After 1 h of perfusion, AST levels in three groups supplemented with pPolyHb were significantly lower than those in basal perfusate group (****$p < 0.0001$) and the groups supplemented with 12% pPolyHb and 24% pPolyHb was significantly lower than 36% pPolyHb group (##$p < 0.01$) **(C)** LDH values of three groups supplemented with pPolyHb were lower than those of basal perfusate group (***$p < 0.001$, ****$p < 0.0001$). The 24% pPolyHb group was significantly lower than 36% pPolyHb (#$p < 0.05$) **(D)** MDA levels in basal perfusate group was significantly higher than that in pPolyHb group (****$p < 0.0001$) (Note: * stands for comparison with the control group, # stands for comparison with 36% pPolyHb, *$p < 0.05$. **$p < 0.01$, ***$p < 0.001$, ****$p < 0.0001$, # Similarly).

Results

Optimal addition ratio of pPolyHb

Liver function tests

Enzyme activity. The release of hepatocyte enzymes (ALT, AST, LDH) in the three groups supplemented with 12% pPolyHb, 24% pPolyHb, and 36% pPolyHb was significantly lower than that in the basal perfusate group. Among the three groups supplemented with pPolyHb, the ALT level in the 24% pPolyHb group increased the most slowly. The AST values of 24% pPolyHb group and 36% pPolyHb group had the same upward trend and similar values, and the AST values of both groups remained at 0–300 (U/L). The most sensitive index of LDH activity increased as 36% pPolyHb group had the highest value, 12% pPolyHb group was close to 24% pPolyHb group. The tissue MDA production in basal perfusate group was significantly higher than that in the three groups supplemented with pPolyHb (Figure 2).

Blood gas analysis

pH. Within 6 h of perfusion, the pH of perfusate did not deviate from the normal range in all groups, but it increased slightly in all groups from the beginning to the end of perfusion (Figure 3A).

pCO_2. At the beginning of perfusion, the pCO_2 of four groups was lower than 50 mmHg, the pCO_2 of the basal perfusate group increased to 130 mmHg with time. pCO_2 increased from 0 h to 1 h in three groups supplemented with pPolyHb. pCO_2 increased slightly from 1 h to 3 h in the 12% pPolyHb group, and then decreased slowly from 3 h to 6 h pCO_2 in 24% pPolyHb group and 36%pPolyHb group tended to be stable after 1 h until the end of perfusion (Figure 3B).

pO_2. Within 6 h, pO_2 in the basal perfusate group decreased from 50 mmHg at the beginning to less than 10 mmHg at the end, while pO_2 in three groups supplemented with pPolyHb was in the range of 83 ± 6.230 mmHg to 108.667 ± 14.364 mmHg (Figure 3C).

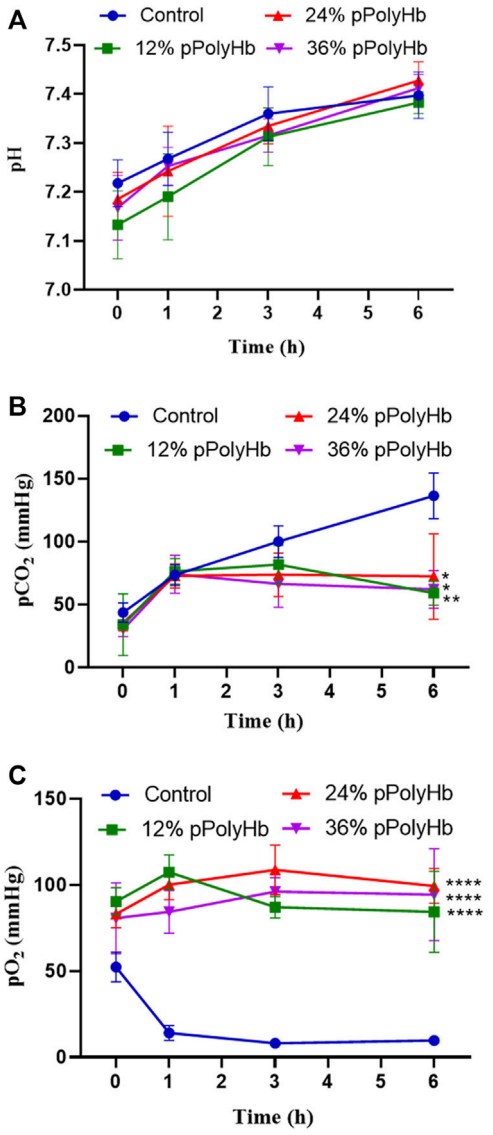

FIGURE 3
(A) There was no significant difference in pH between the four groups during perfusion **(B)** pCO2 in the three groups supplemented with pPolyHb was significantly lower than that in basal perfusate group (*$p < 0.05$, **$p < 0.005$) **(C)** pO2 in the three groups supplemented with pPolyHb during perfusion was significantly higher than that in basal perfusate group (****$p < 0.0001$) (Note: * stands for comparison with the control group).

Electrolyte

During the perfusion period, the change range of Na^+ was relatively stable, ranging from 147.67 ± 3.215 mmol/L to 182.75 ± 8.963 mmol/L, and the change range of K^+ was from 2.03 ± 0.208 mmol/L to 5.63 ± 0.306 mmol/L. The basal perfusate group and three groups supplemented with pPolyHb showed the same trend of change, and the concentration increased with time. Ca^{2+} decreased

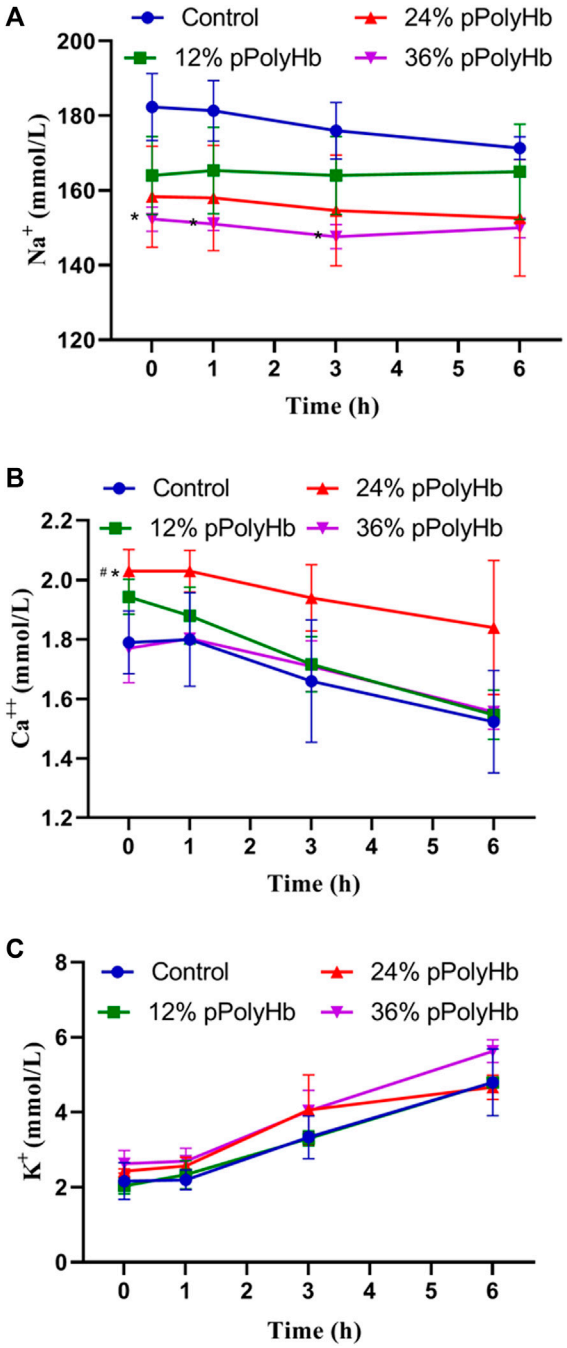

FIGURE 4
(A) There was no significant difference in Na + concentration among the four groups during perfusion (B) After 1 h of perfusion, Ca2+ in the four groups showed a downward trend, and after the end of perfusion, Ca2+ in the 24% pPolyHb group was slightly higher than that in the other three groups (C) There was no significant difference in K+ concentration among the four groups, and it increased at any time (Note: * stands for comparison with the control group, # stands for comparison with 36% pPolyHb, *$p < 0.05$, # Similarly).

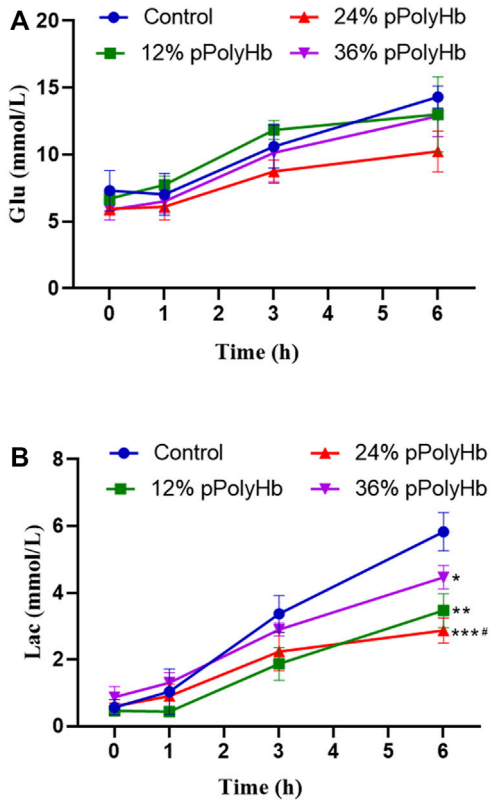

FIGURE 5
(A) The trend in glucose change for each group throughout perfusion. The blood glucose levels in all four perfusion groups rose as perfusion duration was extended, however the 24% pPolyHb group's perfusion group's blood glucose increase trend was the lowest **(B)** The amount of lactic acid created by each group during perfusion, with the control group producing the highest, the 36% pPolyHb group coming in second, and the 24% pPolyHb group coming in last (Note: * stands for comparison with the control group, # stands for comparison with 36% pPolyHb, *$p < 0.05$. **$p < 0.01$, ***$p < 0.001$, ****$p < 0.0001$, # Similarly).

regularly in the range of 1.523 ± 0.172 mmol/L to 2.03 ± 0.07 mmol/L, the highest concentration not exceeding the normal range (Figure 4).

Blood glucose and lactic acid

Blood glucose. Blood glucose increased with perfusion time in all groups and overall changed in the range from 5.867 ± 0.751 mmol/L to 14.3 ± 0.819 mmol/L). There was no significant difference among four groups within 0 h–1 h, but four groups increased significantly within 1h–3 h. At 3 h–6 h, there was also an increase in each group, but the value of three groups supplemented with pPolyHb increased slowly compared with basal perfusate group (Figure 5A).

Lactic acid. With the prolongation of perfusion time, the lactic acid value of four groups gradually increased, and the overall change was in the range of 0.433 ± 0.115 mmol/L to 5.833 ± 0.569 mmol/L. The lactic acid value of the 24% pPolyHb group was 2.233 mmol/L at 3 h, and the other three groups supplemented with pPolyHb was lower than the 3-h threshold of 2.5 mmol/L recommended by Mergental (Mergental et al., 2020) et al. From 3 h to 6 h of perfusion, the lactate increase rate of three groups supplemented with pPolyHb was slowed down, and the most significant was the 24% pPolyHb group, and the lactic acid value at 6 h was still close to the threshold of 2.5 mmol/L. However, the lactic acid value of basal perfusate group continued rising, reaching 3.367 mmol/L at 3 h and 5.833 mmol/L at 6 h (Figure 5B).

Histology

H&E staining. H&E staining was performed on liver slices. Normal rat liver has clear nucleoplasm and nuclear plumpness, without vacuolar degeneration or necrosis. The staining of hepatocytes showed that the nuclei of the basal perfusate fluid group were shrunk, irregular in shape and appeared many vacuoles. 12% pPolyHb group showed clear hepatic lobules and hepatic cords, but multiple punctal necrosis of paravascular hepatocytes. In 24% pPolyHb group, the hepatocytes were arranged neatly, the boundary between nuclear and cytoplasm was clear, and the hepatic lobule structure was intact. 36% pPolyHb group images showed slight atrophy of liver cells (Figure 6A). In conclusion, compared with the basal perfusate group, the liver injury degree of three groups supplemented with pPolyHb after perfusion was reduced, and 24% pPolyHb group had the lowest injury degree.

TUNEL staining was performed on liver tissue sections after different treatments. The results showed that the number of apoptotic cells in basal perfusate group was the highest, and the number of apoptotic cells in 24% pPolyHb group was the lowest (Figure 6B). It was further indicated that the addition of pPolyHb could effectively protect the liver and the degree of liver injury was lower in 24% pPolyHb group.

The expression of apoptotic protein Bcl-2 and bax

The expression of apoptotic protein in liver tissue after perfusion with different pPolyHb content was detected by Western Blot. The results showed that compared with the basal perfusate group, the expression of Bcl-2 was higher and the expression of Bax was lower in the three groups supplemented with pPolyHb, indicating that the addition of pPolyHb in the perfusate had a protective effect. By comparing the values of Bcl-2/Bax, it can be seen that the protein apoptosis rate of the three groups supplemented with pPolyHb was significantly reduced, and 24% pPolyHb had the lowest apoptosis rate (Figure 6C).

Comparison of basal perfusate + 24% pPolyHb with K-H solution and UW solution for liver protection

Liver function test

Enzyme activity. Among the three groups, the values of hepatocyte enzymes (ALT, AST, LDH) in UW solution and

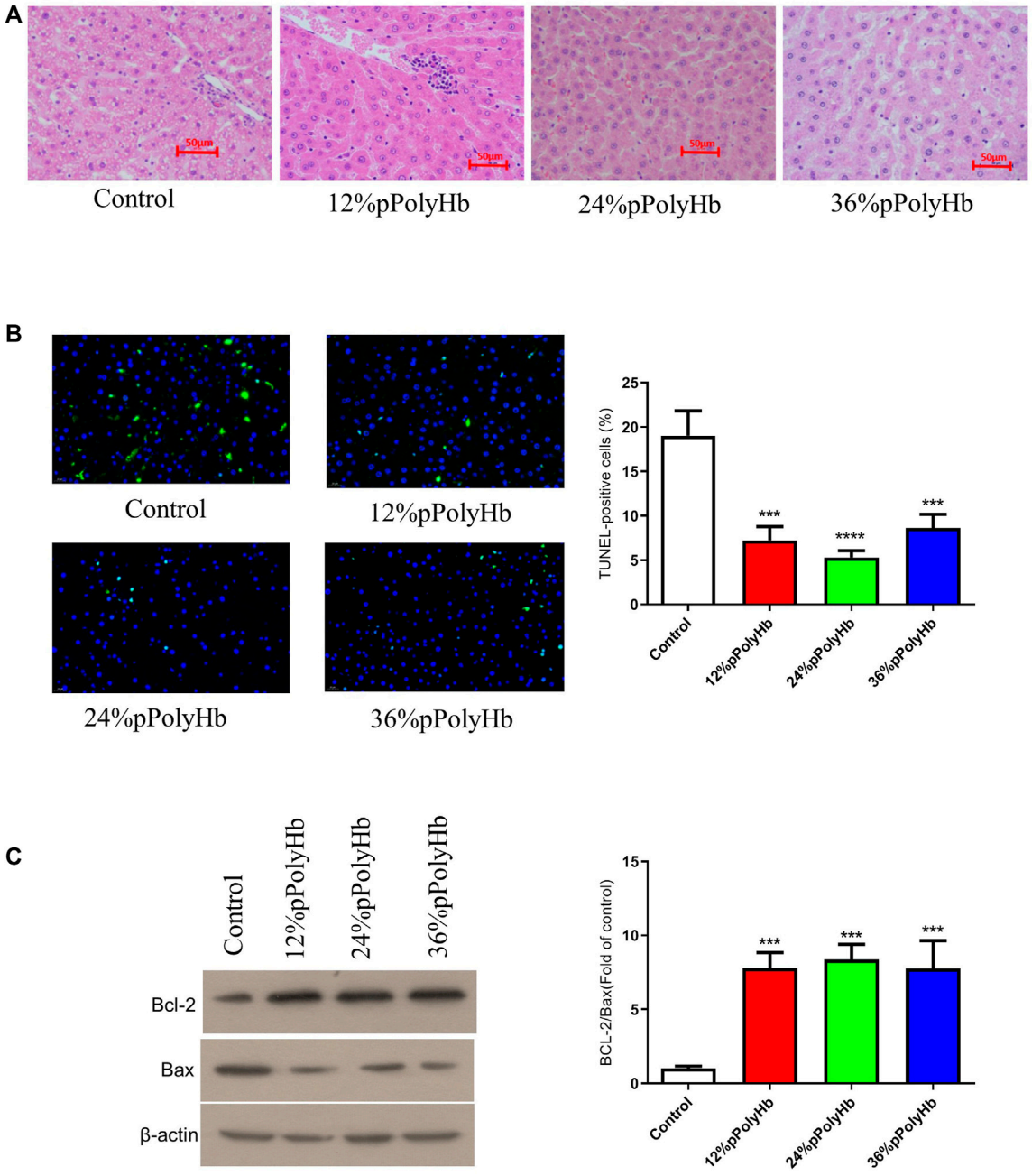

FIGURE 6
(A) H&E straining. Different groups show different physiological morphology, among which 24% pPolyHb group is the best **(B)** TUNEL straining. The control group has the largest number of apoptotic cells. The number of apoptotic cells in 12% pPolyHb group and 36% pPolyHb group is about half of that in control group. The number of apoptotic cells in 24% pPolyHb group was the lowest **(C)** Expression levels of Bax and Bcl-2 in hepatocytes of each group and the ratio of Bcl-2/Bax in each group.

24% pPolyHb group were significantly lower than those in K-H solution group. The amount of hepatocyte enzyme released in K-H solution group was significantly increased after 1 h perfusion. In the 24% pPolyHb group, ALT and AST values increased gradually from 0 h to 6 h, but maintained within the range of 0–200 U/L. LDH also increased gradually, and maintained in the range of 0–400 U/L from the beginning to the end of perfusion. In addition, the MDA value of 24% pPolyHb group and UW solution group was significantly lower than that of K-H solution group (Figure 7).

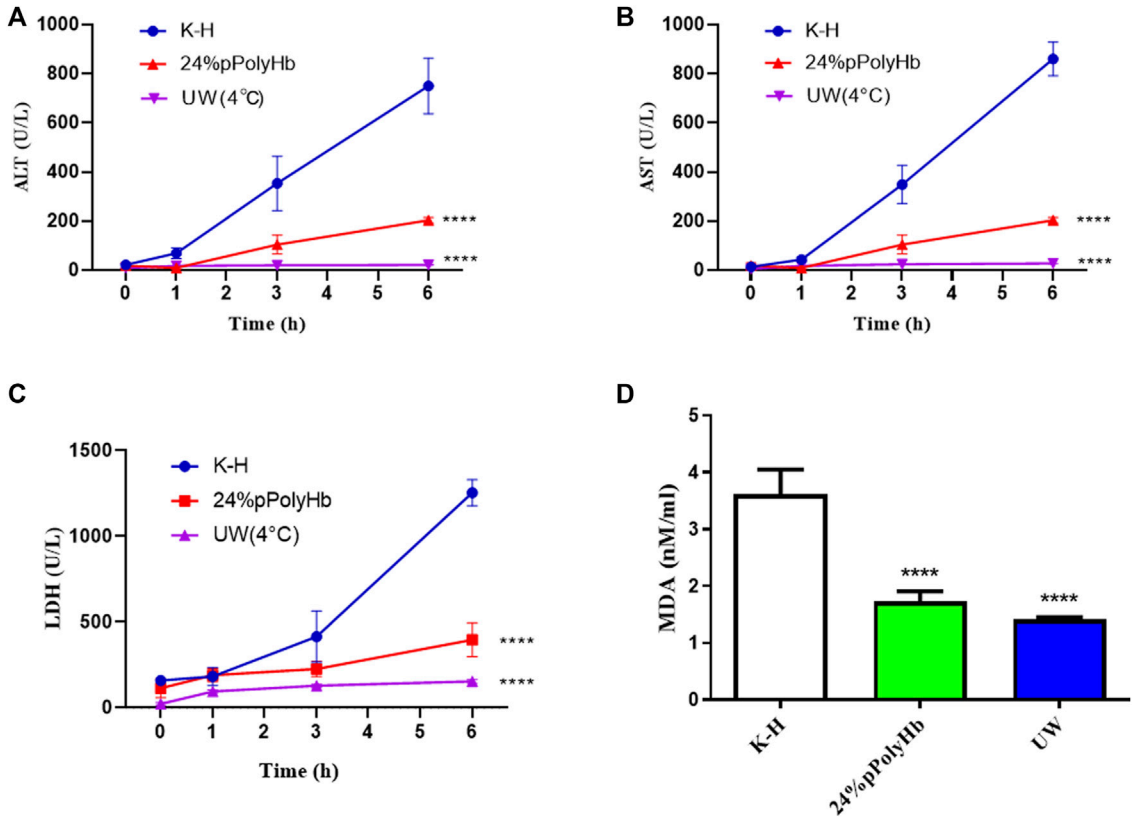

FIGURE 7
(A) Within 1 h after perfusion, ALT of K-H solution group was higher than the other two groups. One hour after perfusion, two groups were significantly lower than K-H solution group (* * * *$p < 0.0001$) **(B)** After 1 h of perfusion, AST of K-H solution group was significantly higher than the other two groups (* * * *$p < 0.0001$) **(C)** After 1 h of perfusion, LDH of K-H solution group was significantly higher than the other two groups (* * * *$p < 0.0001$) **(D)** After 1 h of perfusion, MDA of K-H solution group was significantly higher than that of the other two groups (* * * *$p < 0.0001$).

Histology

The results of H&E staining showed that the hepatic lobules and cords of the liver tissue after perfusing with the 24% pPolyHb group was clear, distinct nucleoplasm, and the nucleolus could be clearly observed. However, the liver tissue perfused with K-H solution was highly vacuolated, and the hepatic lobule structure was changed (Figure 8A). TUNEL staining showed that the number of apoptotic cells in K-H solution group was significantly higher than that in the 24% pPolyHb group (Figure 8B).

Expression of apoptotic protein Bcl-2 and bax

The apoptotic protein expression levels after K-H solution and 24% pPolyHb perfusate treatment were detected by Western Blot. It was found that the expression of Bcl-2 after K-H solution infusion was lower than that after 24% pPolyHb perfusate infusion, and the expression of Bax was higher (Figure 8C).

Discussion

Since the success of the first liver transplantation (LT), it has become a recognized treatment for patients with end-stage liver disease (Adam et al., 2012). Organ preservation is an important part of organ transplantation. The quality of the organ should be maintained during the interval between the removal from the donor and the transplantation into the recipient (Weissenbacher et al., 2019). At present, the most commonly method of organ preservation in clinic is SCS, which goal is to reduce the energy consumption of organs through static low temperature, so as to prolong the preservation time. Although SCS reduces the enzyme activity and oxygen consumption in organs and can maintain the intracellular ion homeostasis and membrane potential, the demand for energy metabolism and oxygen continues (Kasil et al., 2019). Anaerobic metabolism in SCS continues to cause the accumulation of metabolites, which leads to ischemia-reperfusion injury (IRI) after reperfusion of receptor organs (Chouchani et al., 2014). SCS is acceptable for high-quality

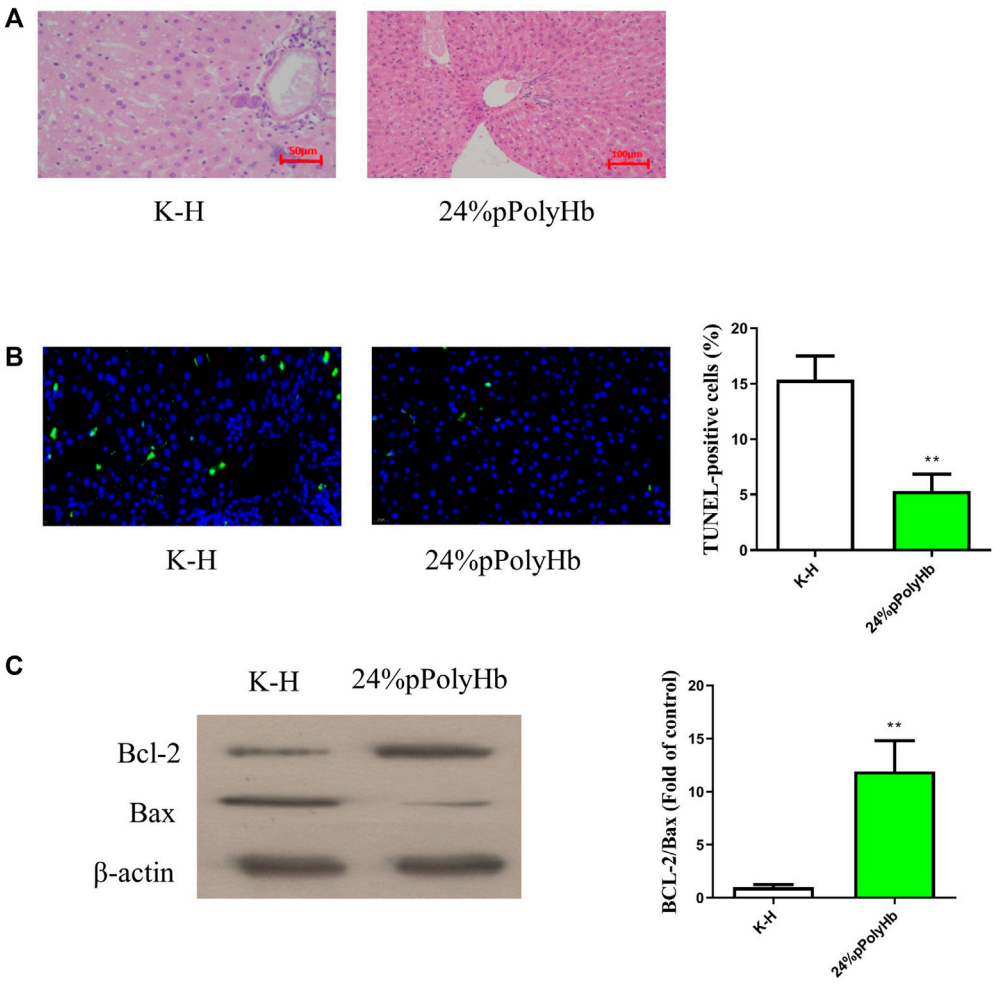

FIGURE 8
(A) H&E staining results. The liver tissue infused with K-H solution was highly vacuolated, and the structure of hepatic lobule was changed. After perfusion of 24% pPolyHb, the liver tissue and hepatic cord were clear, distinct nucleoplasm, and the nucleolus could be clearly observed **(B)** TUNEL staining results. The K-H solution group has a large amount of blue fluorescence. The number of apoptotic cells in K-H solution group was significantly higher than that in 24% pPolyHb group (* $*p < 0.01$) **(C)** Expression of apoptosis related proteins Bax and Bcl-2. The results of Western Blot showed that the expression level of Bcl-2 was higher in 24% pPolyHb group, and the expression level of Bax was lower. According to the histogram, the Bcl-2/Bax of 24% pPolyHb group is significantly higher than that of K-H solution group (* $*p < 0.01$).

organs, but it has limitation in high-risk or marginal organs. NMP allows organs to perform metabolism and liver function synthesis under physiological conditions, which theoretically provides the best condition for evaluating organ survival and integrity before transplantation (von Horn and Minor, 2019). David Nasralla et al. showed in a randomized trial of 220 liver transplants that compared with traditional static refrigeration, normothermic perfusion preservation can reduce graft damage by 50% (Nasralla et al., 2018). In an unprecedented feasibility reasearch, Eshmuminov et al. were able to perfuse the liver allograft for 7 days to keep the liver functional under normal temperature. The experimental results are far-reaching and widely cited, which show that long-term NMP is safe and feasible (Eshmuminov et al., 2020).

Additional oxygen supplementation during organ preservation can promote ATP synthesis and prevent anaerobic metabolism to reduce reperfusion injury (Minor et al., 2011). Nevertheless, direct oxidation may aggravate the oxidative stress damage of the organ if the oxidative metabolism of the graft is seriously damaged. Another method is to use oxygen carriers, especially those based on Hemoglobin-based oxygen carriers (HBOCs). HBOCs were originally studied as blood substitutes, but now they have been extended to the treatment of ischemia and hypoxia (Cao et al., 2021). Recently, the "repositioning" of HBOCs has led to its successful application in organ perfusion fluid, which is considered as an alternative method to improve oxygen supply and protect the optimal metabolic activity.

In this research, we used the hemoglobin oxygen carrier pPolyHb as a major component of perfusate for NMP of rat donor liver. In this paper, the effect of hyperkalemia caused by high concentration of potassium in perfusate on perfusion is not clear (Tan et al., 2005). The ideal composition of NMP perfusate is not yet clear, and most of the existing reports have differences in composition addition and functional differences in the regulation of various components. In this paper, we added some intravenous nutrient elements and trace elements to the perfusate to simulate the normal physiological environment of the liver during NMP and maintain the supply of nutrient elements. Although the mechanism of the necessity of these trace elements for short-term NMP has not been fully understood and confirmed, they may be necessary for long-term perfusion of isolated liver. Hydroxyethyl starch was used because it was isotonic and had a neutral pH, sodium and chlorine content were similar to the extracellular fluid, and salt components such as calcium chloride, potassium dihydrogen phosphate, magnesium sulfate, and potassium hydroxide were used to maintain electrolyte balance of the perfusate. Although the liver itself is expected to produce a certain amount of nutrients, we still add some exogenous nutrients such as glucose and compound amino acid buffer solution as appropriate supplement. On the basis of referring to Butler (García-Gil et al., 2011) basic perfusion formula, the perfusate in this paper has carried out a lot of optimization and improvement work, and the research results show that some data are slightly different from the expected, it demonstrated that our perfusate formula can be further optimized and upgraded in order to obtain better research results.

In hepatocytes, AST and ALT exist inside and outside mitochondria respectively. When liver is damaged, hepatocytes are destroyed, and the intracellular ALT and AST flow out of the cell, resulting in the increase of serum ALT and AST. LDH is widely distributed in the heart, kidney, liver and other sites, and its elevation can indicate myocardial infarction or hepatitis. In this experiment, normal saline was used to dilute the sample before detecting the perfusate, so as to exclude the possibility of false positive LDH. Some end points of our study showed that compared with liver perfusion without pPolyHb perfusate, the values of AST, ALT and LDH of damage markers were significantly decreased after the addition of pPolyHb. Although there is no clear indicator for the threshold of hepatocyte enzymes, the release of hepatocyte enzymes has important reference value for the evaluation of liver viability. In addition, as an oxygen carrier, the main function of pPolyHb is to better carry and release oxygen. In our comparison of partial pressure of oxygen between the group adding pPolyHb of different concentrations and the control group, it can be clearly found that the partial pressure of oxygen in the control group is extremely low, and from the overall curve trend, the partial pressure of oxygen in the 24% pPolyHb group is higher than 12% pPolyHb and 36% pPolyHb, indicating that the oxygen carrying and oxygen releasing capacity is better at this concentration.

Blood glucose is one of the important indicators to detect liver function. When liver function decreases, blood glucose will rise (Micó-Carnero et al., 2022). In this study, we added glucose to the perfusate to provide energy substrate for liver metabolism. In the follow-up test, it was found that the blood glucose increased in 1–3 h. Then it was discovered that the blood glucose of 12% pPolyHb group stopped rising in 3~6 h, at the same time, the rising speed in 24% and 36% pPolyHb groups slowed down. The above results indicated that the liver was in the non-resuscitation state at the initial stage of perfusion, and the liver function declined by degrees. In the later period, the liver gradually recovered its metabolic function and the blood sugar was converted into glycogen then stored in the liver (Matton et al., 2019), thus reduced the measured blood sugar content. It showed that pPolyHb can protect the liver to some extent. Under the condition of hypoxia, blood glucose will undergo a large amount of anaerobic fermentation to convert into lactic acid (Weissenbacher et al., 2022). Lactic acid is an indicator of cell oxygen metabolism. In perfusion, its increase beyond the threshold indicates poor organ preservation effect, impaired liver function, and reduced lactate clearance rate (Aburawi et al., 2019). Previous research results showed that, from the beginning to the end of perfusion, although the lactic acid content in each group increased, the lactic acid value in the middle of perfusion was below the 3-h threshold of 2.5 mmol/L recommended by Mergental et al. At the end of perfusion, the lactic acid value of each group was still around this threshold. Among them, the lactate value of the perfusion group supplemented with 24% pPolyHb was the best, which indicated that the liver status improved after perfusion with 24% pPolyHb, and the lactate clearance ability was gradually restored. At the same time, low lactic acid value indicated that anaerobic metabolism in liver was improved, which further proved that pPolyHb had good oxygen carrying and oxygen releasing capacity.

The results of H&E staining and TUNEL staining after liver tissue sections were consistent: 24% pPolyHb group showed the best morphology of liver cells, and the number of apoptotic cells were the least. The outcomes showed that perfusion with this pPolyHb concentration had the best liver protection effect. Both Bax and Bcl-2 proteins belong to the Bcl-2 gene family, but their regulatory mechanisms are completely different (Tan et al., 2005). The three domains BH1, BH2 and BH3 in Bax gene can promote apoptosis. BH4 contained in Bcl-2 gene is a unique homologous domain of anti-apoptotic protein, which plays a role in inhibiting apoptosis (Sitailo et al., 2009). The comprehensive data of Western Blot analysis showed that the expression of Bax in 24% pPolyHb group was the lowest, and the Bcl-2 was the highest. This illustrated that pPolyHb can protect the liver by changing the expression of Bax and Bcl-2 proteins.

In addition, in the samples treated with pPolyHb perfusion solution, K-H perfusion solution and UW solution respectively, the levels of liver injury indicators in the K-H solution group were significantly higher than the other two groups in terms of ALT, AST, LDH or MDA. According to the results of H&E staining

and TUNEL staining of 24% pPolyHb group and K-H solution group after normothermic machine perfusion, 24% pPolyHb group showed the best results in terms of the morphology of hepatic lobule and hepatic cord in liver tissue and the apoptotic cells. And from the ratio of Bcl-2/Bax, 24% pPolyHb group was significantly higher than K-H solution group, indicating that its addition could conspicuously increase the expression of anti-apoptotic genes and reduce the expression of pro-apoptotic genes. According to the above results, the effect after perfusion with oxygen carrier pPolyHb was obviously better than that after perfusion with K-H solution, which indicated that the addition of pPolyHb enhanced the ability of oxygen carrying and oxygen releasing to a certain extent, and reduced liver injury.

At present, NMP is a research hotspot in the field of organ preservation (Marecki et al., 2017; Nasralla et al., 2018; Bral et al., 2019). This technology has been proved to not only achieve the same preservation effect as cold preserved organs (op den Dries et al., 2016; Dutkowski et al., 2019), but also be able to repair marginal organs and damaged organs in some donor pools, and evaluate the physiological status of donor organs before transplantation. Our research demonstrates that pPolyHb can protect the liver to some extent and has explored the optimal addition ratio of 24%, but there are still some limitations: the number of experimental livers are still small; compared with experimental conditions with perfusion time of 10–24 h, our 6 h *in vitro* operation time is relatively short. In addition, this small animal NMP model does not currently include postperfusion transplantation. Therefore, it is not possible to evaluate liver function after transplantation.

Conclusion

This study preliminarily explored the feasibility of pPolyHb as the main component of liver preservation solution, and proved that the isolated liver perfusion based on pPolyHb can basically maintain the physiological and biochemical functions of the liver within 6 h which confirmed that the pPolyHb based perfusion solution could be applied to the normal temperature machine perfusion of the isolated rat liver.

Data availability statement

The original contributions presented in the study are included in the article/Supplementary Material, further inquiries can be directed to the corresponding author.

Ethics statement

The animal study was reviewed and approved by the Animal Care Committee of Northwest University.

Author contributions

BL, JZ, and CS conceived and designed the experiments. JZ, CS, TZ, YL, and SS performed the experiments. JZ, CS, and TZ wrote the manuscript and analysed the data. CZ and YZ reviewed the manuscript. All authors read, revised, and approved the manuscript.

Funding

This work was supported by the project of the human red blood cell substitute-the pilot test process optimization and function evaluation of glutaraldehyde polymerized porcine hemoglobin (No. 2018YFC1106501).

Acknowledgments

We thank the project of human red blood cell substitute-the pilot test process optimization and function evaluation of glutaraldehyde polymerized porcine hemoglobin for the support of this study.

Conflict of interest

The authors declare that the research was conducted in the absence of any commercial or financial relationships that could be construed as a potential conflict of interest.

Publisher's note

References

Aburawi, M. M., Fontan, F. M., Karimian, N., Eymard, C., Cronin, S., Pendexter, C., et al. (2019). Synthetic hemoglobin-based oxygen carriers are an acceptable alternative for packed red blood cells in normothermic kidney perfusion. *Am. J. Transpl.* 19 (10), 2814–2824. doi:10.1111/ajt.15375

Adam, R., Karam, V., Delvart, V., O'Grady, J., Mirza, D., Klempnauer, J., et al. (2012). Evolution of indications and results of liver transplantation in Europe. A report from the European Liver Transplant Registry (ELTR). *J. Hepatology* 57 (3), 675–688. doi:10.1016/j.jhep.2012.04.015

Bral, M., Dajani, K., Leon Izquierdo, D., Bigam, D., Kneteman, N., Ceresa, C. D. L., et al. (2019). A back-to-base experience of human normothermic *ex situ* liver perfusion: Does the chill kill? *Liver Transpl.* 25 (6), 848–858. doi:10.1002/lt.25464

Brockmann, J., Reddy, S., Coussios, C., Pigott, D., Guirriero, D., Hughes, D., et al. (2009). Normothermic perfusion: a new paradigm for organ preservation. *Ann. Surg.* 250 (1), 1–6. doi:10.1097/SLA.0b013e3181a63c10

Butler, A. J., Rees, M. A., Wight, D. G., Casey, N. D., Alexander, G., White, D. J., et al. (2002). Successful extracorporeal porcine liver perfusion for 72 hr. *Transplantation* 73 (8), 1212–1218. doi:10.1097/00007890-200204270-00005

Cao, M., Wang, G., He, H., Yue, R., Zhao, Y., Pan, L., et al. (2021). Hemoglobin-based oxygen carriers: Potential applications in solid organ preservation. *Front. Pharmacol.* 12, 760215. doi:10.3389/fphar.2021.760215

Chien, S., Zhang, F., Niu, W., Tseng, M. T., and Gray, L., Jr. (2000). Comparison of University of wisconsin, euro-collins, low-potassium dextran, and krebs-henseleit solutions for hypothermic lung preservation. *J. Thorac. Cardiovasc. Surg.* 119 (5), 921–930. doi:10.1016/s0022-5223(00)70087-0

Chouchani, E. T., Pell, V. R., Gaude, E., Aksentijevic, D., Sundier, S. Y., Robb, E. L., et al. (2014). Ischaemic accumulation of succinate controls reperfusion injury through mitochondrial ROS. *Nature* 515 (7527), 431–435. doi:10.1038/nature13909

Clavien, P. A., Harvey, P. R., and Strasberg, S. M. (1992). Preservation and reperfusion injuries in liver allografts. An overview and synthesis of current studies. *Transplantation* 53 (5), 957–978. doi:10.1097/00007890-199205000-00001

de Vries, Y., Matton, A. P. M., Nijsten, M. W. N., Werner, M. J. M., van den Berg, A. P., de Boer, M. T., et al. (2019). Pretransplant sequential hypo- and normothermic machine perfusion of suboptimal livers donated after circulatory death using a hemoglobin-based oxygen carrier perfusion solution. *Am. J. Transpl.* 19 (4), 1202–1211. doi:10.1111/ajt.15228

Dutkowski, P., Guarrera, J. V., de Jonge, J., Martins, P. N., Porte, R. J., and Clavien, P. A. (2019). Evolving trends in machine perfusion for liver transplantation. *Gastroenterology* 156 (6), 1542–1547. doi:10.1053/j.gastro.2018.12.037

Eshmuminov, D., Becker, D., Bautista Borrego, L., Hefti, M., Schuler, M. J., Hagedorn, C., et al. (2020). An integrated perfusion machine preserves injured human livers for 1 week. *Nat. Biotechnol.* 38 (2), 189–198. doi:10.1038/s41587-019-0374-x

Fondevila, C., Hessheimer, A. J., Maathuis, M. H., Muñoz, J., Taurá, P., Calatayud, D., et al. (2011). Superior preservation of DCD livers with continuous normothermic perfusion. *Ann. Surg.* 254 (6), 1000–1007. doi:10.1097/SLA.0b013e31822b8b2f

Fontes, P., Lopez, R., van der Plaats, A., Vodovotz, Y., Minervini, M., Scott, V., et al. (2015). Liver preservation with machine perfusion and a newly developed cell-free oxygen carrier solution under subnormothermic conditions. *Am. J. Transpl.* 15 (2), 381–394. doi:10.1111/ajt.12991

García-Gil, F. A., Serrano, M. T., Fuentes-Broto, L., Arenas, J., García, J. J., Güemes, A., et al. (2011). Celsior versus university of Wisconsin preserving solutions for liver transplantation: postreperfusion syndrome and outcome of a 5-year prospective randomized controlled study. *World J. Surg.* 35 (7), 1598–1607. doi:10.1007/s00268-011-1078-7

Jaeschke, H. (1998). Mechanisms of reperfusion injury after warm ischemia of the liver. *J. Hepatobiliary. Pancreat. Surg.* 5 (4), 402–408. doi:10.1007/s005340050064

Jing, L., Yao, L., Zhao, M., Peng, L. P., and Liu, M. (2018). Organ preservation: from the past to the future. *Acta Pharmacol. Sin.* 39 (5), 845–857. doi:10.1038/aps.2017.182

Kasil, A., Giraud, S., Couturier, P., Amiri, A., Danion, J., Donatini, G., et al. (2019). Individual and combined impact of oxygen and oxygen transporter supplementation during kidney machine preservation in a porcine preclinical kidney transplantation model. *Int. J. Mol. Sci.* 20 (8), 1992. doi:10.3390/ijms20081992

Laing, R. W., Bhogal, R. H., Wallace, L., Boteon, Y., Neil, D. A. H., Smith, A., et al. (2017). The use of an acellular oxygen carrier in a human liver model of normothermic machine perfusion. *Transplantation* 101 (11), 2746–2756. doi:10.1097/tp.0000000000001821

Liu, Q., Nassar, A., Buccini, L., Grady, P., Soliman, B., Hassan, A., et al. (2018). *Ex situ* 86-hour liver perfusion: Pushing the boundary of organ preservation. *Liver Transpl.* 24 (4), 557–561. doi:10.1002/lt.25007

Marecki, H., Bozorgzadeh, A., Porte, R. J., Leuvenink, H. G., Uygun, K., and Martins, P. N. (2017). Liver *ex situ* machine perfusion preservation: A review of the methodology and results of large animal studies and clinical trials. *Liver Transpl.* 23 (5), 679–695. doi:10.1002/lt.24751

Matton, A. P. M., de Vries, Y., Burlage, L. C., van Rijn, R., Fujiyoshi, M., de Meijer, V. E., et al. (2019). Biliary bicarbonate, pH, and glucose are suitable biomarkers of biliary viability during *ex situ* normothermic machine perfusion of human donor livers. *Transplantation* 103 (7), 1405–1413. doi:10.1097/TP.0000000000002500

Mergental, H., Laing, R. W., Kirkham, A. J., Perera, M., Boteon, Y. L., Attard, J., et al. (2020). Transplantation of discarded livers following viability testing with normothermic machine perfusion. *Nat. Commun.* 11 (1), 2939. doi:10.1038/s41467-020-16251-3

Mergental, H., Perera, M. T., Laing, R. W., Muiesan, P., Isaac, J. R., Smith, A., et al. (2016). Transplantation of declined liver allografts following normothermic eEx-sSitu evaluation. *Am. J. Transpl.* 16 (11), 3235–3245. doi:10.1111/ajt.13875

Micó-Carnero, M., Zaouali, M. A., Rojano-Alfonso, C., Maroto-Serrat, C., Ben Abdennebi, H., and Peralta, C. (2022). A potential route to reduce ischemia/reperfusion injury in organ preservation. *Cells* 11 (17), 2763. doi:10.3390/cells11172763

Minor, T., Koetting, M., Koetting, M., Kaiser, G., Efferz, P., Luer, B., et al. (2011). Hypothermic reconditioning by gaseous oxygen improves survival after liver transplantation in the pig. *Am. J. Transpl.* 11 (12), 2627–2634. doi:10.1111/j.1600-6143.2011.03731.x

Nasralla, D., Coussios, C. C., Mergental, H., Akhtar, M. Z., Butler, A. J., Ceresa, C. D. L., et al. (2018). A randomized trial of normothermic preservation in liver transplantation. *Nature* 557 (7703), 50–56. doi:10.1038/s41586-018-0047-9

op den Dries, S., Karimian, N., Sutton, M. E., Westerkamp, A. C., Kuipers, M., Wiersema-Buist, J., et al. (2016). Normothermic machine perfusion reduces bile duct injury and improves biliary epithelial function in rat donor livers. *Liver Transpl.* 22 (7), 994–1005. doi:10.1002/lt.24436(

op den Dries, S., Karimian, N., Sutton, M. E., Westerkamp, A. C., Nijsten, M. W., Gouw, A. S., et al. (2013). *Ex vivo* normothermic machine perfusion and viability testing of discarded human donor livers. *Am. J. Transpl.* 13 (5), 1327–1335. doi:10.1111/ajt.12187

Perk, S., Izamis, M. L., Tolboom, H., Uygun, B., Berthiaume, F., Yarmush, M. L., et al. (2011). A metabolic index of ischemic injury for perfusion-recovery of cadaveric rat livers. *PLoS One* 6 (12), e28518. doi:10.1371/journal.pone.0028518

Schön, M. R., Kollmar, O., Wolf, S., Schrem, H., Matthes, M., Akkoc, N., et al. (2001). Liver transplantation after organ preservation with normothermic extracorporeal perfusion. *Ann. Surg.* 233 (1), 114–123. doi:10.1097/00000658-200101000-00017

Sitailo, L. A., Jerome-Morais, A., and Denning, M. F. (2009). Mcl-1 functions as major epidermal survival protein required for proper keratinocyte differentiation. *J. Invest. Dermatol.* 129 (6), 1351–1360. doi:10.1038/jid.2008.363

Tan, K. O., Fu, N. Y., Sukumaran, S. K., Chan, S. L., Kang, J. H., Poon, K. L., et al. (2005). MAP-1 is a mitochondrial effector of Bax. *Proc. Natl. Acad. Sci. U. S. A.* 102 (41), 14623–14628. doi:10.1073/pnas.0503524102

Tullius, S. G., and Rabb, H. (2018). Improving the supply and quality of deceased-donor organs for transplantation. *N. Engl. J. Med. Overseas. Ed.* 379 (7), 1920–1929. doi:10.1056/nejmra1507080

Vogel, T., Brockmann, J. G., Coussios, C., and Friend, P. J. (2012). The role of normothermic extracorporeal perfusion in minimizing ischemia reperfusion injury. *Transpl. Rev. Orl.* 26 (2), 156–162. doi:10.1016/j.trre.2011.02.004

Vogel, T., Brockmann, J. G., Quaglia, A., Morovat, A., Jassem, W., Heaton, N. D., et al. (2017). The 24-hour normothermic machine perfusion of discarded human liver grafts. *Liver Transpl.* 23 (2), 207–220. doi:10.1002/lt.24672

von Horn, C., and Minor, T. (2019). Modern concepts for the dynamic preservation of the liver and kidneys in the context of transplantation. *Pathologe* 40 (3), 292–298. doi:10.1007/s00292-019-0595-2

Weissenbacher, A., Bogensperger, C., Oberhuber, R., Meszaros, A., Gasteiger, S., Ulmer, H., et al. (2022). Perfusate enzymes and platelets indicate early allograft dysfunction after transplantation of normothermically preserved livers. *Transplantation* 106 (4), 792–805. doi:10.1097/TP.0000000000003857

Weissenbacher, A., Vrakas, G., Nasralla, D., and Ceresa, C. D. L. (2019). The future of organ perfusion and re-conditioning. *Transpl. Int.* 32 (6), 586–597. doi:10.1111/tri.13441

Zhang, W., Yan, K., Dai, P., Tian, J., Zhu, H., and Chen, C. (2012). A novel hemoglobin-based oxygen carrier, polymerized porcine hemoglobin, inhibits H2O2-induced cytotoxicity of endothelial cells. *Artif. Organs* 36 (2), 151–160. doi:10.1111/j.1525-1594.2011.01305.x

Zhu, H., Dang, X., Yan, K., Dai, P., Luo, C., Ma, J., et al. (2011a). Pharmacodynamic study of polymerized porcine hemoglobin (pPolyHb) in a rat model of exchange transfusion. *Artif. Cells Blood Substitutes Biotechnol.* 39 (3), 119–126. doi:10.3109/10731199.2011.559584

Zhu, H., Yan, K., Dang, X., Huang, H., Chen, E., Chen, B., et al. (2011b). Immune safety evaluation of polymerized porcine hemoglobin (pPolyHb): a potential red blood cell substitute. *Artif. Cells Blood Substitutes Biotechnol.* 39 (6), 398–405. doi:10.3109/10731199.2011.631499

frontiers | Frontiers in Bioengineering and Biotechnology

TYPE Original Research
PUBLISHED 08 December 2022
DOI 10.3389/fbioe.2022.1025405

OPEN ACCESS

EDITED BY
Binglan Yu,
Massachusetts General Hospital and Harvard Medical School, United States

REVIEWED BY
Wan Iryani Wan Ismail,
University of Malaysia Terengganu, Malaysia
Lubhan Singh,
Swami Vivekanand Subharti University, India

*CORRESPONDENCE
Sumira Malik,
smalik@rnc.amity.edu
Anuj Ranjan,
randzhan@sfedu.ru
Shafiul Haque,
shafiul.haque@hotmail.com

SPECIALTY SECTION
This article was submitted to Tissue Engineering and Regenerative Medicine, a section of the journal Frontiers in Bioengineering and Biotechnology

RECEIVED 22 August 2022
ACCEPTED 14 November 2022
PUBLISHED 08 December 2022

CITATION
Dhasmana A, Malik S, Sharma AK, Ranjan A, Chauhan A, Harakeh S, Al-Raddadi RM, Almashjary MN, Bawazir WMS and Haque S (2022), Fabrication and evaluation of herbal beads to slow cell ageing. *Front. Bioeng. Biotechnol.* 10:1025405. doi: 10.3389/fbioe.2022.1025405

Fabrication and evaluation of herbal beads to slow cell ageing

Archna Dhasmana[1], Sumira Malik[2]*, Amit Kumar Sharma[3], Anuj Ranjan[4]*, Abhishek Chauhan[5], Steve Harakeh[6], Rajaa M. Al-Raddadi[7], Majed N. Almashjary[8,9,10], Waleed Mohammed S. Bawazir[9,11] and Shafiul Haque[12]*

[1]Himalayan School of Biosciences, Swami Rama Himalayan University, Jolly Grant, Dehradun, Uttarakhand, India, [2]Amity Institute of Biotechnology, Amity University Jharkhand, Ranchi, Jharkhand, India, [3]Department of Biotechnology, Dr KNMIPER, Modinagar, Uttar Pradesh, India, [4]Academy of Biology and Biotechnology, Southern Federal University, Rostov-on-Don, Russia, [5]Amity Institute of Environmental Toxicology, Safety and Management, Amity University, Noida, India, [6]King Fahd Medical Research Center, King Abdulaziz University, Jeddah, Saudi Arabia, [7]Department of Community Medicine, Faculty of Medicine, King Abdulaziz University, Jeddah, Saudi Arabia, [8]Department of Medical Laboratory Sciences, Faculty of Applied Medical Sciences, King Abdulaziz University, Jeddah, Saudi Arabia, [9]Hematology Research Unit, King Fahd Medical Research Center, King Abdulaziz University, Jeddah, Saudi Arabia, [10]Animal House Unit, King Fahd Medical Research Center, King Abdulaziz University, Jeddah, Saudi Arabia, [11]Medical Laboratory Technology Department, Faculty of Applied Medical Sciences, King Abdulaziz University, Jeddah, Saudi Arabia, [12]Research and Scientific Studies Unit, College of Nursing and Allied Health Sciences, Jazan University, Jazan, Saudi Arabia

Several therapies and cosmetics are available commercially to prevent or delay cell ageing, which manifests as premature cell death and skin dullness. Use of herbal products such as *Aloe vera*, curcumin, vitamin C-enriched natural antioxidant, and anti-inflammatory biomolecules are potential ways to prevent or delay ageing. Eggshell membrane (ESM) is also a rich source of collagen; glycosaminoglycans (GAGs) also play an essential role in healing and preventing ageing. It is important to use an extended therapeutic process to prolong the effectiveness of these products, despite the fact that they all have significant anti-ageing properties and the ability to regenerate healthy cells. Encapsulated herbal components are therefore designed to overcome the challenge of ensuring continued treatment over time to prolong the effects of a bioactive component after *in situ* administration. To study their synergistic effects on a cellular level, alginate, Aloe vera, and orange peel extract were encapsulated in bio-polymeric foaming beads and modified with eggshell membrane protein (ESMP) at various concentrations (1 gm, 2 gm, and 5 gm): (A-Av-OP, A-Av-OP-ESMP1, ESMP2, and ESMP3). Analysis of the structural and functional properties of foaming beads showed interconnected 3D porous structure, a surface-functionalized group for entrapment of ESMP, and a significant reduction in pore size (51–35 m) and porosity (80%–60%). By performing DPPH assays, HRBC stabilization assays, and antibacterial tests, the beads were assessed as a natural anti-ageing product with sustained release of molecules effective against inflammatory response, oxidative stress, and microbial contamination. MTT assays were conducted using *in vitro* cell cultures to demonstrate cytocompatibility (in mouse 3T3 fibroblast cells) and cytotoxicity (in human carcinoma HeLa cells). Our study demonstrates that bio-polymeric ESMP beads up to 2 g (A-Av-OP-ESMP2) are practical and feasible natural remedies for suspending defective cell pathways, preventing cell ageing, and promoting healthy cell growth, resulting in a viable and practical natural remedy or therapeutic system.

KEYWORDS

herbal, quercetin, drug, graft, biocompatibility, herbal extracts

Introduction

In the current scenario, biogerontology is a primary area of focus for researchers and scientists (Juengst et al., 2003; Chopra, 2015). The ageing process is a natural phenomenon in which either a single cell or a whole organism undergoes cellular senescence. Significant factors in modern life that may lead to premature ageing include stress, unhealthy food or habits, drugs, smoking, and pollution (Mackenzie and Rakel, 2006; Burokas et al., 2017). Clinically, unhealthy skin may present as acne, wrinkles, dryness, or infections, which are key signs of ageing; the skin is the outermost protective covering of our body and interacts directly with the oxidative environment and harmful radiation (Jemec and Na, 2002; Pillai et al., 2005). Thus, the internal and external organs must be cleansed to overcome these issues and maintain healthy, wrinkle-free, and young-looking skin (Rittié and Fisher, 2015). It has been reported that cell apoptosis due to the shortening of telomeres, harmful UV radiation, glycation, oxidative stress, and hormonal stress causes ageing (Harley et al., 1990; Martin et al., 1993; Cunliffe et al., 2004). In the cellular system, oxygen-derived free radicals are the key players in cell damage, mutation, and early ageing at the cellular and tissue levels. The accretion of endogenous oxygen radicals generated in cells results in oxidative modification of biomolecules such as lipids, proteins, and nucleic acids and has been associated with the ageing and death of all living things (Finkel and Holbrook, 2000).

Cosmetic and therapeutic products, such as anti-ageing creams, masks, sunscreen lotions, moisturizers, and several other anti-ageing medicines, have been associated with prolonged side effects and poor outcomes (Kammeyer and Luiten, 2015; Panich et al., 2016). Herbs or medicinal plants enriched with phytochemicals have potential anti-inflammatory, anti-oxidative, and antimicrobial roles, thereby delaying cellular damage induced by external factors or internal cellular machinery (Pokorný and Schmidt, 2001). Natural antioxidants, such as phenols and flavonoids, slow the endogenous oxidation of a substrate at minute amounts, either through non-enzymatic mechanisms involving uric acid, glutathione, bilirubin, thiols, albumin, and dietary factors or through enzymatic mechanisms involving superoxide dismutases, glutathione peroxidases (GSHPx), and catalase (Sreeramulu et al., 2013). Dietary components have anti-inflammatory and anti-oxidative activity and act through different mechanisms. Free radical scavengers neutralize free radicals directly, reduce peroxide concentrations, repair oxidized membranes, and quench the oxidative capacity of catalytically active iron to decrease the production of reactive oxygen species and lipid metabolism (Miere et al., 2019).

Anti-ageing products contain chemicals from natural products, such as α-hydroxy acids, salicylic acid, hyaluronic acid, and ascorbic acid, along with preservatives for long-term shelf-life (Ahmed et al., 2020). In addition to natural herbal sources, animal products, such as egg shell membrane (ESM), are a rich source of anti-ageing biomolecules, which have traditionally been used as healing and tissue-regenerating biomaterial. Natural components are preferable in producing skin-friendly products. Herein, we report fabrication of a 3D biopolymeric matrix for the treatment of premature cell ageing. Biopolymeric hydrogel beads with Aloe vera, alginate, and orange-peel extract entrapped with eggshell membrane protein (ESMP) were synthesized and evaluated *via* physiochemical characterization and *in vitro* testing for applicability as an anti-ageing product.

It was reported that the lubricant aspect of Aloe vera, enriched with vitamins and fibres, has antioxidant and hydrating gel properties that protect the skin from radiation and thermal or solar burn. It has a prophylactic effect on damaged skin tissue through natural hydration and an antibiotic effect that leads to soothing, cooling, increased elasticity, and promotion of the youthful properties of skin. Clinically, different products are approved to treat skin problems, promote wound healing, slow ageing, heal scratches, and as cleansers to purge the body or skin of impurities (Roth et al., 2001; Surjushe et al., 2008).

Another essential component of healthy skin is hyaluronan or hyaluronic acid. It is a significant component of ESM and has the potential to retain water molecules by efficiently binding to them, thereby maintaining the moisture content of the cell (Papakonstantinou et al., 2012; Burokas et al., 2017). Additionally, the organic components hyaluronic acid, proteoglycans, and collagen in ESM enhance cellular activity and collagen synthesis and inhibit the effects of UV light exposure, thereby preventing premature cell-ageing and inflammation and promoting regeneration of healthy cells (Zhao and Chi, 2009; Kulshreshtha et al., 2020). Hence, ESM is a potentially rich source of components from which to produce beauty products, such as anti-inflammatory creams/lotions, anti-wrinkle agents, antimicrobial wound-healing agents, and moisture-retaining products (Pinsky, 2017; Marimuthu et al., 2020).

Citrus fruits are rich sources of vitamin C, and α-hydroxy acid has natural antibacterial and antioxidant properties. They play vital roles in deferring ageing by enhancing the synthesis of collagen to improve the elasticity and flexibility of the dermal layer of the skin (Pullar et al., 2017; Miastkowska and Sikora, 2018). Products containing citrus fruit extracts have been used medically and sold commercially as skin lighting, dark-spot removal, and anti-wrinkle agents.

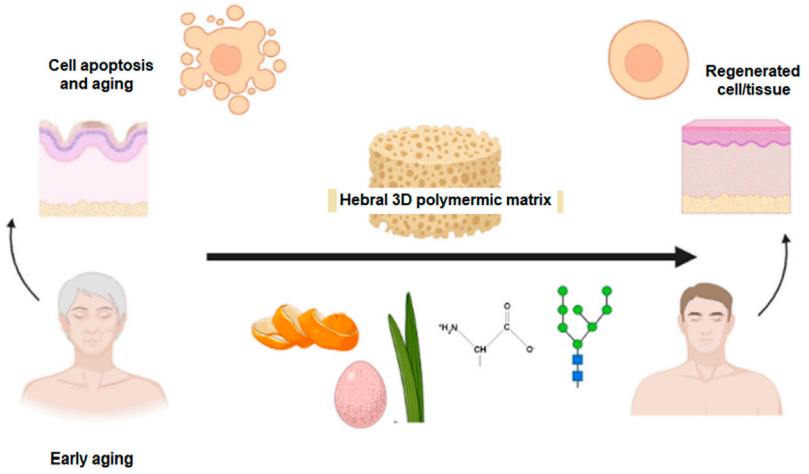

FIGURE 1
Graphical abstract.

Researchers have fabricated alginate beads for the entrapment of bioactive or drug molecules and made polymeric blends containing *Aloe vera*, ESM hydrolysate, and curcumin; these natural matrices for the delivery of therapeutic products for wound dressing and tissue regeneration have demonstrated significant benefit (Pereira, 2013; Shi et al., 2014; Yagi et al., 2018).

The importance of this study is in the development of polymeric beads from natural sources and evaluation of the beads in their capacity to be used in a skin-friendly, biocompatible, non-allergenic, and biodegradable form that is eco-friendly. The bio-polymeric blend of alginate, orange peel powder, and *Aloe vera* enriched with bioactive agents was used in fabrication of the foaming beads with entrapped ESMP at different concentrations (Figure 1). The foaming beads were used as a natural 3D bioactive porous matrix that is a novel formulation for study of the synergistic effects of all components on cellular pathways related to tissue regeneration and remodeling, with the aim of delaying cell apoptosis and/or ageing.

Materials and methods

Materials

Raw material for fabricating bio-polymeric beads was collected, including raw eggshell, orange peel from the campus canteen, and fresh *Aloe vera* leaves from the kitchen garden. Other reagents, including alginate, ethanol, phosphate-buffered saline (PBS), calcium chloride, and acetic acid were purchased from HI media Laboratories, India. All the reagents/chemicals used for fabricating hydrogel beads and in their characterization were of cell culture grade.

Bead fabrication

Bio-polymeric herbal beads of alginate, Aloe vera, and orange peel extract with entrapped ESMP were synthesized using the drop-extrusion crosslinking method in calcium chloride solution. Subsequently, characterization of fabricated samples was carried out to evaluate their applicability in anti-ageing and cell regeneration processes.

(a) ESMP preparation: ESMP solution was prepared according to the previously published protocol (Strohbehn et al., 2013), which is described as follows: briefly, the collected raw eggshell was thoroughly cleaned with double distilled water (ddH2O) and dried at 50°C for 30 min. After drying, the eggshell was soaked in 70% acetic acid for 24 h, with subsequent washing of the decalcified eggshell membrane with ddH2O. Next, the ESMP was dried at 50°C for 4 h and a fine powder was obtained by crushing the ESMP in liquid nitrogen. The ESMP powder was dissolved and incubated in an alkaline solution of sodium hydroxide (NaOH) overnight at 50°C. The dissolved sample was centrifuged and the supernatant collected. ESMP from the solution was then neutralized and lyophilized to form a powdered sample that was stored in the refrigerator.
(b) Preparation of orange peel powder: Collected orange peel was thoroughly washed in ddH2O and dried in a hot-air oven at 37°C. After drying, a fine powder was prepared using a food grinder. The powder was stored in air-tight plastic tubes.
(c) Extraction of Aloe vera gel: Fresh Aloe vera leaves were collected from the college herbal garden. The leaves were washed thoroughly with ddH2O, and the top and bottom

TABLE 1 Composition of the components used to fabricate the ESMP-loaded alginate (A), *Aloe vera* (Av), and orange peel (OP) extract bio-polymeric beads.

Sample type	Bead composition				
	Alginate (%)	Orange powder (%)	*Aloe vera* (ml)	ESMP	$CaCl_2$ (%)
Control (A-Av-OP)	3	2	100	–	1
Sample 1 (A-Av-OP-ESMP1)	3	2	100	1 gm	1
Sample 2 (A-Av-OP-ESMP2)	3	2	100	3 gm	1
Sample 3 (A-Av-OP-ESMP5)	3	2	100	5 gm	1

layers of the leaves were peeled off. The thick, clear gel, or pulpy content of the leaves was collected at the centre. Subsequently, the pulp was blended in a grinder to produce a clear Aloe vera extract.

(d) Preparation of gel beads: Bio-polymeric beads were prepared following the previously published protocol, with some modification in bead composition (Sharma et al., 2012). We generated stable foam containing the bio-polymeric solution with alginate (3 wt %) and orange peel powder (2 wt %) in Aloe vera juice (w/v), which was incubated at 40°C for 2 h on a magnetic stirrer. After mixing, the polymer beads were prepared *via* simple drop-extrusion methods (21G syringe at a height of 10 cm), using a solution of $CaCl_2$ (1 wt %) as a crosslinking agent and ESMP at different ratios, as indicated in Table 1. ESMP was included at different concentrations (1 gm to 3 gm in 100 ml solution) to study physiochemical interaction, dose-dependent effects, and outcome variability in biological effects, as discussed in the following sections.

Fabricated beads were kept in crosslinking solution for 5 min to facilitate efficient crosslinking and ESMP entrapment, then gently washed with ddH2O to remove unbound particles and excess $CaCl_2$. Lastly, the beads were filtered and separated from the solution, then freeze-dried for prolonged storage.

Morphological analysis

The macro-structure of the bio-polymeric beads was determined visibly by macroscopic examination and size dimension (diameter in mm) measurement of a randomly selected 50 beads from each sample using a vernier caliper. However, ultra-structure of the beads was analyzed by studying the cross-sectional area of images of five randomly collected beads captured using a field emission scanning electron microscope (FESEM; QUANTA 200F FEI, Netherlands). The pore size and interconnectivity of the beads were determined by analyzing microscopic images using ImageJ software, and the average dimensions of the beads were determined.

FTIR analysis

The functional and intermolecular interaction that occurs between the samples was determined by FTIR spectra analysis. All the samples were prepared following a previously published protocol (Mackenzie and Rakel, 2006). Briefly, each sample bead was mixed with KBr at a ratio of 1: 900 and ground to a fine powder for FTIR analysis. The absorbance of each sample at wavelength 4000 to 400 cm^{-1} at 2 cm^{-1} resolution was assessed using an FTIR spectrophotometer (Thermo Nicolet, United States), and the generated spectra were analyzed.

Porosity and swelling

Good porosity is required for absorption, vascularization, transport, and release of drug molecules. Therefore, we measured the porosity (χ) of the beads using the liquid dispersion method (Sharma et al., 2012). We measured the void space in the 3D interconnected polymeric beads available to be filled up with the components of the drug/biomolecule by analyzing SEM images of the beads using Image J software, as mentioned previously. The liquid dispersion method and the following equations were used to measure the porosity and the full volume of the freshly prepared foam bead sample (n = 5):

$$\chi = \frac{V_1 - V_3}{V_t} \times 100, \quad (1)$$

$$V_t = V_2 - V_3. \quad (2)$$

In brief, polymeric beads were transferred to a graduated cylinder with a known volume of solvent (V_1); then the volume of solvent after immersion of the beads, V_2, was measured. The volume, V_3, was also measured after removal of the beads at regular time intervals. V_t represents the total volume.

Similarly, bead hydrophilicity, or swelling ratio (S), was determined by immersing the beads in 1X PBS solution for 1 h at room temperature (RT) and measuring their weight at a regular time interval of 10 min. The following equation is used to measure S (Eq. 3). Here, W_s is the weight of wet beads and W_d is the weight of dried beads.

$$S = \frac{W_s - W_d}{W_d} \times 100. \quad (3)$$

All the experiments were repeated five times ($n = 5$), and the mean value was calculated.

In vitro degradation and drug release profile

The rate of degradation of beads was used to measure their stability and was determined under non-enzymatic conditions in a PBS buffer system (Dhasmana et al., 2019). Briefly, 5 gm of each sample bead was incubated in 10 ml 1X PBS (pH 7.4) at 37°C. Beads were taken out of the buffer at regular intervals for weight measurement. The biodegradation rate or weight loss ($n = 3$) was calculated using Eq. 4:

$$\text{weight loss } \% = \frac{W_o - W_t}{W_o} \times 100, \quad (4)$$

where W_0 denotes the initial weight of the scaffold and W_t denotes the weight of the degraded scaffold at different time intervals.

The release of bioactive components from the polymeric bead surface after incubation in PBS buffer was measured using the total immersion method. The absorbance of the ESMP encapsulated bead samples was recorded using a UV-Vis spectrophotometer, and the calibration curve of ESMP (50 μg/ml) was prepared for monitoring drug release. The modified beads were immersed in 150 ml of 1X PBS and placed in a shaking water bath at 37°C. After 12 h of incubation, 2 ml of the sample were taken out at regular time intervals of 30 min, and the absorbance at 412 nm was recorded. After measuring absorbance, the sample was reintroduced into the main flask to maintain constant final volume. The drug release percentage was obtained by comparison with the standard calibration curve.

Antibacterial activity

In vitro antibacterial activity of the beads was tested against Gram-positive (*S. aureus*) and Gram-negative (*E. coli*) bacteria, as described previously (Dhasmana et al., 2019). Briefly, nutrient media was prepared. Subsequently, 2 ml of bacterial suspension or aliquots were added to a culture tube containing 10 ml MH broth, which was then labelled as the positive control culture. However, for the test sample, 5 mg beads of each sample (control and ESMP beads) were added to the culture tubes, along with MH broth and bacterial culture. After inoculation, all the culture tubes were placed in a shaker incubator at 37°C. Absorbance of the culture samples at 570 nm at different predetermined time intervals were measured by taking 2 ml of the liquid culture medium from each sample group. The generated data were then plotted as a bacterial growth curve through which the antibacterial effects of the fabricated sample beads were assessed.

Anti-oxidation analysis

Antioxidant activity of the fabricated polymeric beads was measured *in vitro* using the DPPH assay, as previously described (Eq. 5) (Enkhtuya et al., 2014). Briefly, 0.2 mM DPPH solution in 200 μL absolute ethanol and 800 μL 0.1 M Tris–HCl buffer (pH 7.4) was prepared and kept in the dark at RT. Reagents were then sequentially added to test tubes as follows: Blank contained 3.3 ml ethanol and 0.5 ml sample; the negative control contained 3.5 ml ethanol and 0.3 ml DPPH solution; and the test sample contained 0.5 ml sample, 3 ml absolute ethanol, and 0.3 ml DPPH solution. All samples were mixed well, followed by incubation for 30 min at RT. The absorbance (Abs) of each sample at 517 nm was measured using a UV-vis spectrophotometer (DU 800; Beckman Coulter, Fullerton, CA, United States).

$$\text{AA}\% = 100 - \left[\frac{Abs_{sample} - Abs_{blank}}{Abs_{control}}\right] \times 100. \quad (5)$$

Anti-inflammatory activity

For estimation of the anti-inflammatory activity of the herbal beads, the HRBC membrane sterilization method was used, as previously described (Chowdhury et al., 2014). Briefly, blood samples were collected from a healthy donor and mixed with an equal volume of sterilized Alsever's solution. Next, the blood was centrifuged at 3000 rpm to separate erythrocytes (RBC), which were then washed thoroughly with saline solution (three times), and resuspended at 10% v/v in saline solution.

Different concentrations of sample extract were then mixed separately in 1 ml PBS buffer, 2 ml hyposaline, and 0.5 ml HRBC suspension and incubated at 37°C for 30 min. Following incubation, samples were centrifuged at 3000 rpm for 20 min, and the absorbance of the supernatant at 560 nm was calculated to estimate haemoglobin content and the hemolysis percentage.

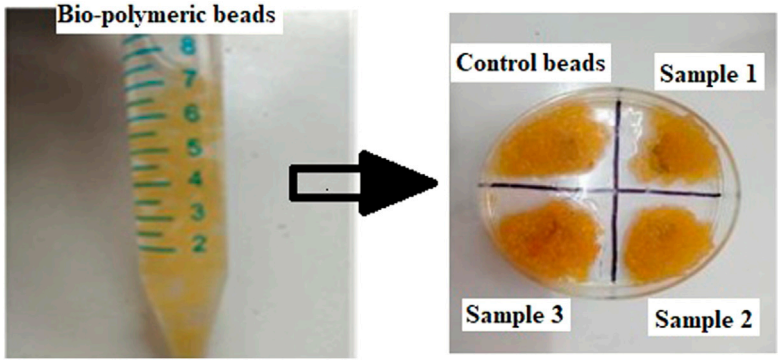

FIGURE 2
Images of the prepared bio-polymeric alginate, *Aloe vera*, and orange peel extract beads containing different concentrations of ESMP.

Here, we set the negative control group as 100%, thus allowing calculation of HRBC membrane stabilization or protection percentage using the following equation.

$$\text{HRBC membrane protection} = 100 - \left(\frac{\text{Abs of test sample}}{\text{absorbance of control}}\right)100. \quad (6)$$

In vitro biocompatibility

In vitro cell culture was used to assess biocompatibility and measure the effects of polymeric herbal bead components on cell viability and proliferation (Dhasmana et al., 2019). Briefly, 10 µl cell suspension (~1×10^3 cells), of either 3T3 mouse fibroblast cells or HeLa carcinoma cells, were seeded over the beads (control: unmodified beads; Samples 1, 2, and 3: ESMP-modified beads at different concentrations) in the tissue culture plate (TCP) wells. TCP wells containing cells cultured without beads were the negative controls. Subsequently, fresh DMEM nutrient medium (990 µl) was added to each TCP well and cells were placed in a CO_2 incubator at 37°C. After 24 h incubation, cell growth and viability were assessed using the MTT assay and by measuring the absorbance of the samples at a wavelength of 490 nm at 1, 3, 5, and 7 days using a microplate reader (TECAN, India).

Statistical analysis

All the experimental data and results were measured quantitatively and are indicated as mean ± standard deviation, with statistical analysis *via* analysis of variance (ANOVA) and calculation of p-value (<0.05) as an indicator of statistical significance.

TABLE 2 Macroscopic size (mm) and pore size (µm) dimensions of fabricated bio-polymeric beads.

Sample type	Bead size (mm)	Pore size (µm)
Control	0.5 ± 0.02	51.01 ± 0.04
Sample 1	0.56 ± 0.10	42.2 ± 0.082
Sample 2	0.73 ± 0.08	40.15 ± 0.05
Sample 3	0.82 ± 0.05	35.22 ± 0.02

Results and discussion

Morphological analysis

Bead morphology and relative size measurements (mean ± SE) were conducted through simple visualization using microscopy. The bead shape was spherical, and bead size ranged from 0.5 to 0.8 mm in diameter (Figure 2; Table 2). The bead ultrastructure represented by the cross-sectional area showed good porosity and pore size ranging from 35 to 50 µm (Figure 3). Good porosity and pore size provide better diffusion of nutrients, vascularization, and migration of cells inside the beads (Tayla et al., 2011). In a previous study, natural polymeric foaming scaffolds had good porosity of up to 90%, with spongy 3D ultrastructure for tissue engineering applications (Sharma et al., 2015). Here, the viscous and unamphiphilic nature of alginate provided good foam stability, and orange peel particles provided stability to the crosslinked matrix. Additionally, the crosslinking of the polymeric beads was performed without using any toxic crosslinking agent, but rather simple alginate bead ionic crosslinking with calcium chloride. The porous

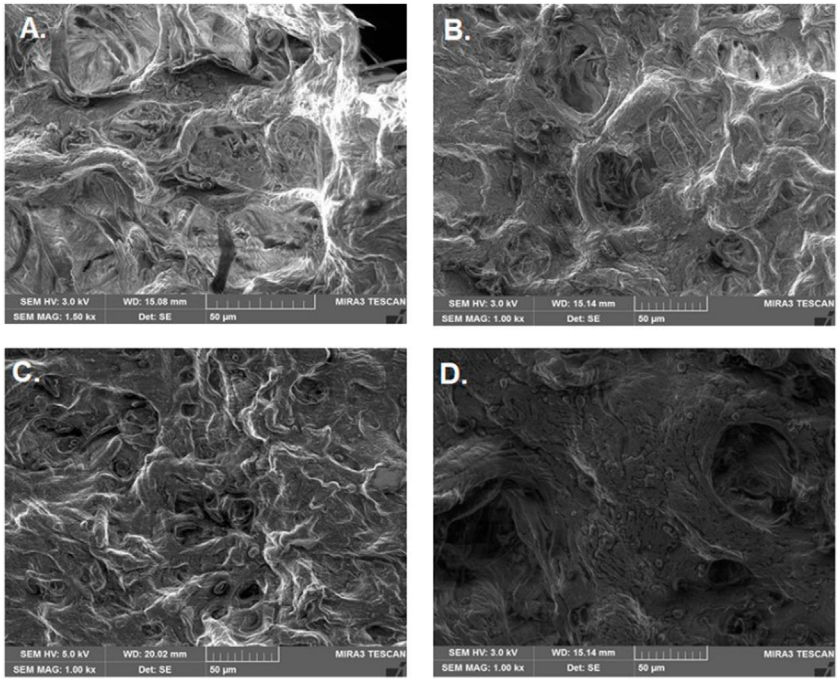

FIGURE 3
Ultrastructure of bio-polymeric beads. **(A)** Control (alginate, *Aloe vera*, and orange peel powder) and **(B–D)** modified beads having different concentrations of ESMP (1, 3, or 5 mg).

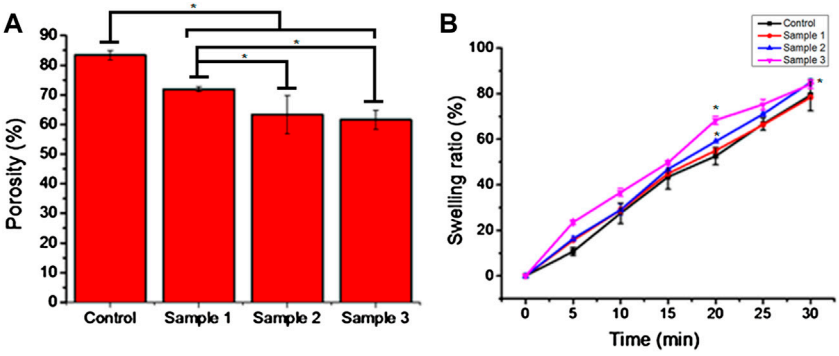

FIGURE 4
Porosity **(A)** and swelling ratio **(B)** of the bio-polymeric beads in 1X PBS solution indicate the hydrophobicity and voids in the control and ESMP-modified beads (samples 1, 2, and 3). Here, * indicates the significant difference between samples ($p < 0.05$).

matrix was designed for the enhanced encapsulation and release of bioactive components, cellular adherence, growth, and proliferation.

Porosity and swelling ratio

The porosity of beads indicates the diffusion rate of molecules through the cell membrane. All the beads demonstrated good porosity, and the porosity of the control sample beads was 80%. However, the porosity of the ESMP-containing beads was significantly reduced as we increased the concentration of ESMP, i.e., 80%–60%, which demonstrates the significant difference in the adsorption of the ESMP particles on the surface of the polymeric matrix (Figure 4A).

The bead swelling ratio or absorption rate showed an excellent rate of sorption and moisture retaining capability of the bio-polymeric beads, i.e., up to 80% (Figure 4B). In a previous

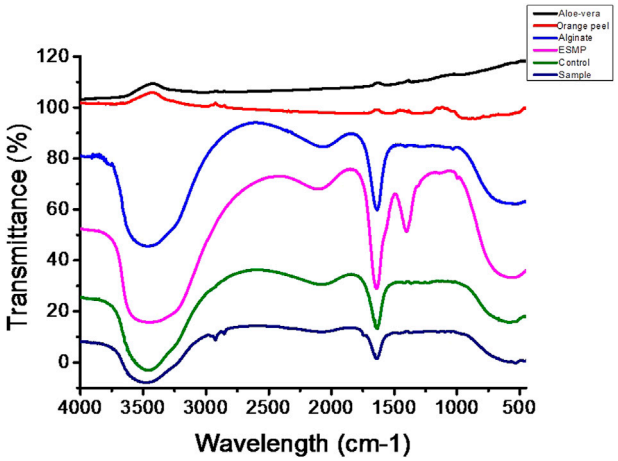

FIGURE 5
FTIR spectra of the bio-polymeric bead components, including those of control bio-polymeric beads (alginate, *Aloe vera*, orange peel), and ESMP-modified sample beads (alginate, *Aloe vera*, orange peel, ESMP).

study, hydrogel fabricated from alginate and *Aloe vera* pulp with good water absorption capacity resulted in the removal of exudate from the wound for better healing (Pereira, 2013).

The chemical composition of bio-polymeric beads has a significant amount of polymeric sugar and amino derivatives along with hydrophilic compounds present in the base-solvent, i.e., Aloe vera pulp, resulting in an excellent swelling ratio and hydrophilicity (Ranjbar-Mohammadi, 2018). Among all the samples, ESMP-containing beads changed the sorption rate most significantly compared to the control sample due to the enrichment of proteins and peptides. Researchers have fabricated ESMP-containing nanofibrous scaffold for healing cutaneous wounds due to their moisture-retaining ability (Mohammadzadeh et al., 2019). In another study, researchers reported that the soluble ESMP proteins used to synthesize hybrid grafts resulted in a controlled sorption rate and strength for better cellular interaction (Choi et al., 2020). Kevin (2020)also reported that the bio-polymeric film containing orange peel powder improves matrix stability and retains moisture for a prolonged time. Thus, all the constituents play an essential role in maintaining the polymeric bead sorption or hydrophobicity for retention of moisture and healthy skin.

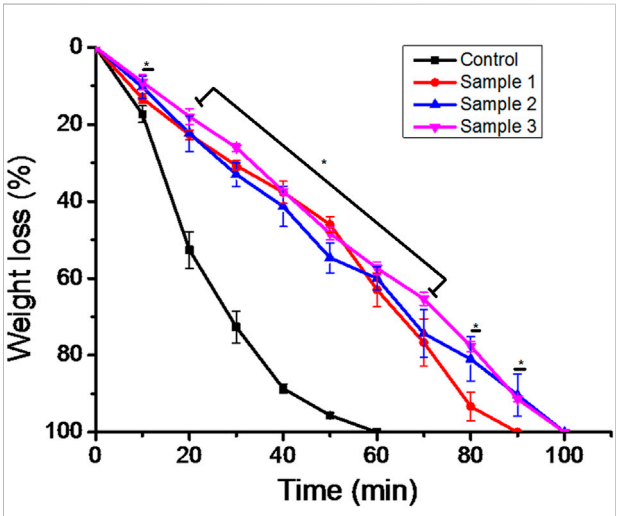

FIGURE 6
In vitro biodegradation of the bio-polymeric beads, including control and ESMP-modified samples, indicating weight loss in the non-enzymatic system of 1X PBS. Here, * indicates the significant difference between samples ($p < 0.05$).

FTIR analysis

The chemical interaction and linkage between the different constituents of bio-polymeric beads assessed *via* FTIR analysis suggested good interaction and bonding (Figure 5). The FTIR spectra of bio-polymeric bead components indicated pure extraction by the presence of functional peaks: orange peel extract—3289 cm^{-1} (O–H stretching), 1750 cm^{-1} (C=O stretching), 1267 cm^{-1} (amide III C–N group), and 1001 cm^{-1} (C–S); Alginate—3445 cm^{-1} (O–H vibration) and 1729 cm^{-1} (C=O stretching) for glucuronic and mannuronic acid units; Aloe vera—3438 cm^{-1} (O–H vibration), 2920 cm^{-1} (symmetric = CH_2 stretching), 1721 cm^{-1} (C=O stretching), and 1580 cm^{-1} (amide II, N–H bending); and ESMP→ 3492 cm^{-1} (O–H, N–H stretching), 2125 cm^{-1} (C–H stretching), 1635 cm^{-1}

(amide I C=O stretching), 1416 cm^{-1} (N–H stretching), and 587 cm^{-1} (C–S stretching), respectively. In the case of control beads of alginate, orange peel, and Aloe vera, the shifting and disappearance of orange peel and Aloe vera functional peaks indicated bonding between the functional groups. However, the stretching mode formed peaks at 3487 and 1742 cm^{-1} for the C–O, O–H, and N–H groups, with asymmetric stretching vibration of C–H bonds. Correspondingly, the ESMP-modified bio-polymeric bead sample showed the same stretching and shifting peaks as observed in the control group. Stretching at 1635, 1416, and 587 cm^{-1} relates to the stretching modes of C-O, N-H, and C-S bonds. The FTIR data confirmed the complete linkage between the functional groups of bio-polymeric bead constituents and free functional groups for better cell attachment. Likewise, other scientists have fabricated biodegradable scaffold and reported peaks for all the essential proteinaceous compounds in the regions: 3200–3500 cm^{-1}, 1600–1700 cm^{-1} (amide I), 1500–1600 cm^{-1} (amide II), and 1200–1300 cm^{-1} (amide III), respectively (Hosseini et al., 2017; Anchor and Zaghouane-Boudiaf, 2020). In another study, FTIR spectra of orange peel extract encapsulated in Ca-alginate beads indicated that the crosslinking between the functional groups results from long-term stability and biological activity of the encapsulated component (Savic Gajic et al., 2021).

In vitro biodegradability and release profile

The biodegradability of the ESMP-modified bio-polymeric beads varied as we increased the concentration of ESMP in the PBS solution (Figure 6). The weight of the sample beads decreased per data collected at regular time intervals and the beads degraded completely within 100 min. In contrast, the control beads degraded more rapidly, within 60 min of incubation, when compared to modified beads, which had prolonged time to degradation. The sample begins losing weight and, at a particular time, the level of biodegradability is constant for both samples 2 and 3. Sample 1 degraded quite early, within 90 min after the control sample, and both final samples degraded after 100 min at constant intervals. In a previous study, polymeric *Aloe vera* showed highly improved water sorption properties that resulted in a faster degradation rate due to the degradable cleavage of the polymeric network (Pereira, 2013). However, in another study, the ESM-*Aloe vera* nanofiber degradability rate significantly improved under prolonged incubation due to the leaching and hydrophilic nature of the ESM (Mohammadzadeh et al., 2019). Similarly, to improve the degradability of gellan gum, ESM was incorporated into the hydrogel fabrication, which then showed up to 30% faster degradation compared to the pure gellan gum hydrogel due to the hydrophilicity of ESM components (Choi et al., 2020). Thus, the complete degradation of all samples in non-enzymatic 1X PBS solution resulted in continuously decreasing weight after a specific time interval.

Additionally, the bead degradation and the release of active components is mandatory for measurement of their effects *in situ*. The degradation of the scaffold or matrix after implantation *in situ* results in the formation of short peptides, molecules either having a toxic effect or activating a signalling response in the dividing cells. Therefore, measuring the biodegradability and release of active components from the matrix is necessary. In recent studies, the alginate-modified drug beads have released dosages for constant and extended-release drug products (Tønnesen and Karlsen, 2002; Liew et al., 2006; Ning et al., 2018). To enhance the bioactivity of the beads, ESMP modification was carried out, and their release profile was measured, showing an initial burst release of up to 80% and subsequent controlled release of the ESMP particles entrapped in the matrix over time (Figure 7). The further compatibility of the bead matrix after degradation and release of biomolecules was measured using *in vitro* cell culture.

Antimicrobial activity

The antimicrobial activity of the bio-polymeric beads examined against both the Gram-positive *Escherichia coli* (*E. coli*) and Gram-negative *Staphylococcus aureus* (*S. auerus*) bacterial strains suppressed growth of bacterial cells over time (Figure 8). The natural component inhibited the growth of bacterial cells in the culture medium and was effective against both bacterial strains. In the control sample, bacterial cells grew steadily, but after 40 min there was a constant slope, as shown. Similarly, sample 1, after 20 min, showed the progressive growth of microbial cells, but at a lower rate than with the control beads. However, in samples 2 and 3, bacterial growth was suppressed, with a constant decrease in absorbance demonstrating the effective antibacterial properties of ESMP hydrolysates in the culture medium. With increased concentration of ESMP in the samples, the reduced absorbance indicated significant bacterial growth reduction and antibacterial effects. A previous study conveyed the antibacterial effects of the short bioactive peptide (e.g., cationic peptides and eicosanoids) at the wound site for better healing of infectious wounds (Zhang et al., 2000). It has been reported that the ESM hydrolysates have antimicrobial activity against several bacteria, including *E. coli* and *S. aureus*, suggesting their potential application to treat acne (Yoo et al., 2014).

Kevin (2020)showed that the biological property of the gelatin film improved along with increased antimicrobial effects after incorporating the orange peel powder against *E. coli* and *S. aureus*. Correspondingly, the bacterial growth in the control and modified sample beads was observed at a high rate, but gradually decreased with a time interval of 20–40 min.

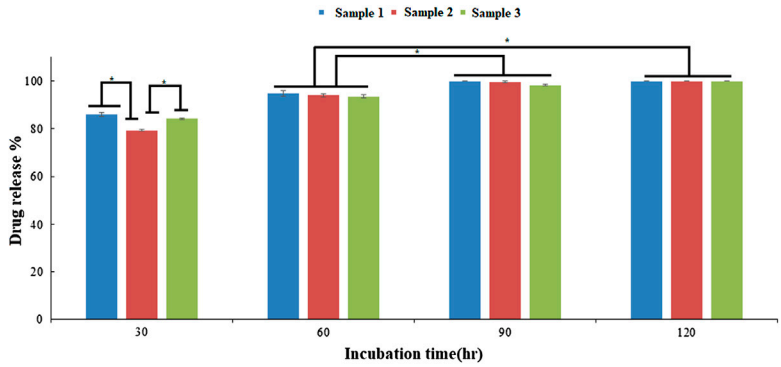

FIGURE 7
In vitro drug release profile of the ESMP entrapped bio-polymeric beads showed constant slow release of ESMP after 30 h incubation and significant progression in release over time (*p-value < 0.05).

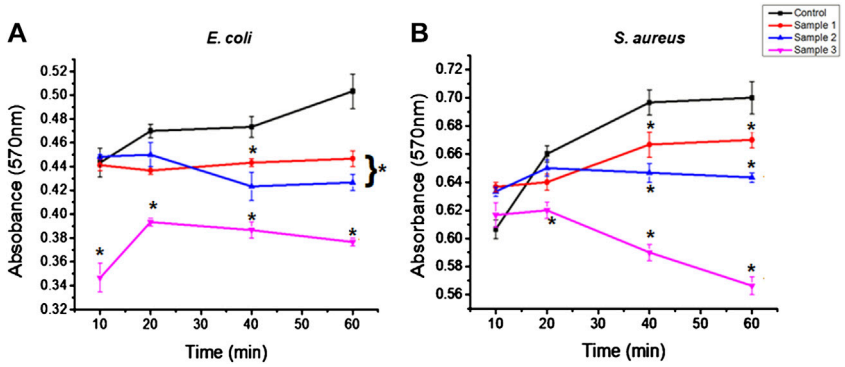

FIGURE 8
Antibacterial effects of the bio-polymeric beads, including control and modified samples, *via* inhibition of the growth of **(A)** Gram-positive and **(B)** Gram-negative bacteria. Here, * indicates the significant difference between samples ($p < 0.05$).

The antibacterial activity of ESMP was observed to be significantly better for *E. coli* than *S. aureus* and to gradually decrease during the incubation time. Thus, many researchers have fabricated skincare or healing agents containing particalized ESM for increased antimicrobial activity and superior anti-inflammatory activity against skin-associated pathogens (Li et al., 2019; Kulshreshtha et al., 2020).

In vitro antioxidant and anti-inflammatory activity

Inflammation is required for better and faster healing of wounds, but prolonged inflammation and oxidative stress due to the formation of free radicals result in chronic wounds and mutations. Thus, anti-inflammatory and anti-oxidative agents are required to suppress the prolonged inflammation, swelling, and evoked immune system to protect the cell from free radicals and delay cell death. It was reported that standard dietary agents enriched with anti-oxidative molecules suppress or inhibit the reactive oxygen species and oxygen-derived free radicals that may result in cellular ageing (Fusco et al., 2007). Many researchers found that the natural components of *Aloe vera*, orange peel, and ESM possess antioxidant and anti-inflammatory properties (Yagi et al., 2002; Das et al., 2011; Yoo et al., 2014). In our study, the bio-polymeric beads showed up to 80% antioxidant activity, with constant increase after the incorporation of ESMP powder at higher concentration in sample 3, i.e., up to 98% (Figure 9A). The HRBC stabilization assay is a standard method to measure the anti-inflammatory activity of drug components or molecules based on the RBC lysis percentage, given the similar cell membrane composition of RBC and lysosomes.

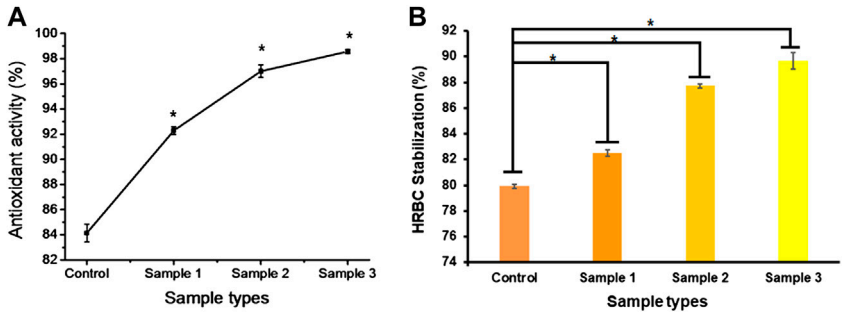

FIGURE 9
In vitro anti-oxidative **(A)** and anti-inflammatory **(B)** effects of bio-polymeric beads indicate significant antioxidant activity and cell lysis protection by natural components. Here, * indicates the significant difference between samples ($p < 0.05$).

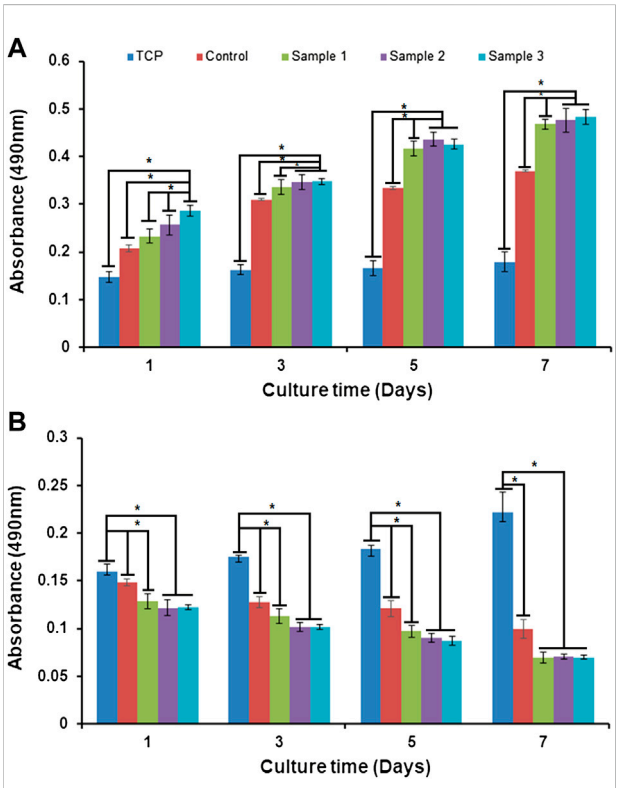

FIGURE 10
In vitro cell biocompatibility *via* MTT assay of **(A)** fibroblast cells and **(B)** carcinoma cells cultured in tissue culture plates (TCP), and with control beads or ESMP-modified sample beads. Here, * indicates the significant difference between samples ($p < 0.05$).

All the bio-polymeric beads showed up to 90% HRBC stabilization. They showed constantly reduced anti-inflammatory effects with increased ESMP powder concentration, i.e., from 90%–80% (Figure 9B), indicating a significant anti-inflammatory effect on red blood cells. Shi et al. (2014) also found potent antioxidant activity of ESM hydrolysate or peptides in human intestinal epithelium for gut healing. In another study, it was demonstrated that both processed ESM powder and its derivatives have immunomodulation and anti-inflammatory effects on immune cells, suppressing the activity of nuclear factor-κB (NF-κB), suggesting potential use as wound dressing material (Vuong et al., 2017). Recently, Savic Gajic et al.(2021)also encapsulated orange peel carotenoids in Ca-alginate beads to protect the antioxidant activity. The alginate encapsulation of natural components improved the anti-oxidative and anti-inflammatory efficiency of the bio-polymeric beads.

In vitro biocompatibility

Biopolymers, alginate, and plant–animal products are naturally biocompatible and therefore serve as non-toxic sources of components widely used in biomedical applications. Alginate is a dressing material for wound healing, encapsulation, and controlled release of biomolecules or drugs in the biological system (Dave, 2019). Additionally, the phenolic components of *Aloe vera* significantly stimulate cell proliferation and migration of skin cells to enhance wound healing (Teplicki et al., 2018). In our study, the MTT assay of cells cultured on the bio-polymeric beads showed cell viability, proliferation, and growth over time (Figure 10). The bio-polymeric matrix showed significant increases in the absorbance of samples cultured with fibroblast cells compared to carcinoma cells. The absorbance of the sample represented the cell growth, with constant increase after incorporation of ESMP components in all modified beads, which indicated biocompatibility. However, in the case of carcinoma cells cultured on beads, cell number and growth gradually decreased over time in all samples, representing toxic effects of their anti-inflammatory and anti-oxidative properties.

In another study, a bio-synthetic, biomimetic, nanofibrous scaffold containing soluble ESM and *Aloe vera* for repairing

cutaneous tissue showed improved cell proliferation over time compared to the control PVA-silk fibroin film (Mohammadzadeh et al., 2019). Recently, fabrication and evaluation of the non-toxic effects of alginate film modified with *Aloe vera* gel and cellulose nanocrystals for wound dressing application were studied (Thomas et al., 2020). The natural 3D porous polymeric matrix enriched with natural anti-oxidative, anti-inflammatory, and growth-promoting molecules resulted in good biocompatibility and anti-cancerous properties of the bio-polymeric beads. The results showed higher cell viability and proliferation with the natural bio-polymeric beads compared to the TCP, which was used as a control.

Conclusion

In this study, the bio-polymeric beads of alginate, orange peel, *Aloe vera*, and ESMP components showed good physiological and *in vitro* biological properties. We know that we need healthy cells for a healthy tissue or organ, and cell ageing is the leading cause of prolonged healing with non-functional tissue regeneration. Today, ageing, from the cellular to the individual level, is a significant problem due to unhealthy lifestyle. There are many anti-ageing products available, but at high cost. Thus, our study to cure or slow down the cell ageing process by focusing on natural by-products showed significant outcomes, such as good hydrophilicity and antibacterial, anti-inflammatory, and anti-oxidative properties that result in better cell growth. The fabricated beads consist of natural bioactive components. They are evaluated as biocompatible products *in vitro* without any significant toxic effects on regular cell lines and *vice versa* for the cancerous cell line. Thus, the fabricated natural polymeric bead components (ESMP, orange peel, *Aloe vera*) enhance their therapeutic index for slowing the ageing process and are potentially applicable as regenerative medicine for bio-functional tissue. We conclude that *in vivo* or pre-clinical trials must be performed to prove the commercial applicability of the beads as consumer-friendly products that can be used as cosmetic or therapeutic products in the same manner as current commercially available dermatological gels, creams, face wash, scrubs, and cleansing agents.

Data availability statement

The raw data supporting the conclusion of this article will be made available by the authors, without undue reservation.

Author contributions

AD and SM contributed to the conception and design of the study. AKS, AR, SM, SH and SFH organized the database. AD performed the statistical analysis. AD, SM, AC, RMA, WMSB and SH wrote the first draft of the manuscript. AD, SM, AR, MNA, SH and SFH wrote sections of the manuscript. All authors contributed to manuscript revision and read and approved the submitted version.

Acknowledgments

This research work was funded by the Institutional Fund projects under grant no. (IFPIP:1866-141-1443). The authors gratefully acknowledge technical and financial support provided by the Ministry of Education and King Abdulaziz University (KAU), Deanship of Scientific Research (DSR), Jeddah, Saudi Arabia.

Conflict of interest

The authors declare that the research was conducted in the absence of any commercial or financial relationships that could be construed as a potential conflict of interest.

Publisher's note

All claims expressed in this article are solely those of the authors and do not necessarily represent those of their affiliated organizations, or those of the publisher, the editors, and the reviewers. Any product that may be evaluated in this article, or claim that may be made by its manufacturer, is not guaranteed or endorsed by the publisher.

References

Ahmed, I. A., Mikail, M. A., Zamakshshari, N., and Abdullah, A. S. H. (2020). Natural anti-aging skincare: Role and potential. *Biogerontology* 21 (3), 293–310. doi:10.1007/s10522-020-09865-z

Anchor, A., and Zaghouane-Boudiaf, H. (2020). Single and competitive adsorption studies of two cationic dyes from aqueous mediums onto cellulose-based modified citrus peels/calcium alginate composite. *Int. J. Biol. Macromol.* 154, 1227–1236. doi:10.1016/j.ijbiomac.2019.10.277

Burokas, A., Arboleya, S., Moloney, R. D., Peterson, V. L., Murphy, K., Clarke, G., et al. (2017). Targeting the microbiota-gut-brain axis: Prebiotics have anxiolytic and antidepressant-like effects and reverse the impact of chronic stress in mice. *Biol. psychiatry* 82 (7), 472–487. doi:10.1016/j.biopsych.2016.12.031

Choi, J., Lee, J., Shin, M. E., Been, S., Lee, D. H., and Khang, G. (2020). Eggshell membrane/gellan gum composite hydrogels with increased degradability, biocompatibility, and anti-swelling properties for effective regeneration of retinal pigment epithelium. *Polymers* 12 (12), 2941. doi:10.3390/polym12122941

Chopra, D. (2015). *Quantum healing: Exploring the frontiers of mind/body medicine*. Bantam.

Chowdhury, A., Azam, S., Jainul, M. A., Faruq, K. O., and Islam, A. (2014). Antibacterial activities and *in vitro* anti-inflammatory (membrane stability) properties of methanolic extracts of Gardenia coronaria leaves. *Int. J. Microbiol.* 2014, 1–5. doi:10.1155/2014/410935

Cunliffe, W. J., Holland, D., and Jeremy, A. (2004). Comedone formation: Etiology, clinical presentation, and treatment. *Clin. dermatology* 22 (5), 367–374. doi:10.1016/j.clindermatol.2004.03.011

Das, S., Mishra, B., Gill, K., Ashraf, M. S., Singh, A. K., Sinha, M., et al. (2011). Isolation and characterization of novel protein with anti-fungal and anti-inflammatory properties from Aloe vera leaf gel. *Int. J. Biol. Macromol.* 48 (1), 38–43. doi:10.1016/j.ijbiomac.2010.09.010

Dave, V. (2019). *Alginates in pharmaceutical and biomedical application: A critique*, 95–123. doi:10.1002/9781119487999.ch6

Dhasmana, A., Singh, L., Roy, P., and Mishra, N. C. (2019). Silk fibroin protein modified acellular dermal matrix for tissue repairing and regeneration. *Mater. Sci. Eng. C* 97, 313–324. doi:10.1016/j.msec.2018.12.038

Enkhtuya, E., Kashiwagi, T., Shimamura, T., Ukeda, H., and Tseye-Oidov, O. (2014). Screening study on antioxidant activity of plants grown wildly in Mongolia. *Food Sci. Technol. Res.* 20 (4), 891–897. doi:10.3136/fstr.20.891

Finkel, T., and Holbrook, N. J. (2000). Oxidants, oxidative stress and the biology of ageing. *Nature* 408, 239–247. doi:10.1038/35041687

Fusco, D., Colloca, G., Lo Monaco, M. R., and Cesari, M. (2007). Effects of antioxidant supplementation on the aging process. *Clin. Interv. Aging* 2 (3), 377–387. PMID: 18044188; PMCID: PMC2685276.

Harley, C. B., Futcher, A. B., and Greider, C. W. (1990). Telomeres shorten during ageing of human fibroblasts. *Nature* 345 (6274), 458–460. doi:10.1038/345458a0

Hosseini, S., Eghbali Babadi, F., Masoudi Soltani, S., Aroua, M. K., Babamohammadi, S., and Mousavi Moghadam, A. (2017). Carbon dioxide adsorption on nitrogen-enriched gel beads from calcined eggshell/sodium alginate natural composite. *Process Saf. Environ. Prot.* 109, 387–399. doi:10.1016/j.psep.2017.03.021

Jemec, G. B., and Na, R. (2002). Hydration and plasticity following long-term use of a moisturizer: A single-blind study. *Acta dermato-venereologica* 82 (5), 322–324. doi:10.1080/000155502320624023

Juengst, E. T., Binstock, R. H., Mehlman, M., Post, S. G., and Whitehouse, P. (2003). Biogerontology, anti-aging medicine, and the challenges of human enhancement. *Hastings Cent. Rep.* 33 (4), 21–30. doi:10.2307/3528377

Kammeyer, A., and Luiten, R. M. (2015). Oxidation events and skin aging. *Ageing Res. Rev.* 21, 16–29. doi:10.1016/j.arr.2015.01.001

Kevin, H. T. (2020). Mechanical, physical, and bio-functional properties of biopolymer films based on gelatin as affected by enriching with orange peel powder. *Polym. Bull.*, 1–16.

Kulshreshtha, G., Ahmed, T. A. E., Wu, L., Diep, T., and Hincke, M. T. (2020). A novel eco-friendly green approach to produce particalized eggshell membrane (PEM) for skin health applications. *Biomater. Sci.* 8 (19), 5346–5361. doi:10.1039/d0bm01110j

Li, X., Cai, Z., Ahn, D. U., and Huang, X. (2019). Development of an antibacterial nanobiomaterial for wound-care based on the absorption of AgNPs on the eggshell membrane. *Colloids Surfaces B Biointerfaces* 183, 110449. doi:10.1016/j.colsurfb.2019.110449

Liew, C. V., Chan, L. W., Ching, A. L., and Heng, P. W. S. (2006). Evaluation of sodium alginate as drug release modifier in matrix tablets. *Int. J. Pharm.* 309 (1-2), 25–37. doi:10.1016/j.ijpharm.2005.10.040

Mackenzie, E. R. and Rakel, B. (Editors) (2006). "Journal of psychiatric and mental health nursing," *Complementary and alternative medicine for older adults: A guide to holistic approaches to healthy ageing* (Springer Publishing Company), 14. 1, 109–110. doi:10.1111/j.1365-2850.2007.01048.x

Marimuthu, C., Chandrasekar, P., Murugan, J., Perumal, K., Marimuthu, I., Sukumar, S., et al. (2020). Application and merits of eggshell membrane in cosmetics. *Res. Jour. Topi. Cosmet. Scie.* 11 (1), 24–31. doi:10.5958/2321-5844.2020.00006.0

Martin, G. R., Danner, D. B., and Holbrook, N. J. (1993). Aging—causes and defenses. *Annu. Rev. Med.* 44 (1), 419–429. doi:10.1146/annurev.me.44.020193.002223

Miastkowska, M., and Sikora, E. (2018). Anti-Aging properties of plant stem cell extracts. *Cosmetics* 5 (4), 55. doi:10.3390/cosmetics5040055

Miere, F. L., Teusdea, A. C., Laslo, V., Fritea, L., Moldovan, L., Costea, T., et al. (2019). Natural polymeric beads for encapsulation of Stellaria media extract with antioxidant properties. *Mat. Plast.* 56, 671–679. doi:10.37358/mp.19.4.5252

Mohammadzadeh, L., Rahbarghazi, R., Salehi, R., and Mahkam, M. (2019). A novel eggshell membrane based hybrid nanofibrous scaffold for cutaneous tissue engineering. *J. Biol. Eng.* 13 (1), 79–15. doi:10.1186/s13036-019-0208-x

Ning, C., Zhou, Z., Tan, G., Zhu, Y., and Mao, C. (2018). Electroactive polymers for tissue regeneration: Developments and perspectives. *Prog. Polym. Sci.* 81, 144–162. doi:10.1016/j.progpolymsci.2018.01.001

Panich, U., Sittithumcharee, G., Rathviboon, N., and Jirawatnotai, S. (2016). Ultraviolet radiation-induced skin aging: The role of DNA damage and oxidative stress in epidermal stem cell damage mediated skin aging. *Stem cells Int.* 2016, 1–14. doi:10.1155/2016/7370642

Papakonstantinou, E., Roth, M., and Karakiulakis, G. (2012). Hyaluronic acid: A key molecule in skin aging. *Dermato-endocrinology* 4 (3), 253–258. doi:10.4161/derm.21923

Pereira, R. F. (2013). Novel alginate/aloe vera hydrogel blends as wound dressings for the treatment of several types of wounds. *ACIDIC* 32. doi:10.3303/CET1332169

Pillai, S., Oresajo, C., and Hayward, J. (2005). Ultraviolet radiation and skin aging: Roles of reactive oxygen species, inflammation and protease activation, and strategies for prevention of inflammation-induced matrix degradation - a review. *Int. J. Cosmet. Sci.* 27 (1), 17–34. doi:10.1111/j.1467-2494.2004.00241.x

Pinsky, M. A. (2017). Efficacy and safety of an anti-aging technology for the treatment of facial wrinkles and skin moisturization. *J. Clin. Aesthet. Dermatol.* 10 (12), 27–35.

Pokorný, J., and Schmidt, S. (2001). Natural antioxidant functionality during food processing. *Antioxidants food*, 331–354. doi:10.1016/9781855736160.4.331

Pullar, J. M., Carr, A., and Vissers, M. (2017). The roles of vitamin C in skin health. *Nutrients* 9 (8), 866. doi:10.3390/nu9080866

Ranjbar-Mohammadi, M. (2018). Characteristics of aloe vera incorporated poly (ε-caprolactone)/gum tragacanth nanofibers as dressings for wound care. *J. Industrial Text.* 47 (7), 1464–1477. doi:10.1177/1528083717692595

Rittié, L., and Fisher, G. J. (2015). Natural and sun-induced aging of human skin. *Cold spring Harb. Perspect. Med.* 5 (1), a015370. doi:10.1101/cshperspect.a015370

Roth, G. S., Ingram, D. K., and Lane, M. A. (2001). Caloric restriction in primates and relevance to humans. *Ann. N. Y. Acad. Sci.* 928 (1), 305–315. doi:10.1111/j.1749-6632.2001.tb05660.x

Savic Gajic, I. M., Savic, I. M., Gajic, D. G., and Dosic, A. (2021). Ultrasound-assisted extraction of carotenoids from orange peel using olive oil and its encapsulation in Ca-alginate beads. *Biomolecules* 11 (2), 225. doi:10.3390/biom11020225

Sharma, C., Dinda, A. K., and Mishra, N. C. (2012). Synthesis and characterization of glycine modified chitosan-gelatin-alginate composite scaffold for tissue engineering applications. *J. Biomater. Tissue Eng.* 2 (2), 133–142. doi:10.1166/jbt.2012.1040

Sharma, C., Dinda, A. K., Potdar, P. D., and Mishra, N. C. (2015). Fabrication of quaternary composite scaffold from silk fibroin, chitosan, gelatin, and alginate for skin regeneration. *J. Appl. Polym. Sci.* 132 (44). doi:10.1002/app.42743

Shi, Y., Kovacs-Nolan, J., Jiang, B., Tsao, R., and Mine, Y. (2014). Antioxidant activity of enzymatic hydrolysates from eggshell membrane proteins and its protective capacity in human intestinal epithelial Caco-2 cells. *J. Funct. Foods* 10, 35–45. doi:10.1016/j.jff.2014.05.004

Sreeramulu, D., Reddy, C. V. K., Chauhan, A., Balakrishna, N., and Raghunath, M. (2013). Natural antioxidant activity of commonly consumed plant foods in India: Effect of domestic processing. *Oxidative Med. Cell. Longev.* 2013, 1–12. doi:10.1155/2013/369479

Strohbehn, R. E., Etzel, L. R., and Figgins, J. (2013). *U.S. Patent and Trademark Office* 8. Washington, DC. U.S. Patent, 425–943.

Surjushe, A., Vasani, R., and Saple, D. (2008). Aloe vera: A short review. *Indian J. dermatol.* 53 (4), 163. doi:10.4103/0019-5154.44785

Tayla, P., Mazur, E., and Mooney, D. J. (2011). Controlled architectural and chemotactic studies of 3D cell migration. *Biomaterials* 32 (10), 2634–2641. doi:10.1016/j.biomaterials.2010.12.019

Teplicki, E., Ma, Q., Castillo, D. E., Zarei, M., Hustad, A. P., Chen, J., et al. (2018). The effects of aloe vera on wound healing in cell proliferation, migration, and viability. *Wounds.* 30 (9), 263–268.

Thomas, D., Nath, M. S., Mathew, N., R, R., Philip, E., and Latha, M. (2020). Alginate film modified with aloe vera gel and cellulose nanocrystals for wound dressing application: Preparation, characterization and *in vitro* evaluation. *J. Drug Deliv. Sci. Technol.* 59, 101894. doi:10.1016/j.jddst.2020.101894

Tønnesen, H. H., and Karlsen, J. (2002). Alginate in drug delivery systems. *Drug Dev. industrial Pharm.* 28 (6), 621–630. doi:10.1081/ddc-120003853

Vuong, T. T., Ronning, S. B., Suso, H. P., Schmidt, R., Prydz, K., Lundstrom, M., et al. (2017). The extracellular matrix of eggshell displays anti-inflammatory activities through NF-κB in LPS-triggered human immune cells. *J. Inflamm. Res.* 10, 83–96. doi:10.2147/jir.s130974

Yagi, A., Kabash, A., Okamura, N., Haraguchi, H., Moustafa, S. M., and Khalifa, T. I. (2002). Antioxidant, free radical scavenging and anti-inflammatory effects of aloesin derivatives in Aloe vera. *Planta Med.* 68 (11), 957–960. doi:10.1055/s-2002-35666

Yagi, A., Megumi, H., Miiko, M., Amal, K., and Suzuka, A. (2018). Nutraceutical aloe vera gel scaffolds for supporting a healthy muscle movement. *J. Gastroenterology Hepatology Res.* 7 (6), 2720–2728. doi:10.17554/j.issn.2224-3992.2018.07.806

Yoo, J., Park, K., Yoo, Y., Kim, J., Yang, H., and Shin, Y. (2014). Effects of eggshell membrane hydrolysates on anti-inflammatory, anti-wrinkle, antimicrobial activity and moisture-protection. *Korean J. food Sci. animal Resour.* 34 (1), 26–32. doi:10.5851/kosfa.2014.34.1.26

Zhang, D. M., Cui, F., Luo, Z., Lin, Y., Zhao, K., and Chen, G. (2000). Wettability improvement of bacterial polyhydroxyalkanoates via ion implantation. *Surf. Coatings Technol.* 131 (1-3), 350–354. doi:10.1016/s0257-8972(00)00810-0

Zhao, Y. H., and Chi, Y. J. (2009). Characterization of collagen from eggshell membrane. *Biotechnology.* 8 (2), 254–258. doi:10.3923/biotech.2009.254.258

frontiers | Frontiers in Medical Technology

TYPE Review
PUBLISHED 23 December 2022
DOI 10.3389/fmedt.2022.1048951

OPEN ACCESS

EDITED BY
Binglan Yu,
Harvard Medical School, United States

REVIEWED BY
Jingxiao Chen,
Jiangnan University, China
Antony P. McNamee,
Griffith University, Australia

*CORRESPONDENCE
Hiromi Sakai
hirosakai@naramed-u.ac.jp

SPECIALTY SECTION
This article was submitted to Regenerative Technologies, a section of the journal Frontiers in Medical Technology

RECEIVED 20 September 2022
ACCEPTED 11 November 2022
PUBLISHED 23 December 2022

CITATION
Sakai H, Kure T, Taguchi K and Azuma H (2022) Research of storable and ready-to-use artificial red blood cells (hemoglobin vesicles) for emergency medicine and other clinical applications.
Front. Med. Technol. 4:1048951.
doi: 10.3389/fmedt.2022.1048951

Research of storable and ready-to-use artificial red blood cells (hemoglobin vesicles) for emergency medicine and other clinical applications

Hiromi Sakai[1]*, Tomoko Kure[1], Kazuaki Taguchi[2] and Hiroshi Azuma[3]

[1]Department of Chemistry, Nara Medical University, Kashihara, Japan, [2]Faculty of Pharmacy, Keio University, Tokyo, Japan, [3]Department of Pediatrics, Asahikawa Medical University, Asahikawa, Japan

Hemoglobin (Hb) is the most abundant protein in blood, with concentration of about 12–15 g/dl. The highly concentrated Hb solution (35 g/dl) is compartmentalized in red blood cells (RBCs). Once Hb is released from RBCs by hemolysis during blood circulation, it induces renal and cardiovascular toxicities. To date, hemoglobin-based oxygen carriers of various types have been developed as blood substitutes to mitigate the Hb toxicities. One method is Hb encapsulation in phospholipid vesicles (liposomes). Although the Hb toxicity can be shielded, it is equally important to ensure the biocompatibility of the liposomal membrane. We have developed Hb-vesicles (HbV). A new encapsulation method using a rotation-revolution mixer which enabled efficient production of HbV with a high yield has considerably facilitated R&D of HbV. Along with our academic consortium, we have studied the preclinical safety and efficacy of HbV extensively as a transfusion alternative, and finally conducted a phase I clinical trial. Moreover, carbonyl-HbV and met-HbV are developed respectively for an anti-inflammatory and anti-oxidative agent and an antidote for poisons. This review paper specifically presents past trials of liposome encapsulated Hb, biocompatible lipid bilayer membranes, and efficient HbV preparation methods, in addition to potential clinical applications of HbV based on results of our *in vivo* studies.

KEYWORDS

artificial oxygen carriers, blood substitutes, translational research, encapsulation, liposome, carbonylhemoglobin, methemoglobin (metHb)

Introduction

Blood donation and transfusion are routinely practiced for sustaining human health and welfare. Their history informs us of the important endeavors of researchers and clinicians at establishing present modes of safer blood transfusion, and we have to continue our endeavors to challenge the remaining difficulties. Screening of the donated blood for hepatitis viruses B, C and E, HIV, west Nile virus etc. by nucleic acid amplification testing (NAT) has mostly eliminated transfusion-related infections.

Nevertheless, emergent infectious viruses threaten humanity continuously. Concentrates of donated red blood cells (RBCs) can be stored in a refrigerator for 6 weeks in the US and EU, but for only 3 weeks in Japan. Rare blood-type RBCs are frozen with a cryoprotectant for long-term storage, but the cryoprotectant must be removed before infusion. Such limited storage conditions impose burdens on logistics, especially for remote islands and rural areas and stockpiling for emergency needs. Crossmatching and blood-type testing immediately before urgent transfusion are particularly time-consuming for life-saving practices. Even in economically developed countries, clinicians experience urgent situations in which blood transfusion is not available to treat patients. These difficulties have spurred us to develop artificial red cells that can eventually be substituted for RBC transfusion where blood transfusion is not available (1). Worldwide deaths from hemorrhage are estimated as 1.9 million per year, with 1.5 million resulting from physical trauma (2).

Hemoglobin (Mw. 64,500) is the most abundant protein in blood. About two million Hb molecules are compartmentalized in a single red blood cell (RBC). The intracellular Hb concentration, which is as high as 35 g/dl, makes the Hb concentration of blood as high as 12–15 g/dl. Because blood type antigens are present on the outer surface of RBCs, an early idea was to use purified Hb as an oxygen-carrying fluid that is free of any blood type. Nevertheless, that effort was unsuccessful because of various toxic effects. In spite of its abundance in blood, Hb becomes toxic when it is released from RBCs. Dissociation of tetramer Hb subunits into two dimers occurs, which proceeds to induce renal toxicity. Entrapment of a gaseous messenger molecule, NO, induces vasoconstriction, hypertension, neurological disturbances, and malfunction of esophageal motor functions (3–6). An aqueous solution of chemically modified Hb-based oxygen carriers (HBOCs) exhibits a colloid osmotic pressure that sometimes exceeds the physiological value (20–25 mmHg) in spite of its low Hb content, thereby having a potential to cause volume overload (7). Some first generation chemically modified HBOCs presented side effects in clinical trials: higher risks of myocardial infarction and death (8, 9). These side effects of molecular Hb imply the importance of the cellular structure and larger particle size of HBOCs (10).

Encapsulation of hemoglobin into liposomes to mimic red blood cells

Concept of hemoglobin encapsulation in liposomes

Pioneering Hb microencapsulation work was first performed by Chang in 1957 (11) using a polymer membrane. Japanese groups followed his attempt to test Hb encapsulation with gelatin, gum Arabic, silicone, etc. (12). Nevertheless, regulating the particle size to be appropriate for blood flow in the capillaries and obtaining sufficient biocompatibility were extremely difficult. Bangham and Horne reported in 1964 that phospholipids assemble to form vesicles in water (13), suggesting that the vesicles (liposomes) can encapsulate water-soluble functional materials in their inner phase (14). The lipid membrane of liposomes somewhat resembles a biomembrane. It should be more biocompatible than a synthetic polymer membrane. Djordjevici and Miller in 1977 first reported a liposome-encapsulated Hb (LEH) as an artificial oxygen carrier (15). Following their trial, many laboratories tested Hb encapsulation using liposomes with various lipid compositions and preparation methods (**Table 1**) (16–44). The addition of cholesterol to phospholipid is a standard method of stabilizing the packing of the lipid membrane and of reducing its curvature to produce larger liposomes. Inclusion of a negatively charged lipid is also a standard recipe to provide negative charges on the liposomal surface, which is effective to reduce the lamellarity of liposomes and to increase the volume of inner aqueous phase, thereby leading to higher Hb encapsulation efficiency (33, 45). Exceptionally, the trials of entry Nos. 3, 5, 16, 21, and 22 did not use negatively charged lipids (18, 20, 42, 43). It is noteworthy that not only liposomes but also polymersomes and other submicrometer capsules made of synthetic biodegradable polymers are tested extensively for Hb encapsulation (46–48). Detailed results of their safety and efficacy studies are awaited.

Optimal lipid compositions for stability and safety of liposome encapsulated hemoglobin

Liposome is categorized as a molecular assembly of lipids formed through hydrophobic interaction among lipids. It is generally regarded as an unstable and fragile capsule, especially when using unsaturated phospholipids such as egg yolk lecithin. To stabilize LEH for long-term storage, polymerizable phospholipids that included diacetylene or diene groups in the phospholipid molecules (entry Nos. 5 & 11) were once tested (5, 28–30). After Hb encapsulation, the lipid was polymerized by UV irradiation or gamma-ray irradiation. In the case of diene-containing phospholipid, the obtained gamma-ray irradiated LEH was so stable that it was able to be frozen and thawed or freeze-dried and rehydrated without structural damage (49). However, one difficulty was clarified from animal experiments: the polymerized liposome could not be metabolized in the reticuloendothelial system. It remained in the liver and spleen for a long time (30). Other trials include surface coverage with polymer chains, such as carboxymethyl chitin (entry No. 3) and actin (entry No. 18)

TABLE 1 Trials of liposome encapsulated Hb with various lipid compositions and preparation methods.

No.	Lipid composition for Hb encapsulation	Points of preparation method	References (Institution)
1970s–1980s			
1	L-α-phosphatidylcholine/cholesterol/palmitic acid	Sonication	(15) (Univ. of Illinois)
2	EYL/cholesterol/bovine brain PS DSPC, DPPC, or DMPC/cholesterol/dicetylphosphate or DMPG	Extrusion	(16, 17) (Naval Res. Lab.)
3	EYL/carboxymethyl chitin	Reverse phase evaporation	(18) (Sci. Univ. Tokyo)
4	EYL/cholesterol/DPPA/α-tocopherol	Reverse phase evaporation, Extrusion	(19) (Univ. California, San Francisco)
5	Diacetylene phospholipid/cholesterol UV polymerization	HbCO, Sonication	(20) (State Univ. N.Y.)
6	HSPC/cholesterol/dicetylphosphate or DMPG (Trehalose is added as a lyoprotectant.)	Microfluidizer	(21, 22) (Naval Res. Lab.)
7	EYL/cholesterol/PS/PA/α-tocopherol	Detergent dialysis	(23) (Univ. Tübingen)
1990s			
8	DSPC/cholesterol/DMPG/α-tocopherol (Trehalose is added as a lyoprotectant.)	Bovine Hb, Thin film hydration and emulsification	(24) (Naval Res. Lab.)
9	HSPC/cholesterol/myristic acid/α-tocopherol/DPPE-PEG	Microfluidizer	(25, 26) (Terumo Corp.)
10	HSPC/DMPG/α-tocopherol/carboxymethyl chitin	Reverse phase evaporation	(27) (McGill Univ.)
11	DODPC/cholesterol/octadecadienoic acid gamma-ray polymerization	HbCO, Extrusion	(28–30) (NOF Corp.)
12	EYL/cholesterol /dicetylphosphate/α-tocopherol	Freeze–thaw method	(31) (Univ. Pennsylvania)
13	DPPC/cholesterol/DPPG or palmitic acid	HbCO, Extrusion	(32, 33) (Waseda Univ.)
14	DPPC/cholesterol/DPPG/DSPE-PEG_{5000}	HbCO, Extrusion	(34) (Waseda Univ.)
15	EYL/cholesterol/α-tocopherol/eggPA	Reverse phase evaporation	(35) (Chung-Yuan Christian Univ.)
16	DSPC/cholesterol/DSPE-PEG_{5000}/α-tocopherol	αα-crosslinked human Hb, Microfluidizer	(36) (Univ. Texas San Antonio)
2000s			
17	DPPC/cholesterol/DHSG/DSPE-PEG_{5000}	HbCO, Extrusion	(37, 38) (Waseda Univ.)
18	DMPC/cholesterol/DMPG/DSPE-PEG_{2000}/actin	Extrusion	(39) (Univ. Notre Dame)
19	HSPC/cholesterol/stearic acid/DSPE-PEG_{5000}	Lipid paste rapid dispersion	(40) (Terumo Corp.)
2010s–2020s			
20	DPPC/cholesterol/HDAS/α-tocopherol/HDAS-PEG_{2000}	High pressure homogenization	(41) (Univ. Notre Dame)
21	EYL/cholesterol/DPSE-PEG_{2000}	Thin film hydration and sonication	(42) (Zhejiang Univ.)
22	DSPC/cholesterol/DSPE-PEG_{5000}	HbCO, cell disruptor	(43) (Ohio State Univ.)
23	DPPC/cholesterol/DHSG/DSPE-PEG_{5000}	HbCO, Rotation-revolution mixer for encapsulation, Decarbonylation and deoxygenation for a long-term storage	(44) (Nara Med. Univ.)

Abbreviations: EYL, egg yolk lecithin; PS, phosphatidylserine; DSPC, 1,2-distearoyl-*sn*-glycero-3-phosphatidylcholine; DPPC, 1,2-dipalmitoyl-*sn*-glycero-3-phosphatidylcholine; DMPC, 1,2-dimyristoyl-*sn*-glycero-3-phosphatidylcholine; DMPG: 1,2-dimyristoyl-*sn*-glycero-3-phosphatidylglycerol; DPPA, 1,2-dipalmitoyl-*sn*-glycero-3-phosphatidic acid; HSPC, hydrogenated soy phosphatidylcholine; DODPC, 1,2-dioctadecadienoyl-*sn*-glycero-3-phosphatidylcholine; DPPE, 1,2-dipalmitoyl-*sn*-glycero-3-phosphatidylethanolamine; DSPE, 1,2-distearoyl-*sn*-glycero-3-phosphatidylethanolamine; DHSG, 1,5-*O*-dihexadecyl-*N*-succinyl-L-glutamate; HDAS, hexadecyl-carbamoyl-methyl-hexadecanoate; HbCO, carbonylhemoglobin.

(18, 39). Rudolph et al. (23) tested freeze-drying and rehydration procedures of LEH in the presence of trehalose as a cryoprotectant as well as a lyoprotectant (entry No. 7). Since Yoshioka et al. reported PEGylation of LEH in 1989, it has become a standard method to stabilize the dispersion state during storage and during blood circulation (Entry No. 9) (50). In our research of so-called Hb-vesicles (HbV), we confirmed that deoxygenated HbV can be stored for over

two years at room temperature using a saturated phospholipid, DPPC, to avoid lipid peroxidation and the combination of PEGylation (44) (**Figure 1**). PEGylation of liposomes is generally intended to prolong their circulation half-lives by the stealth effect (51). An additional benefit of PEGylation is to improve the dispersion state of liposomes during storage and in blood plasma or in plasma expanders (52, 53).

The toxicities of Hb can be shielded by liposomal encapsulation to mimic the physiological structure of erythrocytes. However, another important point is whether the liposomal lipid membrane is sufficiently biocompatible. The surface property of liposome is an important factor to assess safety. Reducing interactions with negatively charged plasma proteins and vascular endothelial cells is important. As shown in **Table 1**, many laboratories use negatively charged phospholipid components such as phosphatidic acid (PA) (19), phosphatidyl serine (PS) (16, 17), phosphatidyl glycerol (PG), and fatty acids (32–34). Later, it was clarified that such negatively charged lipids induce complement activation or platelet activation (40, 54–58). In our case, we use DHSG as a negatively charged synthetic lipid for HbV, which does not induce complement activation or platelet activation in preclinical animal experiments (37, 38, 44, 56–58) (**Figure 1**). Numerous selections of lipid species and compositions are present to make liposomes. Fortunately, the present lipid compositions of HbV: DPPC/cholesterol/DHSG/DSPE-PEG$_{5000}$ show sufficient stability and biocompatibility.

Preparation methods of liposome encapsulated hemoglobin

Because liposomal drugs for cancer and antifungal therapies are approved and because liposomes are used experimentally as a model of biomembrane, various preparation methods have been reported (14). Traditional methods include (i) sonication, (ii) reverse phase-evaporation method using an organic solvent such as diethyl ether, ethanol, or tertial

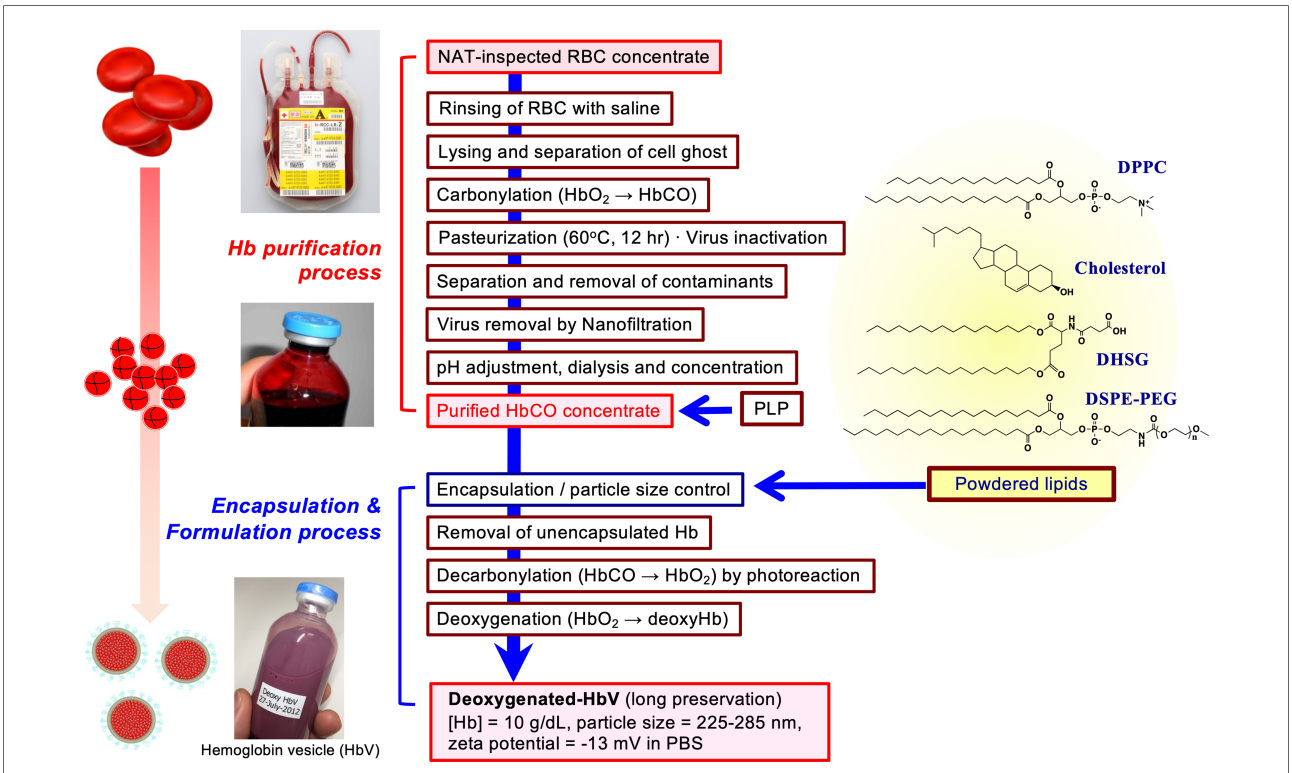

FIGURE 1
Outline of production scheme of HbV. HbCO solution was purified from nucleic acid amplification test (NAT)-inspected human red blood cells concentrate obtained from Japanese Red Cross Kinki Block Blood Center. Cells were rinsed with saline and lysed by gentle osmotic shock. The erythrocyte ghost was separated by ultrafiltration. After carbonylation, the resulting HbCO was pasteurized at 60 °C for 12 h, nano-filtrated, dialyzed, passed through anion-exchanging resins, and ultrafiltered to concentrate to 40 g/dl. Pyridoxal 5′-phosphate (PLP) was added to HbCO at the molar ratio of 1.0. The powdered lipids comprised of 1,2-dipalmitoyl-*sn*-glycero-3-phosphatidylcholine (DPPC), cholesterol, 1,5-*O*-dihexadecyl-*N*-succinyl-L-glutamate (DHSG), and 1,2-distearoyl-*sn*-glycero-3-phosphatidylethanolamine-*N*-poly(ethylene glycol) (PEG$_{5000}$, DSPE-PEG) at a molar ratio of 5:4:0.9:0.03. The HbCO encapsulation and particle size control were performed using the kneading method with a rotation–revolution mixer (44). The unencapsulated Hb was removed by ultrafiltration; HbCO in the vesicles suspended in saline solution was converted to oxyhemoglobin by photoillumination and oxygen flow. The suspension was deoxygenated completely, purged in plastic bags, and sealed with an oxygen adsorber in aluminum bags for long-term storage at 2–8 °C.

butanol, and (iii) solubilization with detergent following dialysis. However, these methods would not be appropriate for Hb encapsulation for *in vivo* use because of the possibility of denaturation of Hb as a protein and incomplete removal of an organic solvent or a detergent. Another method is (iv) extrusion (32, 38). One parameter of LEH to express the oxygen-carrying capacity is the weight ratio of Hb to total lipid: Hb/Lipid. This parameter takes in increasingly larger value with encapsulation of larger amounts of Hb in liposomes with a smaller amount of lipids. Accordingly, the concentration of Hb for encapsulation is expected to be as high as 35–45 g/dl, which is similar to the corpuscular Hb concentration in erythrocytes (35 g/dl). Such a concentrated Hb solution becomes exponentially viscous (50 cP or more) (44, 59). For encapsulation, it must be mixed with lipids (thin lipid films prepared on the inner surface of flask, or freeze-dried lipid powder) (38). The resulting highly viscous mixture is extruded through membrane filters to regulate the particle size. Here the difficulty is clogging of the filter because of the large amount of Hb and lipids. To prevent filter clogging, the amount of lipids had to be reduced to about 6 g/dl, resulting in insufficient encapsulation efficiency to only about 20%. (v) Microfluidizer was often used to reduce the liposome size by a head-on collision of fast fluid flows (21). However, the fluids require lower viscosity for the fast flow and the amount of lipid to be added to Hb is limited, resulting in lower encapsulation efficiency.

To overcome such difficulties in preparation, we developed (vi) a new kneading method with a rotation-revolution mixer (44). The Hb encapsulation efficiency was increased dramatically to about 70%, which is nearly the closest packing factor of 74%, because the kneading method enabled mixing of a highly concentrated carbonylhemoglobin (HbCO) solution (40 g/dl) and a considerably large amount of powdered lipids in only 10–20 min. The high viscosity of the Hb-lipid mixture paste (ca. 10^3–10^5 cP) favorably induces frictional heat by kneading and increases the paste temperature (ca. 60 °C), which facilitates lipid dispersion and liposome formation. During the kneading operation using a thermostable HbCO solution, Hb denaturation was prevented. After HbCO in HbV is converted to HbO_2 by photolysis, HbO_2 is converted to deoxyHb for the long-term storage of HbV. The kneading method is apparently the most suitable for the preparation of HbV made of a viscous paste of the Hb and lipids. Actually, it has enabled scaling up of HbV production and has facilitated preclinical and clinical studies in our project (60).

Safety studies of hemoglobin vesicles

The volumes of blood donation are 200 or 400 ml in Japan. It means that a hemorrhage of 400 ml blood loss does not affect physiological performance to any considerable degree. Therefore, a situation in which a blood substitute is necessary is estimated at a massive hemorrhage of 1,000 ml or more. The Hb concentration of blood is 12–15 g/dl. Blood is a concentrated RBC dispersion suspended in an aqueous solution of plasma proteins and other various solutes. Blood has physiologically adjusted viscosity, and crystalloid and colloid osmotic pressures. A blood substitute should also possess a compatible oxygen-carrying capacity and Hb concentration. In the case of HbV, the Hb concentration is adjusted to 10 g/dl, which is slightly higher than the transfusion trigger: 6–7 g/dl. Not RBCs but plasma proteins show colloid osmotic pressure of whole blood. The HbV is suspended in a physiological saline solution and the suspension does not possess colloid osmotic pressure. Therefore, HbV infusion requires co-injection or addition of plasma expanders such as human serum albumin, hydroxyethyl starch, modified fluid gelatin, or dextran depending on the situation, to adjust the colloid osmotic pressure, as does RBC transfusion (53, 61). Unlike conventional liposomal drugs used for cancer therapy, the volume of HbV for injection should be large: 16 ml/kg or more. Because of the necessity for massive infusion for HbV with high Hb and lipid concentrations, its safety in preclinical stages has been scrutinized in terms of blood compatibility, immunological (62), hematological (57), and cardiovascular effects, vital organ function, biodistribution (63, 64), excretion, etc. No hemolysis of HbV occurs during blood circulation. However, HbV is finally phagocytosed by macrophages, especially in the spleen and liver (65), which causes the main side effect of transient hepatosplenomegaly in rodent models, although the HbV in macrophage phagosomes disappears completely in two weeks; it is excreted through urine and feces (64, 66). Hemosiderin deposition, which is often observed in patients receiving repeated blood transfusion, was confirmed after repeated infusion of HbV in rats (65). All the relevant toxicological data have been reported and summarized elsewhere (67). One important physicochemical characteristic of HbV is that the HbV particles do not form any sediment after conventional centrifugation and show interference effect of "hemolysis" and "lipidemia" on blood clinical chemistry, but they do in the presence of a high molecular weight dextran. This feature enables easy separation of HbV from blood plasma specimen and contributes to accurate analyses in blood clinical chemistry to examine organ function (52).

Potential clinical applications of hemoglobin vesicles

Hemoglobin vesicles as an oxygen carrier

The efficacy of storable and ready-to-use HbV as a transfusion alternative has been tested by many animal

models in our academic consortium, as presented in Table 2 (34, 53, 68–116). The ultimate purpose for R&D of HbV is to use the HbV fluid as a transfusion alternative, especially in urgent situations when RBC transfusion is not available. In fact, HbV has demonstrated effectiveness as a resuscitative fluid in animal models of hemorrhagic shock (72–80), peri-operational or injured uncontrolled massive hemorrhage (81, 84–86), and obstetric hemorrhage (82, 83). Under such circumstances, the level of blood exchange should exceed 50%. Co-injection of a plasma expander is necessary for such extreme conditions to maintain colloid osmotic pressure and the resulting blood volume. Hagisawa et al. clarified that intraosseous infusion of HbV is possible because of its smaller particle size than RBC. It easily enters osseous blood vessels to whole body blood circulation (79). This feature is particularly beneficial when peripheral blood vessels are collapsed and inaccessible. Moreover, HbV can replace packed RBCs as a priming solution for an extracorporeal membrane oxygenator during cardiovascular surgery. As an oxygen carrier, HbV can also be used for oxygen therapeutics for local ischemic diseases, brain protection at apnea, oxygenation of tumors for sensitization (94), and as an ^{15}O carrier for positron emission tomography (95, 96), a perfusate for transplant organs (97–100), and an oxygen carrying medium for cell culturing (101). As a target dye, HbV is useful for dye laser irradiation therapy of port-wine stains (102, 103).

TABLE 2 Potential clinical application of HbV, not only as an O_2-carrier, but also a CO carrier and an antidote, evidenced by academic consortium.

State of HbV	Application	Test Animal Species	References
Deoxy-HbV* (O_2-HbV)	Isovolemic hemodilution (repeated injection at hemorrhage)	Wistar rats, SD rats	(34, 53, 68, 69)
		Syrian golden hamsters	(70, 71)
	Hemorrhagic shock	Wistar rats, Lewis rats	(72–74)
		Jpn or NZ white rabbits	(75–79)
		Beagle dogs	(80)
	Uncontrolled hemorrhage	Wistar rats	(81)
	Obstetric hemorrhage	Jpn white rabbits	(82, 83)
	Perioperational transfusion at pneumonectomy	C57BL/6 mice	(84)
		Wistar rats	(85)
		Beagle dogs	(86)
	Pre-eclampsia	Wistar rats	(87)
	Priming of ECMO	Wistar rats	(88)
	Brain ischemia	Wistar rats	(89)
	Skin flap ischemia	Syrian golden hamsters	(90)
		DDY mice	(91)
	Ischemia-reperfusion injury of heart	Wistar rat heart	(92)
	Brain protection at apnea	SD rats	(93)
	Tumor	C57BL/6 mice	(94)
	^{15}O-PET	SD rats	(95, 96)
	Organ perfusion	BALB/c mice intestine	(97)
		Wistar rat hind leg	(98)
		Cross-bred pig liver	(99, 100)
	Cell culturing	Rat hepatocyte	(101)
	Dye laser irradiation of port-wine stains	Chicken wattle	(102)
		Jpn white rabbits	(103)
CO-HbV	Hemorrhagic shock	Wistar rats	(104, 105)
	Pulmonary fibrosis	Sea-ICR mice	(106)
	Colitis	Sea-ICR mice	(107)
	Pancreatitis	Balb/cN mice, Sea-ICR mice	(108, 109)
	Dye laser irradiation of port-wine stains	Jpn white rabbits	(110)
	Cisplatin-induced acute kidney injury	ICR mice	(111)
	Tracheal transplantation	C57BL/6 mice	(112)
met-HbV	Cyanide poisoning antidote	ddY mice	(113, 114)
	Azide poisoning antidote	ddY mice	(115)
	Hydrogen sulfide poisoning antidote	ddY mice	(116)

Abbreviations: ECMO, extracorporeal membrane oxygenator; PET, positron emission tomograph.
*For oxygen delivery by O_2-HbV, the agent is stored as Deoxy-HbV before infusion.

Hemoglobin vesicles as a carbon monoxide carrier

Carbon monoxide has been tested as an anti-oxidative and anti-inflammatory agent. Direct inhalation of diluted CO gas has been reported, as have the intravenous infusion of CO-bound RBCs and various CO-releasing nanocarriers and molecules (117, 118). Studies have confirmed that CO-bound HbV (CO-HbV) is effective for resuscitation from hemorrhagic shock mitigating ischemia reperfusion injury (104, 105). Moreover, Nagao and Taguchi et al. (106–109) have clarified CO-HbV as a therapeutic agent for colitis, pancreatitis, and cisplatin-induced acute kidney injury (Table 2). After releasing CO, HbV becomes an O_2 carrier (Figure 2). For all experiments, the target molecule of CO should be enzymatic heme proteins related to generation of reactive oxygen species (ROS), such as NADPH oxidase, and cytochrome C oxidase. CO should prevent the activities of such ROS-generating enzymes. CO is well known as a poisonous gas but here, poisoning of ROS is treated by another poison: CO. It is noteworthy that histopathological studies of rat brain have clarified that CO-HbV administration did not lead to marked hippocampal damage (105). Up to 32 ml/kg dosage of CO-HbV did not induce any behavioral abnormalities and the effect of CO-HbV on the central nervous system seems minimal (119).

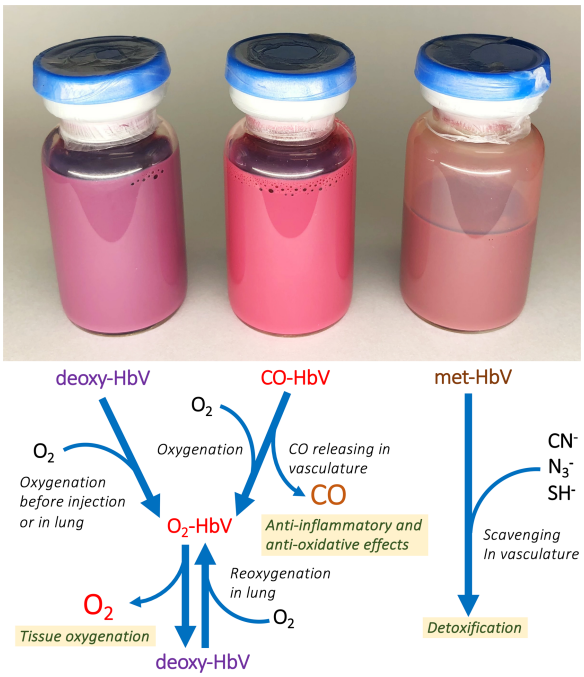

FIGURE 2
Glass vials containing deoxy-HbV, CO-HbV and met-HbV. The colors differ depending on the state of encapsulated Hb. Deoxy-HbV is for an O_2-carrier, CO-HbV for a CO carrier, and metHbV for an antidote of poisonous materials. They can all be stored for years at room temperature.

Hemoglobin vesicles as an antidote

HbO_2 in HbV gradually autoxidizes and becomes metHb, thereby losing its oxygen-carrying capacity. Stoichiometric addition of sodium nitrate to HbO_2 spontaneously converts it to metHb. Suzuki and Taguchi et al. (113–116) clarified that vesicles containing metHb (metHbV) are useful as an antidote for poisons such as cyanide, azide, and hydrogen sulfide, all of which bind strongly to metHb (**Table 2**, **Figure 2**). They confirmed the efficacies of metHbV as antidotes using rodent models. For example, the efficacy as antidotes for cyanide poisoning is higher than conventional treatments with hydroxocobalamin and nitrous acid compounds. Although such an agent would not be required frequently in normal times, it is expected to be indispensable for emergency medicine in some accident-related or disaster-affected situations.

Phase 1 study of hemoglobin vesicles as a transfusion alternative

Many laboratories have attempted Hb encapsulation using liposomes, as shown in **Table 1**. Because of difficulty in ascertaining and developing optimal lipid compositions and efficient production methods, most groups eventually terminated their development. We have continued R&D of HbV and have confirmed their safety and efficacy through abundant preclinical studies. Our new kneading method to encapsulate Hb has facilitated their large-scale production and has supported our R&D projects overall. After full consultation with the Pharmaceuticals and Medical Devices Agency (PMDA), items of evaluations using rodents and dogs under GLP guideline were set in 2016. Subsequently, GLP non-clinical safety evaluations were conducted by private contracting laboratories and were completed in 2019 (60). From 2020, we started a small-scale GMP production of HbV at the Nara Medical University Cell Processing Center. Our academic consortium initiated a phase 1 (first-in-human) study of HbV in 2020 (Registration number, jRCT2011200004) (120) with the close assistance of clinical research organizations of Asahikawa Medical University Hospital Clinical Research Support Center and Hokkaido University Hospital Clinical Research and Medical Innovation Center.

The study examined three cohorts #1, #2, and #3 ($n = 4$), respectively, of 10, 50, and 100 ml dosage. Subjective symptoms, vital signs, electrocardiography, and hematological and biochemical parameters were observed. No severe adverse event was observed for any subject. No hypertension was observed. Some infusion reactions such as fever, fatigue, and conjunctivitis were observed in cohorts #1 and #2 (120), but they resolved promptly without medication. Premedication (dexamethasone, acetaminophen, and famotidine) was introduced for the safety of subjects of cohort #3. No adverse event was observed in the first two subjects. The third subject showed local rash with wheal, which resolved soon without medication after cessation of infusion. Because the coronavirus pandemic affected project rescheduling and because the investigational agent expired, cohort #3 was terminated. No problematic clinical sign was observed from any hematological or biochemical analyte, vital sign, electrocardiograph, etc. Blood specimens of cohort #3 provided concentration profiles of HbV in plasma and revealed that HbV circulate in the bloodstream with half-life of approximately 8 h. The circulation half-life of HbV is known dose-dependent, and it will become longer at a practically higher dosage. Based on the results, we are planning the next clinical trial starting from a 100 ml dose. For that purpose, additional GLP preclinical studies, including developmental toxicity studies, are underway in the ongoing project.

Conclusion

Since the first report of the liposome encapsulated Hb, 45 years have passed. After numerous trials of various lipid compositions and preparation methods, we have ascertained the optimal lipid composition and GMP production method

of HbV, and have completed its GLP preclinical toxicological studies and the phase 1 clinical study. Based on the results, we are planning the next clinical trial starting from a 100 ml dose. As shown in Table 2, HbV is useful not only as a transfusion alternative and as an O_2 carrier, but also as a CO carrier and an antidote for poisoning, which were not expected at the beginning of R&D of HBOCs. Such vast availability to various clinical situations is expected to enhance the contributions of HbV to future human health and welfare. Both CO-HbV and met-HbV are the derivatives of O_2-HbV but different agents. Their preclinical safety and efficacy studies are the target of our research before starting clinical studies. Other HBOCs are expected to have some potential for use in the same manner.

Author contributions

All authors contributed to the article and approved the submitted version.

Funding

This research was supported partly by a Grant-in-Aid for Scientific Research from the Japan Society for the Promotion of Sciences (21H03824), Health and Labour Science Grants (Health Science Research Including Drug Innovation) from the Ministry of Health, Labour and Welfare, Japan (H24-Soyakusougou-Ippan009), and the Japan Agency for Medical Research and Development (AMED, project numbers JP15lk0201034, JP18lk1403022, JP21ym0126034).

Acknowledgments

The authors acknowledge all collaborators in the academic research consortium who contributed considerably to the production and the preclinical and the clinical studies of HbV.

Conflict of interest

HS and KT hold patents related to the production and utilization of hemoglobin vesicles. The remaining authors declare that the research was conducted in the absence of any commercial or financial relationships that could be construed as a potential conflict of interest.

Publisher's note

References

1. Chang TMS, Bulow L, Jahr J, Sakai H, Yang C. *Nanobiotherapeutic based blood substitutes*. Singapore: World Scientific Publishing Co. Pte. Ltd (2022).

2. Cannon JW. Hemorrhagic shock. *New Engl J Med*. (2018) 378(4):370–9. doi: 10.1056/NEJMe1805705

3. Doherty DH, Doyle MP, Curry SR, Vali RJ, Fattor TJ, Olson JS, et al. Rate of reaction with nitric oxide determines the hypertensive effect of cell-free hemoglobin. *Nat Biotechnol*. (1998) 16(7):672–6. doi: 10.1038/nbt0798-672

4. Murray JA, Ledlow A, Launspach J, Evans D, Loveday M, Conklin JL. The effects of recombinant human hemoglobin on esophageal motor function in humans. *Gastroenterology*. (1995) 109:1241–8. doi: 10.1016/0016-5085(95)90584-7

5. Sakai H, Hara H, Yuasa M, Tsai AG, Takeoka S, Tsuchida E, et al. Molecular dimensions of hb-based O_2 carriers determine constriction of resistance arteries and hypertension. *Am J Physiol Heart Circ Physiol*. (2000) 279:H908–15. doi: 10.1152/ajpheart.2000.279.3.H908

6. Sakai H, Sato A, Masuda K, Takeoka S, Tsuchida E. Encapsulation of concentrated hemoglobin solution in phospholipid vesicles retards the reaction with NO, but not CO, by intracellular diffusion barrier. *J Biol Chem*. (2008) 283:1508–17. doi: 10.1074/jbc.M707660200

7. Sakai H, Yuasa M, Onuma H, Takeoka S, Tsuchida E. Synthesis and physicochemical characterization of a series of hemoglobin-based oxygen carriers: objective comparison between cellular and acellular types. *Bioconjugate Chem*. (2000) 11:56–64. doi: 10.1021/bc9900789

8. Natanson C, Kern S, Lurie P, Banks SM, Wolfe SM. Cell-free hemoglobin-based blood substitutes and risk of myocardial infarction and death: a meta-analysis. *JAMA*. (2008) 299:2304–12. doi: 10.1001/jama.299.19.jrv80007

9. Burhop K, Gordon D, Estep T. Review of hemoglobin-induced myocardial lesions. *Artif Cells Blood Subst Biotechnol*. (2004) 32(3):353–74. doi: 10.1081/BIO-200027429

10. Matsuhira T, Sakai H. Artificial oxygen carriers, from nano- to micron-sized particles of hemoglobin composites substituting for red blood cells. *Particuology*. (2022) 64:43–55. doi: 10.1016/j.partic.2021.08.010

11. Chang TMS. *Artificial cells*. Springfield, Illinois: Charles C. Thomas Publisher (1972).

12. Kimoto S, Hori M, Toyoda T, Sekiguchi W. Artificial red cells. *Gekachiryou*. (1968) 19(3):324–32 (in Japanese).

13. Bangham AD, Horne RW. Negative staining of phospholipids and their structure modification by surface-active agents as observed in the electron microscope. *J Mol Biol*. (1964) 8:660–8. doi: 10.1016/S0022-2836(64)80115-7

14. Pattni BS, Chupin VV, Torchilin VP. New developments in liposomal drug delivery. *Chem Rev*. (2015) 115(19):10938–66. doi: 10.1021/acs.chemrev.5b00046

15. Djordjevich L, Miller IF. Lipid encapsulated hemoglobin as a synthetic erythrocyte. *Fed Proc*. (1977) 36:567.

16. Gaber BP, Yager P, Sheridan JP, Chang EL. Encapsulation of hemoglobin in phospholipid vesicles. *FEBS Lett*. (1983) 153:285–8. doi: 10.1016/0014-5793(83)80625-5

17. Farmer MC, Gaber BP. Liposome-encapsulated hemoglobin as an artificial oxygen carrying system. *Methods Enzymol*. (1987) 149:184–200. doi: 10.1016/0076-6879(87)49056-3

18. Kato A, Arakawa M, Kondo T. Liposome-type artificial red blood cells stabilized with carboxymethylchitin. *Nippon Kagaku Kaishi*. (1984) 6:987–91 (in Japanese). doi: 10.1246/nikkashi.1984.987

19. Hunt CA, Burnette RR, MacGregor RD, Strubbe AE, Lau DT, Taylor N, et al. Synthesis and evaluation of prototypal artificial red cells. *Science*. (1985) 230:1165–8. doi: 10.1126/science.4071041

20. Hayward JA, Levine DM, Neufeld L, Simon SR, Johnston DS, Chapman D. Polymerized liposomes as stable oxygen-carriers. *FEBS Lett*. (1985) 187:261–6. doi: 10.1016/0014-5793(85)81255-2

21. Beissinger RL, Farmer MC, Gossage JL. Liposome-encapsulated hemoglobin as a red cell surrogate. *ASAIO Trans*. (1986) 32:58–63.

22. Rudolph AS. The freeze-dried preservation of liposome encapsulated hemoglobin: a potential blood substitute. *Cryobiology*. (1988) 25:277–84. doi: 10.1016/0011-2240(88)90036-3

23. Jopski B, Pirkl V, Jaroni H-W, Schubert R, Schmidt K-H. Preparation of hemoglobin-containing liposomes using octyl glucoside and octyltetraoxyethylene. *Biochim Biophys Acta*. (1989) 978:79–84. doi: 10.1016/0005-2736(89)90501-4

24. Rabinovici R, Rudolph AS, Vernick J, Feuerstein G. A new salutary resuscitative fluid: liposome encapsulated hemoglobin/hypertonic saline solution. *J Trauma*. (1993) 35:121–7. doi: 10.1097/00005373-199307000-00019

25. Yoshioka H. Surface modification of haemoglobin-containing liposomes with poly(ethylene glycol) prevents liposome aggregation in blood plasma. *Biomaterials*. (1991) 12:861–4. doi: 10.1016/0142-9612(91)90075-L

26. Takahashi A. Characterization of neo red cells (NRCs), their function and safety in vivo tests. *Artif Cells Blood Substitutes Immobil Biotechnol*. (1995) 23:347–54. doi: 10.3109/10731199509117951

27. Mobed M, Chang TMS. Preparation and surface characterization of carboxymethylchitin-incorporated submicron bilayer-lipid membrane artificial cells (liposomes) encapsulating hemoglobin. *Biomater Artif Cells Immobilization Biotechnol*. (1991) 19:731–44. doi: 10.3109/10731199109117851

28. Sato T, Kobayashi K, Sekiguchi S, Tsuchida E. Characteristics of artificial red cells: hemoglobin-encapsulated in poly-lipid vesicles. *ASAIO J*. (1992) 38:M580–4. doi: 10.1097/00002480-199207000-00102

29. Sakai H, Takeoka S, Yokohama H, Nishide H, Tsuchida E. Encapsulation of Hb into unsaturated lipid vesicles and gamma-ray polymerization. *Polymer Adv Technol*. (1992) 3:389–94. doi: 10.1002/pat.1992.220030704

30. Akama K, Awai K, Yano Y, Tokuyama S, Nakano Y. In vitro and in vivo stability of polymerized mixed liposomes composed of 2,4-octadecadienoyl groups of phospholipids. *Polymer Adv Technol*. (2000) 11:280–7. doi: 10.1002/1099-1581(200006)11:6<280::AID-PAT942>3.0.CO;2-C

31. Liu L, Yonetani T. Preparation and characterization of liposome-encapsulated haemoglobin by a freeze–thaw method. *J Microencapsulation*. (1994) 11:409–21. doi: 10.3109/02652049409034258

32. Sakai H, Hamada K, Takeoka S, Nishide H, Tsuchida E. Physical properties of hemoglobin vesicles as red cell substitutes. *Biotechnol Progr*. (1996) 12:119–25. doi: 10.1021/bp950068w

33. Takeoka S, Ohgushi T, Terase K, Tsuchida E. Layer-controlled hemoglobin vesicles by interaction of hemoglobin with a phospholipid assembly. *Langmuir*. (1996) 12:1755–9. doi: 10.1021/la940936j

34. Sakai H, Takeoka S, Park SI, Kose T, Izumi Y, Yoshizu A, et al. Surface-modification of hemoglobin vesicles with poly(ethylene glycol) and effects on aggregation, viscosity, and blood flow during 90%-exchange transfusion in anesthetized rats. *Bioconjugate Chem*. (1997) 8:23–30. doi: 10.1021/bc960069p

35. Chung TW, Peng IH. An engineering model to characterize oxygen transfer rates for liposome encapsulated hemoglobin (LEH). *Artif Cells Blood Substit Immobil Biotechnol*. (1998) 26(4):389–98. doi: 10.3109/10731199809117680

36. Phillips WT, Klipper RW, Awasthi VD, Rudolph AS, Cliff R, Kwasiborski V, et al. Polyethylene glycol-modified liposome-encapsulated hemoglobin: a long circulating red cell substitute. *J Pharmacol Exp Ther*. (1999) 288:665–70. https://jpet.aspetjournals.org/content/288/2/665.long

37. Sakai H, Takeoka S, Wettstein R, Tsai AG, Intaglietta M, Tsuchida E. Systemic and microvascular responses to the hemorrhagic shock and resuscitation with hb-vesicles. *Am J Physiol Heart Circ Physiol*. (2002) 283:H1191–9. doi: 10.1152/ajpheart.00080.2002

38. Sou K, Naito Y, Endo T, Takeoka S, Tsuchida E. Effective encapsulation of proteins into size-controlled phospholipid vesicles using freeze-thawing and extrusion. *Biotechnol Progr*. (2003) 19:1547–52. doi: 10.1021/bp0201004

39. Li S, Nickels J, Palmer AF. Liposome-encapsulated actin-hemoglobin (LEAcHb) artificial blood substitutes. *Biomaterials*. (2005) 26:3759–69. doi: 10.1016/j.biomaterials.2004.09.015

40. Pape A, Kertscho H, Meier J, Horn O, Laout M, Steche M, et al. Improved short-term survival with polyethylene glycol modified hemoglobin liposomes in critical normovolemic anemia. *Intensive Care Med*. (2008) 34:1534–43. doi: 10.1007/s00134-008-1082-z

41. Yadav VR, Nag O, Awasthi V. Biological evaluation of liposome-encapsulated hemoglobin surface-modified with a novel PEGylated nonphospholipid amphiphile. *Artif Organs*. (2014) 38(8):625–33. doi: 10.1111/aor.12304

42. Li W, Yang J, Luo L, Jiang M, Qin B, Yin H, et al. Targeting photodynamic and photothermal therapy to the endoplasmic reticulum enhances immunogenic cancer cell death. *Nat Commun*. (2019) 10(1):3349. doi: 10.1038/s41467-019-11269-8

43. Banerjee U, Wolfe S, O'Boyle Q, Cuddington C, Palmer AF. Scalable production and complete biophysical characterization of poly(ethylene glycol) surface conjugated liposome encapsulated hemoglobin (PEG-LEH). *PLoS ONE*. (2022) 17(7):e0269939. doi: 10.1371/journal.pone.0269939

44. Kure T, Sakai H. Preparation of artificial red blood cells (hemoglobin vesicles) using the rotation-revolution mixer for high encapsulation efficiency. *ACS Biomater Sci Eng*. (2021) 7(6):2835–44. doi: 10.1021/acsbiomaterials.1c00424

45. Sou K. Electrostatics of carboxylated anionic vesicles for improving entrapment capacity. *Chem Phys Lipids*. (2011) 164(3):211–5. doi: 10.1016/j.chemphyslip.2011.01.002

46. Rameez S, Bamba I, Palmer AF. Large scale production of vesicles by hollow fiber extrusion: a novel method for generating polymersome encapsulated hemoglobin dispersions. *Langmuir*. (2010) 26(7):5279–85. doi: 10.1021/la9036343

47. Coll-Satue C, Jansman MMT, Thulstrup PW, Hosta-Rigau L. Optimization of hemoglobin encapsulation within PLGA nanoparticles and their investigation as potential oxygen carriers. *Pharmaceutics*. (2021) 13(11):1958. doi: 10.3390/pharmaceutics13111958

48. Mittal N, Rogers S, Dougherty S, Wang Q, Moitra P, Brummet M, et al. Erythromer (EM), a nanoscale bio-synthetic artificial red cell. In: H Liu, AD Kaue, JS Jahr, editors. *Blood substitutes and oxygen biotherapeutics*. Cham, Switzerland: Springer Nature Switzerland AG (2022). p. 253–65.

49. Wang L, Takeoka S, Tsuchida E, Tokuyama S, Mashiko T, Satoh T. Preparation of dehydrated powder of hemoglobin vesicles. *Polymers Adv Technol*. (1992) 3:17–21. doi: 10.1002/pat.1992.220030103

50. Yoshioka H, Suzuki K, Miyauchi Y. *Preventing aggregation of liposomes to use for artificial RBC in plasma by surface modification with PEG. Proceeding of the 11th annual meeting of Japanese membrane association* (1989). p. 49

51. Klibanov AL, Maruyama K, Torchilin VP, Huang L. Amphipathic polyethyleneglycols effectively prolong the circulation time of liposomes. *FEBS Lett*. (1990) 268(1):235–7. doi: 10.1016/0014-5793(90)81016-H

52. Sakai H, Tomiyama K, Masada Y, Takeoka S, Horinouchi H, Kobayashi K, et al. Pretreatment of serum containing hb-vesicels (oxygen carriers) to prevent their interference in laboratory tests. *Clin Chem Lab Med*. (2003) 41:222–31. doi: 10.1515/CCLM.2003.036

53. Sakai H, Miyagawa N, Horinouchi H, Takeoka S, Takaori M, Tsuchida E, et al. Intravenous injection of hb-vesicles (artificial oxygen carriers) after hemodilution with a series of plasma expanders (water-soluble biopolymers) in a rat repeated hemorrhage model. *Polymers Adv Technol*. (2011) 22:1216–22. doi: 10.1002/pat.1964

54. Phillips WT, Klipper R, Fresne D, Rudolph AS, Javors M, Goins B. Platelet reactivity with liposome-encapsulated hemoglobin in the rat. *Exp Hematol*. (1997) 25(13):1347–56. https://pubmed.ncbi.nlm.nih.gov/9406994/

55. Szebeni J, Fontana JL, Wassef NM, Mongan PD, Morse DS, Dobbins DE, et al. Hemodynamic changes induced by liposomes and liposome-encapsulated hemoglobin in pigs: a model for pseudoallergic cardiopulmonary reactions to liposomes. Role of complement and inhibition by soluble CR1 and anti-C5a antibody. *Circulation*. (1999) 99(17):2302–9. doi: 10.1161/01.CIR.99.17.2302

56. Sakai H, Suzuki Y, Sou K, Kano M. Cardiopulmonary hemodynamic responses to the small injection of hemoglobin vesicles (artificial oxygen carriers) in miniature pigs. *J Biomed Mater Res A*. (2012) 100(10):2668–77. doi: 10.1002/jbm.a.34208

57. Abe H, Azuma H, Yamaguchi M, Fujihara M, Ikeda H, Sakai H, et al. Effects of hemoglobin vesicles, a liposomal artificial oxygen carrier, on hematological responses, complement and anaphylactic reactions in rats. *Artif Cells Blood Substit Immobil Biotechnol*. (2007) 35(2):157–72. doi: 10.1080/10731190601188224

58. Sou K, Tsuchida E. Electrostatic interactions and complement activation on the surface of phospholipid vesicle containing acidic lipids: effect of the structure of acidic groups. *Biochim Biophys Acta*. (2008) 1778(4):1035–41. doi: 10.1016/j.bbamem.2008.01.006

59. Takeoka S, Terase K, Yokohama H, Sakai H, Nishide H, Tsuchida E. Interaction between phospholipid assemblies and hemoglobin (Hb). *J Macromol Sci Pure Appl Chem*. (1994) A31(1):97–108. doi: 10.1080/10601329409349720

60. Sakai H, Kobayashi N, Kure T, Okuda C. Translational research of hemoglobin vesicles as a transfusion alternative. *Curr Med Chem*. (2022) 29 (3):591–606. doi: 10.2174/0929867328666210412130035

61. Sakai H, Sato A, Takeoka S, Tsuchida E. Rheological properties of hemoglobin vesicles (artificial oxygen carriers) suspended in a series of plasma substitute solutions. *Langmuir*. (2007) 23:8121–8. doi: 10.1021/la7004503

62. Azuma H, Fujihara M, Sakai H. Biocompatibility of HbV: liposome-encapsulated hemoglobin molecules-liposome effects on immune function. *J Funct Biomater*. (2017) 8(3):E24. doi: 10.3390/jfb8030024

63. Sou K, Klipper R, Goins B, Tsuchida E, Phillips WT. Circulation kinetics and organ distribution of hb-vesicles developed as a red blood cell substitute. *J Pharmacol Exp Ther*. (2005) 312(2):702–9. doi: 10.1124/jpet.104.074534

64. Taguchi K, Urata Y, Anraku M, Maruyama T, Watanabe H, Sakai H, et al. Pharmacokinetic study of enclosed hemoglobin and outer lipid component after the administration of hemoglobin-vesicles as an artificial oxygen carrier. *Drug Metab Dispos*. (2009) 37:1456–63. doi: 10.1124/dmd.109.027094

65. Sakai H, Masada Y, Horinouchi H, Ikeda E, Sou K, Takeoka S, et al. Physiologic capacity of reticuloendothelial system for degradation of hemoglobin-vesicles (artificial oxygen carriers) after massive intravenous doses by daily repeated infusions for 14 days. *J Pharmacol Exp Therap*. (2004) 311:874–84. doi: 10.1124/jpet.104.073049

66. Sakai H, Horinouchi H, Tomiyama K, Ikeda E, Takeoka S, Kobayashi K, et al. Hemoglobin-vesicles as oxygen carriers: influence on phagocytic activity and histopathological changes in reticuloendothelial system. *Am J Pathol*. (2001) 159(3):1079–88. doi: 10.1016/S0002-9440(10)61783-X

67. Sakai H, Horinouchi H, Azuma H, Otagiri M, Kobayashi K. Safety evaluation of artificial red cells (hemoglobin-vesicles) as a transfusion alternative. *Artif Blood*. (2013) 21(1):36–48 (in Japanese).

68. Sakai H, Horinouchi H, Yamamoto M, Ikeda E, Takeoka S, Takaori M, et al. Acute 40 percent exchange-transfusion with hemoglobin-vesicles (HbV) suspended in recombinant human serum albumin solution: degradation of HbV and erythropoiesis in a rat spleen for 2 weeks. *Transfusion*. (2006) 46 (3):339–47. doi: 10.1111/j.1537-2995.2006.00727.x

69. Takase B, Higashimura Y, Asahina H, Masaki N, Kinoshita M, Sakai H. Intraosseous infusion of liposome-encapsulated hemoglobin (HbV) acutely prevents hemorrhagic anemia-induced lethal arrhythmias, and its efficacy persists with preventing proarrhythmic side effects in the subacute phase of severe hemodilution model. *Artif Organs*. (2022) 46(6):1107–21. doi: 10.1111/aor.14170

70. Sakai H, Tsai AG, Kerger H, Park SI, Takeoka S, Nishide H, et al. Subcutaneous microvascular responses to hemodilution with a red cell substitute consisting of polyethyleneglycol-modified vesicles encapsulating hemoglobin. *J Biomed Mater Res*. (1998) 40(1):66–78. doi: 10.1002/(SICI)1097-4636(199804)40:1<66::AID-JBM8>3.0.CO;2-P

71. Sakai H, Tsai AG, Rohlfs RJ, Hara H, Takeoka S, Tsuchida E, et al. Microvascular responses to hemodilution with hb vesicles as red blood cell substitutes: influence of O_2 affinity. *Am J Physiol Heart Circ Physiol*. (1999) 276 (2):H553–62. doi: 10.1152/ajpheart.1999.276.2.H553

72. Sakai H, Masada Y, Horinouchi H, Yamamoto M, Ikeda E, Takeoka S, et al. Hemoglobin-vesicles suspended in recombinant human serum albumin for resuscitation from hemorrhagic shock in anesthetized rats. *Crit Care Med*. (2004) 32(2):539–45. doi: 10.1097/01.CCM.0000109774.99665.22

73. Sakai H, Seishi Y, Obata Y, Takeoka S, Horinouichi H, Tsuchida E, et al. Fluid resuscitation with artificial oxygen carriers in hemorrhaged rats: profiles of hemoglobin-vesicle degradation and hematopoiesis for 14 days. *Shock*. (2009) 31(2):192–200. doi: 10.1097/SHK.0b013e31817d4066

74. Tokuno M, Taguchi K, Yamasaki K, Sakai H, Otagiri M. Long-Term stored hemoglobin-vesicles, a cellular type of hemoglobin-based oxygen carrier, has resuscitative effects comparable to that for fresh red blood cells in a rat model with massive hemorrhage without post-transfusion lung injury. *PLoS One*. (2016) 11(10):e0165557. doi: 10.1371/journal.pone.0165557

75. Yoshizu A, Izumi Y, Park S, Sakai H, Takeoka S, Horinouchi H, et al. Hemorrhagic shock resuscitation with an artificial oxygen carrier, hemoglobin vesicle, maintains intestinal perfusion and suppresses the increase in plasma tumor necrosis factor-alpha. *ASAIO J*. (2004) 50(5):458–63. doi: 10.1097/01.MAT.0000136508.51676.EF

76. Terajima K, Tsueshita T, Sakamoto A, Ogawa R. Fluid resuscitation with hemoglobin vesicles in a rabbit model of acute hemorrhagic shock. *Shock*. (2006) 25(2):184–9. doi: 10.1097/01.shk.0000192118.68295.5d

77. Hagisawa K, Kinoshita M, Takase B, Hashimoto K, Saitoh D, Seki S, et al. Efficacy of resuscitative transfusion with hemoglobin vesicles in the treatment of massive hemorrhage in rabbits with thrombocytopenic coagulopathy and its effect on hemostasis by platelet transfusion. *Shock*. (2018) 50(3):324–30. doi: 10.1097/SHK.0000000000001042

78. Hagisawa K, Kinoshita M, Takikawa M, Takeoka S, Saitoh D, Seki S, et al. Combination therapy using fibrinogen γ-chain peptide-coated, ADP-encapsulated liposomes and hemoglobin vesicles for trauma-induced massive hemorrhage in thrombocytopenic rabbits. *Transfusion*. (2019) 59(10):3186–96. doi: 10.1111/trf.15427

79. Hagisawa K, Kinoshita M, Saitoh D, Morimoto Y, Sakai H. Intraosseous transfusion of hemoglobin vesicles in the treatment of hemorrhagic shock with collapsed vessels in a rabbit model. *Transfusion*. (2020) 60(7):1400–9. doi: 10.1111/trf.15915

80. Yamamoto M, Horinouchi H, Kobayashi K, Seishi Y, Sato N, Itoh M, et al. Fluid resuscitation of hemorrhagic shock with hemoglobin vesicles in beagle dogs: pilot study. *Artif Cells Blood Substit Immobil Biotechnol*. (2012) 40(1–2):179–95. doi: 10.3109/10731199.2011.637929

81. Seishi Y, Horinouchi H, Sakai H, Kobayashi K. Effect of the cellular-type artificial oxygen carrier hemoglobin vesicle as a resuscitative fluid for prehospital treatment: experiments in a rat uncontrolled hemorrhagic shock model. *Shock*. (2012) 38(2):153–8. doi: 10.1097/SHK.0b013e31825ad7cf

82. Yuki Y, Hagisawa K, Kinoshita M, Ishibashi H, Kaneko K, Ishida O, et al. Efficacy of resuscitative infusion with hemoglobin vesicles in rabbits with massive obstetric hemorrhage. *Am J Obstet Gynecol*. (2021) 224 (4):398.e1–398.e11. doi: 10.1016/j.ajog.2020.09.010

83. Ishibashi H, Hagisawa K, Kinoshita M, Yuki Y, Miyamoto M, Kure T, et al. Resuscitative efficacy of hemoglobin vesicles for severe postpartum hemorrhage in pregnant rabbits. *Sci Rep*. (2021) 11(1):22367. doi: 10.1038/s41598-021-01835-w

84. Kohno M, Ikeda T, Hashimoto R, Izumi Y, Watanabe M, Horinouchi H, et al. Acute 40% exchange-transfusion with hemoglobin-vesicles in a mouse pneumonectomy model. *PLoS One*. (2017) 12(6):e0178724. doi: 10.1371/journal.pone.0178724

85. Hashimoto R, Kohno M, Oiwa K, Onozawa H, Watanabe M, Horinouchi H, et al. Immediate effects of systemic administration of Normal and high O_2-affinity haemoglobin vesicles as a transfusion alternative in a rat pneumonectomy model. *BMJ Open Respir Res*. (2020) 7(1):e000476. doi: 10.1136/bmjresp-2019-000476

86. Oiwa K, Kohno M, Onozawa H, Hashimoto R, Masuda R, Watanabe M, et al. Histological evaluation for the efficacy of hemoglobin vesicles in a canine pneumonectomy 30% hemorrhage model. *Artif Blood*. (2021) 29:15 (in Japanese).

87. Li H, Ohta H, Tahara Y, Nakamura S, Taguchi K, Nakagawa M, et al. Artificial oxygen carriers rescue placental hypoxia and improve fetal development in the rat pre-eclampsia model. *Sci Rep*. (2015) 5:15271. doi: 10.1038/srep15271

88. Yamazaki M, Aeba R, Yozu R, Kobayashi K. Use of hemoglobin vesicles during cardiopulmonary bypass priming prevents neurocognitive decline in rats. *Circulation*. (2006) 114(1 Suppl):I220–5. doi: 10.1161/CIRCULATIONAHA.105.000562

89. Komatsu H, Furuya T, Sato N, Ohta K, Matsuura A, Ohmura T, et al. Effect of hemoglobin vesicle, a cellular-type artificial oxygen carrier, on middle cerebral artery occlusion and arachidonic acid-induced stroke models in rats. *Neurosci Lett*. (2007) 421(2):121–5. doi: 10.1016/j.neulet.2007.04.080

90. Plock JA, Tromp AE, Contaldo C, Spanholtz T, Sinovcic D, Sakai H, et al. Hemoglobin vesicles reduce hypoxia-related inflammation in critically ischemic hamster flap tissue. *Crit Care Med*. (2007) 35(3):899–905. doi: 10.1097/01.CCM.0000257463.71761.97

91. Plock JA, Rafatmehr N, Sinovcic D, Schnider J, Sakai H, Tsuchida E, et al. Hemoglobin vesicles improve wound healing and tissue survival in critically ischemic skin in mice. *Am J Physiol Heart Circ Physiol*. (2009) 297(3):H905–10. doi: 10.1152/ajpheart.00430.2009

92. Nakajima J, Bessho M, Adachi T, Yamagishi T, Tokuno S, Horinouchi H, et al. Hemoglobin vesicle improves recovery of cardiac function after ischemia-reperfusion by attenuating oxidative stress in isolated rat hearts. *J Cardiovasc Pharmacol*. (2011) 58(5):528–34. doi: 10.1097/FJC.0b013e31822de06e

93. Naito Y, Sakai H, Inoue S, Kawaguchi M. Hemoglobin vesicles prolong the time to circulatory collapse in rats during apnea. *BMC Anesthesiol*. (2017) 17 (1):44. doi: 10.1186/s12871-017-0338-y

94. Yamamoto M, Izumi Y, Horinouchi H, Teramura Y, Sakai H, Kohno M, et al. Systemic administration of hemoglobin vesicle elevates tumor tissue oxygen tension and modifies tumor response to irradiation. *J Surg Res*. (2009) 151(1):48–54. doi: 10.1016/j.jss.2007.12.770

95. Kobayashi M, Mori T, Kiyono Y, Tiwari VN, Maruyama R, Kawai K, et al. Cerebral oxygen metabolism of rats using injectable ^{15}O-oxygen with a steady-state method. *J Cereb Blood Flow Metab*. (2012) 32(1):33–40. doi: 10.1038/jcbfm.2011.125

96. Tiwari VN, Kiyono Y, Kobayashi M, Mori T, Kudo T, Okazawa H, et al. Automatic labeling method for injectable ^{15}O-oxygen using hemoglobin-containing liposome vesicles and its application for measurement of brain oxygen consumption by PET. *Nucl Med Biol*. (2010) 37(1):77–83. doi: 10.1016/j.nucmedbio.2009.08.004

97. Verdu EF, Bercik P, Huang XX, Lu J, Al-Mutawaly N, Sakai H, et al. The role of luminal factors in the recovery of gastric function and behavioral changes after chronic Helicobacter pylori infection. *Am J Physiol Gastrointest Liver Physiol*. (2008) 295(4):G664–70. doi: 10.1152/ajpgi.90316.2008

98. Araki J, Sakai H, Takeuchi D, Kagaya Y, Tashiro K, Naito M, et al. Normothermic preservation of the rat hind limb with artificial oxygen-carrying hemoglobin vesicles. *Transplantation*. (2015) 99(4):687–92. doi: 10.1097/TP.0000000000000528

99. Shonaka T, Matsuno N, Obara H, Yoshikawa R, Nishikawa Y, Ishihara Y, et al. Impact of human-derived hemoglobin based oxygen vesicles as a machine perfusion solution for liver donation after cardiac death in a pig model. *PLoS One*. (2019) 14(12):e0226183. doi: 10.1371/journal.pone.0226183

100. Iwata H, Toriumi A, Ishii D, Yamamoto A, Sato Y, Takahashi H, et al. Applicability of hemoglobin vesicles as transplantable liver perfusion preservation solution. *Artif Blood*. (2021) 29(1):43–9.

101. Montagne K, Huang H, Ohara K, Matsumoto K, Mizuno A, Ohta K, et al. Use of liposome encapsulated hemoglobin as an oxygen carrier for fetal and adult rat liver cell culture. *J Biosci Bioeng*. (2011) 112(5):485–90. doi: 10.1016/j.jbiosc.2011.07.004

102. Rikihisa N, Watanabe S, Satoh K, Saito Y, Sakai H. Photosensitizer effects of artificial red cells on dye Laser irradiation in an animal model assuming port-wine stain treatment. *Plast Reconstr Surg*. (2017) 139(3):707e–16e. doi: 10.1097/PRS.0000000000003082

103. Shimanouchi K, Rikihisa N, Saito Y, Iuchi K, Tsumura N, Sakai H, et al. Artificial red blood cells increase large vessel wall damage and decrease surrounding dermal tissue damage in a rabbit auricle model after subsequent flashlamp-pumped pulsed-dye laser treatment. *J Dermatol*. (2021) 48(5):600–12. doi: 10.1111/1346-8138.15805

104. Sakai H, Horinouchi H, Tsuchida E, Kobayashi K. Hemoglobin vesicles and red blood cells as carriers of carbon monoxide prior to oxygen for resuscitation after hemorrhagic shock in a rat model. *Shock*. (2009) 31(5):507–14. doi: 10.1097/SHK.0b013e318188f83d

105. Okuda C, Sakai H. Effect of carbon monoxide administration using haemoglobin-vesicles on the hippocampal tissue. *Artif Cells Nanomed Biotechnol*. (2022) 50(1):1–9. doi: 10.1080/21691401.2022.2027428

106. Nagao S, Taguchi K, Sakai H, Tanaka R, Horinouchi H, Watanabe H, et al. Carbon monoxide-bound hemoglobin-vesicles for the treatment of bleomycin-induced pulmonary fibrosis. *Biomaterials*. (2014) 35(24):6553–62. doi: 10.1016/j.biomaterials.2014.04.049

107. Nagao S, Taguchi K, Miyazaki Y, Wakayama T, Chuang VT, Yamasaki K, et al. Evaluation of a new type of nano-sized carbon monoxide donor on treating mice with experimentally induced colitis. *J Control Release*. (2016) 234:49–58. doi: 10.1016/j.jconrel.2016.05.016

108. Nagao S, Taguchi K, Sakai H, Yamasaki K, Watanabe H, Otagiri M, et al. Carbon monoxide-bound hemoglobin vesicles ameliorate multiorgan injuries induced by severe acute pancreatitis in mice by their anti-inflammatory and antioxidant properties. *Int J Nanomedicine*. (2016) 11:5611–20. doi: 10.2147/IJN.S118185

109. Taguchi K, Nagao S, Maeda H, Yanagisawa H, Sakai H, Yamasaki K, et al. Biomimetic carbon monoxide delivery based on hemoglobin vesicles ameliorates acute pancreatitis in mice via the regulation of macrophage and neutrophil activity. *Drug Deliv*. (2018) 25(1):1266–74. doi: 10.1080/10717544.2018.1477860

110. Rikihisa N, Shimanouchi K, Saito Y, Sakai H, Mitsukawa N. Carbon monoxide combined with artificial blood cells acts as an antioxidant for tissues thermally damaged by dye laser irradiation. *Burns*. (2022): S0305-4179(22)00063-8. in press. doi: 10.1016/j.burns.2022.03.009. [Online ahead of print]

111. Taguchi K, Suzuki Y, Tsutsuura M, Hiraoka K, Watabe Y, Enoki Y, et al. Liposomal artificial red blood cell-based carbon monoxide donor is a potent renoprotectant against cisplatin-induced acute kidney injury. *Pharmaceutics*. (2021) 14(1):57. doi: 10.3390/pharmaceutics14010057

112. Watabe Y, Taguchi K, Sakai H, Enoki Y, Maruyama T, Otagiri M, et al. Bioinspired carbon monoxide delivery using artificial blood attenuates the progression of obliterative bronchiolitis via suppression of macrophage activation by IL-17A. *Eur J Pharm Biopharm*. (2022) 170:43–51. doi: 10.1016/j.ejpb.2021.11.011

113. Suzuki Y, Taguchi K, Kure T, Sakai H, Enoki Y, Otagiri M, et al. Liposome-encapsulated methemoglobin as an antidote against cyanide poisoning. *J Control Release*. (2021) 337:59–70. doi: 10.1016/j.jconrel.2021.07.015

114. Suzuki Y, Taguchi K, Kure T, Enoki Y, Otagiri M, Sakai H, et al. Long-term pharmaceutical stability of liposome-encapsulated methemoglobin as an antidote for cyanide poisoning. *Int J Pharm*. (2021) 610:121260. doi: 10.1016/j.ijpharm.2021.121260

115. Suzuki Y, Taguchi K, Hanyu S, Kure T, Enoki Y, Otagiri M, et al. Oxidized artificial red blood cell rescues the lethal toxidrome of azide poisoning mice via recovering cytochrome c oxidase activity. *J Drug Delivery Sci Technol*. (2022) 71:103282. doi: 10.1016/j.jddst.2022.103282

116. Suzuki Y, Taguchi K, Kure T, Enoki Y, Otagiri M, Sakai H, et al. Liposomal methemoglobin as a potent antidote for hydrogen sulfide poisoning. *Toxicol Appl Pharmacol*. (2022) 450:116159. doi: 10.1016/j.taap.2022.116159

117. Siracusa R, Schaufler A, Calabrese V, Fuller PM, Otterbein LE. Carbon monoxide: from poison to clinical trials. *Trends Pharmacol Sci*. (2021) 42(5):329–39. doi: 10.1016/j.tips.2021.02.003

118. Misra H, Lickliter J, Kazo F, Abuchowski A. PEGylated carboxyhemoglobin bovine (SANGUINATE): results of a phase I clinical trial. *Artif Organs*. (2014) 38(8):702–7. doi: 10.1111/aor.12341

119. Sakai H, Yasuda S, Okuda C, Yamada T, Owaki K, Miwa Y. Examination of central nervous system by functional observation battery after massive intravenous infusion of carbon monoxide-bound and oxygen-bound hemoglobin vesicles in rats. *Curr Res Pharmacol Drug Discovery*. (2022) 3:100135. doi: 10.1016/j.crphar.2022.100135

120. Azuma H, Amano T, Kamiyama N, Takehara N, Jingu M, Takagi H, et al. First-in-human phase 1 trial of hemoglobin vesicles as artificial red blood cells developed for use as a transfusion alternative. *Blood Adv*. (2022) 6(21):5711–5. doi: 10.1182/bloodadvances.2022007977

frontiers | Frontiers in Medicine

TYPE Review
PUBLISHED 04 January 2023
DOI 10.3389/fmed.2022.1035150

OPEN ACCESS

EDITED BY
Binglan Yu,
Massachusetts General Hospital and Harvard Medical School, United States

REVIEWED BY
Chun Li,
Peking University People's Hospital, China
Thomas Ming Swi Chang,
McGill University, Canada

*CORRESPONDENCE
Lailiang Ou
✉ ouyll@nankai.edu.cn

SPECIALTY SECTION
This article was submitted to Precision Medicine, a section of the journal Frontiers in Medicine

RECEIVED 09 September 2022
ACCEPTED 29 November 2022
PUBLISHED 04 January 2023

CITATION
Yu Y and Ou L (2023) The development of immunosorbents for the treatment of systemic lupus erythematosus *via* hemoperfusion. *Front. Med.* 9:1035150. doi: 10.3389/fmed.2022.1035150

The development of immunosorbents for the treatment of systemic lupus erythematosus *via* hemoperfusion

Yameng Yu[1,2] and Lailiang Ou[1]*

[1]Key Laboratory of Bioactive Materials, Ministry of Education, College of Life Sciences, Nankai University, Tianjin, China, [2]Beijing Key Laboratory of Digital Stomatology, NMPA Key Laboratory for Dental Materials, Department of Dental Materials, Peking University School and Hospital of Stomatology, National Center of Stomatology, National Clinical Research Center for Oral Diseases, National Engineering Laboratory for Digital, Material Technology of Stomatology, Research Center of Engineering and Technology for Computerized Dentistry Ministry of Health, Beijing, China

Systemic lupus erythematosus (SLE) is an autoimmune disease (AID) that involves multiple organ systems and is characterized by elevated levels of autoantibodies (ANA) and immune complexes. The immunoadsorption technique uses an extracorporeal clearance process to remove pathogenic toxins from patients' blood and alleviate disease symptoms. An immunosorbent is a key component of the immunoadsorption system that determines therapeutic efficacy and safety. Immunosorbents are prepared by immobilizing antibodies, antigens, or ligands with specific physicochemical affinities on a supporting matrix. Immunosorbents and pathogenic toxins bind *via* affinity adsorption, which involves electrostatic interactions, hydrogen bonds, hydrophobic interactions, and van der Waals forces. Immunosorbents are classified on the basis of their interaction mechanism with toxins into three categories: non-selective, semi-selective, and highly selective. This review aimed to summarize the current status of various commercial immunosorbents that are used to treat SLE. Moreover, recent developments in immunosorbents have heightened the need for a brief discussion about specific ligands and a supporting matrix.

KEYWORDS

immunosorbent, systemic lupus erythematosus, hemoperfusion, autoimmune disease, anti-double-stranded DNA antibody

1. Introduction of immunoadsorption in the treatment of systemic lupus erythematosus

The immunoadsorption technique uses extracorporeal perfusion to selectively remove pathogenic toxins from patients with autoimmune diseases (AIDs) to purify the blood and alleviate disease symptoms (1). In contrast to traditional blood purification techniques, immunoadsorption is a novel treatment strategy based on antigen–antibody

interactions. The immunoadsorption process is therefore unique to pathogenic toxins. It is important to note that immunosorbents play an essential role in determining therapeutic efficiency and safety as a result of direct contact with pathogenic toxins and blood components. A typical immunosorbent consists of a matrix and specific ligands, such as antigens, antibodies, or a ligand with specific physicochemical affinities (2, 3). Immunoadsorption is classified into two types: plasma perfusion and whole blood perfusion (4). In the former case, plasma must be separated before purification. Instead, blood is introduced directly into the adsorption column during whole blood perfusion, where pathogenic substances are selectively adsorbed by immunosorbents. Pure blood is reintroduced into a patient's body to achieve therapeutic goals.

Systemic lupus erythematosus (SLE) is an AID that can cause immune system dysfunction, loss of autoimmune tolerance, and abnormal activation of autoreactive lymphocytes, which can cause tissue and organ damage (5, 6). SLE is characterized by the production of various antibodies against deoxyribonucleic acid (DNA). The level of anti-double-stranded DNA (anti-dsDNA) antibodies is closely related to disease activity, which can cause pathology by directly inducing cell apoptosis. In addition to their direct effects, anti-dsDNA antibodies can also exert pathogenic effects in an indirect manner *via* circulating antigen–antibody complexes that form during the course of the disease (7, 8). Therefore, the removal of anti-dsDNA antibodies is widely recognized as an efficient treatment strategy that can benefit overall clinical outcomes (9–11). Plasma exchange can remove approximately 49–89% of autoantibodies (ANA) from the plasma of a patient but adverse effects limit the technique, resulting, for example, in a reduction of essential plasma components and in the induction of allergic reactions and viral contamination (12). In 1979, Terman et al. (13) published a case report involving DNA-activated carbon as an adsorbent for the removal of anti-dsDNA antibodies from the plasma of a patient with severe SLE. Since then, a wide range of immunosorbents containing specific ligands have been developed to remove anti-dsDNA antibodies from patients' blood *via* hemoperfusion (1–3). This study discusses the latest developments of various immunosorbents, from synthetic methodologies to technical specifications and therapeutic efficiencies.

2. Ligands for immunosorbents

The binding between immunosorbents and pathogenic toxins is based on affinity adsorption, which includes electrostatic interactions, hydrogen bonds, hydrophobic interactions, and van der Waals forces (14). According to the ligand and autoantibody binding principle, immunosorbents can be classified into three categories, as illustrated in Figure 1.

2.1. Dextran sulfate

Dextran sulfate is a specific ligand widely used in SLE immunosorbents and is an anionic dextran derivative with high binding affinity to anti-dsDNA antibodies *via* the cross-reactivity of repeating negatively charged units (15, 16). Liposorber LA40 (Kanegafuchi Chemical Industry) is a blood lipid purification system that contains cellulose gels grafted with dextran sulfate to selectively remove low-density lipoproteins (LDLs) from patients with familial hypercholesterolemia. Kinoshita et al. (17) reported that the Liposorber system could be highly effective in safely removing anti-dsDNA antibodies and immune complexes from the plasma of patients with SLE. In this study, 2 L of plasma were treated with a dextran sulfate gel column, and an anti-dsDNA antibody adsorption rate was achieved at up to 40%. Other biochemical indicators besides blood lipids, such as albumin, show no significant changes during immunoadsorption. However, anti-dsDNA antibodies have a lower adsorption capacity than LDL, total cholesterol, and triglycerides, which causes atherosclerosis. Based on those results, the Selesorb column was designed to achieve higher adsorption selectivity by increasing the amount of dextran sulfate immobilization and narrowing the cellulose matrix's pore diameter to match the size of anti-dsDNA antibodies. Anti-dsDNA antibody removal efficiency significantly increased as a result of the optimized pore diameter and ligand grafting density, and it was approximately two times as high as that of the Liposorber system (18).

The Selesorb system comprises two alternate columns, each containing 150 ml of porous cellulose beads grafted with dextran sulfate ligands and connected to a regenerating apheresis unit to recover adsorption efficiency during the treatment. Currently, the Selesorb system has been successfully utilized to treat patients with SLE. The relevant case series are summarized in Table 1. Suzuki et al. (21) reported a clinical trial of six patients with SLE who received Selesorb immunoadsorption. The levels of anti-dsDNA antibodies could be rapidly reduced after 2–4 treatment procedures for all subjects, and the mean adsorbing ratio of the antibodies was ∼55.6% ± 4.6%. The symptoms improved in three subjects with proteinuria and four with lymphocytopenia after the apheresis procedure. In addition, Selesorb immunoadsorption could also remove anticardiolipin antibodies and immune complexes from the plasma of patients with SLE and improve the vascular changes and symptoms of arthralgia, rashes, and lymphocytopenia (20, 24). However, adverse events accompanied by treatment with Selesorb were also reported, including nausea, vomiting, hypotension, cardiopalmus, dizziness, chills, and thrombocytopenia. These

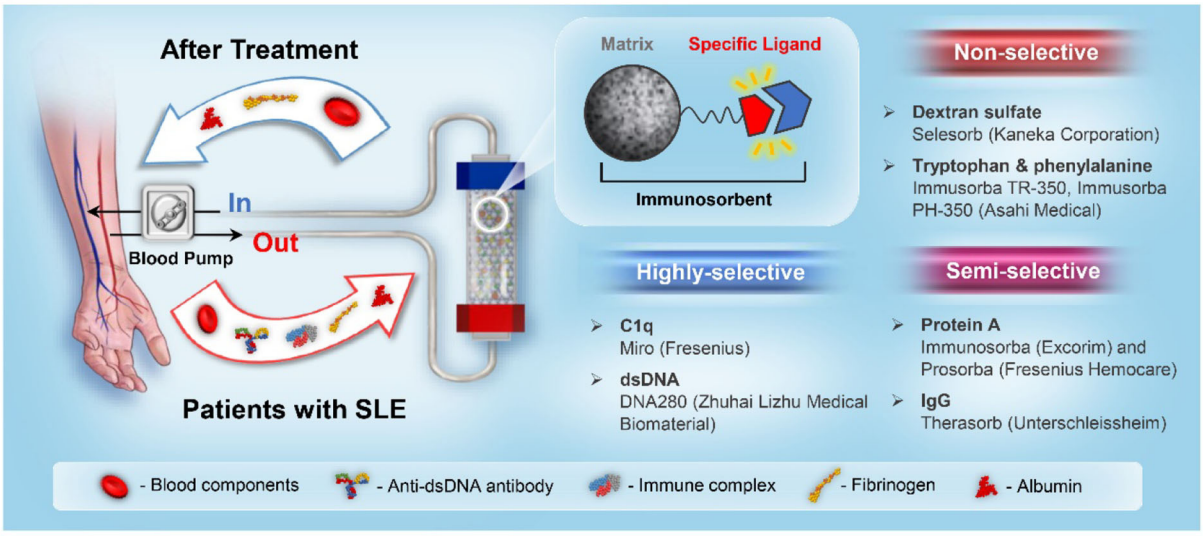

FIGURE 1
A schematic illustration of the SLE immunoadsorption system and immunosorbent classification.

TABLE 1 A summary of the case reports with the application of Selesorb in the treatment of systemic lupus erythematosus (SLE).

Subject number	Outcome parameters	Therapeutic effect	References
$n = 1$	IgG, IgM immune complexes	Restored renal function	(19)
$n = 1$	IgG, IgM, IgA, C3	Improvement of skin lesions	(20)
$n = 6$	Proteinuria, anti-dsDNA antibody, CIC	Improvement of symptoms	(21)
$n = 6$	ACL, anti-dsDNA antibody	Decreased titers of pathogenic toxins	(22)
$n = 19$	SLEDAI, anti-dsDNA antibody	Decreased titers of pathogenic toxins	(23)

symptoms were considered to be derived from hypovolemia or vasovagal reactions that are sometimes observed during extracorporeal therapies (18).

2.2. Tryptophan and phenylalanine

Tryptophan and phenylalanine can be used as ligands to develop non-biological immunosorbents for the removal of pathogenic factors, such as anti-acetylcholine receptor antibodies, anti-ganglioside antibodies, and anti-DNA antibodies, *via* physicochemical interactions, including hydrophobic force or ionic interactions. Immusorba (Asahi Medical) was the first immunosorbent product bearing non-biological ligands; this system contains two types of columns, namely Immusorba TR and Immusorba PH, depending on the immobilized amino acid of the adsorbent (25, 26). Tryptophan is used as a ligand for Immusorba TR, and phenylalanine is used as a ligand for Immusorba PH. Porous poly(vinyl alcohol), a supporting matrix, was treated with epichlorohydrin to activate the matrix, followed by covalent immobilization of tryptophan or phenylalanine to prepare adsorbents. A schematic illustration of immunoadsorption using Immusorba TR and Immusorba PH is shown in Figure 2.

An *in vitro* study demonstrated that both Immusorba TR-350 and Immusorba PH-350 possess high removal efficiencies of anti-dsDNA antibodies and circulating immune complexes (CICs) from the plasma of patients with SLE. The reduction rate of anti-dsDNA antibodies was ∼65% ± 15% on Immusorba TR-350 and 75% ± 14% on Immusorba PH-350. The reduction rate of CIC was ∼75% ± 2% on Immusorba TR-350 and 74% ± 3% on Immusorba PH-350 (27, 28). Avenhaus et al. (28) evaluated the adsorption efficiency and underlying binding mechanism of Immusorba in an *in vitro* miniature mode to simulate the immunoadsorption procedure. The average reduction rate of anti-dsDNA antibodies was significantly higher than that of both immunoglobin G (IgG) and total protein. Hydrophobic interactions served as the predominant force in the binding between the ligand phenylalanine and pathogenic antibodies. Sugimoto et al. (29) reported a clinical trial of six patients with lupus nephritis (LN) associated with proteinuria and abnormal sedimentation on urinalysis. Those patients were treated by immunoadsorption plasmapheresis using Immusorba PH-350. The levels of anti-DNA antibodies decreased significantly after

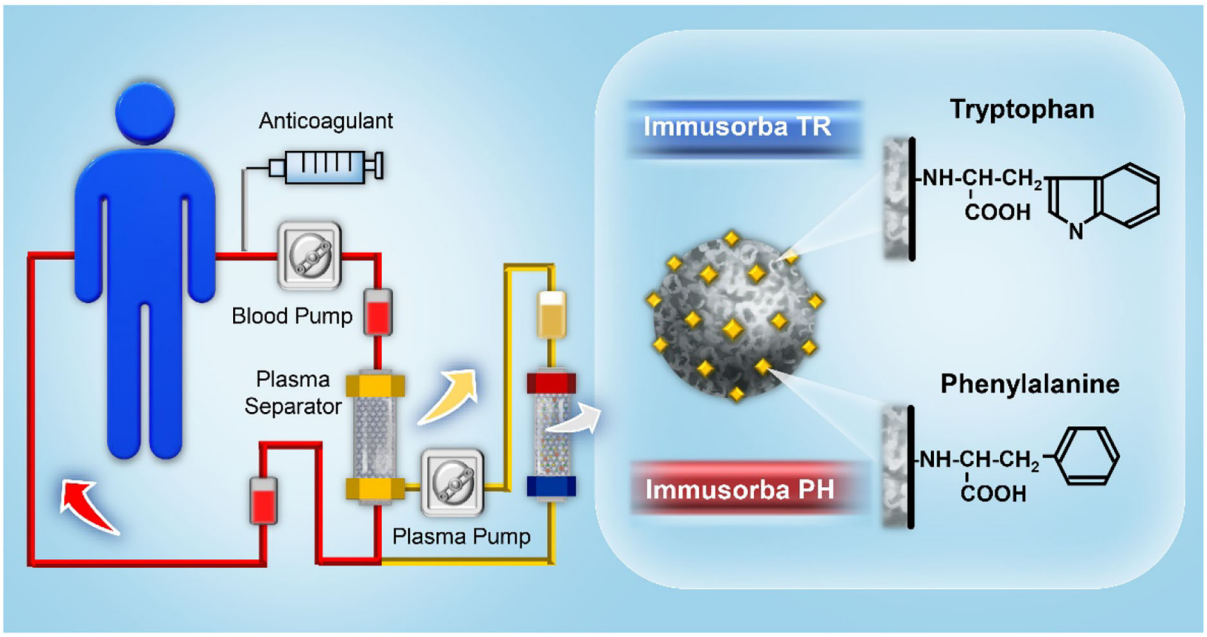

FIGURE 2
A schematic illustration of immunoadsorption using Immusorba TR and Immusorba PH.

apheresis. The levels of urinary protein, immune complexes, and other pathogenic substances were also reduced, indicating the treatment efficiency of LN.

Similar to the dextran sulfate gel column, few studies showed that an immunosorbent bearing tryptophan or phenylalanine is applicable to more than one disease due to its broad-spectrum adsorption properties (30, 31). Non-selective adsorption might induce non-ideal consumption of fibrinogen. *In vitro* and *ex vivo* biocompatibility studies showed that fibrinogen concentration decreased remarkably to around 50% (32). Therefore, to avoid the consumption of beneficial serum components during apheresis, immunosorbents with highly specific ligands are required to provide superior therapeutic efficacy in the treatment of SLE.

2.3. Staphylococcal protein A

Staphylococcus aureus protein A can selectively bind to the heavy chain within the fragment crystallizable (Fc) region of antibodies, particularly those of the IgG class. To date, two types of immunosorbents that use protein A as a specific ligand have been approved for clinical use by the US Food and Drug Administration, namely Immunosorba (Excorim) and Prosorba (Fresenius Hemocare) (33, 34). As shown in Figure 3, the supporting matrix is the crucial difference between the two immunosorbents. Protein A is immobilized onto agarose beads by cyanogen bromide activation, whereas protein A is coupled to a silica matrix by Prosorba.

The Immunosorba system consists of two adsorption columns and an elution monitor (35). During the treatment, both columns are used alternately in the adsorption–elution procedure, which allows the previously saturated column to be regenerated for a new perfusion cycle. Due to the high regeneration efficiency (more than 20 times) and large plasma operating volume, the levels of ANA in the patient's blood can be considerably decreased with the treatment of the Immunosorba protein A system. As the binding affinity between protein A and immunoglobulins is much higher than that of tryptophan, phenylalanine, or dextran sulfate, Immunosorba exhibited superior adsorption efficiency of protein A for CIC (73 ± 0%) and anti-dsDNA antibodies (83 ± 2%) from the plasma of patients with SLE compared to non-selective adsorbents (27). The Immunosorba protein A system can be used to remove total IgG, ANA, and CIC with concomitant amelioration of inflammation. A case report of eight patients with life-threatening or severe therapy-resistant SLE revealed that disease remission was achieved in seven patients with immunoadsorption (36). After the treatment, lupus activity measured by the systemic lupus activity measure (SLAM) index decreased from 23.8 ± 4.2 to 7.9 ± 4.3, and the best treatment efficacy was achieved through daily immunoadsorption.

Unlike the Immunosorba system, the Prosorba system only possesses one disposable column containing 200-mg protein A-immobilized silica beads (125 g). The maximum

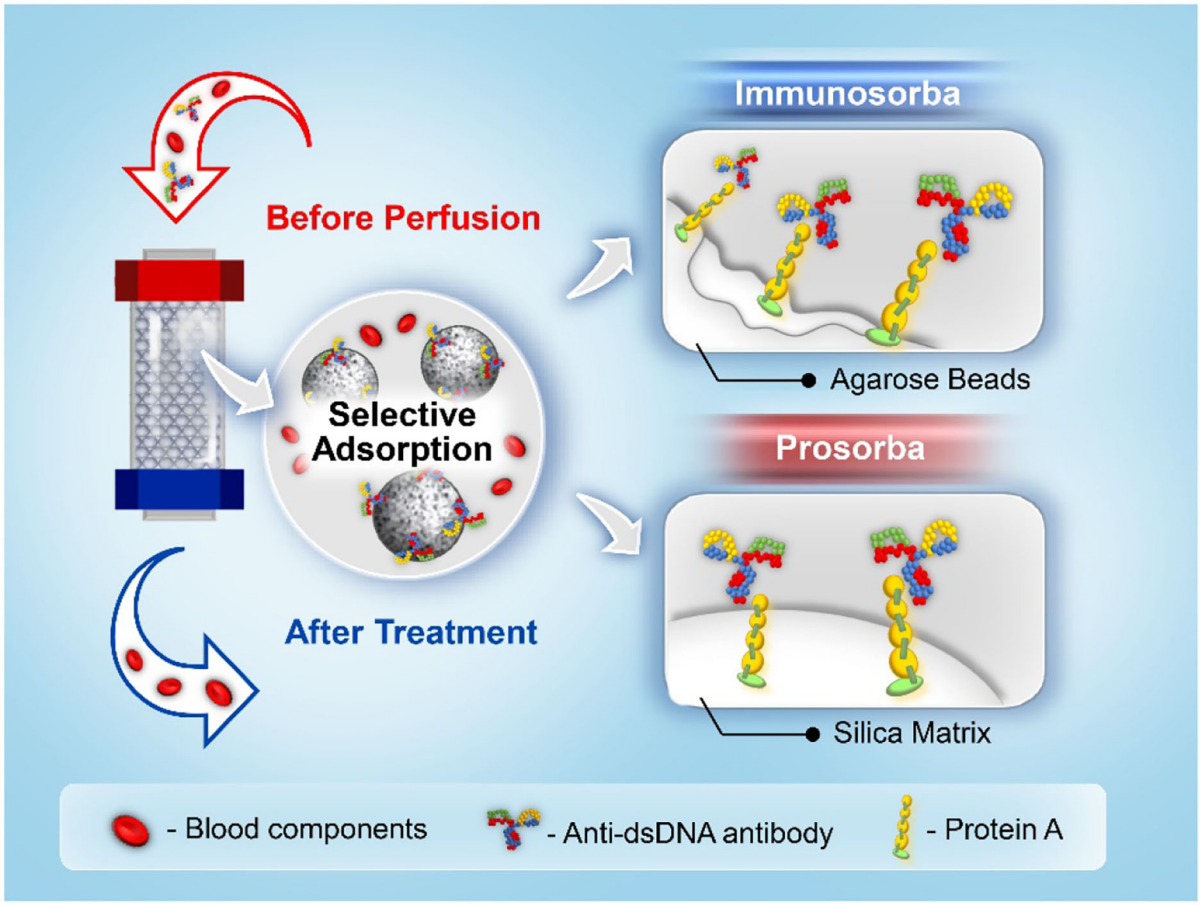

FIGURE 3
A schematic illustration of protein A Immunosorba and Prosorba.

operating volume of the plasma in the Prosorba system is restricted to 2,000 ml, resulting in a relatively lower amount of immunoglobulins and a relatively lower removal capacity of CIC than that of Immunosorba (37). However, it has been reported that the leakage of protein A from the adsorbent during the treatment may have adverse effects in clinical applications (38). Protein A is a B-cell superantigen that evolved in Staphylococcus to weaken the host antibody-mediated defenses; thereby, exposure to protein A during the treatment might induce an immunosuppressive effect (39). The Food and Drug Administration (FDA) has discontinued the application of Prosorba since 2006 due to the aforementioned adverse effects in clinical use, and the Prosorba system has not been available (40).

2.4. Immunoglobin G

Immunoglobin G is recognized as a four-chain monomer, accounting for 75% of the total amount of serum immunoglobin, and is the most essential component of antibodies in serum and extracellular fluids. IgG-based immunosorbents were developed, namely Therasorb, which utilizes polyclonal sheep antihuman IgG antibodies covalently coupled with cellulose beads to remove immune complexes and pathogenic antibodies through highly specific antigen–antibody interactions (41).

The Ig-Therasorb system comprises two columns containing 150 ml of the adsorbent and can be regenerated using glycine buffer *via* an automatic adsorption–desorption apparatus. It has been widely reported that Ig-Therasorb immunoadsorption can reduce the anti-dsDNA antibody levels, disease activity, and proteinuria. The results are summarized in Table 2. Gaubitz et al. (43) reported a randomized trial to compare the efficiency of Ig-Therasorb and Immusorba PH-350 in treating patients with SLE. Approximately 20 patients suffering from moderate or severe SLE were randomized to receive hemoperfusion with either Ig-Therasorb or Immusorba PH-350. Both immunoadsorption systems showed satisfactory removal efficiencies of pathogenic antibodies without causing

TABLE 2 Summary of the case reports involving the application of Ig-Therasorb in treating SLE.

Subject number	Outcome parameters	Therapeutic effect	References
$n = 16$	Anti-dsDNA antibody	Reduced proteinuria and disease activity	(42)
$n = 10$	Anti-dsDNA antibody	Decreased SLAM scores and anti-dsDNA antibody level	(43)
$n = 1$	Anti-dsDNA antibody	Decreased proteinuria and anti-dsDNA antibody level	(44)
$n = 16$	Anti-dsDNA antibody	Decreased disease activity and anti-dsDNA antibody level	(45)
$n = 2$	-	Safe and well tolerated in pregnant women	(46)

any adverse side effects. The removal rates of anti-ds-DNA antibodies were ∼61.0 ± 10.8% and 50.8 ± 6.6% for Ig-Therasorb and Immusorba PH-350, respectively. The higher antibody binding efficacy might be attributable to the particular mode of action of IgG compared to the hydrophobic interactions of phenylalanine. The clinical outcomes of both systems were similar after 1 month of treatment. Still, the number of non-responders was higher in Immusorba PH-350 than in Ig-Therasorb due to the interindividual variability, different indications, and disease duration and severity of the small subject group. Nevertheless, some studies reported the occurrence of infections that may prevent the further application of this system (42, 45).

2.5. C1q

C1q is a component of the first complement component C1, with a molecular weight of 410 kDa. The C1q molecule is a heterohexamer composed of six subunits, each of which is composed of three polypeptide chains. Those peptide chains are connected by disulfide bonds to form a collagen-like structure, which can provide specific binding forces with CIC through the globular C-terminus. Gazitt et al. (47) developed a C1q-based immunosorbent that uses agarose polyacrolein microsphere beads as the supporting matrix to remove CIC in patients with AIDs based on this principle.

Miro (Fresenius) is a single-use immunosorbent containing 300 ml of C1q-immobilized porous polymer beads. Pfueller et al. (48) reported the results of a case report involving eight patients with SLE who received C1q immunoadsorption. The results demonstrated that the reduction of the European Consensus Lupus Activity Measurement score was observed in seven out of eight patients, the decrease in CIC-IgG was observed in five of eight patients, and the reduction of C1q-bearing immune complexes was observed in seven of eight patients. Furthermore, the inflammation parameters, such as the erythrocyte sedimentation rate, C-reactive protein, and the fibrinogen levels, were also decreased for all subjects. The satisfactory treatment efficacy of the C1q immunoadsorption system may be attributable to the multifunctional interactions between C1q and the pathogenic factors, such as CIC, anti-C1q ANA, and inflammatory proteins.

2.6. Double-stranded DNA

Double-stranded DNA is a DNA molecule composed of two single strands of DNA joined by the complementary action of bases. In 1979, Terman et al. (13) in a case report (13), demonstrated the use of DNA collodion charcoal immunosorbent to treat a 29-year-old woman with severe LN. Calf thymus DNA was immobilized in collodion membranes that were adhered to small charcoal particles as the adsorbents. Immune complexes and ssDNA antibodies could be substantially reduced by extracorporeal immunoadsorption. However, hemoperfusion with activated charcoal may result in adverse effects, such as particle embolism, and damage to blood cells, which can be alleviated by modifying collodion-activated charcoal with albumin to enhance blood compatibility (49).

In addition to activated charcoal, various porous supporting matrices based on chitosan, Sepharose, and cellulose have been developed for DNA immobilization. Yu et al. (50) developed a DNA-based immunosorbent with the immobilization of calf thymus DNA onto hydroxyethyl-crosslinked chitosan beads *via* the activation of cyanogen bromide (Figure 4A). The adsorbent could effectively reduce the levels of anti-DNA antibodies in the serum of patients with SLE by 65.33% and could be regenerated for three adsorption cycles by glycine–hydrochloride (HCL). However, the preservation methods affected the performance of antibody adsorption. The adsorption capacity was found to be higher in dry conditions than in wet conditions. The decreased adsorption capacity might be attributed to the decomposition or hydrolyzation of the immobilized DNA under wet conditions.

To improve the grafting capacity and stability while reducing the leakage of the coupled DNA molecules, Kong et al. (51) developed an efficient strategy for DNA immobilization using Sepharose 4FF as the supporting matrix and 5-norbornene-2,3-dicarboximido carbonochloridate (Cl-CO-ONB) for matrix activation (Figure 4B). The coupling efficiency was investigated by varying pH, temperature, reaction time, DNA concentration, and the activation level of the supporting matrix. The results showed that the maximum amount of immobilized DNA was approximately 1.0 mg/ml under an optimal reaction condition, and the amount of DNA immobilization increased with increasing concentration and activation levels. The adsorbent

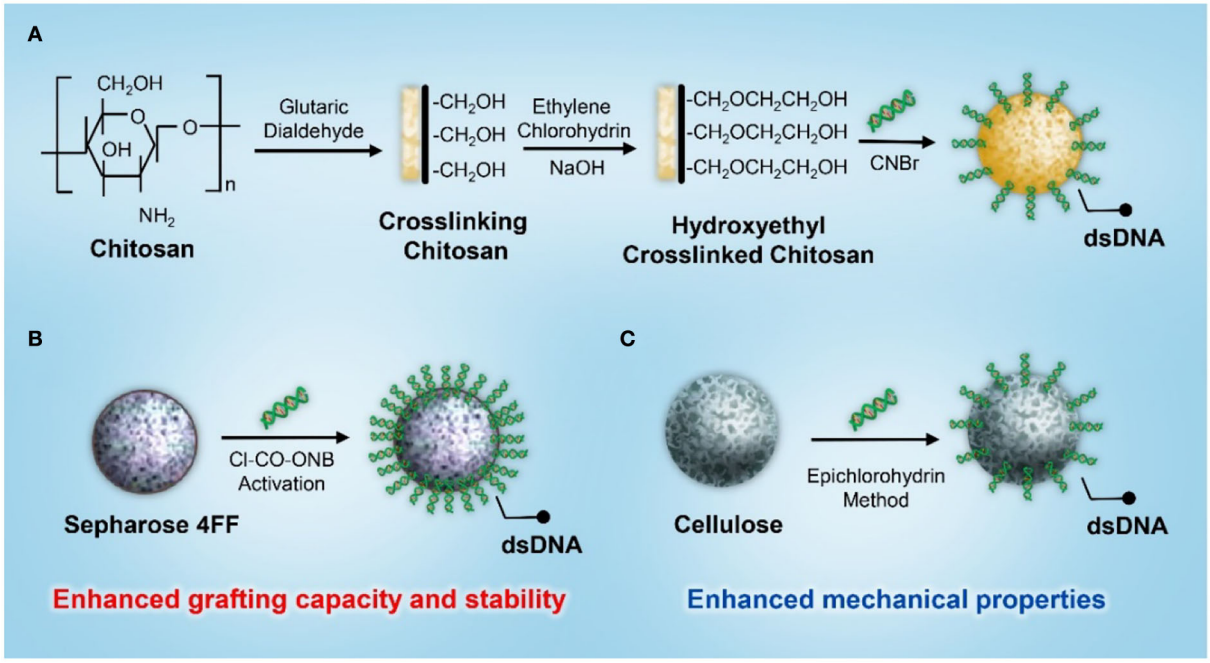

FIGURE 4
A schematic illustration of the synthesis of a dsDNA-based immunosorbent using **(A)** chitosan, **(B)** Sepharose 4FF, and **(C)** cellulose as the supporting matrix.

exhibited excellent adsorption capacity and efficacy for anti-DNA antibodies. The removal rate of anti-DNA antibodies from the plasma of patients with SLE was approximately 80–90%. In addition, the adsorption rate for both normal IgG and total protein was <15%, indicating satisfactory adsorption selectivity against beneficial blood components. However, Sepharose's poor flow through parameter and narrowed column type adaptation restricted its further application in SLE hemoperfusion, so different supporting matrices and coupling strategies were investigated in the development of a DNA-based immunosorbent. Based on its superior mechanical properties and the capacity to fulfill a relatively large column, cellulose was applied as the supporting matrix for DNA immobilization (Figure 4C). A cellulose-based DNA immunosorbent exhibited excellent adsorption capacity, and the antibody removal rate was ∼80% at an adsorption ratio of 20:1 (plasma/adsorbent, v/v) (52).

In 1988, Yang et al. (53) reported a study on a new DNA immune adsorbent for hemoperfusion in SLE therapy. In this study, a patient with SLE who had high levels of anti-DNA antibodies and immune complexes was successfully treated with whole blood perfusion using a DNA immunosorbent. Calf thymus DNA was applied as the specific ligand and immobilized onto carbonized resin beads with an immobilization amount of 98–98.5%, and no leakage was detected during the perfusion process. Anti-DNA antibody levels decreased sharply from 56.34 to 0.8% after 2.5 h of hemoperfusion without significant clinical complications. Yu et al. (54) reported that 30 cases of clinical trials were performed in 12 hospitals in China using type I (DNA immobilized on the carbonized resin) and type II (DNA immobilized on cellulose) adsorbents for immunoadsorption. The levels of anti-DNA antibodies could be reduced by ∼40–70% after whole blood perfusion; almost all the symptoms could be relieved, and some subjects were free from medicine administration. Type II adsorbents possessed a higher DNA immobilization capacity (0.6 mg/ml) than type I adsorbents (0.4 mg/ml). *In vitro* static adsorption experiments revealed that anti-DNA antibody removal efficiency on type II adsorbents was approximately 60%, which was significantly higher than that on type I adsorbents (30%). The high adsorption capacity might be attributable to the introduction of 1,6-hexamethylene diamine, which is the space arm during the preparation of adsorbents so that the steric hindrance effect could be effectively mitigated in the DNA immobilization and antibody adsorption processes.

In 2015, Xu et al. (55) conducted a study to evaluate the therapeutic efficacy of DNA280 (Zhuhai Lizhu Medical Biomaterial), a DNA immunoadsorption system comprising an enveloped carbonized resin as a matrix and purified DNA molecule fragments as ligands. This study involved 57 patients with severe SLE who received immunoadsorption between January 2007 and December 2013. The levels of ANA and anti-ds-DNA antibodies in such patients could be significantly

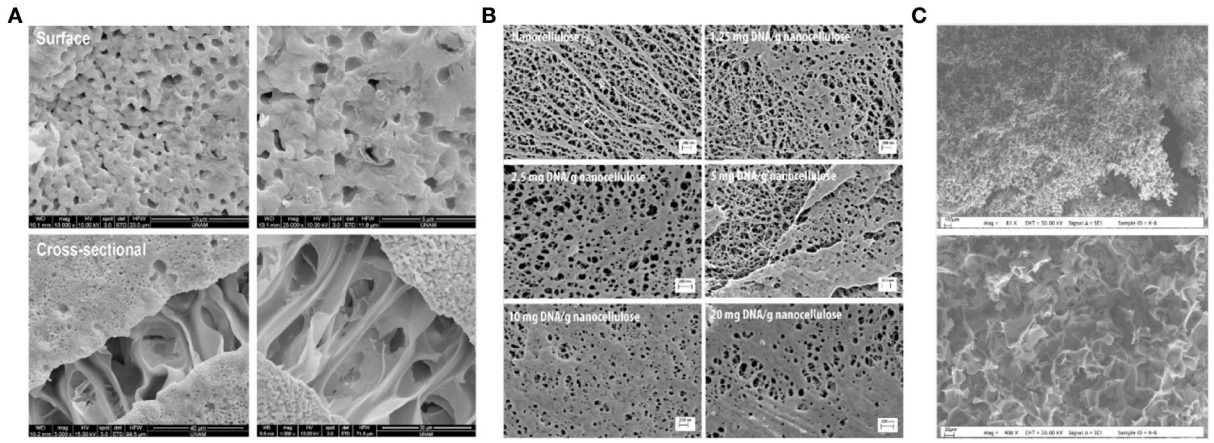

FIGURE 5
Scanning electron microscope images of **(A)** PHEMAAL membranes (57), **(B)** nanocellulose samples with indicated amounts of immobilized DNA (58), and **(C)** PHEMA cryogel (59).

reduced *via* immunoadsorption. The levels of immunological parameters, such as erythrocyte sedimentation rate, C-reactive protein, serum creatinine, and urine protein, were also significantly decreased compared to those before the treatment, and no severe adverse effects were observed during or after the treatment. However, the fabrication procedure of DNA280 was relatively complicated due to the cumbersome processes of matrix preparation, DNA extraction, and purification. Consequently, cost efficiency for such immunosorbents should be considered and improved.

3. Recent developments in immunosorbents for SLE

3.1. Advances in the supporting matrix

Although immunoadsorption has been recognized as an effective therapeutic strategy for SLE, there are some non-negligible issues with the treatment procedure. For example, the compressed pressure of adsorbents in the column caused a reduced flow rate, especially when dealing with highly viscous blood samples (56, 57). Porous membranes are therefore considered alternative adsorbent geometries that can be applied under low-pressure conditions. Poly (2-hydroxyethyl methacrylate) (PHEMA) porous membrane possesses a large specific surface area, high chemical, biological, and mechanical stabilities, strong hydrophilicity, and antifouling properties, making it an ideal support matrix for the preparation of an immunosorbent for SLE. Uzun et al. (57) immobilized DNA onto a PHEMA-based microporous membrane (PHEMAAL-DNA) for the selective removal of anti-dsDNA antibodies from the plasma of patients with SLE. To further improve the compatibility of the blood membrane, N-methacryloyl-L-alanine (MAAL) was introduced as a monomer to copolymerize with HEMA to form the PHEMAAL membrane. As shown in Figure 5A, the membrane surface seems to be rough and heterogeneous, with largely interconnected pores of approximately 5–10 μm. The microporous structure and higher inner surface area could effectively decrease diffusional resistance and facilitate the mass transfer of anti-dsDNA antibodies. Anti-dsDNA antibody adsorption capacity was approximately 68×10^3 IU/g. The levels of anti-dsDNA antibodies can be decreased from their initial value of 875–144 IU/ml. The adsorption membrane also exhibited excellent blood compatibility due to the incorporation of hydrophilic MAAL, which could effectively reduce blood cell adhesion and non-specific protein adsorption.

Cellulose materials have been widely applied in immunoadsorption due to their desired mechanical strength, physicochemical stability, and biocompatibility. However, conventional cellulose-based immunosorbents are limited in their ability to graft ligands owing to their low porosity and surface area. As compared to conventional cellulose materials, nanocellulose exhibits a surface area that is nearly two orders of magnitude greater than conventional cellulose materials. Based on this unique property, Xu et al. (58) prepared a DNA-immobilized immunosorbent using the nanocellulose membrane as the supporting matrix. As shown in Figure 5B, the non-coated nanocellulose exhibited a fibrous structure, and with an increased amount of immobilized DNA, new structures progressively emerged in the form of patches that covered the voids between the nanofibers. These patches become denser at the highest degree of DNA binding, which causes them to clog the pore structure. The nanocellulose-based DNA

membrane exhibited a high affinity for binding with anti-ds-DNA IgG *in vitro*. The binding capacity was quantitatively dependent on the number of immobilized DNA ligands on the membrane.

Apart from the membrane, macroporous cryogel was applied as the supporting matrix to prepare an immunosorbent to facilitate blood cells passing through, rather than being blocked by, the pores. Özgür (59) modified PHEMA cryogel with polyethyleneimine (PEI) and DNA for the removal of anti-dsDNA antibodies from the plasma of patients with SLE. The cryogel-based adsorbent possessed a high porosity, approximately 67.5%, and interconnected macropores of 10–200 μm (Figure 5C). As a result of its macroporosity and interconnected pore structure, the adsorbent had a meager flow resistance. The maximum adsorption capacity of the anti-dsDNA antibody was approximately 70×10^3 IU/g. The levels of an anti-dsDNA antibody in SLE plasma could be decreased from 780 to 80 IU/ml after adsorption.

3.2. Adsorbents using 4-mercaptoethylpyridine as a ligand

Applications of immunosorbents that use proteins or antibodies as ligands are limited because of their high cost and lack of stability. 4-Mercaptoethylpyridine (MEP, MW 139 Da) is a synthetic compound with desirable hydrophobicity that can be used to capture and purify antibodies from complex feedstock *via* hydrophobic interactions. Ren et al. (60) developed an MEP-grafted Sepharose gel to remove ANA from the serum of patients with AIDs. The MEP grafting density was optimized to achieve the maximum binding capacity for anti-dsDNA antibodies. The MEP Sepharose gel with a ligand density of 98.9 μmol/ml could remove 80% of the anti-dsDNA antibodies. Moreover, MEP-grafted Sepharose gel exhibited a lower degree of individual differences compared to Protein A-Sepharose. Out of the 14 serum samples derived from patients with SLE, 11 samples had markedly reduced antinuclear antibody titers. Albumin, fibrinogen, and other plasma components would not be virtually affected by the immunosorbent.

4. Conclusion

In the last three decades, immunoadsorption has been extensively used for treating patients with SLE who are refractory to conventional therapies. Unlike plasma exchange, immunoadsorption can effectively remove pathogenic antibodies and immune complexes without altering the levels of beneficial blood components. Immunosorbents containing non-selective or semi-selective ligands, such as dextran sulfate, phenylalanine, tryptophan, protein A, and IgG, have been commercially used over the past few decades. Among these, immunoadsorption columns, such as Ig-Therasorb and protein A Immunosorba, can remove disease-specific antibodies with a high affinity, making them valuable treatment options for SLE. Selesorb and Immusorba are examples of low-affinity columns that exhibit lower levels of efficacy. Ligands with higher selectivity are still being investigated, such as C1q and dsDNA. A non-selective or sim-selective immunosorbent may reduce the levels of beneficial plasma components and proteins after purification. A highly selective immunosorbent has the potential to bind to pathogenic antibodies with high specificity. However, further investigation is warranted to confirm its safety and efficacy. Recently, several studies focused on optimizing the supporting matrix and developing novel specific ligands to reduce treatment costs further and improve therapeutic efficacy and safety.

Author contributions

YY: writing–original draft. LO: writing–review and editing. All authors contributed to the article and approved the submitted version.

Acknowledgments

The authors gratefully acknowledge funding from the National Natural Science Foundation of China (No. 82172093).

Conflict of interest

The authors declare that the research was conducted in the absence of any commercial or financial relationships that could be construed as a potential conflict of interest.

Publisher's note

References

1. Chang TMS, Endo Y, Nikolaev VG, Tani T, Yu Y, Zheng WH, et al. *Hemoperfusion, Plasmaperfusion and Other Clinical Uses of General, Biospecific, Immuno and Leucocyte Adsorbents*. Singapore: World Scientific (2017).

2. Nakaji S. Current topics on immunoadsorption therapy. *Therap Apher*. (2001) 5:301–5. doi: 10.1046/j.1526-0968.2001.00360.x

3. Stummvoll G. Immunoadsorption (IAS) for systemic lupus erythematosus. *Lupus*. (2011) 20:115–9. doi: 10.1177/0961203310389487

4. Kadar JG, Borberg H. Biocompatibility of extracorporeal immunoadsorption systems. *Trans Sci*. (1990) 11:223–39. doi: 10.1016/0955-3886(90)90099-5

5. Fanouriakis A, Kostopoulou M, Alunno A, Aringer M, Bajema I, Boletis JN, et al. 2019 update of the EULAR recommendations for the management of systemic lupus erythematosus. *Annal Rheumat Dis*. (2019) 78:736–45. doi: 10.1136/annrheumdis-2019-215089

6. Mok C, Lau C. Pathogenesis of systemic lupus erythematosus. *J Clin Pathol*. (2003) 56:481–90. doi: 10.1136/jcp.56.7.481

7. Koffler D, Carr R, Agnello V, Thoburn R, Kunkel H. Antibodies to polynucleotides in human sera: antigenic specificity and relation to disease. *J Exp Med*. (1971) 134:294–312. doi: 10.1084/jem.134.1.294

8. Giles BM, Boackle SA. Linking complement and anti-dsDNA antibodies in the pathogenesis of systemic lupus erythematosus. *Immunol Res*. (2013) 55:10–21. doi: 10.1007/s12026-012-8345-z

9. Larosa M, Iaccarino L, Gatto M, Punzi L, Doria A. Advances in the diagnosis and classification of systemic lupus erythematosus. *Expert Rev Clin Immunol*. (2016) 12:1309–20. doi: 10.1080/1744666X.2016.1206470

10. Strand V, Crawford B. Improvement in health-related quality of life in patients with SLE following sustained reductions in anti-dsDNA antibodies. *Exp Rev Pharm Outcomes Res*. (2005) 5:317–26. doi: 10.1586/14737167.5.3.317

11. Zabriskie JB. *Essential Clinical Immunology*. Cambridge: Cambridge University Press (2009).

12. Traeger J, Laville M, Serres P, Cronenberger M, Thomas M, Rey M, et al. A new device for specific extracorporeal immunoadsorption of anti-DNA antibodies. *In vitro* and *in vivo* results. *Annales Med Int*. (1992) 143:7–12.

13. Terman D, Buffaloe G, Cook G, Sullivan M, Mattioli C, Tillquist R, et al. Extracorporeal immunoadsorption: initial experience in human systemic lupus erythematosus. *Lancet*. (1979) 314:824–7. doi: 10.1016/S0140-6736(79)92177-9

14. Winchester JF, Kellum JA, Ronco C, Brady JA, Quartararo PJ, Salsberg JA, et al. Sorbents in acute renal failure and the systemic inflammatory response syndrome. *Blood Purif*. (2003) 21:79–84. doi: 10.1159/000067860

15. Aotsuka S, Funahashi T, Tani N, Okawa-Takatsuji M, Kinoshita M, Yokohari R, et al. Adsorption of anti-dsDNA antibodies by immobilized polyanionic compounds. *Clin Exp Immunol*. (1990) 79:215–20. doi: 10.1111/j.1365-2249.1990.tb05181.x

16. Matsuki Y, Suzuki K, Kawakami M, Ishizuka T, Kawaguchi Y, Hidaka T, et al. High-avidity anti-DNA antibody removal from the serum of systemic lupus erythematosus patients by adsorption using dextran sulfate cellulose columns. *J Clin Apher*. (1996) 11:30–5. doi: 10.1002/(SICI)1098-1101(1996)11:1<30::AID-JCA7>3.0.CO;2-C

17. Kinoshita M, Aotsuka S, Funahashi T, Tani N, Yokohari R. Selective removal of anti-double-stranded DNA antibodies by immunoadsorption with dextran sulphate in a patient with systemic lupus erythematosus. *Annal Rheum Dis*. (1989) 48:856–60. doi: 10.1136/ard.48.10.856

18. Kutsuki H, Takata S, Yamamoto K, Tani N. Therapeutic selective adsorption of anti-DNA antibody using dextran sulfate cellulose column (selesorb) for the treatment of systemic lupus erythematosus. *Therap Apher*. (1998) 2:18–24. doi: 10.1111/j.1744-9987.1998.tb00068.x

19. Stefanutti C, Vivenzio A, Giacomo SDi, Mareri M, Ceccarelli F, Valesini G, et al. Cyclophosphamide and immunoadsorption apheresis treatment of lupus nephritis nonresponsive to drug therapy alone. *BioDrugs*. (2005) 19:129–33. doi: 10.2165/00063030-200519020-00004

20. Braun N, Jünger M, Klein R, Gutenberger S, Guagnin M, Risler T, et al. Dextran sulfate (Selesorb) plasma apheresis improves vascular changes in systemic lupus erythematosus. *Therap Apher*. (2002) 6:471–7. doi: 10.1046/j.1526-0968.2002.00408.x

21. Suzuki K, Hara M, Harigai M, Ishizuka T, Hirose T, Matsuki Y, et al. Continuous removal of anti-DNA antibody, using a new extracorporeal immunoadsorption system, in patients with systemic lupus erythematosus. *Arthr Rheumat*. (1991) 34:1546–52. doi: 10.1002/art.1780341211

22. Hashimoto H, Tsuda H, Kanai Y, Kobayashi S, Hirose S, Shinoura H, et al. Selective removal of anti-DNA and anticardiolipin antibodies by adsorbent plasmapheresis using dextran sulfate columns in patients with systemic lupus erythematosus. *J Rheumatol*. (1991) 18:545–51.

23. Suzuki K. The role of immunoadsorption using dextran-sulfate cellulose columns in the treatment of systemic lupus erythematosus. *Therapeutic Apher*. (2000) 4:239–43. doi: 10.1046/j.1526-0968.2000.00178.x

24. Asahi T, Yamamoto T, Kutsuki H. Blood purification therapies using dextran sulfate cellulose columns Liposorber and Selesorb. *Therap Apher Dial*. (2003) 7:73–7. doi: 10.1046/j.1526-0968.2003.00018.x

25. Hirata N, Kuriyama T, Yamawaki N. Immusorba Tr and Ph. *Therap Apher Dial*. (2003) 7:85–90. doi: 10.1046/j.1526-0968.2003.00010.x

26. Yoshida M, Tamura Y, Yamada Y, Yamawaki N, Yamashita Y. Immusorba TR and Immusorba PH: basics of design and features of functions. *Therap Apher*. (1998) 2:185–92. doi: 10.1111/j.1744-9987.1998.tb00102.x

27. Ikonomov V, Samtleben W, Schmidt B, Blumenstein M, Gurland H. Adsorption profile of commercially available adsorbents: an *in vitro* evaluation. *Int J Artif Organs*. (1992) 15:312–9. doi: 10.1177/039139889201500511

28. Avenhaus B, Avenhaus W, Schneider M, Domschke W, Gaubitz M. Development of an in vitro miniature model to simulate immunoadsorption in patients with systemic lupus erythematosus. *J Clin Apher*. (2002) 17:183–9. doi: 10.1002/jca.10034

29. Sugimoto K, Yamaji K, Yang KS, Kanai Y, Tsuda H, Hashimoto H, et al. Immunoadsorption plasmapheresis using a phenylalanine column as an effective treatment for lupus nephritis. *Therap Apher Dial*. (2006) 10:187–92. doi: 10.1111/j.1744-9987.2006.00362.x

30. Fu G, Yu H, Yuan Z, Liu B, Shen B, He B, et al. Chitosan adsorbents carrying amino acids for selective removal of low density lipoprotein. *Artif Blood Subst Biotechnol*. (2004) 32:303–13. doi: 10.1081/BIO-120037835

31. Fu G, Shi K, Yuan Z, He B, Liu B, Shen B, et al. Preparation of tryptophan modified chitosan beads and their adsorption of low density lipoprotein. *Chin Sci Bullet*. (2003) 48:2303–7. doi: 10.1360/03wb0052

32. Yamazaki Z, Fujimori Y, Takahama T, Inoue N, Wada T, Kazama M, et al. Efficiency and biocompatibility of a new immunosorbent. *ASAIO J*. (1982) 28:318–23.

33. Braun N, Gutenberger S, Erley CM, Risler T. Immunoglobulin and circulating immune complex kinetics during immunoadsorption onto protein A sepharose. *Trans Sci*. (1997) 19:25–31. doi: 10.1016/S0955-3886(97)00099-4

34. Samuelsson G. What's happening? Protein A columns: current concepts, and recent advances. *Trans Sci*. (1999) 21:215–7. doi: 10.1016/S0955-3886(99)00096-X

35. Pineda AA, Vamvakas EC. Specialized therapeutic hemapheresis: present and future. *Vox Sang*. (2002) 83:41–4. doi: 10.1111/j.1423-0410.2002.tb05265.x

36. Braun N, Erley C, Klein R, Kötter I, Saal J, Risler T, et al. Immunoadsorption onto protein A induces remission in severe systemic lupus erythematosus. *Nephrol Dial Transpl*. (2000) 15:1367–72. doi: 10.1093/ndt/15.9.1367

37. Felson DT, LaValley MP, Baldassare AR, Block JA, Caldwell JR, Cannon GW. The Prosorba column for treatment of refractory rheumatoid arthritis: a randomized, double-blind, sham-controlled trial arthritis and rheumatism *Off J Am College Rheumatol*. (1999) 42:2153–9. doi: 10.1002/1529-0131(199910)42:10<2153::AID-ANR16>3.0.CO;2-W

38. Sasso EH, Merrill C, Furst DE. Immunoglobulin binding properties of the Prosorba immunadsorption column in treatment of rheumatoid arthritis. *Therap Apher*. (2001) 5:84–91. doi: 10.1046/j.1526-0968.2001.005002084.x

39. Goodyear CS, Silverman GJ. Death by a B cell superantigen: *in vivo* VH-targeted apoptotic supraclonal B cell deletion by a staphylococcal toxin. *J Exp Med*. (2003) 197:1125–39. doi: 10.1084/jem.20020552

40. Sanchez AP, Cunard R, Ward DM. The selective therapeutic apheresis procedures. *J Clin Apher*. (2013) 28:20–9. doi: 10.1002/jca.21265

41. Graninger M, Schmaldienst S, Derfler K, Graninger W. Immunoadsorption therapy (therasorb) in patients with severe lupus erythematosus. *Acta Med Austriaca*. (2002) 29:26–9. doi: 10.1046/j.1563-2571.2002.01040.x

42. Stummvoll GH, Aringer M, Smolen JS, Schmaldienst S, Jimenez-Boj E, Hörl WH, et al. IgG immunoadsorption reduces systemic lupus erythematosus activity, and proteinuria: a long term observational study. *Annal Rheumat Dis*. (2005) 64:1015–21. doi: 10.1136/ard.2004.029660

43. Gaubitz M, Seidel M, Kummer S, Schotte H, Perniok A, Domschke W, et al. Prospective randomized trial of two different

immunoadsorbers in severe systemic lupus erythematosus. *J Autoimmun.* (1998) 11:495–501. doi: 10.1006/jaut.1998.0229

44. Schmaldienst S, Jansen M, Hollenstein U, Graninger W, Regele H, Hörl WH, et al. Treatment of systemic lupus erythematosus by immunoadsorption in a patient suffering from tuberculosis. *Am J Kidney Dis.* (2002) 39:415–8. doi: 10.1053/ajkd.2002.30564

45. Stummvoll GH, Aringer M, Jansen M, Smolen JS, Derfler K, Graninger WB, et al. Immunoadsorption as a rescue therapy in systemic lupus erythematosus: considerations on safety and efficacy. *Wien Klin Wochenschr.* (2004) 116:716–24. doi: 10.1007/s00508-004-0232-8

46. Dittrich E, Schmaldienst S, Langer M, Jansen M, Hörl WH, Derfler K, et al. Immunoadsorption and plasma exchange in pregnancy. *Kidney Blood Pressure Res.* (2002) 25:232–9. doi: 10.1159/000066343

47. Gazitt Y, Margel S, Lerner A, Wands J, Shouval D. Development of a novel Clq immunoadsorbent for removal of circulating immunecomplexes: quantitative isolation of hepatitis B virus surface antigen and immunecomplexes. *Immunol Lett.* (1985) 11:1–8. doi: 10.1016/0165-2478(85)90135-X

48. Pfueller B, Wolbart K, Bruns A, Burmester GR, Hiepe F. Successful treatment of patients with systemic lupus erythematosus by immunoadsorption with a C1q column: a pilot study. *Arthr Rheumat.* (2001) 44:1962–3. doi: 10.1002/1529-0131(200108)44:8<1962::AID-ART335>3.0.CO;2-R

49. Chang TM. *First Design and Clinical Use in Patients of Surface Modified Sorbent Hemoperfusion Based on Artificial Cells for Poisoning, Kidney Failure, Liver Failure and Immunology. Hemoperfusion, Plasmaperfusion and Other Clinical Uses Of General, Biospecific, Immuno and Leucocyte Adsorbents*. Singapore: World Scientific (2017).

50. Yu YH, He BL. The preparation of immunoadsorbents and their adsorption properties for anti-DNA antibodies in SLE serum. *React Funct Polymers.* (1999) 41:191–5. doi: 10.1016/S1381-5148(99)00028-0

51. Kong DL, Schuett W, Boeden HF, Kunkel S, Holtz M, Matic G, et al. Development of a DNA immunoadsorbent: coupling DNA on sepharose 4FF by an efficient activation method. *Artif Org.* (2000) 24:845–51. doi: 10.1046/j.1525-1594.2000.06618.x

52. Kong D, Schuett W, Dai J, Kunkel S, Holtz M, Yamada R, et al. Development of Cellulose-DNA Immunoadsorbent. *Artif Org.* (2002) 26:200–8. doi: 10.1046/j.1525-1594.2002.06721.x

53. Yan Y, Yao-Ting Y, Ji-Chang S, Shao-Cheng Q, Wu-Lie Q, Xin-Hua S, et al. A new DNA immune adsorbent for hemoperfusion in SLE therapy: a clinical trial. *Artif Org.* (1998) 12:444–6. doi: 10.1111/j.1525-1594.1988.tb02799.x

54. Kong DL, Chen CZ, Lin EF, Yu YT. Clinical trials of type I, and in vitro studies of type II immunoadsorbents for systemic lupus erythematosus therapy. *Artif Org.* (1998) 22:644–50. doi: 10.1046/j.1525-1594.1998.06010.x

55. Xu L, Wu X, Zou Y. Clinical efficacy comparison of HA280 and DNA280 immunoadsorption column in treating systemic lupus erythematosus. *Modern Rheumatol.* (2016) 26:94–8. doi: 10.3109/14397595.2015.1056955

56. Dancette OP, Taboureau JL, Tournier E, Charcosset C, Blond P. (1999). Purification of immunoglobulins G by protein A/G affinity membrane chromatography. *J Chromatograph Biomed Sci Appl.* (1999) 723:61–8. doi: 10.1016/S0378-4347(98)00470-8

57. Uzun L, Yavuz H, Osman B, Çelik H, Denizli A. Poly (hydroxyethyl methacrylate) based affinity membranes for in vitro removal of anti-dsDNA antibodies from SLE plasma. *Int J Biol Macromol.* (2010) 47:44–9. doi: 10.1016/j.ijbiomac.2010.03.022

58. Xu C, Carlsson DO, Mihranyan A. Feasibility of using DNA-immobilized nanocellulose-based immunoadsorbent for systemic lupus erythematosus plasmapheresis. *Colloids Surf Biointerf.* (2016) 143:1–6. doi: 10.1016/j.colsurfb.2016.03.014

59. Özgür E, Bereli N, Türkmen D, Ünal S, Denizli A. PHEMA cryogel for in-vitro removal of anti-dsDNA antibodies from SLE plasma. *Mat Sci Eng.* (2011) 31:915–20. doi: 10.1016/j.msec.2011.02.012

60. Ren J, Jia L, Xu L, Lin X, Pi Z, Xie J, et al. Removal of autoantibodies by 4-mercaptoethylpyridine-based adsorbent. *J Chromatograph.* (2009) 877:1200–4. doi: 10.1016/j.jchromb.2009.03.017

frontiers | Frontiers in Bioengineering and Biotechnology

TYPE Review
PUBLISHED 09 February 2023
DOI 10.3389/fbioe.2023.1072937

OPEN ACCESS

EDITED BY
Binglan Yu,
Massachusetts General Hospital and Harvard Medical School, United States

REVIEWED BY
Thomas Ming Swi Chang,
McGill University, Canada
Franck Zal,
Hemarina (France), France

*CORRESPONDENCE
Hongli Zhu,
zhuyjw1971@nwu.edu.cn

SPECIALTY SECTION
This article was submitted to Tissue Engineering and Regenerative Medicine, a section of the journal Frontiers in Bioengineering and Biotechnology

RECEIVED 18 October 2022
ACCEPTED 31 January 2023
PUBLISHED 09 February 2023

CITATION
Shen C, Cheng H, Zong T and Zhu H (2023), The role of normothermic machine perfusion (NMP) in the preservation of *ex-vivo* liver before transplantation: A review. *Front. Bioeng. Biotechnol.* 11:1072937. doi: 10.3389/fbioe.2023.1072937

The role of normothermic machine perfusion (NMP) in the preservation of *ex-vivo* liver before transplantation: A review

Chuanyan Shen[1], Hongwei Cheng[1], Tingting Zong[1] and Hongli Zhu[1,2,3]*

[1]The College of Life Sciences, Northwest University, Xi'an, Shaanxi, China, [2]National Engineering Research Center for Miniaturized Detection Systems, Northwest University, Xi'an, China, [3]Key Laboratory of Resource Biology and Biotechnology in Western China, Ministry of Education, School of Medicine, Northwest University, Xi'an, China

The discrepancy between the number of patients awaiting liver transplantation and the number of available donors has become a key issue in the transplant setting. There is a limited access to liver transplantation, as a result, it is increasingly dependent on the use of extended criteria donors (ECD) to increase the organ donor pool and address rising demand. However, there are still many unknown risks associated with the use of ECD, among which preservation before liver transplantation is important in determining whether patients would experience complications survive after liver transplantation. In contrast to traditional static cold preservation of donor livers, normothermic machine perfusion (NMP) may reduce preservation injury, improve graft viability, and potentially *ex vivo* assessment of graft viability before transplantation. Data seem to suggest that NMP can enhance the preservation of liver transplantation to some extent and improve the early outcome after transplantation. In this review, we provided an overview of NMP and its application in *ex vivo* liver preservation and pre-transplantation, and we summarized the data from current clinical trials of normothermic liver perfusion.

KEYWORDS

liver transplantation, normothermic machine perfusion, marginal liver, expanded criteria donor, donation after cardiac death

Abbreviations: AOC, Artificial Oxygen Carriers; AST, Aspartate aminotransferase; CS, Cold storage; DBD, Donate after brain death; DCD, Donation after cardiac death; EAD, Early allograft dysfunction; ECD, Expanded criteria donor; FDA, Food and Drug Administration; GDH, Glutamate dehydrogenase; HMP, Hypothermic machine perfusion; HOPE, Hypothermic Oxygenated Perfusion; ICS, Ischemic cold storage; LFTs, Liver Function Tests; LT, Liver Transplantation; MDA, Malondialdehyde; MP, Machine Perfusion; NEVLP, Normothermic ex vivo liver perfusion; NMP, Normothermic Machine Perfusion; NMP-L, Normothermic Machine Perfusion Liver; NRP, Normothermic regional perfusion; OC, Oxygen Carrier; OCS, Organ Care System; PNF, Primary Non-Function; PS, Preservation solution; RCT, Randomized controlled trials; SCS, Static cold storage; SNMP, Subnormothermic machine perfusion.

1 Introduction

Patients with liver cirrhosis, decompensated illnesses, acute liver failure, hepatocellular carcinoma, and other irreversible liver disorders are currently treated with liver transplantation as a first choice (Liu et al., 2014). However, the discrepancy between the lack of liver donors and the rising number of patients awaiting transplantation is continually growing. At the same time, due to the donor factors and preservation technology, many marginal livers, such as old donor livers and fatty donor livers are abandoned (Liu et al., 2014). Numerous transplantation facilities all across the world have begun to experiment with so-called expanded standard donors, namely donation after cardiac death (DCD) donors, as a result of the severe liver donor scarcity (Badawy et al., 2020). In general, all donors who raise the possibility of early organ failure or malfunction, including expanded standard liver (Liu et al., 2014) donors can be listed for early organ non-function and late organ inactivation (Parente et al., 2020). However, the following issues will unavoidably occur from the use of ECD liver: 1) ECD graft is related to the increased risk of primary organ dysfunction or initial liver dysfunction (Chen et al., 2017). 2) ECD and DCD livers have poor tolerance to ischemia-reperfusion injury. 3) DCD liver has frequent biliary complications, such as ischemic cholangiopathy, and poor survival rate of the corresponding graft (Jay et al., 2011).

All donated organs are typically preserved using static cold storage (SCS) (Vogel et al., 2017). In contrast, the goal of normothermic storage is to preserve cell metabolism by simulating the natural environment. To sustain the aerobic circulation of the liver *in vitro*, NMP provides oxygen and nutrition at 37°C, which could decrease the risk associated with marginal liver transplantation (steatosis, aging, and donation after circulatory death) (Aufhauser and Foley, 2021). Machine perfusion has been proven in a series of clinical trials to increase the efficacy of allogeneic liver transplantation, reduce the risk of ischemia-reperfusion injury, and decrease the incidence of early allograft liver transplantation malfunction, biliary problems, and ischemic cholangiopathy. The liver transplantation conducted with the marginal liver and preserved by Machine Perfusion (MP) showed that the transplantation rate increases, which can expand the liver donor pool, thereby saving more lives of patients with advanced liver disease. Gaurav et al. (2022) conducted a single center, retrospective analysis of data collected on 233 DCD liver transplants perfused using SCS, normothermic regional perfusion (NRP), or NMP between January 2013 and October 2020. This is the first direct comparison of SCS with both *in situ* and *ex situ* normothermic preservation techniques in DCD liver transplantation from a single center, and one of the largest series of NRP and DCD-NMP to date. In this study, the researchers found that compared to SCS, both NMP and NRP livers had better early transplant outcomes and better early allograft function.

2 Development of organ preservation and perfusate

The issue of organ donors is a significant segment in organ transplantation, and the preservation of organs *in vitro* is the most crucial link in this chain. Organ transplantation research is challenging because once the organ is removed, the original blood circulation ceases instantly. The first goal of organ perfusion was to maximally eliminate toxic metabolites (Collins and Wicomb, 1992) generated by cells during ischemia in the shortest amount of time. While cryopreservation can keep cell metabolism at a low level, preventing cell damage, it cannot achieve perfect preservation result (Hartley et al., 1971). Collins et al. conceptualized and produced the initial cryopreservation solution to immerse isolated organs, such as heart, kidney, liver, and lung (Collins et al., 1969). The preservation effect was great in those primary organs and thus was given the name Euro Collins in 1980 (Aydin et al., 1982; Guibert et al., 2011). Its chemical stability and composition have been improved, and it can provide better protection for organs under long-term cold ischemia. The University of Wisconsin (UW) in the United States developed a cold organ preservation solution in the 1980s that was primarily made up of various carbohydrate substances (Wahlberg et al., 1986) and used primarily for the preservation of abdominal organs. The cold preservation solution for organs that has been used for long time is currently considered as the gold standard (Stewart, 2015). Although UW solution has been in the leading position of organ preservation solution for many years, studies have shown that kidney preservation causes the increase of epithelial Na^+ channel (ENaC) activity, which leads to the dysfunction of ENaC and the decrease of renal function (Khedr et al., 2019). The histidine tryptophan ketoglutarate solution (HTK), sometimes known as HTK solution, was created in 1975 by Bretsheneider et al. (Wechsler et al., 1986). HTK solution was first utilized to maintain abdominal cavity organs, then utilized to maintain the heart when Flaming et al. discovered its favorable preservation effect (Flameng et al., 1988). Rauen et al. used six different preservation solutions to culture hepatocytes and evaluated their toxicity. The results showed that HTK solution had obvious toxicity during cold culture, which may be related to the histidine contained in it (Rauen and de Groot, 2008).

Celsior, a cold heart preservation solution created by Pasteur-Mérieux in 1994, it was also used in the preservation of thoracic and abdominal organs (Karam et al., 2005). When Takahiko Kiyooka et al. (2016) evaluated the preservation effects of Celsior solution (CS) and UW solution on the heart, they found that the antioxidant effect of CS was noticeably better than UW solution. However, the preservation effect of CS on most abdominal organs is limited (Bessems et al., 2005). At present, most researchers are trying to add additional nutrients and antioxidants into a number of established preservation solutions to improve their preservation effect.

Ectopic perfusion of human donor liver using NMP is conducted at a temperature of 37°C. This technique can be used throughout the preservation period of the liver. Pre-transplantation assessment tests and clinical studies using NMP method are now underway (Mergental et al., 2016; Watson et al., 2016; Haque et al., 2021). The aim of NMP is to restore cell metabolism by keeping organs at their normal temperature and providing adequate oxygen and nutrient supply. For mechanical perfusion at normothermic temperature, it is now established practice to use whole blood that has been diluted, heparinized, and pH balanced as the starting point of the perfusate. After adding to the perfusate, red blood cells have the function of transporting oxygen, which could maximize the

physiological environment *in vitro* and delaying the occurrence of interstitial edema in the liver during MP. op den Dries et al. (2013) established the make-up and ratio of the perfusate for mechanical perfusion at room temperature at the first time, which contains all the nutrients, oxygen, and safeguards required for a typical liver metabolism. Based on concentrated red blood cells, plasma, and albumin, this formula also contains trace elements, antibiotics, and nutritional solution. At present, the perfusate used by major transplantation centers is basically based on this formula with various substances added.

3 The use of blood substitutes on MP

NMP frequently makes use of red blood cell (RBC-based) perfusate (op den Dries et al., 2013; Perera et al., 2016; Selzner et al., 2016; Bral et al., 2017). Cellular oxygen consumption is positively connected with temperature, organ metabolism depends on oxygen to create adenosine triphosphate, and NMP demands plenty oxygen. The most physiological oxygen transporters are human red blood cells, however since human blood products are expensive due to short storage time, cross-matching requirement, blood borne infections, and logistical difficulties.

At present, the effective artificial oxygen transporters are hemoglobin based oxygen carrier (HBOC). Many oxygen carriers are used in clinical and NMP, including Hemoglobin Vesicles (Taguchi et al., 2009; Kure and Sakai, 2021), Hemoglobin based oxygen carrier-201 (HBOC-201) (Jahr et al., 2008), Hemoglobin M101 from Hemarina (Kaminski et al., 2019; Alix et al., 2020), and Perfluorocarbons (Riess, 2001; Menz et al., 2018). There are advantages and disadvantages. HBOC-201 is a polymerized Hb made from a bovine Hb source. Hb was extracted and purified from bovine red blood cells (RBCs), and then cross-linked to enhance its stability. In addition, HBOC-201 is less viscous than RBC, has long shelf life of three years, compatible with all blood types. In a protocol for a prospective single-arm study, Van Leeuwen et al. heated discarded human donor livers from hypothermic to normothermic temperatures with HBOC-201. In this study, substandard livers were continually oxygenated and perfused, increasing the usage of donor organs that were previously rejected. Importantly, HBOC-201 can be used during the HMP phase which avoids the need to change the perfusion fluid when switching from hypothermia to normothermia (de Vries et al., 2018; Matton et al., 2018; van Leeuwen et al., 2019). Although HBOC-201 received human use approval in South Africa and veterinary use in the US, due to vasoconstriction effects, Food and Drug Administration (FDA) has not approved HBOCs for human use in the US. This product has been evaluated in non-cardiac surgery patients and trauma patients, and is under further clinical investigation for treatment of life-threatening anaemia (Sen Gupta, 2019).

To address the urgent medical need in liver transplantation, VirTech Bio, Inc. (VTB) has explored using a non-cellular HBOC to address the concept that effective oxygenation of isolated *ex vivo* organs is the key point in organ transplantation (Chang et al., 2022). Thus, VTB is testing a novel HBOC product, VIR-XVl, in combination with MP to improve donor organ preservation. VIR-XVl is a purified, glutaraldehyde polymerized, high molecular weight (>1,000 kD) HBOC. It is designed as a hemoglobin hyperpolymer for retention in the *ex vivo* perfusate system and is formulated at a high oxygen carrying capacity. It is deoxygenated, stable at room temperature, and stored in oxygen-impermeable bags or bottles. Unlike RBC, VIR-XVl is universally compatible, sterile, free from potential infectious disease and able for off-shelf use. VIR-XVl demonstrated 1) improved efficacy in providing prolonged hepatic oxygenation, 2) was able to provide normal hepatic functions (e.g., lactate clearance and sustained pH) over a 12-h period, 3) normal anatomical hepatic features after 12-h of *ex vivo* preservation, 4) mitochondrial function was sustained within normal range during the 12-h *ex vivo* period, 5) the magnitude of NO oxidation (nitrite and nitrate levels) was lower compared to previous published data, and 6) hepatocytes sustained full cellular integrity over the 12-h period, including normal anatomical features for mitochondria. Taken together, these parameters indicate that the VIR-XVl maintained intact and fully functional during the 12-h study.

OxyVita is a new generation of HBOC. The OxyVita has been shown to be extremely resistant to breakdown and unfolding, resulting in a molecule that not only starts out as a large polymer, but should stay as such after injection. The zero-link polymerization technology, at its core, is based on removing any residual linking agents within the polymer itself. This eliminates concerns of reverse reactions or decomposition due to non-specific binding, temperature and pressure changes also eliminate the risks of residual linker toxicity.

Hemoglobin-vesicles (Hb-Vs) are phospholipid vesicles containing human-derived Hb. The diameter of the vesicles is 250–280 nm, which is smaller than that of RBCs. Hb-Vs are saturated for 50% at an O_2 pressure between 9 mm Hg and 30 mm Hg. They do not contain clinically relevant RBC antigens and have a longer shelf life than RBCs. The porcine models of using Hb-Vs for perfusion (Shonaka et al., 2018; Shonaka et al., 2019) showed increased O_2 consumption during subnormothermic machine perfusion (SNMP) and decreased alanine aminotransferase and lactate dehydrogenase levels after reperfusion compared to hypothermic machine perfusion (HMP) and SNMP, without an additional OC.

$HEMO_2$life was the first HBOC recently approved by the European Health authorities. The natural extracellular Hb equivalent Hemarina M101 ($HEMO_2$life®, France) is obtained from a marine invertebrate: Arenicola marina, a lugworm. It is composed of 156 globins and 44 non-globin linker chains that can carry up to 156 O_2 molecules when saturated, which results in a high O_2-binding capacity. Hemarina M101 is active over a large range of temperatures (4°C to 37°C) and releases O_2 according to a simple gradient that does not require any allosteric effector. The molecule possesses intrinsic Cu/Zn-superoxide dismutase antioxidant activity that, to a certain extent, protects tissue from superoxide radicals (Rousselot et al., 2006). $HEMO_2$life®, which contains M101 has been used for static cold storage (SCS) and has shown superior results in organ preservation. In an obese Zucker rat model (Asong-Fontem et al., 2021) et al., a total of 36 livers were procured from obese Zucker rats and randomly divided into three groups, i.e., control, SCS-24H and SCS-24H + M101 (M101 at 1 g/L), mimicking the gold standard of organ preservation. *Ex situ* machine perfusion for 2 h was used to evaluate the quality of the livers. Perfusates were sampled for

functional assessment, biochemical analysis and subsequent biopsies were performed for assessment of ischemia-reperfusion markers. Transaminases, Glutamate dehydrogenase (GDH) and lactate levels at the end of reperfusion were significantly lower in the group preserved with M101 ($p < 0.05$). Protection from reactive oxygen species (low Malondialdehyde (MDA) and higher production of NO_2-NO_3) and less inflammation (HMGB1) were also observed in this group ($p < 0.05$). These data demonstrate, for the first time, that the addition of $HEMO_2life^{®}$ to the preservation solution significantly protects steatotic livers during SCS by decreasing reperfusion injury and improving graft function. In addition, M101 the only Oxygen Carrier (OC) compatible for a wide range of temperatures, suggesting that it can be used in hypothermia as well as normothermia.

4 Present situation and research progress of NMP

The history of NMP began with the development of a perfusion chamber for organ preservation at room temperature in 1935 by Alexis Carell and Charles Lindbergh (Lindbergh, 1935). However, due to the complexity of the technology, this technology did not attract widespread attention and use at that time. Then, in the 1960s, a research team investigated (Starzl et al., 1963) the technology of dynamic perfusion preservation of isolated liver. However, because of difficult logistics and financial issues, little attention was paid to this technology. Organ transplantation still requires expanding the donor pool and using marginal organs for transplantation in the 21st century due to the lack of donors. Clinical trails, however, have demonstrated that marginal organs may raise patients post-transplant problems, for example, ischemic cholangiopathy and primary reactive disease may be caused by marginal liver (Foley et al., 2011; Hoyer et al., 2015). People's interest in NMP has returned because it may be utilized to provide new sources of liver grafts, assess the viability of enlarged standard donors (including fatty liver transplants), and enhance organ function. Guarrera et al. (2010) successfully completed the first clinical trial using low-temperature mechanical perfusion, and the post-operative blood transaminase and serum bilirubin levels of patients were successfully decreased, demonstrating the viability of its clinical application. After that, DCD donors received oxygenated hypothermic mechanical perfusion, which produced positive clinical outcomes (Dutkowski et al., 2014). After successful clinical trials, DCD donors were subsequently employed for normothermic machine perfusion of liver transplants.

Clinical findings show that the perfused liver in the first phase clinical trial of NMP (Ravikumar et al., 2016) has stable hemodynamic, synthetic, and metabolic capabilities throughout perfusion, and this may reduce the inherent danger of transplanted marginal organs. In this pilot investigation for a European (Selzner et al., 2016) clinical NEVLP trial of assessing safety and feasibility utilizing Steen solution based on human albumin, all NMP grafts functioned well following transplantation. Numerous animal investigations have demonstrated that marginal grafts kept using NMP have superior transplantation outcomes than those stored with CS, and clearly outperform typical static cryopreservation in terms of minimizing cell damage and post-transplantation survival rates (Schön et al., 2001; Brockmann et al., 2009; Fondevila et al., 2011; Knaak et al., 2014; Liu et al., 2016).

By combining *in situ* normothermic regional perfusion (NRP) with normothermic mechanical perfusion, the De Carlis et al. (2017) team successfully used DCD donors in clinical liver transplantation and the survival rate after 6 months of follow-up was 100%. In 4 abandoned human donor livers, op den Dries et al. (2013) performed mechanical perfusion at room temperature for 6 h. After 30 min, the metabolic lactic acid value reduced to a normal level, suggesting the recovery of liver function, and the perfusion of the portal vein and hepatic artery essentially recovered. Both before and after perfusion, there was no liver tissue deterioration. The first clinical trial of marginal donor liver transplantation following extracorporeal normothermic mechanical perfusion was finished in 2016 by Perera et al. (2016). The donor suffered a cardiac arrest during the procedure, which resulted in inadequate liver perfusion 109 min later. However, lactic acid levels were decreased and bile started to come out of the donor liver after two hours of normothermic mechanical perfusion. The patient had a transplant after 6.5 h of normothermic mechanical perfusion. During the follow-up period, there were no biliary complications and the surgical recovery went pretty smoothly. The liver transplantation experiment using 20 donor livers following normothermic mechanical perfusion was reported by Ravikumar et al. (2016). Nine hours of normothermic mechanical perfusion were given to the donor livers before transplantation. The liver function and blood gas readings were essentially normal during the perfusion period. NMP models the reperfusion under physiological circumstances perfectly. NMP can successfully save marginal donor liver, as demonstrated by experimental investigations and clinically successful cases, although it also has certain hazards. In case of equipment failure, the liver must be abandoned. Therefore, the NMP equipment has high requirements, and the setting of perfusate and perfusion parameters also needs further discussion.

5 ECD and NMP

Around two billion individuals worldwide have hepatitis B, and one million of them pass away from the disease late consequences, according to WHO figures (Zanierato et al., 2020). Since there are not enough donor livers to meet the rapidly rising demand for liver transplants, DCD donors and other extended standard donor livers are gradually being used. Expanded standard donor liver has not yet been well defined (Vodkin and Kuo, 2017). Currently, several ECD markers that are often utilized include. 1) Elderly donors; 2) Liver donors with bullous steatosis; 3) DCD donors; 4) Organ malfunction during donor donation; 5) Dead donors of hypoxia and cerebrovascular accident; 6) Donors of extrahepatic malignant tumors include donors with extremely contagious illnesses. DCD donors are now the most frequent ECD donors. In the United States, the percentage of liver transplants employing DCD donors has increased (Manyalich et al., 2018) for the last ten year. The primary factor impeding the extensive use of DCD donors is the post-transplant ischemic bile duct damage (Reich et al., 2009). Given that DCD donors are unique, one of the primary variables causing ischemic biliary problems following DCD donor liver surgery is their long-term heat ischemia. In addition, postoperative biliary problems are significantly influenced by the length of cold ischemia and the age of the donor liver. The latest advancement of mechanical

perfusion has greatly enhanced the preservation quality of DCD donor organs compared to earlier times. Given the features of mechanical perfusion at normal temperature, it is now one of the most promising approaches for DCD donors. The incidence of postoperative biliary problems is higher in DCD donors than in conventional donors because the perfusion impact of typical static cryopreservation on the donor liver is not optimal. The metabolic condition of liver cells during mechanical perfusion of a liver transplant can be significantly improved, which lowers the risk of patient postoperative problems (Angelico et al., 2016).

6 Feasibility evaluation of NMP application before liver transplantation

The risk assessment of whether an isolated liver meets the criteria for transplantation has not been established until now. Liver donor criteria usually include age, recipient criteria, and gross appearance of the liver. The subjective, unstandardized assessment of the surgeon is an important reference for the acceptability of the donor liver. The lack of objective, independent predictors and variables to predict graft function after transplantation leads to the discarding of potentially functional livers. In the clinical practice of NMP, such as elderly donor liver or steatosis liver with DCD can get objective evaluation, which has a positive effect on whether more donor liver can be applied in clinical transplantation (Ceresa et al., 2018; Resch et al., 2020). NMP was used to evaluate the graft survival rate before donor liver transplantation, which includes liver function parameters such as metabolic acidosis, pH stability, stable hepatic artery and portal vein hemodynamics, decreased transaminase levels, glucose parameters and bile production. The survival rate test provided objective evidence of liver function.

Mergental et al. (2016) reported the survival assessment of five liver transplants through normothermic mechanical liver perfusion Normothermic *ex vivo* liver perfusion (NMP-L). Evaluation protocols included perfusate lactate, bile production, vascular flow, and liver appearance. Before NMP, all the livers were exposed to static refrigeration at different periods, and the grafts played an immediate role after transplantation. During an average follow-up of 7 months (ranging from 6 to 19 months), liver function tests were normal. In this study, the researchers successfully evaluated and resuscitated a batch of "rejected" liver transplant patients by testing the viability of some high-risk donor livers during NMP-L, and the patients recovered after transplanting these high-risk donor livers. This pilot study shows that a proportion of high-risk donor livers might be transplanted by subjecting them to viability testing during NMP-L, without compromising patient safety in a cohort of low-risk recipients.

Thomas Vogel et al. (2017) Conducted a 24-Hour Normothermic Machine Perfusion of Discarded Human Liver Grafts at the Oxford Transplant Centre. Thirteen human liver grafts which had been discarded for transplantation, were entered into this study. Organ procurement was performed after cardiac arrest (Donation after circulatory death, DCD) in nine of 13 liver donors (69%). The results suggest that normothermic perfusion preservation of human livers for 24 h was shown to be technically feasible. Human liver grafts, all of which had been discarded for transplantation, showed organ viability with respect to metabolic and synthetic liver function (to varying degrees). In this study, researchers demonstrated good correlation between bile production during normothermic perfusion and histologic examination post-perfusion. Bile production was significantly correlated with better histological grading (p = 0.001). The researchers also concluded that prolonged normothermic preservation might allow time for recovery, and it might also offer a useful platform for therapeutic delivery (steatosis reduction). NMP allows functional parameters to be measured as a marker of the viability of the organ: prolonged NMP might allow clinicians to accept a high-risk organ on the basis (possibly of greatest value).

Mergental et al. (2020) conducted a prospective, non-randomized, adaptive phase 2 trial in a large single center, and objectively evaluated the livers discarded by 31 British centers that met specific high-risk criteria using NMP. In this first systematic study on objective survival criteria for livers that meet the specific high-risk characteristics of initially considered "non-transplantable" organs, the 31 livers were evaluated for activity with a lactate clearance rate (≤) of 2.5 mmoL/L within 4 h, of which 22 (71%) livers were transplanted after a median preservation time of 18 h, and the survival time was 100.90 days. During a median follow-up period of 542 days, four patients (18%) developed biliary stricture and needed re-transplantation, other patients had good liver function. Among them, 71% of abandoned livers can be successfully transplanted, and the 90 days survival rate of patients and grafts is 100%. The 1-year patient and graft survival rates were 100% and 86%, respectively.

Quintini et al. (2022) performed NMP evaluation on 21 livers from other transplant centers that were rejected (which were considered to use SCS non-transplantable grafts), with perfusion times ranging from 3 h 49 min to 10 h 29 min. Six of them were discarded after NMP because they did not meet liver survival criteria, and the remaining 15 were considered suitable for transplantation. None of the patients had primary non-function after transplantation. During the follow-up period of 8 weeks–14 months, except one patient had ischemic cholangiopathy 4 months later, the other patients had good liver function. A total of 71.5% of the abandoned livers that received extracorporeal normothermic machine perfusion were successfully transplanted after organ perfusion and activity index evaluation.

Watson et al. (2018) conducted a pre-implantation evaluation on 47 cases of liver that were considered not eligible for liver transplantation. They evaluated liver viability of orthotopic perfusion and determined the parameters that may be valuable within an acceptable range. The researchers analyzed the characteristics of perfusion, and evaluated liver viability included transaminase release, glucose metabolism, lactate clearance and acid-base balance, which can evaluate the liver survival rate during normothermic perfusion. They proposed that the assessment of bile pH value may provide valuable insights into the integrity of bile ducts and the risk of ischemic bile duct disease after transplantation. Among the 47 liver donors, 22 liver donors received liver transplantation. The liver cell damage was reflected in the concentration of aminotransferase, which was related to the peak transaminase level after transplantation. Among the 47 livers receiving normothermic perfusion, the ALT was< 6000 IU/L in all but six livers within 2 h. The researchers tended to use ALT as a marker of hepatocellular carcinoma, and they found no evidence to support the effect of bile production on the outcome after transplantation.

According to the previous research reports, although there is no completely determined standard for the evaluation of liver function

by NMP before liver transplantation, the currently widely accepted evaluation standards (Watson et al., 2018) include: lactic acid clearance rate in perfusion fluid, pH dynamic balance (no need to continuously supplement bicarbonate), stable hepatic artery and portal vein hemodynamics, decreased transaminase level, blood glucose, bile glucose, the concentrations of glucose, bile bicarbonate and bile lactate dehydrogenase in the perfusate. The activity test before transplantation will greatly reduce the risks associated with marginal donor organs, thereby lowering the threshold for retrieving such organs, reducing the risk of primary non-function after transplantation, and the rejection of organs and enable more patients to obtain rescue opportunities.

7 The trail results of NMP in liver transplantation

Ravikumar et al. (2016) conducted a Phase 1 (First-in-Man) clinical trial of liver transplantation after *ex vivo* normothermic machine perfusion. In this Phase 1 trial, NMP livers were matched 1:2 to cold-stored livers. Twenty patients underwent liver transplantation after NMP. This first report of liver transplantation using NMP-preserved livers demonstrates the safety and feasibility of using this technology from retrieval to transplantation, including transportation. NMP may be valuable in increasing the number of donor livers and improving the function of transplantable organs. The primary endpoint was 30-day graft survival. The results showed the procedure is feasible and safe. All livers enrolled into the study were successfully transplanted with 100% 30-day recipient and graft survival. This is the first report of normothermic perfusion in clinical liver transplantation. This preservation methodology potentially reduces the risk inherent in transplanting marginal donor organs. The researchers believe that normothermic preservation may substantially improve organ utilization.

According to a report of Watson (Watson et al., 2016) on a 57-year-old DCD donor, after circulatory death, the liver obtained from the donor underwent 350 min of cold ischemia and then was perfused and transplanted into the recipient at normothermic temperature. After receiving the transplantation, the patient returned to normal and was discharged on the eighth day. The liver biochemistry was normal from the 19th day and remained normal since then. The donor common bile duct resected at the time of transplantation showed that the peribiliary gland was retained, and cholangiography 6 months after transplantation showed no signs of bile duct disease.

Nasralla et al. (2018) carried out a randomized trial of 220 cases of liver transplantation, which is the first known randomized controlled trial comparing the effects of machine perfusion technology and traditional static refrigeration in human liver transplantation. In this study, the liver was divided into static cold storage group (N = 100) and NMP group (N = 120). The rejection rate of SCS group was 24.1%, higher than that of NMP group (11.7%) (one liver was discarded due to the failure of perfusion equipment). From cold perfusion of donor aorta to reperfusion of recipient aorta, the average total preservation time of NMP group was 11 h and 54 min, which was higher than that of SCS group (7 h and 45 min). Post reperfusion syndrome was more common in SCS group (32 of 97 cases) than in NMP group (15 of 121 cases). The results of AST and EAD, clinically recognized biomarkers for long-term transplantation and patient survival, showed that the peak AST (main result) in the first 7 days after transplantation in the NMP group was reduced by 49.4% compared with the SCS group. The evaluation data of the incidence of EAD showed that the incidence of EAD in the NMP group (12 out of 119 cases) was 74% lower than that in the SCS group (29 out of 97 cases). "Transplanted livers were shown to function better if they had been preserved using a novel technology, NMP. The benefit was most pronounced in the most marginal donor livers, particularly those originating from DCD donors," noted by Nasralla. The trial demonstrates that NMP is feasible and effective for organ preservation and, if successfully translated to clinical practice, could reduce tissue injury associated with liver transplants and enable better assessment of organ quality to ultimately improve liver transplantation outcomes.

Ceresa et al. (2019) carried out a multicenter prospective study to evaluate the safety and feasibility of normothermic mechanical perfusion after static cold storage (PSCS-NMP) in liver transplantation. In this study, for ensuring consistency intervention tests, 31 cases (23 DBD and 8 DCD) of donor liver stored in low temperature environment 3–8 h with NMP circuit for infusion, and the clearance of lactic acid, glucose metabolism, pH to maintain, bile, transaminase level and flow rate of infusion, and other data were measured. The overall results showed that the survival rate of the graft was 94% and the incidence of EAD was 13% within 30 days. Patient and graft survival (including one functional graft death) at 12 months was 84%, and patient survival was 90%.

In a pilot, open, randomized, prospective trial, Ghinolfi et al. (2019) randomized 20 primary liver transplant recipients from elderly (≥70 years old) liver donors, including 10 patients in NMP group and 10 patients in CS group. The survival rate of grafts and patients at 6 months, IRI assessed by transaminase peak within 7 days after operation, the incidence of biliary complications at 6 months after operation, and liver and bile duct histology were evaluated. The results showed that one patient in the NMP group lost the graft due to hepatic artery thrombosis (HAT), and the patient survived after 1 year of re-transplantation. One patient in the CS group died of septic shock after re admission due to intestinal obstruction. The histological analysis of this study did not show the main benefits of the NMP group, and its biopsy results were comparable to those of the CS group. However, the investigators pointed out that NMP may detect bile duct injury caused by IRI earlier than other clinical variables.

Bral et al. (2017) conducted a single center experiment. Donor livers were grouped according to a 1:3 ratio of NMP group (N = 10) and SCS group (N = 30). The results showed that the 30 days graft survival rate was the same between the two groups, and there was no significant difference in the 6-month graft survival rate. PNF was not observed in NMP group or SCS group. There was no case of post reperfusion syndrome in the NMP graft, but the intensive care and hospital stay in the NMP group were significantly prolonged. In this study, no significant difference in early receptor transaminases between NMP and SCS preserved grafts was observed. This study considered that NMP had potential technical risks and emphasized the need for a larger randomized study. In a non-randomized pilot study conducted by Bral et al. (2019) from February 2015 to June 2018, 46 cases (3 of them were discarded due to poor ectopic perfusion function) were NMP, including 17 liver donors who purchased their livers locally for NMP immediately, 26 liver donors who purchased their livers from remote locations, first

preserved and transported to the recipient center by SCS, and then NMP was performed. In these two groups of NMP circulation, all livers showed stable portal vein and hepatic artery flow rates, The researchers found that there was a significant correlation between the AST level of the NMP loop and the subsequent EAD of the recipient (r = 0.33; 95% confidence interval, 0.02–0.58; p = 0.03). During the 6-month follow-up, none of the patients receiving NMP transplantation developed ischemic cholangiopathy (IC). The purpose of this study is to explore whether liver transplantation can be delivered from the donor center of SCS until NMP was started at the recipient center, because this will simplify logistics and reduce the cost of the transplantation process. In fact, the results of this study indicate that NMP after SCS can be safely used for low-risk DCD and DBD grafts.

For the three years from November 2016 to October 2019, Markmann et al. (2022) designed and conducted a multicenter randomized clinical trial (International Randomized Trial to Evaluate the Effectiveness of the Portable Organ Care System Liver for Preserving and Assessing Donor Livers for Transplantation). This randomized trial was conducted in 20 US liver transplantation programs, it compared outcomes for 300 recipients of livers preserved using either Organ Care System (OCS) (n = 153) or Ischemic cold storage (ICS) (n = 147). The primary effectiveness end point was incidence of EAD. The primary safety end point was the number of liver graft-related severe adverse events within 30 days after transplant. Secondary end points included OCS Liver *ex vivo* assessment capability of donor allografts, extent of reperfusion syndrome, incidence of IBC at 6 and 12 months, and overall recipient survival after transplant. Among the per-protocol patients (293 patients), 151 were in the OCS-liver group and 142 were in the ICS group. The primary effectiveness end point was met by a significant decrease in EAD (27 of 150 [18%] vs. 44 of 141 [31%]; p = .01). The OCS Liver preserved livers had significant reduction in histopathologic evidence of ischemia-reperfusion injury after reperfusion (less moderate to severe lobular inflammation: nine of 150 [6%] for OCS Liver vs. 18 of 141 [13%] for ICS; p = .004). The OCS Liver was also associated with significant reduction in incidence of IBC 6 months (1.3% vs. 8.5%; p = .02) and 12 months (2.6% vs. 9.9%; p = .02) after transplant. This multicenter randomized clinical trial provides the first indication, that normothermic machine perfusion preservation of deceased donor livers reduces both posttransplant EAD and IBC. Use of the OCS Liver also resulted in increased use of livers from donors after cardiac death. Together these findings indicate that OCS Liver preservation is associated with superior posttransplant outcomes and increased donor liver use.

8 Advantages and limitations of NMP

8.1 Advantages

1. NMP can test the safety and feasibility of transplant donors before transplantation.
2. NMP can dynamically evaluate liver transplantation.
3. NMP may detect bile duct injury caused by IRI earlier than other clinical variables.
4. NMP helps to reduce macrovascular hepatic steatosis.

8.2 Limitations

1. The liver active markers during NMP perfusion should be standardized, which is the key to promote safely and rapidly this field.
2. Physiological mechanism of NMP activates liver donors and optimizes existing technologies.

9 Conclusion

The purpose of this review is to provide an overview of NMP and its application in the preservation of liver before *ex vivo* transplantation, and a retrospective analysis of the current trails on the preservation and transplantation of human liver by normothermic machine perfusion. The feasibility evaluation study of NMP applied to liver transplantation shows that objective and definite criteria for liver function indexes of liver transplantation are needed to ensure that the donor liver can be successfully transplanted into a patient. NMP-L provides survival parameters of liver function before marginal donor liver transplantation, which can increase organ utilization and reduce patient mortality. The use of NMP-L in liver transplantation and preservation shows that it has such evaluation function and has certain feasibility. NMP has advantages in increasing the utilization rate of marginal liver and alleviating the shortage of donor livers for liver transplantation. Future double-blinded, randomized, large clinical trials will be required to evaluate the benefits of NMP technology.

Author contributions

CS collected literature, collated data, and the main writing of the article. HZ, HC, and TZ reviewed the manuscript. All authors read, revised, and approved the manuscript.

Acknowledgments

We thank the project of human red blood cell substitute-the pilot test process optimization and function evaluation of glutaraldehyde polymerized porcine hemoglobin for the support of this study.

Conflict of interest

The authors declare that the research was conducted in the absence of any commercial or financial relationships that could be construed as a potential conflict of interest.

Publisher's note

References

Alix, P., Val-Laillet, D., Turlin, B., Ben Mosbah, I., Burel, A., Bobillier, E., et al. (2020). Adding the oxygen carrier M101 to a cold-storage solution could be an alternative to HOPE for liver graft preservation. *JHEP Rep.* 2 (4), 100119. doi:10.1016/j.jhepr.2020.100119

Angelico, R., Perera, M. T., Ravikumar, R., Holroyd, D., Coussios, C., Mergental, H., et al. (2016). Normothermic machine perfusion of deceased donor liver grafts is associated with improved postreperfusion hemodynamics. *Transpl. Direct* 2 (9), e97. doi:10.1097/txd.0000000000000611

Asong-Fontem, N., Panisello-Rosello, A., Lopez, A., Imai, K., Zal, F., Delpy, E., et al. (2021). A novel oxygen carrier (M101) attenuates ischemia-reperfusion injuries during static cold storage in steatotic livers. *Int. J. Mol. Sci.* 22 (16), 8542. doi:10.3390/ijms22168542

Aufhauser, D. D., Jr., and Foley, D. P. (2021). Beyond ice and the cooler: Machine perfusion strategies in liver transplantation. *Clin. Liver Dis.* 25 (1), 179–194. doi:10.1016/j.cld.2020.08.013

Aydin, G., Okiye, S. E., and Zincke, H. (1982). Successful 24-hour preservation of the ischemic canine kidney with Euro-Collins solution. *J. Urol.* 128 (6), 1401–1403. doi:10.1016/s0022-5347(17)53517-x

Badawy, A., Kaido, T., and Uemoto, S. (2020). Current status of liver transplantation using marginal grafts. *J. Invest. Surg.* 33 (6), 553–564. doi:10.1080/08941939.2018.1517197

Bessems, M., Doorschodt, B. M., van Vliet, A. K., and van Gulik, T. M. (2005). Improved rat liver preservation by hypothermic continuous machine perfusion using polysol, a new, enriched preservation solution. *Liver Transpl.* 11 (5), 539–546. doi:10.1002/lt.20388

Bral, M., Dajani, K., Leon Izquierdo, D., Bigam, D., Kneteman, N., Ceresa, C. D. L., et al. (2019). A back-to-base experience of human normothermic *ex situ* liver perfusion: Does the chill kill? *Liver Transpl.* 25 (6), 848–858. doi:10.1002/lt.25464

Bral, M., Gala-Lopez, B., Bigam, D., Kneteman, N., Malcolm, A., Livingstone, S., et al. (2017). Preliminary single-center Canadian experience of human normothermic *ex vivo* liver perfusion: Results of a clinical trial. *Am. J. Transpl.* 17 (4), 1071–1080. doi:10.1111/ajt.14049

Brockmann, J., Reddy, S., Coussios, C., Pigott, D., Guirriero, D., Hughes, D., et al. (2009). Normothermic perfusion: A new paradigm for organ preservation. *Ann. Surg.* 250 (1), 1–6. doi:10.1097/SLA.0b013e3181a63c10

Ceresa, C. D. L., Nasralla, D., Coussios, C. C., and Friend, P. J. (2018). The case for normothermic machine perfusion in liver transplantation. *Liver Transpl.* 24 (2), 269–275. doi:10.1002/lt.25000

Ceresa, C. D. L., Nasralla, D., Watson, C. J. E., Butler, A. J., Coussios, C. C., Crick, K., et al. (2019). Transient cold storage prior to normothermic liver perfusion may facilitate adoption of a novel technology. *Liver Transpl.* 25 (10), 1503–1513. doi:10.1002/lt.25584

Chang, T. M. S., Bulow, L., Jahr, J. S., Sakaia, H., and Yang, C. (2022). *Chengmin nanobiotherapeutic based blood substitutes*.

Chen, G., Wang, C., Ko, D. S., Qiu, J., Yuan, X., Han, M., et al. (2017). Comparison of outcomes of kidney transplantation from donation after brain death, donation after circulatory death, and donation after brain death followed by circulatory death donors. *Clin. Transpl.* 31 (11), e13110. doi:10.1111/ctr.13110

Collins, G. M., Bravo-Shugarman, M., and Terasaki, P. I. (1969). Kidney preservation for transportation. Initial perfusion and 30 hours' ice storage. *Lancet* 2 (7632), 1219–1222. doi:10.1016/s0140-6736(69)90753-3

Collins, G. M., and Wicomb, W. N. (1992). New organ preservation solutions. *Kidney Int. Suppl.* 38, S197–S202.

De Carlis, R., Di Sandro, S., Lauterio, A., Ferla, F., Dell'Acqua, A., Zanierato, M., et al. (2017). Successful donation after cardiac death liver transplants with prolonged warm ischemia time using normothermic regional perfusion. *Liver Transpl.* 23 (2), 166–173. doi:10.1002/lt.24666

de Vries, Y., van Leeuwen, O. B., Matton, A. P. M., Fujiyoshi, M., de Meijer, V. E., and Porte, R. J. (2018). *Ex situ* normothermic machine perfusion of donor livers using a haemoglobin-based oxygen carrier: A viable alternative to red blood cells. *Transpl. Int.* 31 (11), 1281–1282. doi:10.1111/tri.13320

Dutkowski, P., Schlegel, A., de Oliveira, M., Müllhaupt, B., Neff, F., and Clavien, P. A. (2014). HOPE for human liver grafts obtained from donors after cardiac death. *J. Hepatol.* 60 (4), 765–772. doi:10.1016/j.jhep.2013.11.023

Flameng, W., Dyszkiewicz, W., and Minten, J. (1988). Energy state of the myocardium during long-term cold storage and subsequent reperfusion. *Eur. J. Cardiothorac. Surg.* 2 (4), 244–255. doi:10.1016/1010-7940(88)90079-6

Foley, D. P., Fernandez, L. A., Leverson, G., Anderson, M., Mezrich, J., Sollinger, H. W., et al. (2011). Biliary complications after liver transplantation from donation after cardiac death donors: An analysis of risk factors and long-term outcomes from a single center. *Ann. Surg.* 253 (4), 817–825. doi:10.1097/SLA.0b013e3182104784

Fondevila, C., Hessheimer, A. J., Maathuis, M. H., Muñoz, J., Taurá, P., Calatayud, D., et al. (2011). Superior preservation of DCD livers with continuous normothermic perfusion. *Ann. Surg.* 254 (6), 1000–1007. doi:10.1097/SLA.0b013e31822b8b2f

Gaurav, R., Butler, A. J., Kosmoliaptsis, V., Mumford, L., Fear, C., Swift, L., et al. (2022). Liver transplantation outcomes from controlled circulatory death donors: SCS vs *in situ* NRP vs *ex situ* NMP. *Ann. Surg.* 275 (6), 1156–1164. doi:10.1097/sla.0000000000005428

Ghinolfi, D., Rreka, E., De Tata, V., Franzini, M., Pezzati, D., Fierabracci, V., et al. (2019). Pilot, open, randomized, prospective trial for normothermic machine perfusion evaluation in liver transplantation from older donors. *Liver Transpl.* 25 (3), 436–449. doi:10.1002/lt.25362

Guarrera, J. V., Henry, S. D., Samstein, B., Odeh-Ramadan, R., Kinkhabwala, M., Goldstein, M. J., et al. (2010). Hypothermic machine preservation in human liver transplantation: The first clinical series. *Am. J. Transpl.* 10 (2), 372–381. doi:10.1111/j.1600-6143.2009.02932.x

Guibert, E. E., Petrenko, A. Y., Balaban, C. L., Somov, A. Y., Rodriguez, J. V., and Fuller, B. J. (2011). Organ preservation: Current concepts and new strategies for the next decade. *Transfus. Med. Hemother* 38 (2), 125–142. doi:10.1159/000327033

Haque, O., Raigani, S., Rosales, I., Carroll, C., Coe, T. M., Baptista, S., et al. (2021). Thrombolytic therapy during *ex-vivo* normothermic machine perfusion of human livers reduces peribiliary vascular plexus injury. *Front. Surg.* 8, 644859. doi:10.3389/fsurg.2021.644859

Hartley, L. C., Collins, G. M., and Clunie, G. J. (1971). Kidney preservation for transportation. Function of 29 human-cadaver kidneys preserved with an intracellular perfusate. *N. Engl. J. Med.* 285 (19), 1049–1052. doi:10.1056/nejm197111042851903

Hoyer, D. P., Paul, A., Gallinat, A., Molmenti, E. P., Reinhardt, R., Minor, T., et al. (2015). Donor information based prediction of early allograft dysfunction and outcome in liver transplantation. *Liver Int.* 35 (1), 156–163. doi:10.1111/liv.12443

Jahr, J. S., Moallempour, M., and Lim, J. C. (2008). HBOC-201, hemoglobin glutamer-250 (bovine), Hemopure (Biopure Corporation). *Expert Opin. Biol. Ther.* 8 (9), 1425–1433. doi:10.1517/14712598.8.9.1425

Jay, C. L., Lyuksemburg, V., Ladner, D. P., Wang, E., Caicedo, J. C., Holl, J. L., et al. (2011). Ischemic cholangiopathy after controlled donation after cardiac death liver transplantation: A meta-analysis. *Ann. Surg.* 253 (2), 259–264. doi:10.1097/SLA.0b013e318204e658

Kaminski, J., Hannaert, P., Kasil, A., Thuillier, R., Leize, E., Delpy, E., et al. (2019). Efficacy of the natural oxygen transporter HEMO(2) life(®) in cold preservation in a preclinical porcine model of donation after cardiac death. *Transpl. Int.* 32 (9), 985–996. doi:10.1111/tri.13434

Karam, G., Compagnon, P., Hourmant, M., Despins, P., Duveau, D., Noury, D., et al. (2005). A single solution for multiple organ procurement and preservation. *Transpl. Int.* 18 (6), 657–663. doi:10.1111/j.1432-2277.2005.00083.x

Khedr, S., Palygin, O., Pavlov, T. S., Blass, G., Levchenko, V., Alsheikh, A., et al. (2019). Increased ENaC activity during kidney preservation in Wisconsin solution. *BMC Nephrol.* 20 (1), 145. doi:10.1186/s12882-019-1329-7

Kiyooka, T., Oshima, Y., Fujinaka, W., Iribe, G., Shimizu, J., Mohri, S., et al. (2016). Celsior preserves cardiac mechano-energetics better than University of Wisconsin solution by preventing oxidative stress. *Interact. Cardiovasc Thorac. Surg.* 22 (2), 168–175. doi:10.1093/icvts/ivv324

Knaak, J. M., Spetzler, V. N., Goldaracena, N., Boehnert, M. U., Bazerbachi, F., Louis, K. S., et al. (2014). Subnormothermic *ex vivo* liver perfusion reduces endothelial cell and bile duct injury after donation after cardiac death pig liver transplantation. *Liver Transpl.* 20 (11), 1296–1305. doi:10.1002/lt.23986

Kure, T., and Sakai, H. (2021). Preparation of artificial red blood cells (hemoglobin vesicles) using the rotation-revolution mixer for high encapsulation efficiency. *ACS Biomater. Sci. Eng.* 7 (6), 2835–2844. doi:10.1021/acsbiomaterials.1c00424

Lindbergh, C. A. (1935). An apparatus for the culture of whole organs. *J. Exp. Med.* 62 (3), 409–431. doi:10.1084/jem.62.3.409

Liu, Q., Nassar, A., Farias, K., Buccini, L., Mangino, M. J., Baldwin, W., et al. (2016). Comparing normothermic machine perfusion preservation with different perfusates on porcine livers from donors after circulatory death. *Am. J. Transpl.* 16 (3), 794–807. doi:10.1111/ajt.13546

Liu, Q., Vekemans, K., Iania, L., Komuta, M., Parkkinen, J., Heedfeld, V., et al. (2014). Assessing warm ischemic injury of pig livers at hypothermic machine perfusion. *J. Surg. Res.* 186 (1), 379–389. doi:10.1016/j.jss.2013.07.034

Manyalich, M., Nelson, H., and Delmonico, F. L. (2018). The need and opportunity for donation after circulatory death worldwide. *Curr. Opin. Organ Transpl.* 23 (1), 136–141. doi:10.1097/mot.0000000000000486

Markmann, J. F., Abouljoud, M. S., Ghobrial, R. M., Bhati, C. S., Pelletier, S. J., Lu, A. D., et al. (2022). Impact of portable normothermic blood-based machine perfusion on outcomes of liver transplant: The OCS liver PROTECT randomized clinical trial. *JAMA Surg.* 157 (3), 189–198. doi:10.1001/jamasurg.2021.6781

Matton, A. P. M., Burlage, L. C., van Rijn, R., de Vries, Y., Karangwa, S. A., Nijsten, M. W., et al. (2018). Normothermic machine perfusion of donor livers without the need for human blood products. *Liver Transpl.* 24 (4), 528–538. doi:10.1002/lt.25005

Menz, D. H., Feltgen, N., Menz, H., Müller, B. K., Lechner, T., Dresp, J., et al. (2018). How to ward off retinal toxicity of perfluorooctane and other perfluorocarbon liquids? *Invest. Ophthalmol. Vis. Sci.* 59 (12), 4841–4846. doi:10.1167/iovs.18-24698

Mergental, H., Laing, R. W., Kirkham, A. J., Perera, M., Boteon, Y. L., Attard, J., et al. (2020). Transplantation of discarded livers following viability testing with normothermic machine perfusion. *Nat. Commun.* 11 (1), 2939. doi:10.1038/s41467-020-16251-3

Mergental, H., Perera, M. T., Laing, R. W., Muiesan, P., Isaac, J. R., Smith, A., et al. (2016). Transplantation of declined liver allografts following normothermic *ex-situ* evaluation. *Am. J. Transpl.* 16 (11), 3235–3245. doi:10.1111/ajt.13875

Nasralla, D., Coussios, C. C., Mergental, H., Akhtar, M. Z., Butler, A. J., Ceresa, C. D. L., et al. (2018). A randomized trial of normothermic preservation in liver transplantation. *Nature* 557 (7703), 50–56. doi:10.1038/s41586-018-0047-9

op den Dries, S., Karimian, N., Sutton, M. E., Westerkamp, A. C., Nijsten, M. W., Gouw, A. S., et al. (2013). *Ex vivo* normothermic machine perfusion and viability testing of discarded human donor livers. *Am. J. Transpl.* 13 (5), 1327–1335. doi:10.1111/ajt.12187

Parente, A., Osei-Bordom, D. C., Ronca, V., Perera, M., and Mirza, D. (2020). Organ restoration with normothermic machine perfusion and immune reaction. *Front. Immunol.* 11, 565616. doi:10.3389/fimmu.2020.565616

Perera, T., Mergental, H., Stephenson, B., Roll, G. R., Cilliers, H., Liang, R., et al. (2016). First human liver transplantation using a marginal allograft resuscitated by normothermic machine perfusion. *Liver Transpl.* 22 (1), 120–124. doi:10.1002/lt.24369

Quintini, C., Del Prete, L., Simioni, A., Del Angel, L., Diago Uso, T., D'Amico, G., et al. (2022). Transplantation of declined livers after normothermic perfusion. *Surgery* 171 (3), 747–756. doi:10.1016/j.surg.2021.10.056

Rauen, U., and de Groot, H. (2008). Inherent toxicity of organ preservation solutions to cultured hepatocytes. *Cryobiology* 56 (1), 88–92. doi:10.1016/j.cryobiol.2007.09.003

Ravikumar, R., Jassem, W., Mergental, H., Heaton, N., Mirza, D., Perera, M. T., et al. (2016). Liver transplantation after *ex vivo* normothermic machine preservation: A phase 1 (First-in-Man) clinical trial. *Am. J. Transpl.* 16 (6), 1779–1787. doi:10.1111/ajt.13708

Reich, D. J., Mulligan, D. C., Abt, P. L., Pruett, T. L., Abecassis, M. M., D'Alessandro, A., et al. (2009). ASTS recommended practice guidelines for controlled donation after cardiac death organ procurement and transplantation. *Am. J. Transpl.* 9 (9), 2004–2011. doi:10.1111/j.1600-6143.2009.02739.x

Resch, T., Cardini, B., Oberhuber, R., Weissenbacher, A., Dumfarth, J., Krapf, C., et al. (2020). Transplanting marginal organs in the era of modern machine perfusion and advanced organ monitoring. *Front. Immunol.* 11, 631. doi:10.3389/fimmu.2020.00631

Riess, J. G. (2001). Oxygen Carriers ("Blood Substitutes")Raison d'Etre, Chemistry, and Some Physiology *Blut ist ein ganz besondrer Saft*. *Chem. Rev.* 101 (9), 2797–2920. doi:10.1021/cr970143c

Rousselot, M., Delpy, E., Drieu La Rochelle, C., Lagente, V., Pirow, R., Rees, J. F., et al. (2006). Arenicola marina extracellular hemoglobin: A new promising blood substitute. *Biotechnol. J.* 1 (3), 333–345. doi:10.1002/biot.200500049

Schön, M. R., Kollmar, O., Wolf, S., Schrem, H., Matthes, M., Akkoc, N., et al. (2001). Liver transplantation after organ preservation with normothermic extracorporeal perfusion. *Ann. Surg.* 233 (1), 114–123. doi:10.1097/00000658-200101000-00017

Selzner, M., Goldaracena, N., Echeverri, J., Kaths, J. M., Linares, I., Selzner, N., et al. (2016). Normothermic *ex vivo* liver perfusion using steen solution as perfusate for human liver transplantation: First North American results. *Liver Transpl.* 22 (11), 1501–1508. doi:10.1002/lt.24499

Sen Gupta, A. (2019). Hemoglobin-based oxygen carriers: Current state-of-the-art and novel molecules. *Shock* 52 (1), 70–83. doi:10.1097/shk.0000000000001009

Shonaka, T., Matsuno, N., Obara, H., Yoshikawa, R., Nishikawa, Y., Gouchi, M., et al. (2018). Application of perfusate with human-derived oxygen carrier solution under subnormothermic machine perfusion for donation after cardiac death liver grafts in pigs. *Transpl. Proc.* 50 (9), 2821–2825. doi:10.1016/j.transproceed.2018.02.184

Shonaka, T., Matsuno, N., Obara, H., Yoshikawa, R., Nishikawa, Y., Ishihara, Y., et al. (2019). Impact of human-derived hemoglobin based oxygen vesicles as a machine perfusion solution for liver donation after cardiac death in a pig model. *PLoS One* 14 (12), e0226183. doi:10.1371/journal.pone.0226183

Starzl, T. E., Marchioro, T. L., Vonkaulla, K. N., Hermann, G., Brittain, R. S., and Waddell, W. R. (1963). Homotransplantation of the liver in humans. *Surg. Gynecol. Obstet.* 117, 659–676.

Stewart, Z. A. (2015). UW solution: Still the "gold standard" for liver transplantation. *Am. J. Transpl.* 15 (2), 295–296. doi:10.1111/ajt.13062

Taguchi, K., Urata, Y., Anraku, M., Maruyama, T., Watanabe, H., Sakai, H., et al. (2009). Pharmacokinetic study of enclosed hemoglobin and outer lipid component after the administration of hemoglobin vesicles as an artificial oxygen carrier. *Drug Metab. Dispos.* 37 (7), 1456–1463. doi:10.1124/dmd.109.027094

van Leeuwen, O. B., de Vries, Y., Fujiyoshi, M., Nijsten, M. W. N., Ubbink, R., Pelgrim, G. J., et al. (2019). Transplantation of high-risk donor livers after *ex situ* resuscitation and assessment using combined hypo- and normothermic machine perfusion: A prospective clinical trial. *Ann. Surg.* 270 (5), 906–914. doi:10.1097/sla.0000000000003540

Vodkin, I., and Kuo, A. (2017). Extended criteria donors in liver transplantation. *Clin. Liver Dis.* 21 (2), 289–301. doi:10.1016/j.cld.2016.12.004

Vogel, T., Brockmann, J. G., Quaglia, A., Morovat, A., Jassem, W., Heaton, N. D., et al. (2017). The 24-hour normothermic machine perfusion of discarded human liver grafts. *Liver Transpl.* 23 (2), 207–220. doi:10.1002/lt.24672

Wahlberg, J. A., Southard, J. H., and Belzer, F. O. (1986). Development of a cold storage solution for pancreas preservation. *Cryobiology* 23 (6), 477–482. doi:10.1016/0011-2240(86)90056-8

Watson, C. J. E., Kosmoliaptsis, V., Pley, C., Randle, L., Fear, C., Crick, K., et al. (2018). Observations on the *ex situ* perfusion of livers for transplantation. *Am. J. Transpl.* 18 (8), 2005–2020. doi:10.1111/ajt.14687

Watson, C. J., Kosmoliaptsis, V., Randle, L. V., Russell, N. K., Griffiths, W. J., Davies, S., et al. (2016). Preimplant normothermic liver perfusion of a suboptimal liver donated after circulatory death. *Am. J. Transpl.* 16 (1), 353–357. doi:10.1111/ajt.13448

Wechsler, A. S., Abd-Elfattah, A. S., Murphy, C. E., Salter, D. R., Brunsting, L. A., and Goldstein, J. P. (1986). Myocardial protection. *J. Card. Surg.* 1 (3), 271–306. doi:10.1111/j.1540-8191.1986.tb00715.x

Zanierato, M., Dondossola, D., Palleschi, A., and Zanella, A. (2020). Donation after circulatory death: Possible strategies for *in-situ* organ preservation. *Minerva Anestesiol.* 86 (9), 984–991. doi:10.23736/s0375-9393.20.14262-7

frontiers | Frontiers in Medical Technology

TYPE Original Research
PUBLISHED 21 February 2023
DOI 10.3389/fmedt.2023.1074643

OPEN ACCESS

EDITED BY
Binglan Yu,
Massachusetts General Hospital and Harvard Medical School, United States

REVIEWED BY
Smrithi Padmakumar,
Spark Therapeutics Inc., United States
Luciana Magalhães Rebelo Alencar,
Federal University of Maranhão, Brazil

*CORRESPONDENCE
Raymond C. Koehler
✉ rkoehler@jhmi.edu

SPECIALTY SECTION
This article was submitted to Regenerative Technologies, a section of the journal Frontiers in Medical Technology

RECEIVED 19 October 2022
ACCEPTED 13 January 2023
PUBLISHED 21 February 2023

CITATION
Wang J, Shi Y, Cao S, Liu X, Martin LJ, Simoni J, Soltys BJ, Hsia CJC and Koehler RC (2023) Polynitroxylated PEGylated hemoglobin protects pig brain neocortical gray and white matter after traumatic brain injury and hemorrhagic shock.
Front. Med. Technol. 5:1074643.
doi: 10.3389/fmedt.2023.1074643

Polynitroxylated PEGylated hemoglobin protects pig brain neocortical gray and white matter after traumatic brain injury and hemorrhagic shock

Jun Wang[1], Yanrong Shi[1], Suyi Cao[1], Xiuyun Liu[1], Lee J. Martin[2], Jan Simoni[3], Bohdan J. Soltys[3], Carleton J. C. Hsia[3] and Raymond C. Koehler[1]*

[1]Department of Anesthesiology and Critical Care Medicine, Johns Hopkins University, Baltimore, MD, United States, [2]Department of Pathology, Johns Hopkins University, Baltimore, MD, United States, [3]AntiRadical Therapeutics LLC, Sioux Falls, SD, United States

Polynitroxylated PEGylated hemoglobin (PNPH, aka SanFlow) possesses superoxide dismutase/catalase mimetic activities that may directly protect the brain from oxidative stress. Stabilization of PNPH with bound carbon monoxide prevents methemoglobin formation during storage and permits it to serve as an anti-inflammatory carbon monoxide donor. We determined whether small volume transfusion of hyperoncotic PNPH is neuroprotective in a porcine model of traumatic brain injury (TBI) with and without accompanying hemorrhagic shock (HS). TBI was produced by controlled cortical impact over the frontal lobe of anesthetized juvenile pigs. Hemorrhagic shock was induced starting 5 min after TBI by 30 ml/kg blood withdrawal. At 120 min after TBI, pigs were resuscitated with 60 ml/kg lactated Ringer's (LR) or 10 or 20 ml/kg PNPH. Mean arterial pressure recovered to approximately 100 mmHg in all groups. A significant amount of PNPH was retained in the plasma over the first day of recovery. At 4 days of recovery in the LR-resuscitated group, the volume of frontal lobe subcortical white matter ipsilateral to the injury was 26.2 ± 7.6% smaller than homotypic contralateral volume, whereas this white matter loss was only 8.6 ± 12.0% with 20-ml/kg PNPH resuscitation. Amyloid precursor protein punctate accumulation, a marker of axonopathy, increased in ipsilateral subcortical white matter by 132 ± 71% after LR resuscitation, whereas the changes after 10 ml/kg (36 ± 41%) and 20 ml/kg (26 ± 15%) PNPH resuscitation were not significantly different from controls. The number of cortical neuron long dendrites enriched in microtubules (length >50 microns) decreased in neocortex by 41 ± 24% after LR resuscitation but was not significantly changed after PNPH resuscitation. The perilesion microglia density increased by 45 ± 24% after LR resuscitation but was unchanged after 20 ml/kg PNPH resuscitation (4 ± 18%). Furthermore, the number with an activated morphology was attenuated by 30 ± 10%. In TBI pigs without HS followed 2 h later by infusion of 10 ml/kg LR or PNPH, PNPH remained neuroprotective. These results in a gyrencephalic brain show that resuscitation from TBI + HS with PNPH protects neocortical gray matter, including dendritic microstructure, and white matter axons and myelin. This neuroprotective effect persists with TBI alone, indicating brain-targeting benefits independent of blood pressure restoration.

KEYWORDS

controlled cortical impact, frontal lobe damage, hemoglobin-based oxygen carrier, dendrite/axon rescue, neuroprotection

Introduction

Traumatic brain injury (TBI) produces an immediate mechanical injury to brain tissue followed by the secondary injury that evolves over acute, subacute, and chronic stages instigated by imbalances in neurotransmitter signal processing and connectivity, mitochondrial dysfunction, oxidative stress, and neuroinflammation (1–5). With moderate or severe TBI, early treatment focuses on maintaining mean arterial blood pressure (MABP) and minimizing brain swelling to mitigate intracranial hypertension. Both factors influence the cerebral pressure gradient, which can be particularly critical in TBI victims because autoregulation-maintained cerebral blood flow can be impaired in some patients (6). Several studies have demonstrated that clinical outcome correlates with maintenance of cerebral perfusion pressure in the range where the limited post-traumatic vascular autoregulatory mechanisms remain operative (7–9). Furthermore, some TBI victims suffer systemic organ-wide multi-trauma accompanied by hemorrhage shock (HS) that can exacerbate brain injury by reducing MABP and blood O_2-carrying capacity due to the loss of red blood cells. Consequently, an ideal therapeutic for TBI + HS should have pleiotropic multi-target properties that serve not only as a resuscitation fluid to restore perfusion pressure and O_2 carrying capacity, but also to directly protect the brain from secondary injury cascades associated with oxidative stress and neuroinflammation.

Polynitroxylated PEGylated hemoglobin (PNPH, SanFlow™) is in advanced preclinical development both as a nanobiotherapeutic and as a third-generation blood substitute (10, 11). It is a manufactured ~8 nm nanoparticle with bovine hemoglobin as the protein center and with bound nitroxide groups and conjugated PEG. Here, we propose that PNPH meets the criteria for a pleiotrophic multitarget resuscitation fluid for several reasons. First, PNPH has the ability to carry O_2 into the microcirculation and, owing to its high affinity for O_2, will unload O_2 preferentially in tissue with low PO_2 driven by diffusion gradient. Moreover, because PNPH is in the plasma compartment, it can deliver O_2 to capillaries that are poorly perfused by red blood cells and improve the homogeneous delivery of O_2. Second, the PEGylation increases hemoglobin's oncotic pressure and allows it to be used as a small volume resuscitation fluid, which is of logistical benefit for use in the field and military settings (12, 13). The high oncotic pressure also serves to limit cerebral edema after TBI (12, 13). Third, the PEGylation provides the additional benefit of increasing the molecular radius so that it is not filtered in the renal glomeruli or in other vascular beds (14), thereby extending its circulating half-life and reducing the need for frequent infusions. The restrained extravasation also reduces abluminal scavenging of nitric oxide by hemoglobin and associated vasoconstriction (15–17), which was an adverse effect of earlier generations of cell-free crosslinked hemoglobin solutions (18) that failed in clinical trials (19). Fourth, PNPH is stored with carbon monoxide (CO) bound to the heme to prevent autooxidation to methemoglobin (metHb) and thus extend its shelf life. Furthermore, when infused into the circulation, the CO is released and re-equilibrates with red blood cell-based hemoglobin and other heme moieties in the tissue. The resulting low partial pressure of CO is known to exert anti-inflammatory effects as shown by the use of other CO donors (20, 21). Fifth, PNPH has nitroxide moieties conjugated to lysine residues on the hemoglobin molecule and these moieties react with superoxide anion (22, 23), effectively serving as a plasma-based superoxide dismutase to protect the endothelium from oxidative stress and leukocyte adhesion (24, 25). Interestingly, PNPH also has been shown to protect cultured neurons from the toxic effects of native hemoglobin and elevated glutamate (26). Thus, any extravasation of PNPH at a site of blood-brain barrier breakdown after TBI will be less toxic than native hemoglobin and could even exert direct neuroprotective effects against excitotoxicity by virtue of its antioxidant properties. One concern with the use of cell-free hemoglobin is that it undergoes oxidation to the ferric state, wherein it can be further oxidized to the highly reactive ferryl state in the presence of H_2O_2 (27). However, the nitroxide moieties also possess peroxidase activity that limits oxidation to the ferryl state (28, 29), thereby limiting toxicity of hemoglobin outside of the red blood cell. Hence, PNPH has many characteristics suitable both for fluid resuscitation from TBI + HS and protecting the brain vasculature and parenchyma.

Previously, PNPH was found to help maintain dilation of pial arteries, improve collateral blood flow, and reduce infarct volume in ischemic stroke (30). In a mouse model of TBI + HS, PNPH was more effective than crystalloid or whole blood in restoring arterial pressure and that resuscitation with PNPH ameliorated cerebral edema and neurodegeneration in hippocampus (12, 13, 26). Likewise, in a guinea pig model of TBI + HS, resuscitation with PNPH was superior to lactated Ringer's (LR) solution in restoring arterial pressure, preserving hippocampal viable neurons and reducing loss of white matter (31). Based on these encouraging results in rodents, testing the efficacy of PNPH in a large animal model was now deemed warranted for possible clinical translation.

Pigs are used increasingly as a large animal for TBI studies (32). In most studies, they typically range in age from 4 days (neonatal model) (33), to 1 month (toddler model) (34), and to 35–45 kg (pre-pubertal juvenile model) (35); the latter are considered pediatric models. Because sexually mature adult domestic pigs are more difficult to accommodate logistically in most laboratories, minipig strains provide an alternative adult model (36, 37), but their financial cost is considerably greater than domestic pigs. Here, we used 3-month-old juvenile pigs (approximately 30 kg) in our model of TBI + HS for testing the therapeutic efficacy of PNPH at doses of 10 or 20 ml/kg (300–600 ml for a 30-kg pig). Like humans, pigs have a large gyrencephalic brain and abundant white matter. Others have established a swine model of TBI + HS induced by controlled cortical impact (CCI) combined with 2 h of HS followed by therapeutic resuscitation for evaluating hematologic and cerebral biochemical effects at 6-h survival (38–41) and neurologic deficits with longer-term survival (35, 42). We adapted this model for neuropathological evaluation at 4 days after injury to interrogate the effects of PNPH on evolving brain damage in survivors.

Our first objective was to evaluate two doses of PNPH during the resuscitation from TBI + HS on histopathological outcomes, including cortical contusion injury volume, loss of subcortical white matter, impairment of axonal transport as a functional marker of axonal injury, dendritic damage as assessed by microtubule-associated protein disintegration, and microglia morphology as a marker of neuroinflammation. The experimental protocol for TBI + HS utilized CCI followed by 2 h of arterial hypotension induced by 30 ml/kg hemorrhage. Pigs were then resuscitated with 60 ml/kg infusion of

LR or 10 or 20 ml/kg of PNPH. This study was intended to inform whether a single infusion of PNPH at resuscitation from TBI + HS could sustain improvement of histological markers of secondary brain injury over a 4-day period. The 4-day recovery period allows time for secondary neuronal injury processes and inflammation to develop. Furthermore, having a neuroprotective agent that mitigates acute secondary injury and sustains brain viability for several days is also of clinical importance in some military arenas and in remote civilian settings, wherein blood typing and storage are not always available and patient transport to advanced critical care units may take several days.

Our second objective was to determine whether PNPH has neuroprotective efficacy after TBI in the absence of induced HS. In previous work in mouse and guinea pig (26, 31), PNPH infusion restored mean arterial pressure (MAP) more quickly than infusion of LR. Thus, the neuroprotection seen in these earlier studies may have been attributed to the hemodynamic benefits of PNPH. To determine whether protection can occur independent of effects on MAP, we conducted a second experiment to test the efficacy of PNPH infusion after TBI alone.

Methods

Surgical preparation

All procedures on pigs were approved by the Johns Hopkins University Animal Care and Use Committee and by the Animal Care and Use Review Office of the US Army Medical Research and Materiel Command for Award Number W81XWH-19-C-0022 (Fort Detrick, MD). In conducting research using animals, the investigators adhered to the Animal Welfare Act Regulations and other Federal statutes relating to animals and experiments involving animals and the principles set forth in the current version of the Guide for the Care and Use of Laboratory Animals, National Research Council.

Because there can be sex differences in the response to TBI (43, 44) and TBI in the young and in military personnel is more prevalent in males (45), the study was conducted in male pigs. A total of 48 pigs weighing 28 ± 2 kg and approximately 3 months of age were used in the overall study. The experimental protocols for the TBI + HS experiment and the TBI alone experiment are delineated in **Figure 1**. The pigs were sedated with intramuscular injection of Telazol (50 mg/ml tiletamine and 50 mg/ml zolazepam, 4.4 mg/kg each component), ketamine 2.2 mg/kg and xylazine 2.2 mg/kg. Isoflurane (4% in 30% O_2) was administered *via* face mask to produce an anesthetic depth for oral intubation of the trachea. After a surgical plane of anesthesia was achieved, as assessed by the lack of limb withdrawal to hoof pinching and by looseness of muscle tone in the jaw, anesthesia was maintained with 2% isoflurane in approximately 30% O_2 with mechanical ventilation of the lungs. The antibiotic Baytril 10 mg/kg (100 mg/ml) was injected intramuscularly. Surgery was conducted using aseptic techniques. Through a 5-cm neck incision, an external jugular vein was isolated by blunt dissection. The vein was ligated and a catheter was advanced toward the heart and secured with another ligature. For arterial catheterization, we chose the axillary artery

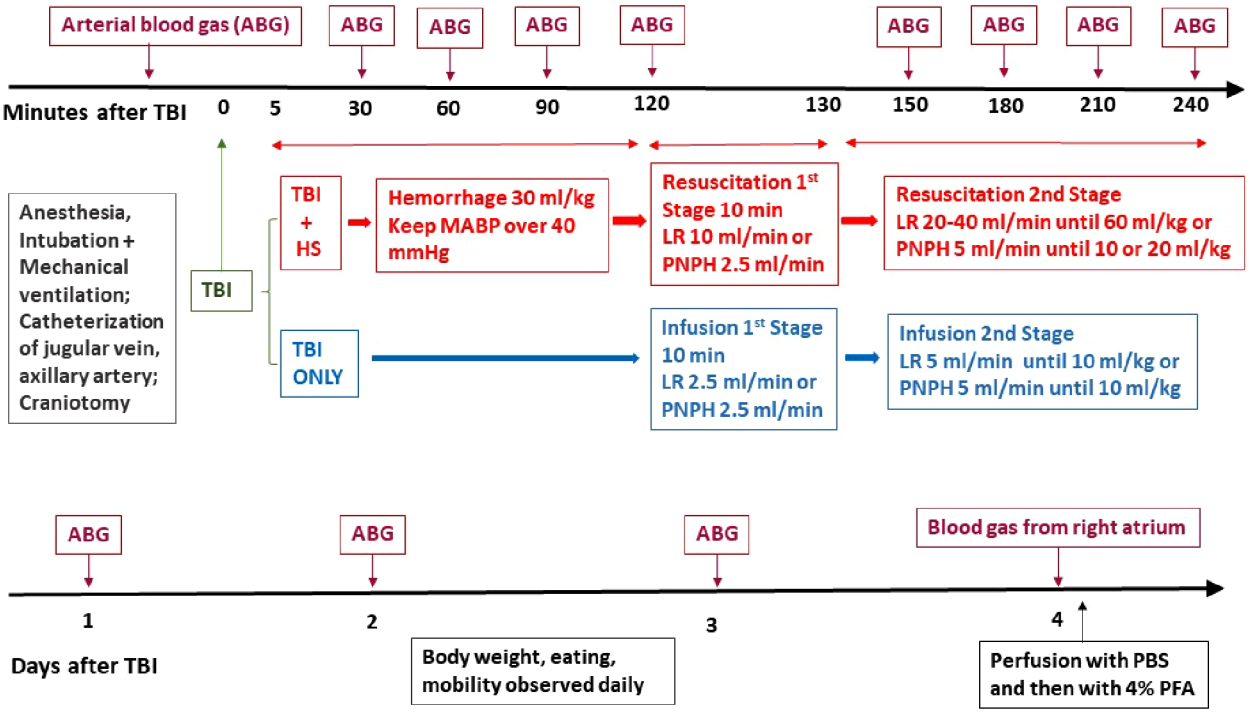

FIGURE 1
Schematic outline of time line of protocol for TBI + hemorrhagic shock (HS) and TBI only experiments on pigs during the first 4 h of recovery (top) and during the 4-day survival period (bottom). ABG, arterial blood gas; CCI, controlled cortical impact; LR, lactated Ringer's solution; PBS, phosphate-buffered saline; PFA, paraformaldehyde.

because occlusion of the carotid artery could limit cerebral blood flow after TBI and catheterization of the femoral artery can limit use of the hindlimb. An incision was made in the axilla, and the axillary artery was isolated, ligated, and cannulated with a flexible polyvinyl catheter that minimized kinking. The arterial and venous catheters were tunneled subcutaneously to the back of the neck, where they exited through a small incision. Pigs were able to bear weight on the forelimb and ambulate on the day after surgery.

Traumatic brain injury

Pigs were injected with fentanyl 20 μg/kg bolus and followed by continuous infusion of 20 μg/kg/h through the jugular vein catheter while maintained on isoflurane anesthesia. They were placed in a stereotactic head holder that was placed on the base of the impactor frame to prevent movement of the head during impact. The CCI model was similar to that described by others (38). A 20 mm diameter craniotomy was made over the right frontal cortex centered 1 cm anterior to the bregma and 1 cm lateral to the midline. The dura remained intact. Once the craniotomy was complete, the isoflurane concentration was decreased to 1%. At 5 min before the TBI, the isoflurane was stopped while fentanyl continued to be infused. TBI was produced with a CCI device (Custom Design and Fabrication, Inc., Sandston, VA, USA) that used a linear electric motor accelerator to control an impactor with a 15 mm diameter and a rounded tip. We used a 10 cm inward displacement of the dura at a velocity of 5 m/s for a duration of 50 ms. After CCI, gel foam was inserted into the craniotomy and sealed with tissue glue. The scalp incision was closed, and lidocaine hydrochloride cream (2.0%) was topically applied to all surgical incisions. The pigs remained sedated by infusing 0.1 mg/kg midazolam while continuing the infusion of 20 μg/kg/h fentanyl. For postoperative analgesia, they received a subcutaneous injection of sustained-release buprenorphine (0.12 mg/kg). They typically became responsive and were extubated at 3–5 h after TBI and were placed in a recovery cage for additional physiology monitoring for the first 4 h after TBI. When they were able to stand, they were returned to their pen in the central housing facility and continued to be observed for full mobility, which usually occurred within 6 h after TBI. Pigs were observed at least twice per day over the 4-day recovery period and were assessed for appetite, urination, defecation, mobility and level of awareness.

Hemorrhagic hypotension

In the first experiment with TBI + HS, hemorrhage was produced by withdrawing 30 ml/kg of blood starting 5 min after TBI. Because very low mean arterial pressure (MAP) will decrease coronary blood flow and cardiac contractility, hemorrhage sometimes needs to be briefly interrupted to prevent loss of cardiac function (42). In our protocol, blood withdrawal was temporarily stopped when MAP fell to 35–40 mmHg and resumed when MAP began to recover above 40 mmHg. When the targeted amount of blood had been removed, blood withdrawal ceased and MAP was allowed to spontaneously increase above 40 mmHg. Thus, we used a variable rate of blood withdrawal to achieve a fixed volume of hemorrhage while attempting to avoid MAP < 35 mmHg and minimize the risk of cardiogenic shock.

Treatment groups

In the first experiment, pigs were randomized to groups undergoing TBI followed by 2 h of hemorrhagic hypotension and then fluid resuscitation with 60 ml/kg lactated Ringer's (LR) solution ($n = 7$), 10 ml/kg PNPH ($n = 8$), or 20 ml/kg PNPH ($n = 8$). In the second experiment, pigs undergoing TBI without hemorrhagic hypotension were randomized to fluid treatment with 10 ml/kg LR solution ($n = 6$) or 10 ml/kg PNPH ($n = 9$) starting 2 h after TBI. A sham-operated group underwent catheterization and craniotomy, but without CCI or hemorrhage ($n = 5$). Because the craniotomy itself can potentially cause inflammation in the meninges and in cortex, brains from a naïve group without surgery were also collected ($n = 5$).

Fluid treatment commenced 2 h after TBI in those with and without induced hemorrhagic hypotension. Because PEGylation conveys hyper-oncotic properties to the molecule, smaller infusion volumes of PNPH are needed to restore MAP than LR. In addition, rapid fluid resuscitation can cause a rapid increase in preload and afterload, which can lead to pulmonary edema when cardiac contractility is already compromised by low perfusion pressure. Because cardiac output can be reduced and cerebral edema worsened with rapid LR infusion, others recommend using stepwise increases in infusion rates (39). Therefore, we performed fluid resuscitation with stepwise increasing infusion rates. In the group resuscitated with LR after hemorrhage, infusion started at a rate of 10 ml/min for 5 min (50 ml), then 20 ml/min for 22.5 min (additional 450 ml), and lastly at 60 ml/min until 60 ml/kg was infused (twice the hemorrhage volume). In the group without hemorrhage and treated with LR, infusion was stopped when a total of 10 ml/kg was infused. For the PNPH infusion groups, resuscitation commenced with a priming dose of LR infused at a rate of 10 ml/min for 5 min followed by PNPH infusion at a rate of 2.5 ml/min for 10 min and then at 5 ml/min until the targeted dose of 10 or 20 ml/kg was achieved. In the pigs that underwent hemorrhage, an additional LR infusion was performed at the end of the infusion period until the total of PNPH + LR equaled 30 ml/kg (the hemorrhage volume). If mean arterial pressure dropped below 40 mmHg during HS or early resuscitation, epinephrine was infused to maintain coronary perfusion pressure and avoid irreversible shock.

Throughout the first 4 h after TBI or sham surgery, arterial blood pressure was recorded and arterial blood samples (0.5 ml) were obtained hourly. The samples were analyzed for pH, blood gases, Hb concentration, metHb, COHb, and glucose with an ABL800Flex blood gas machine (Radiometer Inc., Brea, CA USA). In the group receiving PNPH, the remaining blood sample was centrifuged to obtain plasma, which was then analyzed for Hb concentration. Rectal temperature also was monitored.

On day 1, 2, 3 and 4 of recovery, a 1 ml blood sample was withdrawn from the arterial catheter for analysis of total blood Hb concentration, metHb, and COHb. The plasma Hb was also

analyzed in the PNPH groups. If the arterial catheter was not patent, then samples were drawn from the jugular vein. Values from arterial and venous blood were combined for statistical analysis because the Hb concentration, metHb, and COHb from the 2 sites are expected to be similar. On day 4, piglets were deeply anesthetized and perfused transcardially with cold phosphate-buffered saline (PBS) followed by cold 4% paraformaldehyde. The thoracic aorta was clamped to direct fixative to the upper body. The quality of ongoing and final tissue fixation was judged by neck and facial muscle firmness. The heads were removed and placed in 4% paraformaldehyde to allow for *in situ* post-fixation of the brain within the skull overnight. Then the brains were carefully dissected and placed in a solution of 4% paraformaldehyde and 30% sucrose in PBS at 4°C. Using the optic chiasm and pons as landmarks, the brain was cut into 3 blocks. The anterior third block was cut into 50 μm sections with a sliding microtome and serially allocated into three 12-well plates and repeating the order 1–36.

Lesion volume and white matter volume analysis

Evaluation of neuropathology was performed with blinding to treatment group. Histologic sections from the anterior third of the brain, encompassing the frontal lobes, were used to estimate the ipsilateral and contralateral hemisphere volume of structurally normal appearing cerebral cortex and the volume of peri-lesion subcortical white matter. Every 12th serial coronal section was stained with 0.1% Luxol fast blue followed by 0.1% cresyl violet staining after dehydration in a series of increasing alcohol concentrations. Luxol fast blue staining was used to identify white matter. Cresyl violet was used to counterstain tissue sections for lesion identification and neocortex loss. Using Image J software, we traced the area of each hemisphere excluding the contusion injury (cavity plus pale cresyl violet stained tissue) and the area of white matter in each hemisphere. We calculated the volume by summing section area × 600 μm spacing between sections along the entire axial length of the anterior third of the cerebral hemisphere. The percentage of contusion injury volume was calculated 100 (left–right)/left hemisphere volume. The percentage of white matter volume loss was calculated as 100 (left–right)/left white matter volume. For this analysis, 15–20 brain sections were used to calculate the percentage of contusion injury volume and the percentage of white matter volume loss for each brain.

Immunohistochemistry and immunofluorescence

Immunostaining for amyloid precursor protein (APP) was used as a surrogate marker for impairment of axonal transport because it is known to accumulate when transport function in axons is blocked (46). Neuronal somatodendritic integrity was assessed by immunostaining for the cytoskeletal protein microtubule-associated protein-2 (MAP-2). Assessment of microglia morphology was performed with immunostaining for Iba-1. Immunohistochemistry was performed on 50 μm free-floating sections under moderate shaking. Before staining, the sections were incubated 30 min in 0.3% hydrogen peroxide to quench endogenous peroxidases. After three washing steps in 0.1 M phosphate buffer (pH 7.4), non-specific antibody binding sites were blocked with using 10% normal goat serum. Different free-floating sections were incubated overnight at 4 °C with anti-MAP-2 (1 : 500, monoclonal mouse-IgG; Millipore, MAB3418), anti-APP (1 : 500, monoclonal mouse-IgG; Millipore, MAB348), or anti-Iba-1 (1 : 500, polyclonal rabbit-IgG; Wako, 019-19741) in 5% normal goat serum. After several washes, sections were incubated for 2 h at room temperature with secondary antibodies. For APP and MAP-2 staining, biotinylated anti-mouse-IgG, 1 : 500, Vector, BA9200 was used, and the streptavidin/horseradish peroxidase detection was performed according to the manufacturer's recommendations. These sections were incubated with the substrate diaminobenzidine (DAB, D3939; Sigma-Aldrich Company, St. Louis, MO, United States) for 10 min at room temperature. For Iba-1 staining, Alexa Fluor 594 sary antibody (1:500, Invitrogen, #A-11037) was used. Immunofluorescent images were obtained with a Leica microscope (model DMi8 with THUNDER Imager 3D software).

Stereological measurement for APP-positive particles

Stereological measurements were made by using a Nikon Eclipse 90i microscope (Nikon, Tokyo, Japan) attached to a Qimage Retiga-2000R camera, which was connected to a workstation with Stereo Investigator software (Version 10; MicroBrightField, Williston, VT, USA). Every 12th section was examined, placing the analyzed sections 600 μm apart. Using a 2× objective, we traced the entire area of subcortical white matter for outlining the region of interest to be used in the stereological analysis. Then we counted the APP-positive particles under a 40× objective. We identified particles as being a brown dot that first came into focus within the optical dissector counting frame. The counting frame was 150 × 150 μm with a grid size of 3,000 × 3,000 μm. The dissector height was set at 10 μm with an upper and lower guard zone of 1 μm. This analysis used 11–14 coronal sections and 98–176 sampling fields to ensure that at least 100 particles were counted per brain (range 118–1086) to obtain the estimate of the total number of APP-positive particles within the entire subcortical white matter area.

MAP-2 immunohistochemistry analysis

Processes stained for MAP-2 had a more fragmented appearance after TBI, indicative of disruption of microtubules. As a measure of dendrite integrity, we counted the number of MAP-2–immunopositive processes with a length >50 μm within the plane of sectioning of the 50 μm-thick sections. This 50 μm threshold length was based on a preliminary survey of the images in the TBI brains where many of the fragmented dendrites were <50 μm in length. For this analysis, adjacent images of the entire cortical mantle of the gyrus lateral to the contused gyrus were obtained at 40× and the image tiles were stitched together to obtain a single composite image. For each brain, 10–12 sections spaced 600 μm

apart were analyzed and the number of long processes per coronal section were averaged. Counting was performed on approximately 100 fields of view (0.25 mm^2 area each) per section spread over a 5 × 5 mm area of the cortical mantle. For each brain, approximately 1,000 fields were used to obtain the number of MAP-2 immunostained processes >50 μm per section.

Iba-1 immunohistochemistry analysis

Iba-1 immunofluorescent images were obtained on 3 coronal sections for each brain. On each section, 3 fields of view at 40× power were analyzed in the peri-lesion area. For each brain, an average value was obtained from the 9 fields of view. The total number of Iba-1–positive cells were counted to quantify the number of microglia/macrophages in the peri-lesion area. In addition, we quantified three different kinds of morphologies of these cells. Those with a small cell body area and long processes were regarded as ramified microglia. Those with a larger cell body area and shorter processes were regarded as hypertrophic microglia. Those which almost had no long, thin processes were regarded as fully activated bushy microglia. Because the hypertrophied and bushy morphologies were not always distinguishable, these two morphologies were combined for statistical purposes.

Statistical analysis

All data were analyzed by GraphPad Prism version 6 statistical software. Measurement data were expressed by mean ± standard deviation. Statistical analysis included all pigs that completed the protocol and survived for brain perfusion and fixation: The number of pigs in each group was: 5 naïve, 5 sham surgery, 5 TBI + HS + 60 ml/kg LR, 4 TBI + HS + 10 ml/kg, PNPH, 5 TBI + HS + 20 ml/kg PNPH, 6 TBI alone + 10 ml/kg LR, and 6 TBI alone + 10 ml/kg PNPH. For histologic analysis, the naïve and sham groups were combined into a single control group of 10 pigs since all of the histologic values were similar in each group. The TBI + HS experiment and the TBI alone experiment were analyzed with separate one-way analysis of variance (ANOVA) for each experiment. If the F value was significant, then we used the Holm-Sidak procedure to keep the family-wise error at <0.05 for multiple comparisons. In the TBI + HS experiment, there were 5 comparisons of interest. We compared the combined Naïve + Sham group with (1) TBI + HS + LR, (2) TBI + HS + 10 ml/kg PNPH and (3) TBI + HS + 20 ml/kg PNPH; and we compared TBI + HS + LR with (4) TBI + HS + 10 ml/kg PNPH and (5) TBI + HS + 20 ml/kg PNPH. In the TBI alone experiment, there were 3 comparisons of interest. We compared the combined naïve + Sham group with (1) the TBI + LR group and (2) the TBI + 10 ml/kg PNPH group; and we compared the TBI + LR group with (3) the TBI + 10 ml/kg PNPH group. For physiologic measurements, some missing values occurred because of difficulty in drawing arterial blood samples or because of technical problems with the blood gas analyzer. In addition, some sham-operated pigs regained consciousness more quickly than the TBI pigs and were too active to obtain MAP and blood sample measurements at the 120–240 min time points, resulting in $n = 2–3$ at these times. Because of the small sample size, the sham group was not included in the statistical comparisons for MAP and blood sample analysis.

Results

Enrollment and attrition

In the TBI + HS experiment, 33 pigs were enrolled in the TBI + HS study and assigned to an intention-to-treat group prior to the day of surgery. Of these, 24 survived and were used for neuropathologic analysis. These included: (1) 5 naïve pigs perfused with fixative to provide normal brain histology, (2) 5 survivors from sham surgery, (3) 5 survivors from TBI + HS + LR resuscitation (mortality = 2 of 7 pigs: one pig died during surgery from presumed arrhythmia, 1 pig died 4 h after TBI), (4) 4 survivors from 10 ml/kg PNPH resuscitation (mortality = 4 of 8 pigs: one pig died during hemorrhage before the start of resuscitation; two pigs were hypotensive during resuscitation and died at 2.5–4 h after TBI; one pig completed the resuscitation protocol, but its arterial catheter accidently got pulled out when the pig was waking up from anesthesia and moving its legs, which resulted in a second episode of hypotension; this pig was humanely euthanized), (5) 5 survivors from 20 ml/kg PNPH resuscitation (mortality = 3 of 8 pigs: one pig died during hemorrhage before the start of resuscitation; two pigs were hypotensive during resuscitation and died at 2.5–3 h after TBI). Thus, among the groups destined to undergo TBI + HS, 14 of 23 pigs completed the protocol.

In the TBI alone experiment, 15 pigs were enrolled and 12 survived and were used for neuropathologic analysis. These included: (1) 6 survivors from TBI + LR infusion (no mortality) and (2) 6 survivors from TBI + 10 ml/kg PNPH infusion (mortality = 3 of 9: two pigs had severe hypotension leading to cardiac arrest during infusion; one pig failed to fully regain consciousness).

Physiological results with TBI + HS

The time course of physiologic data is presented for the survivors from each group in **Figure 2** and the individual data are shown at each time point in **Supplementary Figures S1–S5**. All TBI + HS groups subjected to HS had a similar level of MAP at the time of TBI and had a similar level of hypotension during the 2 h of HS (**Figure 2A**). In all TBI + HS groups, MAP recovered to their pre-injury levels within 30–60 min of the start of fluid resuscitation. All groups had further increases in MAP to approximately 100 mmHg as pigs awakened at variable times. Thus, the different resuscitation fluid composition and volumes were well matched to yield a similar recovery of MAP. This allowed comparisons of potential neuroprotective effects to be independent of the recovery of MAP.

The concentration of hemoglobin (Hb) decreased during the fluid resuscitation with LR at 150 and 180 min after TBI (30 and 60 min of fluid infusion) compared to the PNPH groups, which were infused at a slower rate (**Figure 2B**). PNPH is nearly saturated with carbon monoxide (CO) to prevent metHb formation during storage. During the infusion of PNPH, CO is released from PNPH and equilibrates with native Hb. The total blood COHb (plasma plus red blood cell Hb) increased progressively during PNPH infusion but remained

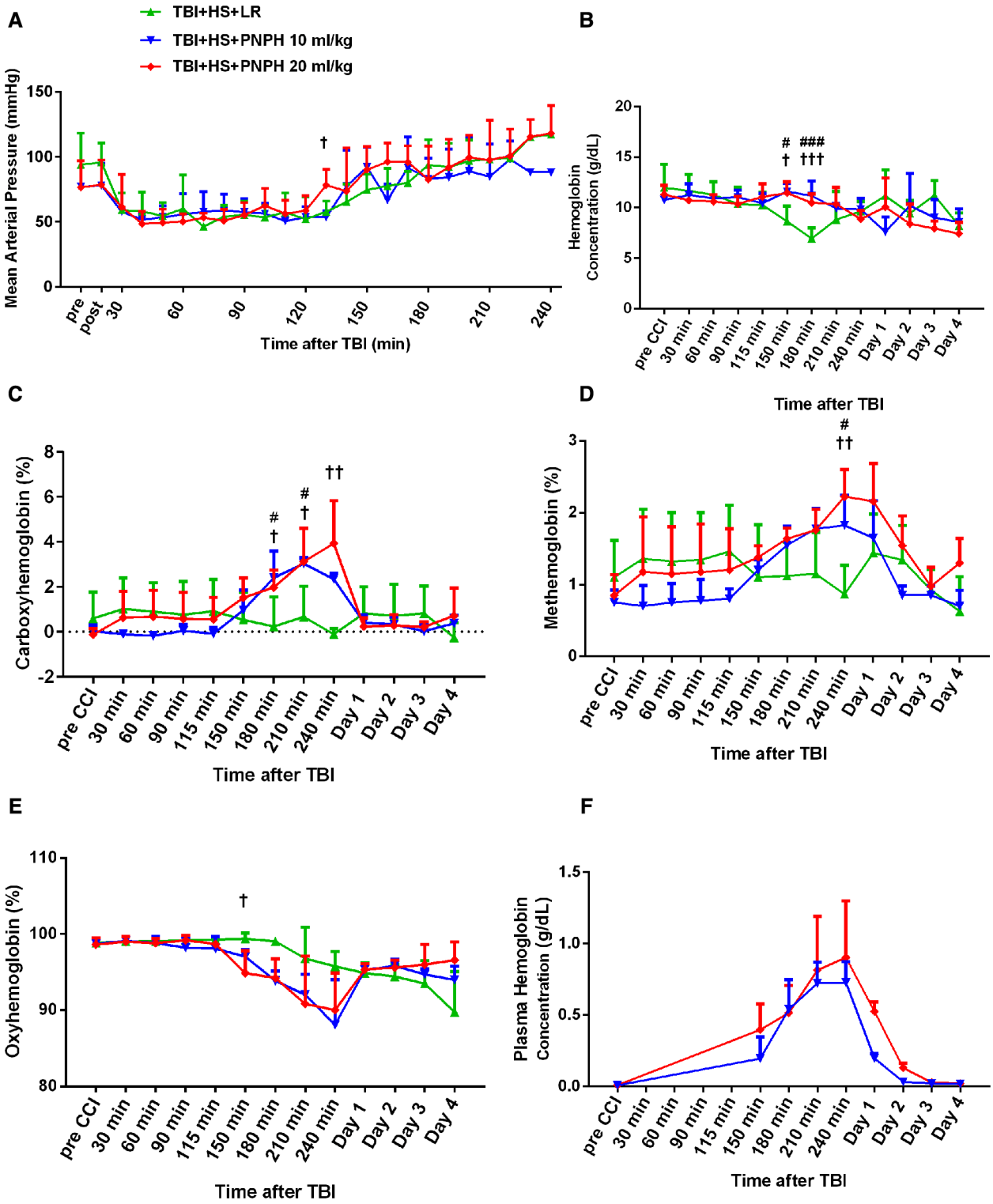

FIGURE 2
Time course of mean arterial pressure (A), hemoglobin concentration (B), percent of carboxyhemoglobin (C), percent of methemoglobin (D), and percent of oxygenated hemoglobin (E) in whole blood for groups of pigs subjected to TBI and 120 min of hemorrhagic shock (HS) followed by infusion of 60 ml/kg lactated Ringer's (LR) solution, 10 ml/kg PNPH, or 20 ml/kg PNPH. Sample sizes per time point were 3–5 for LR group, 3–4 for 10 ml/kg PNPH group, and 4–5 for 20 ml/kg PNPH group (smaller sample sizes occurred at 180–240 min when arterial blood samples could no longer be drawn because the pig was too active or the subcutaneously-routed catheter was inoperable). Individual data are shown in Supplemental Figures 1–5. PNPH infusion produced increases in plasma hemoglobin concentration that subsided over 1–2 days (F). Values are means ± SD. $^{\#}P < 0.05$, $^{\#\#\#}P < 0.001$ TBI + HS + LR vs. TBI + HS + 10 ml/kg PNPH; $^{\dagger}P < 0.05$, $^{\dagger\dagger}P < 0.01$ TBI + HS + LR vs. TBI + HS + 20 ml/kg PNPH. Significance determined by one-way ANOVA and the Holm-Sidak procedure for multiple comparisons.

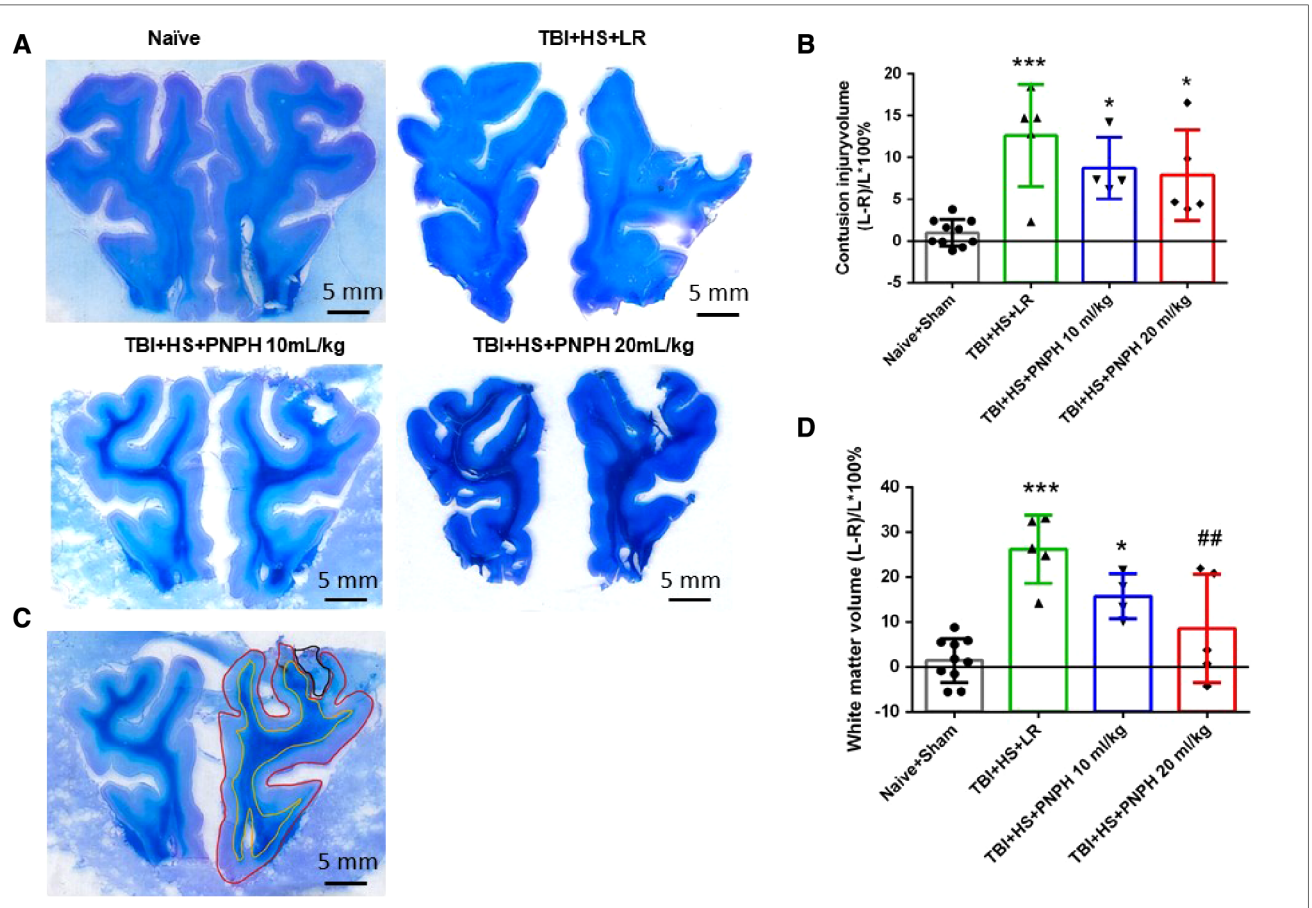

FIGURE 3
Effect of PNPH on contusion injury volume and volumetric white matter loss in frontal lobe after TBI + hemorrhagic shock (HS). (**A**) Representative coronal sections (both hemispheres, top is superior) of frontal lobe of normal pig brain and brains 4 days after TBI and resuscitation with 60 ml/kg lactated Ringer's (LR) solution and 10 and 20 ml/kg PNPH. Gray matter is visualized with cresyl violet staining and subcortical white matter myelin is visualized with Luxol fast blue staining. (**B**) Area delineated by red trace is the entire histologically normal hemisphere, area delineated by the yellow trace is the subcortical white matter, and area circled by the black trace is the contusion site. (**C**) Contusion injury volume (intact tissue difference of left minus right hemisphere as a percentage of left hemisphere volume contralateral to the injury site) of pigs subjected to TBI + HS followed by resuscitation at 120 min with LR ($n = 5$) or 10 ml/kg PNPH ($n = 4$) and 20 ml/kg PNPH ($n = 5$). The normal variation in the difference of left minus right hemisphere volume as a percentage of left hemisphere volume is shown for the combined Naïve ($n = 5$) and Sham ($n = 5$) group. (**D**) Volume of white matter loss in the same brains was calculated as the difference between left minus right subcortical white matter volume normalized by the left subcortical white matter volume (contralateral volume). The loss of white matter seen in the LR group was attenuated in the 20 ml/kg PNPH group. Mean ± SD and individual data for each pig are shown. $^{*}P < 0.05$, $^{***}P < 0.001$ vs. combined Naïve and Sham groups. $^{\#\#}P < 0.05$ vs. LR group determined by one-way ANOVA and the Holm-Sidak procedure for multiple comparisons.

below 4% (Figure 2C). COHb recovered to normal levels by Day 1. PNPH infusion also resulted in a significant increase in metHb by 240 min after TBI compared to the LR group (Figure 2D), but the elevation was only about 1% metHb and resolved by 1–2 days. Together, the increase in COHb and metHb will act to decrease the fraction of total Hb that was carrying oxygen (FHbO2). Although there was a trend for FHbO2 to decrease at 210 and 240 min when COHb and metHb were at their peak levels, the decrease in FHbO2 was variable and did not significantly differ from values in the group resuscitated with LR at these time points (Figure 2E). The concentration of Hb in the plasma increased to 0.71 ± 0.16 g/dl after infusion of 10 ml/kg PNPH and then declined to 0.21 ± 0.03 g/dl on Day 1 and to 0.03 ± 0.02 g/dl on Day 2 (Figure 2F). After 20 ml/kg PNPH infusion, plasma Hb concentration increased to 0.84 ± 0.40 g/dl and declined to 0.52 ± 0.07 g/dl on Day 1 and to 0.13 ± 0.04 g/dl on Day 2 as PNPH was slowly cleared from the circulation. Thus, a significant amount of PNPH was retained in the circulation over the first two days of recovery.

Neuropathologic results with TBI + HS

Representative coronal brain sections stained with Luxol fast blue followed by cresyl violet are shown from a naïve pig and TBI + HS pigs resuscitated with LR and PNPH (Figure 3A). At 4 days of recovery, cavitation with some remnants of hemorrhage were evident in the cerebral cortex and underlying white matter. The areas used for measuring intact hemisphere volume and white matter volume are illustrated by the red and yellow traces, respectively, in Figure 3B. Contusion injury area measurements included the cavity and tissue with atypical sparse cresyl violet staining. The remaining area of histologically normal tissue in the injured hemisphere was subtracted from the area of the contralateral hemisphere and summed across the frontal lobe to estimate the contusion lesion volume, which was normalized by the contralateral hemisphere volume. Because the Sham group had minor differences between the volume of each hemisphere volume, pigs in this group were combined with the Naïve group as a single

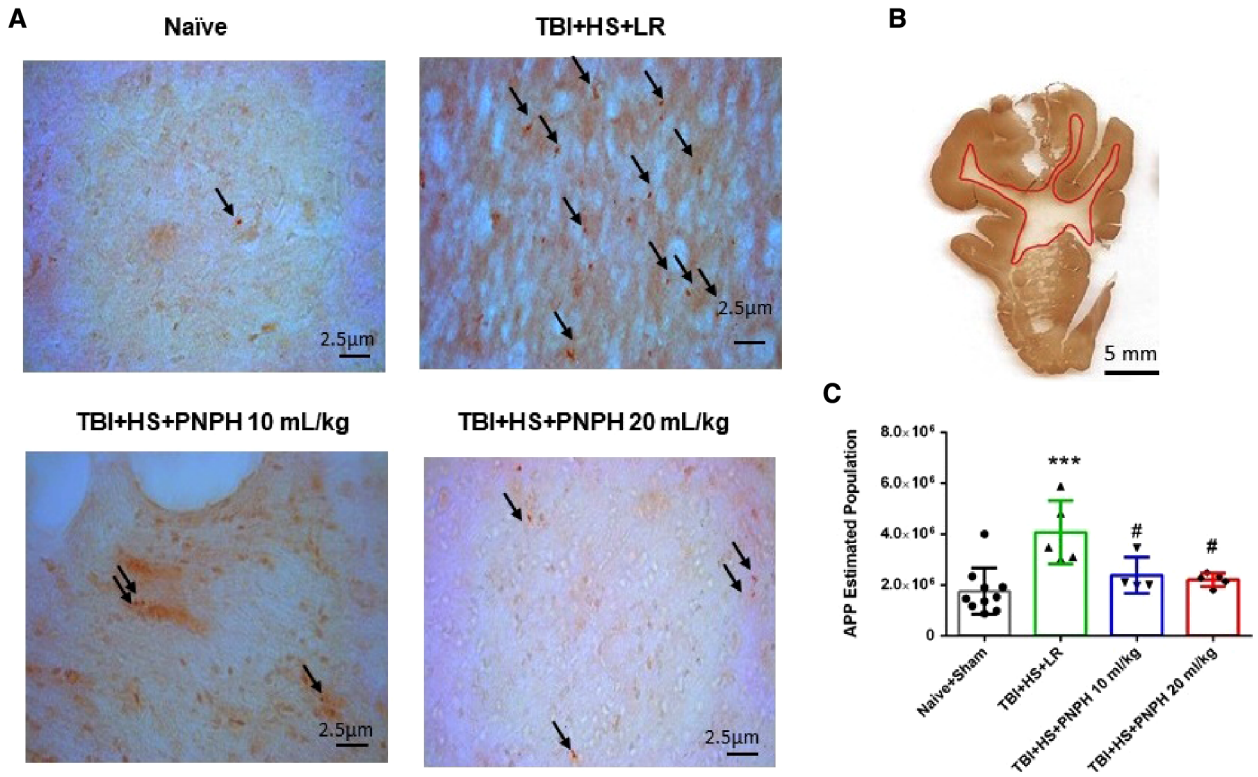

FIGURE 4
Effect of PNPH on amyloid precursor protein (APP) punctate accumulation after TBI + hemorrhagic shock (HS). (**A**) Representative images of APP immunostaining from naïve pig and TBI + HS pigs resuscitated with 60 ml/kg lactated Ringer's (LR) solution or 10 ml/kg PNPH and 20 ml/kg PNPH. Arrows point to particles of APP accumulation. (**B**) The area of subcortical white used in the analysis is illustrated with the red trace. (**C**) The number of APP particles throughout subcortical white matter was estimated with the optical fractionator method of unbiased stereology and are plotted for the combined Naïve + Sham group ($n = 10$) and for TBI + HS groups resuscitated with 60 ml/kg LR ($n = 5$), 10 ml/kg PNPH ($n = 4$), and 20 ml/kg PNPH ($n = 5$). Both doses of PNPH blunted the increase in APP particles seen in the LR group. Mean ± SD and individual data for each pig are shown. $^{***}P < 0.001$ vs. combined Naïve + Sham group. $^{\#}P < 0.05$ vs. LR group determined by one-way ANOVA and the Holm-Sidak procedure for multiple comparisons.

control group for statistical analysis. One-way ANOVA indicated a significant overall effect of treatment among the four groups [$F(3,20) = 10.463$; $P < 0.001$]. Contusion injury volume averaged 13%, 9%, and 8% of the homotypic contralateral hemisphere volume in the TBI + HS groups resuscitated with 60 ml/kg LR, 10 ml/kg PNPH, and 20 ml/kg PNPH, respectively (Figure 3C). Contusion injury volume exhibited considerable variability and no significant differences were noted among the 3 TBI + HS groups with TBI + HS with the Holm-Sidak procedure.

White matter loss, relative to the homotypic contralateral white matter volume, averaged 26% in the frontal lobe in the TBI group resuscitated with LR, 16% in the group resuscitated with 10 ml/kg PNPH, and 9% in the group resuscitated with 20 ml/kg PNPH (Figure 3D). The overall effect of group intervention was significant by one-way ANOVA [$F(3,20) = 13.233$; $P < 0.001$]. Multiple comparisons with the Holm-Sidak procedure indicated that the level in the 20 ml/kg PNPH group was significantly less than the level in the LR group ($P = 0.006$) but was not significantly different than the measurements in the Naïve + Sham group ($P = 0.18$). This result suggests that PNPH protects white matter in a gyrencephalic brain where there is an abundance of subcortical white matter.

Axonopathy was assessed by APP staining as interpreted by accumulation of punctate immunoreactivity in the white matter seen as brown particulate inclusions on DAB immunohistochemistry (Figure 4A). Using 11–14 equally spaced coronal sections per brain, unbiased stereological analysis was performed over the entire area of subcortical white matter. An example of the area included in the analysis is shown by the outlined red trace in Figure 4B. One-way ANOVA indicated a significant overall effect of group intervention [$F(3,20) = 7.898$; $P < 0.001$]. The Holm-Sidak procedure for multiple comparisons indicated a consistent increase in the estimated APP particles, from 1,749,836 ± 908,968 in the combined group Sham + Naïve group to 4,066,307 ± 1,244,399 in the TBI + HS group resuscitated with LR ($P < 0.001$, Figure 4C). In contrast, the estimated number of APP particles in groups resuscitated with 10 ml/kg PNPH (2,385,524 ± 715,346) and 20 ml/kg PNPH (2,201,756 ± 257,790) were not significantly different from the Sham + Naïve group ($P > 0.5$). Moreover, APP particle accumulation in the 10 ml/kg and 20 ml/kg PNPH groups were significantly less than that in the LR group ($P < 0.05$). These results indicate a significant rescue of neuronal axonal transport with PNPH resuscitation from TBI + HS.

To assess neuronal dendrite integrity in neocortical gray matter of frontal lobe, we examined the number of long MAP-2–positive processes in the plane of the section. In Figure 5A, arrows point to the MAP-2–positive dendritic segments with >50 μm length. Counting was performed on 10–12 equally spaced coronal sections throughout the neocortex of the gyrus adjacent to the contusion as outlined in Figure 5B. One-way ANOVA indicated a significant

10.3389/fmedt.2023.1074643

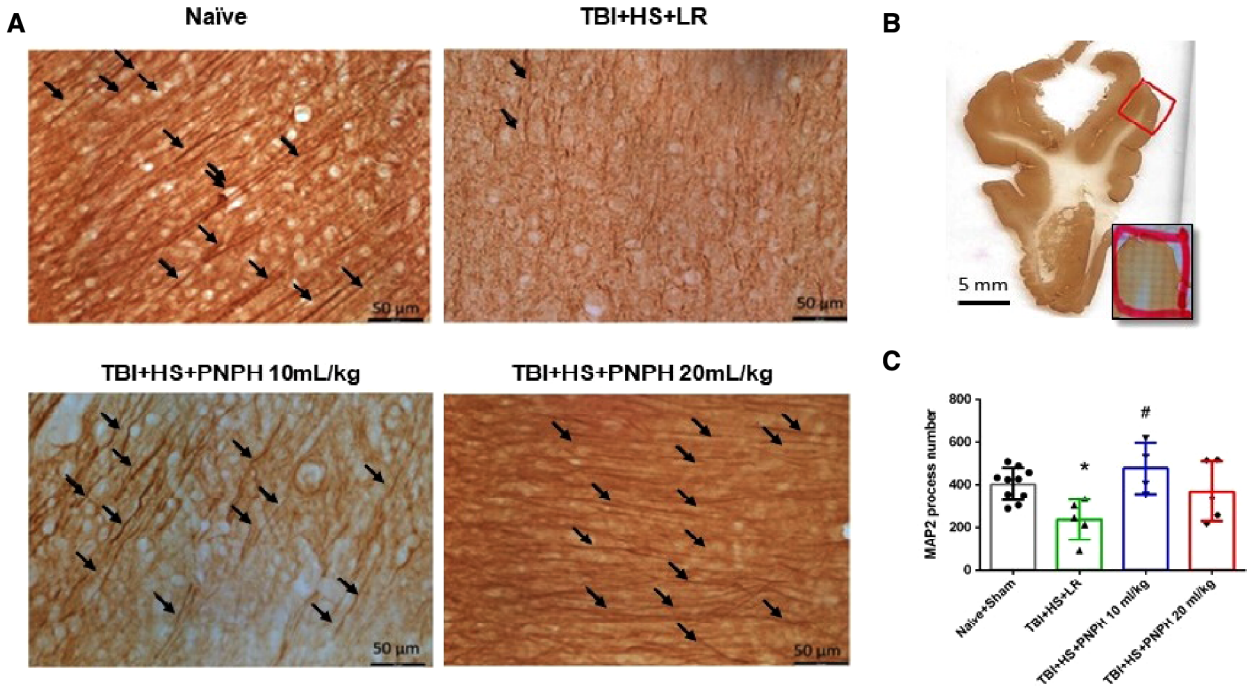

FIGURE 5
Effect of PNPH on MAP-2–identified gray matter neuronal dendrites after TBI + hemorrhagic shock (HS). (**A**) Representative images of MAP-2 immunostaining from naïve pig and TBI pigs resuscitated with 60 ml/kg lactated Ringer's (LR) solution or 10 ml/kg PNPH and 20 ml/kg PNPH. Arrows point to dendritic segments with >50 μm length from the gyrus of the cortex adjacent to the gyrus where the controlled cortical impact was produced. (**B**) The area used for MAP-2 analysis is outlined in the gyrus adjacent to the impacted gyrus. (**C**) The number of long dendrites in neocortex per coronal section averaged over 10–12 sections are plotted for the combined Naïve + Sham group ($n = 10$) and for TBI + HS groups resuscitated with 60 ml/kg LR ($n = 5$), 10 ml/kg PNPH ($n = 4$), and 20 ml/kg PNPH ($n = 5$). The dose of 10 ml/kg of PNPH blocked the decrease in long dendrites seen in the LR group. Mean ± SD and individual data for each pig are shown. $^{*}P < 0.05$ vs. combined Naïve + Sham group, $^{\#}P < 0.05$ vs. TBI + HS + LR group determined by one-way ANOVA and the Holm-Sidak procedure for multiple comparisons.

overall effect of group intervention [F (3,20) = 4.615; $P = 0.013$]. The number of long dendritic processes per coronal section was reduced from 403 ± 75 in the Naïve + Sham group to 237 ± 95 in the TBI + HS + LR group ($P < 0.05$), whereas the number of long dendrites in the groups resuscitated with 10 ml/kg PNPH (406 ± 121) and 20 ml/kg PNPH (368 ± 139) were not significantly different from the Sham + Naïve group (Figure 5C). Furthermore, the value in the 10 ml/kg PNPH group was significantly greater than that seen with LR resuscitation ($P < 0.05$).

We next performed assessment of Iba1-positive cells to quantify microglial cell number and morphologic appearance in the cerebral cortex adjacent to the contusion. In each of 3 sections, we counted three fields of view as shown as Figure 6A, and obtained an average value from the total of 9 fields for each brain. We quantified the number of Iba-1–immunopositive cells, the number of immunopositive cells with a small soma and ramified process morphology, and the number of immunopositive cells with a large soma and shorter processes (hypertrophic microglia) or essentially no processes (bushy microglia). Examples are shown in Figure 6B. One-way ANOVA indicated a significant overall effect of group intervention for the total Iba-1–immunopositive cell number [F (3,20) = 5.187; $P = 0.008$], for the number of ramified microglia [F (3,20) = 7.360; $P = 0.002$], and for the number of hypertrophic and bushy microglia [F (3,20) = 35.002; $P < 0.001$]. For TBI + HS with LR resuscitation, the total Iba-1 immunopositive–cell number was significantly increased compared with Naïve + Sham group ($P < 0.01$). This increase was modestly but significantly reduced with 20 ml/kg PNPH resuscitation compared to LR resuscitation ($P = 0.04$) and not significantly different from the level in the Naïve + Sham group (Figure 6C). TBI + HS produced an overall decrease in the number of microglia with ramified processes without significant differences between the LR group and the two PNPH groups (Figure 6D). The decrease in ramified microglia was associated with an increase in the number of microglia with hypertrophic and bushy appearance in all three TBI + HS groups compared to the Naïve + Sham group. Treatment with 20 ml/kg PNPH treatment modestly reduced the number of hypertrophic and bushy Iba1-positive microglia when compared with LR-treated TBI piglets ($P = 0.04$; Figure 6E).

Physiological results with TBI alone

The time course of physiologic data is presented for the survivors from each group in the TBI alone experiment in Figure 7, and the individual data are shown at each time point in Supplementary Figures S6–S10. Before TBI, MAP was approximately 80 mmHg and remained stable during the first 2 h after TBI in the absence of hemorrhagic shock in the groups destined to receive 10 ml/kg LR or 10 ml/kg PNPH at 2 h (Figure 7A). Afterwards, MAP gradually increased in both TBI groups as the pigs regained consciousness. Some pigs receiving PNPH had brief episodes of arterial

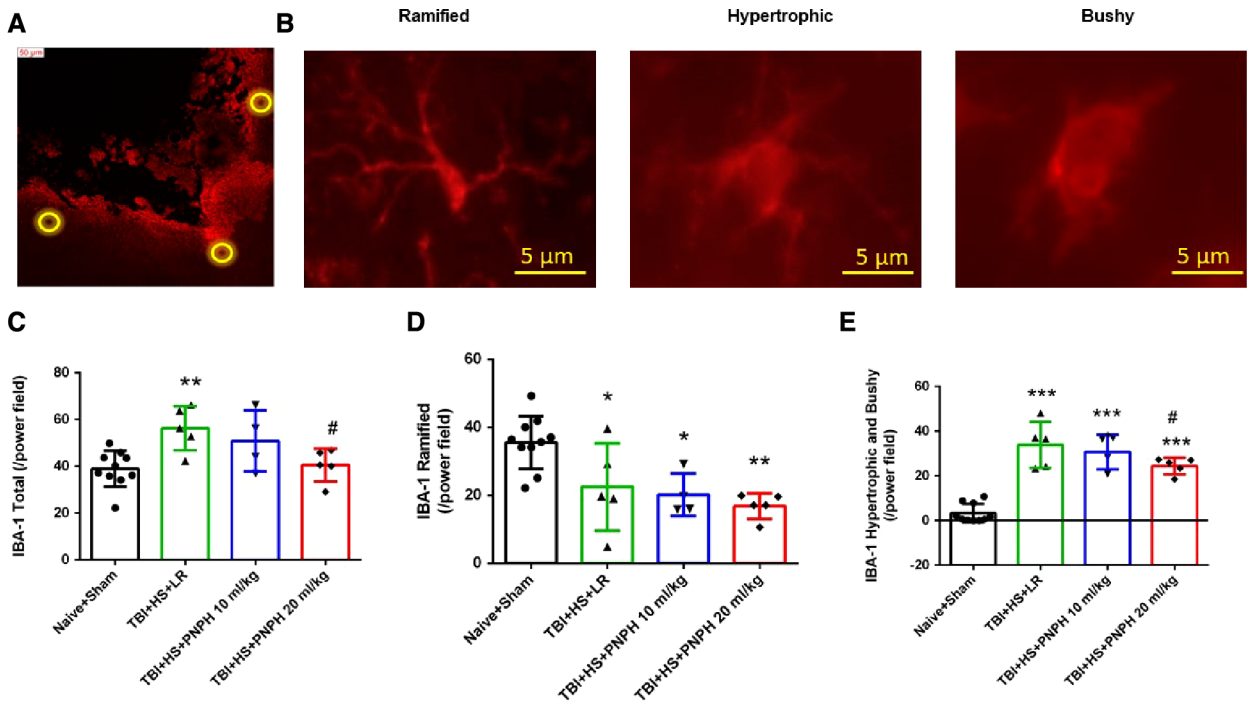

FIGURE 6
Effect of PNPH on microglial activation after TBI + hemorrhagic shock (HS). (**A**) Example of three fields selected for counting in the peri-lesion cortex on each side of the contusion and near the inner depth of the contusion. (**B**) Representative images of three morphologies of microglial cells: ramified, hypertrophic, and bushy. The number of Iba-1–positive cells (**C**), ramified Iba-1–positive cells (**D**), and hypertrophic plus bushy Iba-1–positive cells (**E**) are plotted for the combined Naïve + Sham group ($n = 10$) and for TBI + HS groups resuscitated with 60 ml/kg lactated Ringer's (LR) solution ($n = 5$), 10 ml/kg PNPH ($n = 4$), and 20 ml/kg PNPH ($n = 5$). The dose of 20 ml/kg PNPH attenuated the increased in microglia density and the number of hypertrophic/bushy microglia. Mean ± SD and individual data for each pig are shown. $^{*}P < 0.05$, $^{**}P < 0.01$, $^{***}P < 0.001$ vs. combined Naïve and Sham groups; $^{\#}P < 0.05$ vs. LR group determined by one-way ANOVA and the Holm-Sidak procedure for multiple comparisons.

hypotension that were restored by infusion of epinephrine. However, infusion of epinephrine sometimes resulted in an overshoot in MAP, which may have accounted for the elevated MAP seen at 150 min and 180 min time points after TBI. The oncotic effect of PNPH might also be a factor in this early increase in MAP. At the remaining time points, MAP in both TBI groups was similar to that in the sham group.

During the first 4 h after TBI, both groups had similar levels of whole blood Hb (Figure 7B), FHbO2 (Figure 7C), and metHb (Figure 7D). PNPH infusion resulted in the expected increase in whole blood COHb, but the peak level was only 2% COHb and was eliminated by day 1 (Figure 7E). Plasma Hb concentration increased to 0.51 ± 0.06 g/dl after 10 ml/kg PNPH infusion and declined to 0.11 ± 0.06 and 0.02 ± 0.01 g/dl on days 1 and 2, respectively (Figure 7F).

Neuropathology with TBI alone

Representative cresyl violet/Luxol fast blue-stained images of coronal brain sections are shown from a naïve pig and pigs with 10 ml/kg LR and 10 ml/kg PNPH infusion started 2 h after TBI (Figure 8A). Contusion lesion volume displayed an overall group effect [F (2,19) = 7.513; $P = 0.004$], but there was no significant difference ($P = 0.17$) between the TBI groups receiving LR and PNPH (Figure 8B). The volume of the subcortical white matter on the impacted side relative to the contralateral side displayed an overall group effect [F (2,19) = 6.826; $P = 0.006$]. Compared to the Naïve + Sham group, the TBI group receiving LR exhibited a significant loss of white matter volume ipsilateral to the injury ($P = 0.022$) (Figure 8C). In the TBI group receiving PNPH, the loss of white matter volume was significantly attenuated compared to the group receiving LR ($P = 0.027$). The value in the PNPH group did not significantly differ from the value in the Naïve + Sham group ($P = 0.99$).

Examples of APP immunoreactive particles are shown in Figure 9A for sections from naïve, TBI + LR, and TBI + PNPH pigs, and the area of subcortical white matter used in the stereological analysis is shown in Figure 9B. The quantification of APP particles in subcortical white matter in the TBI alone experiment (Figure 9C) showed a significant overall effect of group intervention [F (2,19) = 7.513; $P = 0.004$]. The Holm-Sidak procedure for multiple comparisons indicated that the estimate of the number of APP particles in the TBI + LR group (3,826,066 ± 1,977,136) was significantly greater than the number in the Naïve + Sham group (1,749,836 ± 908,968, $P = 0.007$). The number in the TBI + LR group was also significantly greater than that in the TBI + PNPH group (1,365,371 ± 429,906, $P = 0.007$). Interestingly, the value in the TBI + PNPH group was not significantly different from that in the Naïve + Sham group. Thus, the benefit of PNPH treatment on both white matter volume and APP accumulation seen in the TBI + HS experiment persisted in the absence of hemorrhagic shock.

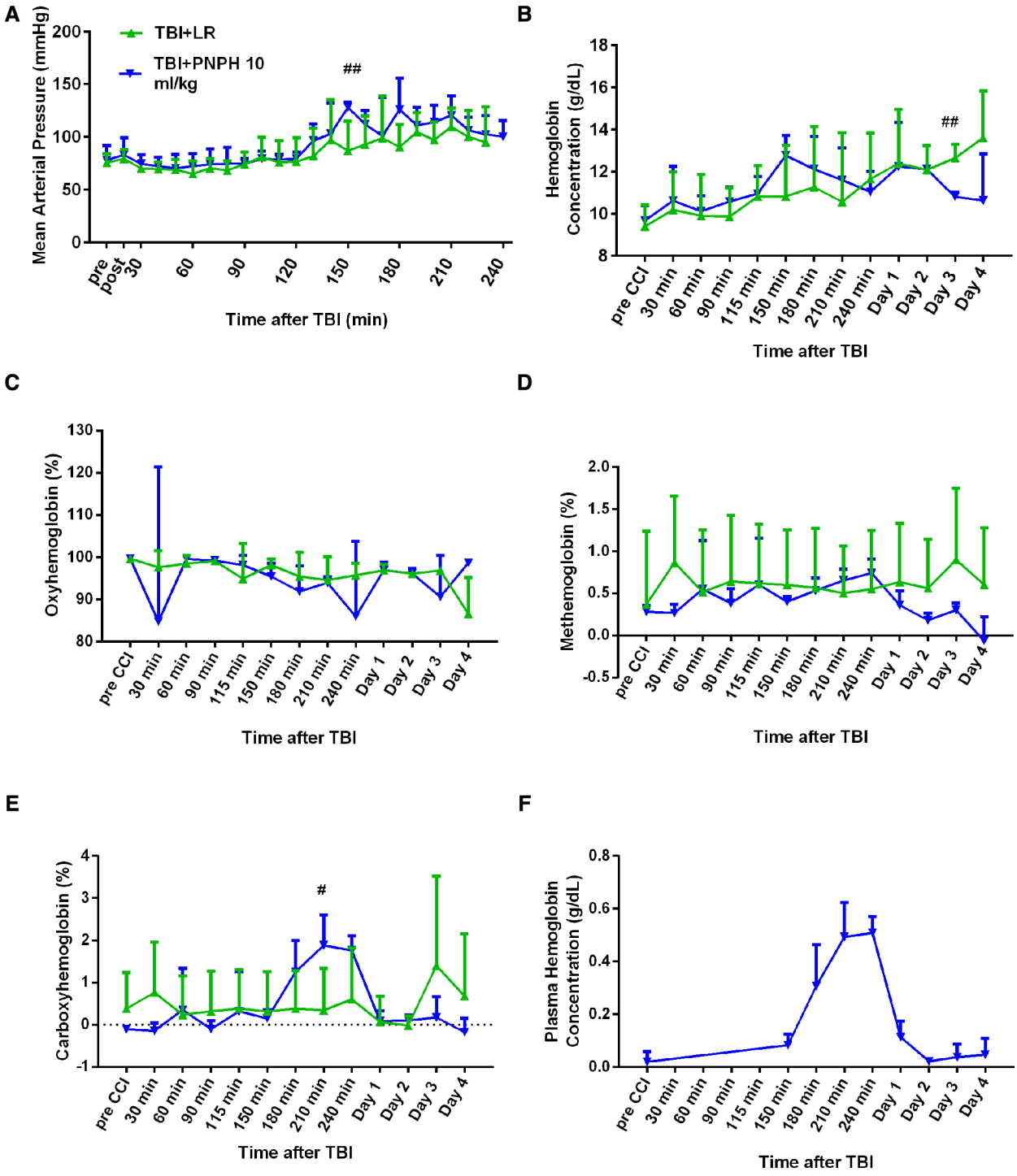

FIGURE 7
Systemic physiologic changes after TBI without hemorrhagic shock. Mean arterial pressure (A), hemoglobin concentration (B), percent of oxygenated hemoglobin (C), percent of methemoglobin (D), and percent of carboxyhemoglobin (E) in whole blood for pigs subjected to TBI followed by infusion of 10 ml/kg of lactated Ringer's (LR) solution or PNPH at 120–180 after TBI. Sample sizes per time point were 4–6 for LR group and 5–6 for 10 ml/kg PNPH group (smaller sample sizes occurred at 180–240 min when arterial blood samples could no longer be drawn because the pig was too active or the subcutaneously-routed catheter was inoperable). Individual data are shown in Supplemental Figures 6–10. PNPH infusion produced an increase in plasma hemoglobin concentration (F). Values are means ± SD. $^{\#}P < 0.05$, $^{\#\#}P < 0.01$ LR infusion vs. PNPH infusion group determined by one-way ANOVA.

Images of MAP-2–positive dendritic segments with >50 μm length in the gyrus adjacent to the contusion are shown in Figure 10A for brains from the TBI alone experiment, and an example of the area of the gyrus used in the analysis is shown in Figure 10B. As occurred with TBI + HS, one-way ANOVA indicated a significant overall effect of group intervention on dendritic integrity [F (2,19) = 40.465; $P < 0.001$]. The Holm-Sidak procedure for multiple comparisons revealed a marked decrease in the number of intact

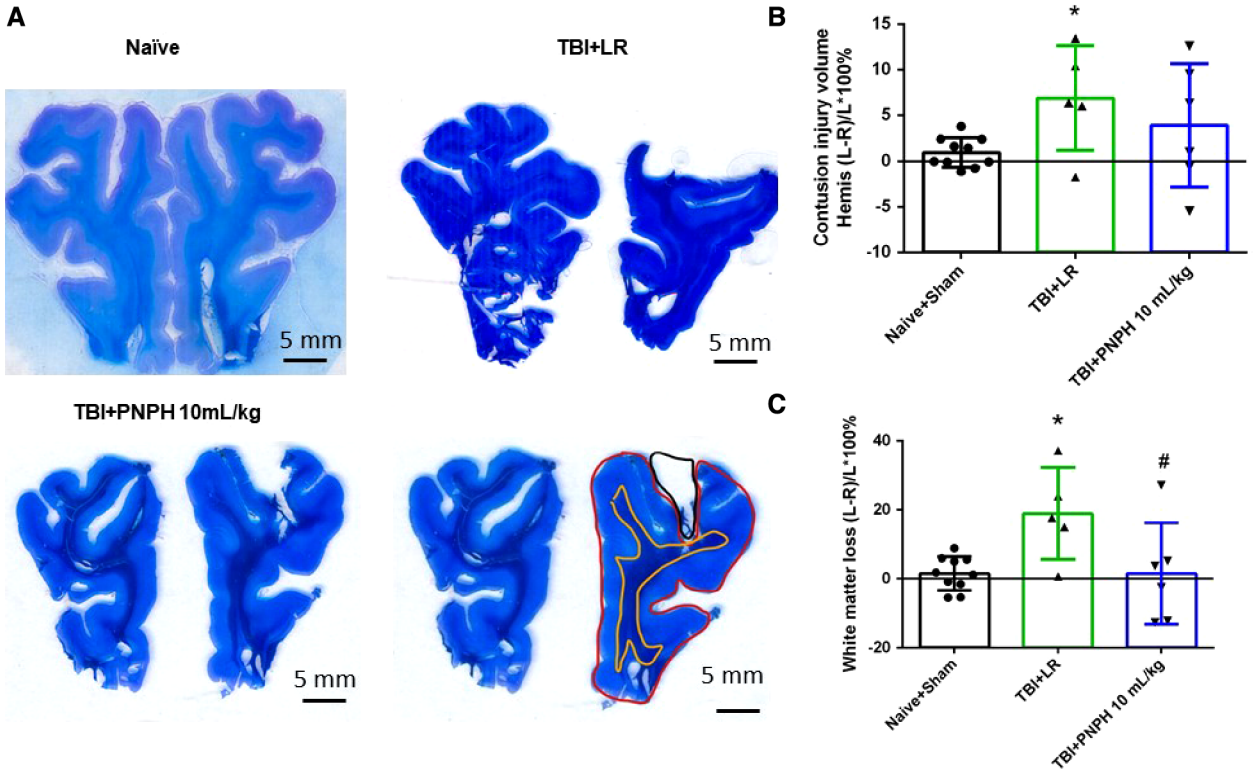

FIGURE 8
Effect of PNPH on frontal lobe contusion injury volume and volumetric white matter loss after TBI without hemorrhagic shock. (A) Representative coronal sections (both hemispheres, top is superior) of frontal lobe of normal pig brain and brains 4 days after TBI and infusion of 10 ml/kg lactated Ringer's (LR) solution and 10 ml/kg PNPH. Gray matter is visualized with cresyl violet staining and subcortical white matter myelin is visualized with Luxol fast blue staining. Area delineated by red trace is the entire histologically normal hemisphere, area delineated by the yellow trace is the white matter, and area delineated by the black trace is the contusion site. (B) Contusion injury volume (intact tissue difference of left minus right hemisphere as a percentage of left hemisphere volume contralateral to the injury site) of pigs subjected to TBI followed at 120 min with LR ($n = 6$) or PNPH ($n = 6$). The normal variation in the difference of left minus right hemisphere volume as a percentage of left hemisphere volume is shown for the combined Naïve ($n = 5$) and Sham ($n = 5$) group. (C) Volume of white matter loss in the same brains was calculated as the difference between left minus right subcortical white matter volume normalized by the left subcortical white matter volume (contralateral volume). White matter loss was decreased with PNPH treatment. Mean ± SD and individual data for each pig are shown. $^{*}P < 0.05$ vs. Naïve + Sham group, $^{\#}P < 0.05$ vs. LR group determined by one-way ANOVA and the Holm-Sidak procedure for multiple comparisons.

dendritic processes with a length >50 μm in the TBI group treated with LR (139 ± 35 per coronal section; $P < 0.001$) compared to the Naive + Sham group (403 ± 75 per coronal section) (Figure 10C). Treatment with PNPH greatly attenuated this decrease in long dendrites (349 ± 36 per coronal section; $P < 0.001$ from LR group), and the values were only marginally different from the Naïve + Sham group ($P = 0.09$). Again, the benefit of PNPH treatment after TBI did not require the presence of HS.

With TBI alone, the density of Iba-1–positive cell counts showed no overall effect among the three groups [F (2,19) = 1.620; $P = 0.22$] (Figure 11A). Analysis of the number of Iba-1–positive cells classified as having ramified processes yielded an overall group effect [F (2,19) = 27.810; $P < 0.001$] accompanied by significant decreases in the LR and PNPH groups compared to the Naïve + Sham group (Figure 11B). The difference between the LR and PNPH groups was not significant. On the other hand, the number of hypertrophic/bushy Iba-1–positive cells at 4 days after TBI alone displayed an overall group effect [F (2,19) = 42.107; $P < 0.001$] in which the significant increase seen with LR infusion ($P < 0.001$) compared to the Naive + Sham group was significantly attenuated with PNPH treatment ($P = 0.011$ vs. LR group).

Discussion

The CCI model of TBI has been used in infant and prepubertal juvenile pigs, but many studies had short survival times of 6 h or less (38, 47) and the number of studies with neuropathologic analysis at longer survival time is limited (34, 48, 49). Unique features in the present study include the immunohistochemical analysis of cellular changes in neocortical regions adjacent to the impacted gyrus. We purposely performed the impact over the dorsolateral frontal lobe region to avoid direct injury to primary somatosensory and motor neocortices that could adversely affect the pig's mobility and ability to eat and drink. Also noteworthy is that the pigs were approximately 3-months old, an age that approximates the age range that often appears in the literature for pre-pubertal swine models of TBI + HS (35, 38–42). The weight of the brain at this age is approximately 75% of those in fully mature pigs (50). Thus, the brains are likely to have undergoing myelination and brain development, which may have influenced neuronal vulnerability.

Our first main finding is that resuscitation from TBI + HS with 10 ml/kg and 20 ml/kg PNPH at 2 h after TBI substantially ameliorated the overall loss of white matter and neuronal cellular

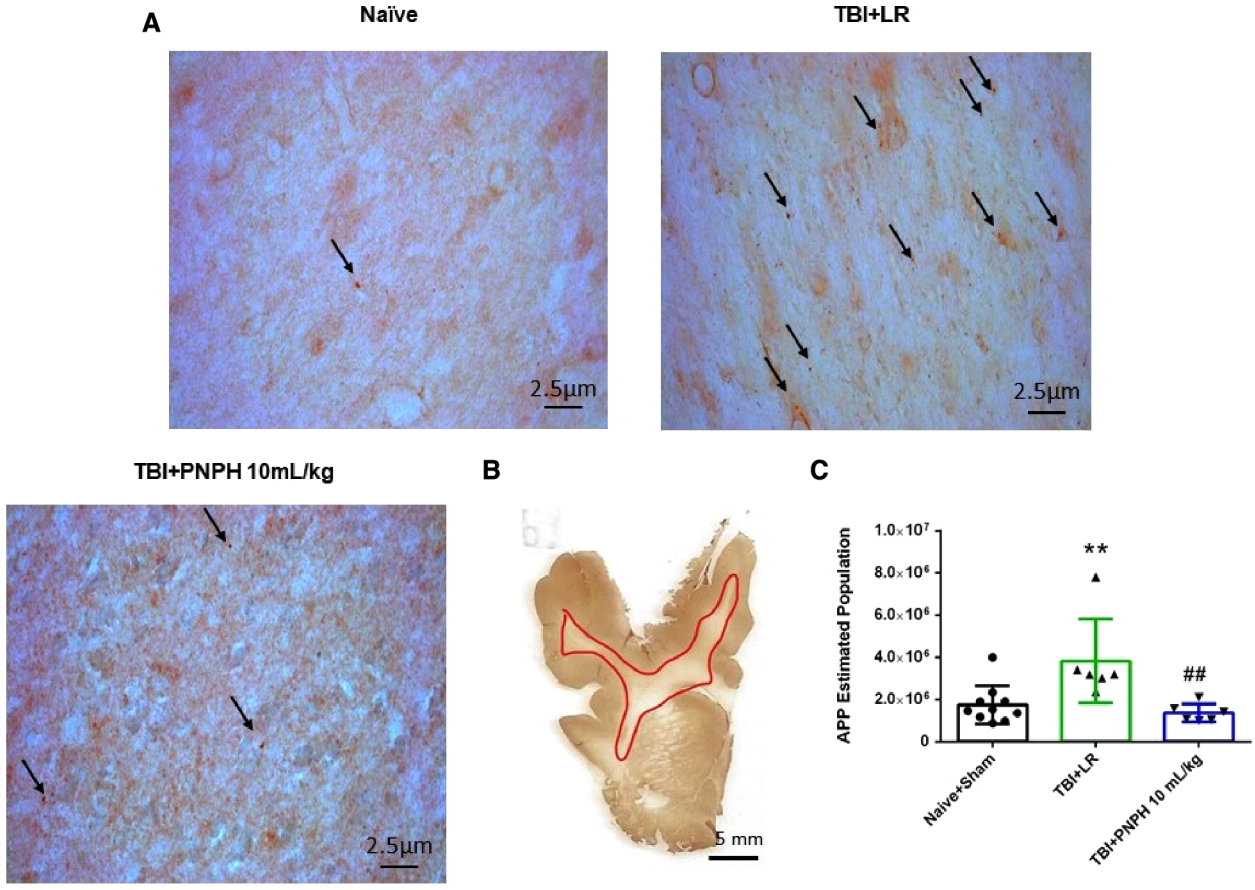

FIGURE 9
Effect of PNPH on APP expression after TBI without HS. (**A**) Representative images of APP immunostaining from naïve pig and pigs infused with 10 ml/kg LR or 10 ml/kg PNPH at 2 h after TBI. Arrows point to particles of APP accumulation. (**B**) The area of subcortical white used in the analysis is illustrated with the red trace. (**C**) The number of APP particles throughout subcortical white matter was estimated with the optical fractionator method of unbiased stereology and are plotted for the combined Naïve + Sham group ($n = 10$) and for TBI groups infused with 10 ml/kg LR ($n = 6$) and 10 ml/kg PNPH ($n = 6$). APP particles increased after TBI with LR infusion but not after PNPH infusion. Mean ± SD and individual data for each pig are shown. $^{**}P < 0.01$ vs. combined naïve and sham groups, $^{\#\#}P < 0.01$ vs. LR group determined by one-way ANOVA and the Holm-Sidak procedure for multiple comparisons.

injury in the gyrus adjacent to the impact. The cerebroprotection was associated with an improvement in gray and white matter and an attenuation of neuroinflammation as assessed by morphologic changes of microglia. Specifically, PHPH protected neocortical neuron dendrites as seen by MAP-2 immunoreactivity, diminished axonopathy as revealed by APP immunoreactivity, and rescued myelination perturbation as seen by the Luxol fast blue staining. The second main finding was that similar benefits were observed when PNPH was infused 2 h after TBI without intervening HS, thereby implying that hemorrhagic hypotension is not a requirement for cerebroprotection by PNPH in this large animal model of TBI and that the cerebroprotection is not completely dependent on a faster restoration of MAP by PNPH infusion. This protection is presumably attributable to nitroxide-based scavenging of superoxide and peroxynitrite within the vascular space, resulting in less vascular damage and inflammation, and possibly in the extravascular space where there is blood-brain barrier disruption (23, 24). Moreover, PNPH serves as a CO-releasing molecule that likely reinforces the anti-inflammatory effects exerted by nitroxide free radical scavenging (20) and that can promote cerebral vasodilation, even in the absence of nitroxide conjugation to PEG-Hb (51, 52). Furthermore, the ability of plasma-based PNPH to enter compressed capillaries that restrict red blood cell entry and to reduce edema (12, 13) may also improve microcirculatory hemodynamics independent of changes in MAP.

We analyzed the volumetric change of intact tissue after CCI and found that although the contusion injury volume in cerebral cortex was, on average, smaller in the groups treated with PNPH, the variability was relatively large and the difference from the LR-treated group did not attain statistical significance in either the TBI + HS experiment or the TBI alone experiment. Variability in contusion volume in the CCI model is not unusual. The coefficient of variation of contusion volume in the TBI + HS + LR group obtained histologically on Day 4 was 48% (SD = 6.11%; mean = 12.60%) and is comparable to that reported by others (42) in a TBI + HS swine model with T2 MRI measurements of edema on Day 3 after CCI (coefficient of variation of 46%, SD = 551 mm^3, mean = 1,202 mm^3). In rodent CCI models, variability has been attributed to several factors related to the instrumentation, experimental protocol, and presence of hemorrhage (53, 54). For CCI in a gyrencephalic brain, there are many complex considerations such as whether the center of the impact

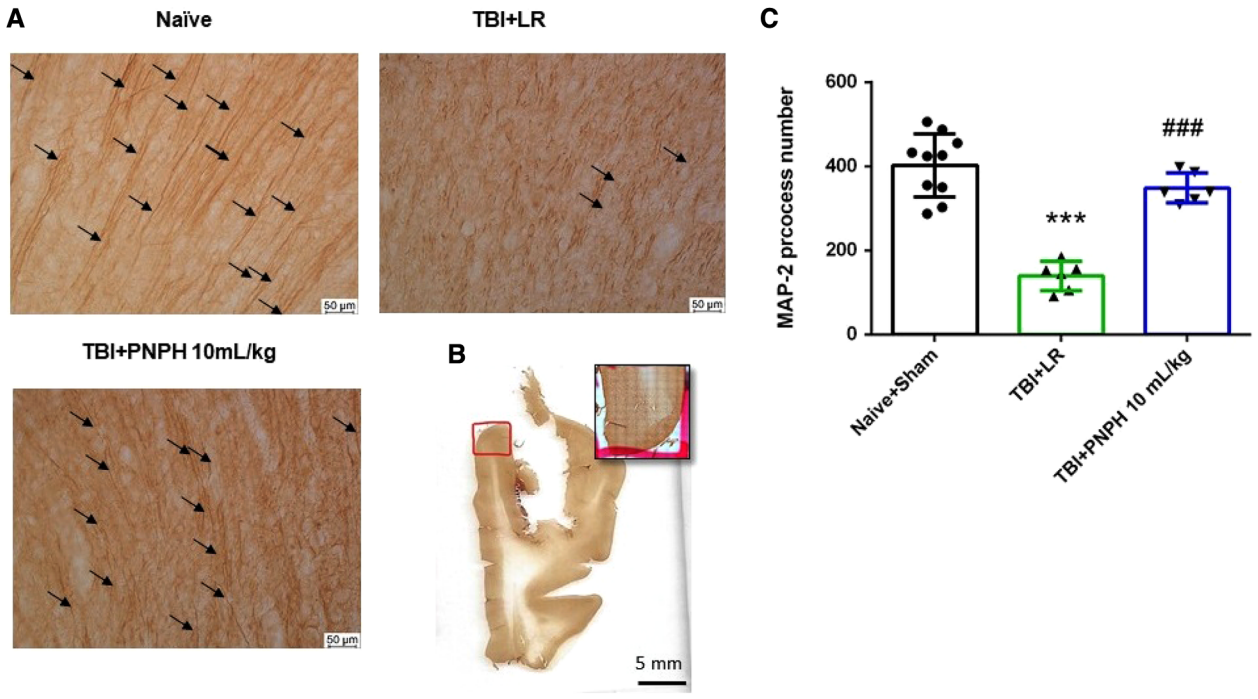

FIGURE 10
Effect of PNPH on MAP-2–identified gray matter neuronal dendrites after TBI without hemorrhagic shock. (**A**) Representative images of MAP-2 immunostaining from naïve pig and pigs infused with 10 ml/kg LR or 10 ml/kg PNPH 2 h after TBI. Arrows point to dendritic segments with >50 μm length from gyrus of the cortex adjacent to the gyrus where CCI was produced. (**B**) Example of area of gyrus analyzed is outlined in red. (**C**) The number of long neocortical dendrites per coronal section averaged over 10–12 sections are plotted for the combined Naïve + Sham group ($n = 10$) and for TBI groups infused with 10 ml/kg LR ($n = 6$) and 10 ml/kg PNPH ($n = 6$). The number of long dendrites was decreased in the TBI group infused with LR compared to the Naïve + Sham group and to the TBI group infused with PNPH. Mean ± SD and individual data for each pig are shown. $^{***}P < 0.001$ vs. combined Naïve + Sham groups, $^{###}P < 0.001$ vs. LR group determined by one-way ANOVA and the Holm-Sidak procedure for multiple comparisons.

approximates the center of the underlying gyrus or is over a sulcus and whether the trajectory of the subcortical white matter is parallel or perpendicular to the impact force. It should also be noted that contusion injury volume may continue to expand beyond 4 days, and a treatment effect might have become more evident at a later time point.

White matter volume was measured by staining of myelin with Luxol fast blue on sections in the frontal lobe. The 26% decrease in subcortical white matter volume relative to the contralateral white matter volume seen in the TBI + HS + LR group was substantially attenuated with PNPH resuscitation. In the case of TBI alone, PNPH almost completely prevented white matter loss. To specifically assess axonopathy, we measured accumulation of APP particles, which are known to accumulate after disruption of axonal transport induced by TBI (55). Moreover, TBI is considered a risk factor for Alzheimer's disease, either as a precipitating event or by accelerating development of the disease (56). The accumulation of APP after TBI and increased amyloidogenic (Aβ-producing) processing of APP by β-secretase has been postulated as a major cause of brain accumulation of Aβ (57, 58). TBI produced an increase the number of APP-positive white matter inclusions (brown dots) in both the TBI + HS and TBI alone experiments. Remarkably, treatment with PNPH largely prevented the increase in APP particle accumulation after TBI + HS and TBI alone. Together with the results of white matter volumetric improvement, PNPH appears to mitigate markers of axonopathy and myelin loss.

MAP-2 is a neuron-specific cytoskeletal protein that stabilizes microtubules in dendrites and the cell body by linking with intermediate filaments and other microtubules. Because MAP-2 is found along the length of the microtubules that are enriched in neuron dendrites, it is a reliable marker of dendrite integrity. We found significant neocortical dendritic disruption, as indicated by a decrease in the length of continuous MAP-2 stained dendrites within the plane of the tissue sections. The decrease in the number of dendrites with a length greater than 50 μm was measured in cerebral cortex independent of layer throughout the gyrus adjacent to the gyrus that was impacted and thus is indicative on neuronal injury remote from the contusion. This decrease occurred in the LR groups with and without concomitant HS and thus is primarily related to the CCI itself. Importantly, treatment with PNPH ameliorated the decrease in the number of long dendrites in gray matter. This observation indicates that cytoskeletal disruption in gray matter remote from the mechanically induced contusion is a treatable phenomenon, even when the treatment is delayed by 2 h after the primary insult. Therefore, delayed PNPH infusion has the capability of rescuing not only axonopathy, but also dendrites.

Neuroinflammation after TBI is usually accompanied by morphologic changes in microglia consisting of increased size of the cell body, less ramification of fine processes giving rise to shorter, hypertrophic processes, and in some cases, severe shortening and thickening of processes around the cell body that convey a bushy appearance (44, 48). As expected, pig brains in the

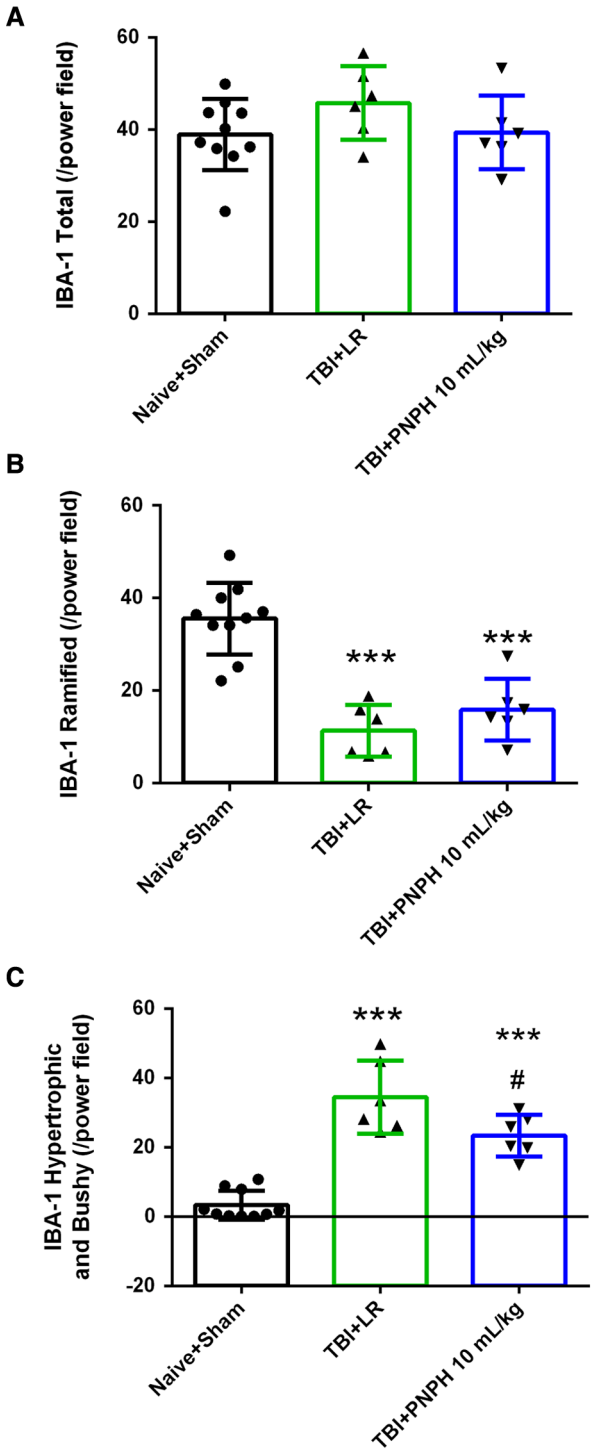

FIGURE 11
Effect of PNPH on microglial activation after TBI without HS. The number of Iba-1–positive cells (**A**), ramified Iba-1–positive cells (**B**), and hypertrophic plus bushy Iba-1–positive cells (**C**) are plotted for the combined Naïve + Sham group ($n = 10$) and for TBI groups infused with 10 ml/kg lactated Ringer's (LR) solution ($n = 6$) and 10 ml/kg PNPH ($n = 6$). The number of Iba-1–positive cells did not change significantly 4 days after TBI, whereas the number of Iba-1 cells classified as ramified decreased significantly in both TBI groups. Hypertrophic and bushy Iba-1 cell number markedly increased in the TBI group with LR infusion and the increase was attenuated with PNPH infusion. Mean ± SD and individual data for each pig are shown. ***$P < 0.001$ vs. combined Naïve + Sham group, $^{\#}P < 0.05$ vs. TBI group with LR treatment determined by one-way ANOVA and the Holm-Sidak procedure for multiple comparisons.

TBI + HS and TBI alone protocols presented with these characteristic changes. Interestingly, treatment with PNPH in both protocols attenuated the increase in the number of microglia with the hypertrophy and bushy appearance without affecting the decrease in microglia with fine process ramification. This pattern suggests that microglia are still activated but that not as many are in an overt pro-inflammatory state. Measurements of cytokines would be needed to help confirm this interpretation. In addition, the number of positive Iba1-positive cells significantly increased at 4 days after TBI + HS with LR resuscitation, and this increase was significantly reduced by treatment with 20 ml/kg PNPH. Although some of the increase may be attributable to infiltrating macrophages, it seems likely that PNPH also limited microglia proliferation. The latter would also be consistent with an anti-inflammatory effect of PNPH.

Previous studies with PNPH resuscitation from TBI + HS in mouse (12, 13, 26) and guinea pig (31) demonstrated faster recovery of MAP than with LR. Here, we did not observe substantial differences in the rate of MAP recovery after TBI + HS among groups, most likely because we used a faster rate of LR infusion to achieve a greater total treatment volume with LR (twice the hemorrhage volume) than with PNPH over a similar amount of time. Moreover, the infusion time was prolonged so as not to produce rapid changes in preload or afterload on the heart.

Infusion of 10 and 20 ml/kg PNPH produced dose-dependent increases in the plasma concentration of this cell-free Hb. Measurable levels were detected at 1 day after 10 ml/kg infusion and at 2 days after 20 ml/kg infusion. These recovery levels are consistent with a circulating half-life in the range of 12–24 h that is dependent on the amount of infused PNPH (zero-order clearance kinetics) in this large animal model. The peak concentration of Hb in the plasma remained less than 1 g/dl. PNPH resuscitation after TBI + HS limited the decrease in total blood Hb concentration seen with LR resuscitation. The concentration of Hb in the plasma may have contributed to attenuating the decrease in total Hb, but the larger volume of LR infused at a faster rate than PNPH is probably another factor that needs to be considered in the more profound hemodilution observed in the TBI + HS + LR group.

One concern with the use of cell-free Hb is that metHb can increase and produce oxidative stress. However, the percent of metHb in whole blood increased by only 1% of all Hb at 240 min after TBI + HS and subsided by one day. No significant elevations of metHb were observed with PNPH infusion in the TBI alone group. Thus, adverse effects on metHb levels are minimal with PNPH infusion, likely because the nitroxide groups on the molecule limit autooxidation (22, 23). Moreover, any adverse effects of this mild increase in metHb is expected to be alleviated by the peroxidase activity of nitroxides limiting the transition of the heme iron from the ferric to the highly reactive ferryl state (28, 29).

PNPH is stored as COHb to prevent autooxidation before it is infused. Upon infusion, CO is released and exchanges with Hb in red blood cells. The level of COHb increased to approximately 2% after infusion of 10 ml/kg PNPH and 4% after infusion of 20 ml/kg PNPH. This reservoir of CO storage may provide anti-inflammatory effects for the early hours after TBI until the CO is excreted by the lungs (20, 21). Importantly, these low levels of COHb did not have a significant effect on the fraction of arterial Hb carrying oxygen.

Although PNPH treatment provided significant cerebroprotection in 4-day survivors in both the TBI + HS and TBI alone models, a major limitation was that PNPH also produced severe hypotension in many of the pigs and required infusion of epinephrine to maintain MAP above 40 mmHg in many of the pigs. In some cases, the infusion of epinephrine was inadequate to prevent cardiac arrest. When the hypotension occurred, it was usually rapid. In some pigs, the MAP began to drop as early as 2 min into the infusion when the pig received only 5 ml of PNPH, which is a small volume relative to the >2 L blood volume of a 28-kg pig. This effect was unexpected because hypotension was not observed in mouse or guinea pig during PNPH infusion. The solvent for PNPH was dialyzed extensively against LR to remove all free reagents that could affect cardiac function and cause hypotension. One consideration is that pseudo-anaphylactic reaction to the PEG itself, although infrequent (59), might become more probable by changes in the immune milieu 2 h after TBI in 3-month-old swine. Left ventricular function has been reported to be depressed over the early hours after TBI in the absence of HS in 26-kg pigs (60), comparable to the size pig we used, and may provide the conditions for increased sensitivity to an anaphylactic stimulus. The use of midazolam to provide sedation after TBI may have also suppressed reflex sympathetic activity. Further work is needed to identify the underlying mechanism before recommending PNPH for use in non-human primates and humans.

Conclusion

Collectively, the presented data on myelin staining, APP particle number, dendrite length and microglial activation indicate that resuscitation from TBI with PNPH is superior in survivors in protecting the peri-contusion brain tissue compared to resuscitation with LR. These results extend previous work in rodent models of TBI + HS and demonstrate that PNPH possesses the capability to protect various aspects of neuronal integrity in the large gyrencephalic brain of the pig. This protection persisted when PNPH infusion was delayed by 2 h after TBI in the absence of HS. However, adverse effects on cardiac function and hemodynamics that appear to be specific to swine need to be further investigated before translation to human use.

Data availability statement

The raw data supporting the conclusions of this article will be made available by the authors, without undue reservation.

Ethics statement

The animal study was reviewed and approved by All procedures on pigs were approved by the Johns Hopkins University Animal Care and Use Committee and by the Animal Care and Use Review Office of the US Army Medical Research and Materiel Command (Fort Detrick, MD). In conducting research using animals, the investigators adhered to the Animal Welfare Act Regulations and other Federal statutes relating to animals and experiments involving animals and the principles set forth in the current version of the Guide for the Care and Use of Laboratory Animals, National Research Council.

Author contributions

JW, LJM, JS, BJS, CJCH, and RCK conceptualized and designed the study. JW, YS, SC, XL, LJM, and RCK performed the experiments and acquired data. JS synthesized the PNPH. JW and RCK analyzed the data. JW and RCK drafted the manuscript. All authors contributed to the article and approved the submitted version.

Funding

This work was supported by the US Army Medical Research and Materiel Command under Contract Number W81XWH19C0022 to CJCH and RCK. The views, opinions and/or findings contained in this report are those of the authors and should not be construed as an official Department of the Army position, policy or decision unless so designated by other documentation. Support was also received from the National Institutes of Health R01 HL139543 to RCK.

Acknowledgments

The authors express their appreciation to Shawn Adams and Natalia Rivera Diaz for their excellent technical assistance.

Conflict of interest

JS and BJS are employees of AntiRadical Therapeutics, LLC. CJCH holds shares in AntiRadical Therapeutics, LLC, which holds the license for polynitroxylated PEGylated hemoglobin.

The remaining authors declare that the research was conducted in the absence of any commercial or financial relationships that could be construed as a potential conflict of interest.

Publisher's note

Supplementary material

The Supplementary Material for this article can be found online at: https://www.frontiersin.org/articles/10.3389/fmedt.2023.1074643/full#supplementary-material.

References

1. Doganyigit Z, Erbakan K, Akyuz E, Polat AK, Arulsamy A, Shaikh MF. The role of neuroinflammatory mediators in the pathogenesis of traumatic brain injury: a narrative review. *ACS Chem Neurosci*. (2022) 13(13):1835–48. doi: 10.1021/acschemneuro.2c00196

2. Hakiminia B, Alikiaii B, Khorvash F, Mousavi S. Oxidative stress and mitochondrial dysfunction following traumatic brain injury: from mechanistic view to targeted therapeutic opportunities. *Fundam Clin Pharmacol*. (2022) 36(4):612–62. doi: 10.1111/fcp.12767

3. Hoffe B, Holahan MR. Hyperacute excitotoxic mechanisms and synaptic dysfunction involved in traumatic brain injury. *Front Mol Neurosci*. (2022) 15:831825. doi: 10.3389/fnmol.2022.831825

4. Shao F, Wang X, Wu H, Wu Q, Zhang J. Microglia and neuroinflammation: crucial pathological mechanisms in traumatic brain injury-induced neurodegeneration. *Front Aging Neurosci*. (2022) 14:825086. doi: 10.3389/fnagi.2022.825086

5. Thapa K, Khan H, Singh TG, Kaur A. Traumatic brain injury: mechanistic insight on pathophysiology and potential therapeutic targets. *J Mol Neurosci*. (2021) 71(9):1725–42. doi: 10.1007/s12031-021-01841-7

6. Czosnyka M, Brady K, Reinhard M, Smielewski P, Steiner LA. Monitoring of cerebrovascular autoregulation: facts, myths, and missing links. *NeurocritCare*. (2009) 10(3):373–86. doi: 10.1007/s12028-008-9175-7

7. Sviri GE, Aaslid R, Douville CM, Moore A, Newell DW. Time course for autoregulation recovery following severe traumatic brain injury. *J Neurosurg*. (2009) 111(4):695–700. doi: 10.3171/2008.10.17686

8. Hlatky R, Furuya Y, Valadka AB, Gonzalez J, Chacko A, Mizutani Y, et al. Dynamic autoregulatory response after severe head injury. *J Neurosurg*. (2002) 97(5):1054–61. doi: 10.3171/jns.2002.97.5.1054

9. Brady KM, Shaffner DH, Lee JK, Easley RB, Smielewski P, Czosnyka M, et al. Continuous monitoring of cerebrovascular pressure reactivity after traumatic brain injury in children. *Pediatrics*. (2009) 124(6):e1205–12. doi: 10.1542/peds.2009-0550

10. Day WG, Soltys BJ, Cole J, Simoni J, Hsia CJC, Lin AH. *Potential value of polynitoxylated PEGylated hemoglobin (SanFlow) in pre-hospital medicine in austere environments including military deployments, disasters and remote emergencies*. Blood Substitutes and Oxygen Biotherapeutics ed. Cham, Switzerland: Springer Nature (2022).

11. Hsia CJ, Ma L. A hemoglobin-based multifunctional therapeutic: polynitroxylated pegylated hemoglobin. *Artif Organs*. (2012) 36(2):215–20. doi: 10.1111/j.1525-1594.2011.01307.x

12. Brockman EC, Bayir H, Blasiole B, Shein SL, Fink EL, Dixon C, et al. Polynitroxylated-pegylated hemoglobin attenuates fluid requirements and brain edema in combined traumatic brain injury plus hemorrhagic shock in mice. *J Cereb Blood Flow Metab*. (2013) 33(9):1457–64. doi: 10.1038/jcbfm.2013.104

13. Brockman EC, Jackson TC, Dixon CE, BayIr H, Clark RS, Vagni V, et al. Polynitroxylated pegylated hemoglobin-A novel, small volume therapeutic for traumatic brain injury resuscitation: comparison to whole blood and dose response evaluation. *J Neurotrauma*. (2017) 34(7):1337–50. doi: 10.1089/neu.2016.4656

14. Nho K, Glower D, Bredehoeft S, Shankar H, Shorr R, Abuchowski A. PEG-bovine hemoglobin: safety in a canine dehydrated hypovolemic-hemorrhagic shock model. *BiomaterArtifCells Immobilization Biotechnol*. (1992) 20(2–4):511–24. doi: 10.3109/10731199209119677

15. Asano Y, Koehler RC, Ulatowski JA, Traystman RJ, Bucci E. Effect of cross-linked hemoglobin transfusion on endothelial-dependent dilation in cat pial arterioles. *Am J Physiol*. (1998) 275(4):H1313–21. doi: 10.1152/ajpheart.1998.275.4.H1313

16. Sampei K, Ulatowski JA, Asano Y, Kwansa H, Bucci E, Koehler RC. Role of nitric oxide scavenging in vascular response to cell-free hemoglobin transfusion. *Am J Physiol Heart Circ Physiol*. (2005) 289(3):H1191–201. doi: 10.1152/ajpheart.00251.2005

17. Rebel A, Cao S, Kwansa H, Dore S, Bucci E, Koehler RC. Dependence of acetylcholine and ADP dilation of pial arterioles on heme oxygenase after transfusion of cell-free polymeric hemoglobin. *Am J Physiol Heart Circ Physiol*. (2006) 290(3):H1027–H37. doi: 10.1152/ajpheart.00500.2005

18. Saxena R, Wijnhoud AD, Man in 't Veld AJ, van den Meiracker AH, Boomsma F, Przybelski RJ, et al. Effect of diaspirin cross-linked hemoglobin on endothelin-1 and blood pressure in acute ischemic stroke in man. *J Hypertens*. (1998) 16(10):1459–65. doi: 10.1097/00004872-199816100-00009

19. Saxena R, Wijnhoud AD, Carton H, Hacke W, Kaste M, Przybelski RJ, et al. Controlled safety study of a hemoglobin-based oxygen carrier, DCLHb, in acute ischemic stroke. *Stroke*. (1999) 30(5):993–6. doi: 10.1161/01.STR.30.5.993

20. Fagone P, Mazzon E, Bramanti P, Bendtzen K, Nicoletti F. Gasotransmitters and the immune system: mode of action and novel therapeutic targets. *Eur J Pharmacol*. (2018) 834:92–102. doi: 10.1016/j.ejphar.2018.07.026

21. Wang J, Zhang D, Fu X, Yu L, Lu Z, Gao Y, et al. Carbon monoxide-releasing molecule-3 protects against ischemic stroke by suppressing neuroinflammation and alleviating blood-brain barrier disruption. *J Neuroinflammation*. (2018) 15(1):188. doi: 10.1186/s12974-018-1226-1

22. Krishna MC, Russo A, Mitchell JB, Goldstein S, Dafni H, Samuni A. Do nitroxide antioxidants act as scavengers of O2-. or as SOD mimics? *J Biol Chem*. (1996) 271(42):26026–31. doi: 10.1074/jbc.271.42.26026

23. Buehler PW, Haney CR, Gulati A, Ma L, Hsia CJ. Polynitroxyl hemoglobin: a pharmacokinetic study of covalently bound nitroxides to hemoglobin platforms. *Free RadicBiolMed*. (2004) 37(1):124–35. doi: 10.1016/j.freeradbiomed.2004.04.008

24. Saetzler RK, Arfors KE, Tuma RF, Vasthare U, Ma L, Hsia CJ, et al. Polynitroxylated hemoglobin-based oxygen carrier: inhibition of free radical-induced microcirculatory dysfunction. *Free Radic Biol Med*. (1999) 27(1–2):1–6. doi: 10.1016/S0891-5849(99)00037-4

25. Okayama N, Park JH, Coe L, Granger DN, Ma L, Hisa CJ, et al. Polynitroxyl alpha alpha-hemoglobin (PNH) inhibits peroxide and superoxide-mediated neutrophil adherence to human endothelial cells. *Free Radic Res*. (1999) 31(1):53–8. doi: 10.1080/10715769900300591

26. Shellington DK, Du L, Wu X, Exo J, Vagni V, Ma L, et al. Polynitroxylated pegylated hemoglobin: a novel neuroprotective hemoglobin for acute volume-limited fluid resuscitation after combined traumatic brain injury and hemorrhagic hypotension in mice. *Crit Care Med*. (2011) 39(3):494–505. doi: 10.1097/CCM.0b013e318206b1fa

27. Alayash AI. Oxygen therapeutics: can we tame haemoglobin? *NatRevDrug Discov*. (2004) 3(2):152–9. doi: 10.1038/nrd1307

28. Stoyanovsky DA, Kapralov A, Huang Z, Maeda A, Osipov A, Hsia CJ, et al. Unusual peroxidase activity of polynitroxylated pegylated hemoglobin: elimination of H(2)O(2) coupled with intramolecular oxidation of nitroxides. *Biochem Biophys Res Commun*. (2010) 399(2):139–43. doi: 10.1016/j.bbrc.2010.07.030

29. Krishna MC, Samuni A, Taira J, Goldstein S, Mitchell JB, Russo A. Stimulation by nitroxides of catalase-like activity of hemeproteins. Kinetics and mechanism. *J Biol Chem*. (1996) 271(42):26018–25. doi: 10.1074/jbc.271.42.26018

30. Cao S, Zhang J, Ma L, Hsia CJC, Koehler RC. Transfusion of polynitroxylated pegylated hemoglobin stabilizes pial arterial dilation and decreases infarct volume after transient middle cerebral artery occlusion. *J Am Heart Assoc*. (2017) 6(9):e006505. doi: 10.1161/JAHA.117.006505

31. Seno S, Wang J, Cao S, Saraswati M, Park S, Simoni J, et al. Resuscitation with macromolecular superoxide dismutase/catalase mimetic polynitroxylated PEGylated hemoglobin offers neuroprotection in Guinea pigs after traumatic brain injury combined with hemorrhage shock. *BMC Neurosci*. (2020) 21(1):22. doi: 10.1186/s12868-020-00571-7

32. Kinder HA, Baker EW, West FD. The pig as a preclinical traumatic brain injury model: current models, functional outcome measures, and translational detection strategies. *Neural Regen Res*. (2019) 14(3):413–24. doi: 10.4103/1673-5374.245334

33. Kilbaugh TJ, Bhandare S, Lorom DH, Saraswati M, Robertson CL, Margulies SS. Cyclosporin A preserves mitochondrial function after traumatic brain injury in the immature rat and piglet. *J Neurotrauma*. (2011) 28(5):763–74. doi: 10.1089/neu.2010.1635

34. Kinder HA, Baker EW, Howerth EW, Duberstein KJ, West FD. Controlled cortical impact leads to cognitive and motor function deficits that correspond to cellular pathology in a piglet traumatic brain injury model. *J Neurotrauma*. (2019) 36(19):2810–26. doi: 10.1089/neu.2019.6405

35. Williams AM, Dennahy IS, Bhatti UF, Halaweish I, Xiong Y, Chang P, et al. Mesenchymal stem cell-derived exosomes provide neuroprotection and improve long-term neurologic outcomes in a swine model of traumatic brain injury and hemorrhagic shock. *J Neurotrauma*. (2019) 36(1):54–60. doi: 10.1089/neu.2018.5711

36. Mayer AR, Dodd AB, Rannou-Latella JG, Stephenson DD, Dodd RJ, Ling JM, et al. 17alpha-Ethinyl estradiol-3-sulfate increases survival and hemodynamic functioning in a large animal model of combined traumatic brain injury and hemorrhagic shock: a randomized control trial. *Crit Care*. (2021) 25(1):428. doi: 10.1186/s13054-021-03844-7

37. Mayer AR, Ling JM, Dodd AB, Rannou-Latella JG, Stephenson DD, Dodd RJ, et al. Reproducibility and characterization of head kinematics during a large animal acceleration model of traumatic brain injury. *Front Neurol*. (2021) 12:658461. doi: 10.3389/fneur.2021.658461

38. Imam AM, Jin G, Duggan M, Sillesen M, Hwabejire JO, Jepsen CH, et al. Synergistic effects of fresh frozen plasma and valproic acid treatment in a combined model of traumatic brain injury and hemorrhagic shock. *Surgery*. (2013) 154(2):388–96. doi: 10.1016/j.surg.2013.05.008

39. Sillesen M, Jin G, Johansson PI, Alam HB. Resuscitation speed affects brain injury in a large animal model of traumatic brain injury and shock. *Scand J Trauma Resusc Emerg Med*. (2014) 22:46. doi: 10.1186/s13049-014-0046-2

40. Hwabejire JO, Jin G, Imam AM, Duggan M, Sillesen M, Deperalta D, et al. Pharmacologic modulation of cerebral metabolic derangement and excitotoxicity in a porcine model of traumatic brain injury and hemorrhagic shock. *Surgery*. (2013) 154(2):234–43. doi: 10.1016/j.surg.2013.04.008

41. Dekker SE, Bambakidis T, Sillesen M, Liu B, Johnson CN, Jin G, et al. Effect of pharmacologic resuscitation on the brain gene expression profiles in a swine model of traumatic brain injury and hemorrhage. *J Trauma Acute Care Surg*. (2014) 77(6):906–12; discussion 12. doi: 10.1097/TA.0000000000000345

42. Halaweish I, Bambakidis T, He W, Linzel D, Chang Z, Srinivasan A, et al. Early resuscitation with fresh frozen plasma for traumatic brain injury combined with hemorrhagic shock improves neurologic recovery. *J Am Coll Surg*. (2015) 220 (5):809–19. doi: 10.1016/j.jamcollsurg.2015.01.057

43. Arambula SE, Reinl EL, El Demerdash N, McCarthy MM, Robertson CL. Sex differences in pediatric traumatic brain injury. *Exp Neurol*. (2019) 317:168–79. doi: 10.1016/j.expneurol.2019.02.016

44. Villapol S, Loane DJ, Burns MP. Sexual dimorphism in the inflammatory response to traumatic brain injury. *Glia*. (2017) 65(9):1423–38. doi: 10.1002/glia.23171

45. Lu VM, Hernandez N, Wang S. National characteristics, etiology, and inpatient outcomes of pediatric traumatic brain injury: a KID study. *Childs Nerv Syst*. (2022) 38 (8):1541–7. doi: 10.1007/s00381-022-05544-1

46. Koo EH, Sisodia SS, Archer DR, Martin LJ, Weidemann A, Beyreuther K, et al. Precursor of amyloid protein in Alzheimer disease undergoes fast anterograde axonal transport. *Proc Natl Acad Sci U S A*. (1990) 87(4):1561–5. doi: 10.1073/pnas.87.4.1561

47. Nikolian VC, Dekker SE, Bambakidis T, Higgins GA, Dennahy IS, Georgoff PE, et al. Improvement of blood-brain barrier integrity in traumatic brain injury and hemorrhagic shock following treatment with valproic acid and fresh frozen plasma. *Crit Care Med*. (2018) 46(1):e59–66. doi: 10.1097/CCM.0000000000002800

48. Irvine KA, Bishop RK, Won SJ, Xu J, Hamel KA, Coppes V, et al. Effects of veliparib on microglial activation and functional outcomes after traumatic brain injury in the rat and pig. *J Neurotrauma*. (2018) 35(7):918–29. doi: 10.1089/neu.2017.5044

49. Kinder HA, Baker EW, Wang S, Fleischer CC, Howerth EW, Duberstein KJ, et al. Traumatic brain injury results in dynamic brain structure changes leading to acute and chronic motor function deficits in a pediatric piglet model. *J Neurotrauma*. (2019) 36 (20):2930–42. doi: 10.1089/neu.2018.6303

50. Conrad MS, Dilger RN, Johnson RW. Brain growth of the domestic pig (Sus scrofa) from 2 to 24 weeks of age: a longitudinal MRI study. *Dev Neurosci*. (2012) 34(4):291–8. doi: 10.1159/000339311

51. Zhang J, Cao S, Kwansa H, Crafa D, Kibler KK, Koehler RC. Transfusion of hemoglobin-based oxygen carriers in the carboxy state is beneficial during transient focal cerebral ischemia. *J Appl Physiol*. (2012) 113(11):1709–17. doi: 10.1152/japplphysiol.01079.2012

52. Cipolla MJ, Linfante I, Abuchowski A, Jubin R, Chan SL. Pharmacologically increasing collateral perfusion during acute stroke using a carboxyhemoglobin gas transfer agent (sanguinate) in spontaneously hypertensive rats. *J Cereb Blood Flow Metab*. (2017) 38(5):755–66. doi: 10.1177/0271678X17705567

53. Siebold L, Obenaus A, Goyal R. Criteria to define mild, moderate, and severe traumatic brain injury in the mouse controlled cortical impact model. *Exp Neurol*. (2018) 310:48–57. doi: 10.1016/j.expneurol.2018.07.004

54. Sellappan P, Cote J, Kreth PA, Schepkin VD, Darkazalli A, Morris DR, et al. Variability and uncertainty in the rodent controlled cortical impact model of traumatic brain injury. *J Neurosci Methods*. (2019) 312:37–42. doi: 10.1016/j.jneumeth.2018.10.027

55. Wang J, Hamm RJ, Povlishock JT. Traumatic axonal injury in the optic nerve: evidence for axonal swelling, disconnection, dieback, and reorganization. *JNeurotrauma*. (2011) 28(7):1185–98. doi: 10.1089/neu.2011.1756

56. Dams-O'Connor K, Guetta G, Hahn-Ketter AE, Fedor A. Traumatic brain injury as a risk factor for Alzheimer's disease: current knowledge and future directions. *Neurodegener Dis Manag*. (2016) 6(5):417–29. doi: 10.2217/nmt-2016-0017

57. Johnson VE, Stewart W, Smith DH. Traumatic brain injury and amyloid-beta pathology: a link to Alzheimer's disease? *Nat Rev Neurosci*. (2010) 11(5):361–70. doi: 10.1038/nrn2808

58. Johnson VE, Stewart W, Smith DH. Widespread tau and amyloid-beta pathology many years after a single traumatic brain injury in humans. *Brain Pathol*. (2012) 22 (2):142–9. doi: 10.1111/j.1750-3639.2011.00513.x

59. Padin-Gonzalez E, Lancaster P, Bottini M, Gasco P, Tran L, Fadeel B, et al. Understanding the role and impact of poly (ethylene glycol) (PEG) on nanoparticle formulation: implications for COVID-19 vaccines. *Front Bioeng Biotechnol*. (2022) 10:882363. doi: 10.3389/fbioe.2022.882363

60. Adedipe A, John AS, Krishnamoorthy V, Wang X, Steck DT, Ferreira R, et al. Left ventricular function in the initial period after severe traumatic brain injury in swine. *Neurocrit Care*. (2022) 37(1):200–8. doi: 10.1007/s12028-022-01468-5

frontiers | Frontiers in Molecular Biosciences

TYPE Original Research
PUBLISHED 16 March 2023
DOI 10.3389/fmolb.2023.1133985

OPEN ACCESS

EDITED BY
Andrea Mozzarelli,
University of Parma, Italy

REVIEWED BY
Hiromi Sakai,
Nara Medical University, Japan
Stefano Bruno,
University of Parma, Italy

*CORRESPONDENCE
Leif Bülow,
leif.bulow@kilu.lu.se

SPECIALTY SECTION
This article was submitted to Structural Biology, a section of the journal Frontiers in Molecular Biosciences

RECEIVED 03 January 2023
ACCEPTED 01 March 2023
PUBLISHED 16 March 2023

CITATION
Kettisen K, Nyblom M, Smeds E, Fago A and Bülow L (2023), Structural and oxidative investigation of a recombinant high-yielding fetal hemoglobin mutant. *Front. Mol. Biosci.* 10:1133985. doi: 10.3389/fmolb.2023.1133985

Structural and oxidative investigation of a recombinant high-yielding fetal hemoglobin mutant

Karin Kettisen[1], Maria Nyblom[2], Emanuel Smeds[3,4], Angela Fago[5] and Leif Bülow[1]*

[1]Pure and Applied Biochemistry, Department of Chemistry, Lund University, Lund, Sweden, [2]Lund Protein Production Platform, Department of Biology, Lund University, Lund, Sweden, [3]Infection Medicine, Department of Clinical Sciences, Lund University, Lund, Sweden, [4]Anesthesiology and Intensive Care, Department of Clinical Sciences, Lund University, Lund, Sweden, [5]Zoophysiology, Department of Biology, Aarhus University, Aarhus, Denmark

Human fetal hemoglobin (HbF) is an attractive starting protein for developing an effective agent for oxygen therapeutics applications. This requires that HbF can be produced in heterologous systems at high levels and in a homogeneous form. The introduction of negative charges on the surface of the α-chain in HbF can enhance the recombinant production yield of a functional protein in *Escherichia coli*. In this study, we characterized the structural, biophysical, and biological properties of an HbF mutant carrying four additional negative charges on each α-chain (rHbFα4). The 3D structure of the rHbFα4 mutant was solved with X-ray crystallography at 1.6 Å resolution. Apart from enabling a higher yield in recombinant protein production in *E. coli*, we observed that the normal DNA cleavage activity of the HbF was significantly lowered, with a four-time reduced rate constant for the rHbFα4 mutant. The oxygen-binding properties of the rHbFα4 mutant were identical to the wild-type protein. No significant difference between the wild-type and rHbFα4 was observed for the investigated oxidation rates (autoxidation and H_2O_2-mediated ferryl formation). However, the ferryl reduction reaction indicated some differences, which appear to be related to the reaction rates linked to the α-chain.

KEYWORDS

fetal hemoglobin, protein surface net charge, oxygen binding, redox reactions, DNA cleavage, X-ray crystallography

1 Introduction

To enable the design of a safe and functional oxygen therapeutic, a suitable oxygen-carrying component is essential. In humans, hemoglobin (Hb) is the oxygen-carrying protein responsible for transporting oxygen from the lungs to all tissues in the body. Due to the appropriate oxygen transport characteristics of human Hb, this protein has a central role in the development of a class of oxygen therapeutic products called hemoglobin-based oxygen carriers (HBOCs) (Alayash, 2014). No HBOC product to date has been approved for human use by key government agencies such as the European Medicines Agency (EMA) or the Food and Drug Administration (FDA). The persistent safety issues associated with HBOCs have been proposed to largely stem from toxic side

effects of cell-free Hb, such as endothelial nitric oxide scavenging, oxidative side reactions, and heme-associated inflammatory responses (Buehler et al., 2010). These side effects are normally *in vivo* kept under control by inherent protective systems against hemolysis, including the plasma proteins haptoglobin, hemopexin, and α1-microglobulin (Alayash et al., 2013; Ascenzi et al., 2005). However, under more challenging conditions, for example, by applying significant amounts of extracellular Hb formulated as oxygen therapeutics, these systems can easily be overwhelmed and Hb-mediated toxicity will occur (Bozza and Jeney, 2020). To tackle these issues, significant efforts have been spent on engineering human Hb for HBOC use, both to clarify the origin of the toxic side reactions and to identify ways to control harmful activities (Varnado et al., 2013; Olson, 2020). Besides engineering the Hb molecule itself to achieve the required qualities, future development will also require efficient recombinant protein production systems capable of large-scale manufacture of such designed Hb molecules. Thus, an aspect to consider for efficient production of Hb in heterologous hosts is the protein design to enhance yield and stability during protein production.

Human hemoglobins are made up of four subunits, forming a heterotetramer of two α-type globins (α, ζ) and two β-type globins (β, γ, δ, ε) (Schechter, 2008). The most common variant, adult human hemoglobin (HbA, $\alpha_2\beta_2$) has been used as a component to formulate many HBOCs. An alternative human protein is the fetal human hemoglobin (HbF), which carries the same α-subunits as HbA, but the α-subunits are paired with two γ-subunits instead of β-subunits. The γ- and β-subunit are largely similar but differ in their amino acid sequences at 39 or 40 residues (the γ-globin genes (HBG1 and HBG2) differ at one residue). The differences are manifested as a reduced sensitivity of the oxygen affinity to the allosteric effector 2,3-diphosphoglycerate (DPG) (Bauer et al., 1968; Bunn and Briehl, 1970), a higher alkali denaturation resistance (Perutz, 1974), and a lower tetramer-dimer dissociation constant (Yagami et al., 2002) compared to the adult protein. Recombinantly produced wild type (wt) HbA and wt HbF were compared side by side in terms of oxidative reactivity in a study by Simons et al. (2018), which concluded that both proteins have favorable qualities in diverse redox-related aspects, and from that perspective, neither Hb appeared more suitable than the other as an HBOC starting material. Still, the enhanced stability of HbF compared to HbA is an argument in favor of HbF as a more attractive candidate for large-scale production. Optimization of culture conditions can markedly improve HbF production and a lesser fraction of non-desirable Hb (consisting of e.g., the soluble β-type subunit homotetramers) were seen with HbF compared to HbA (Ratanasopa et al., 2016). We recently revisited a laboratory-scale protocol for shake flask HbF production and found that wt HbF yield in *Escherichia coli* flask cultures could be increased to ~30 mg purified Hb/L (Kettisen and Bulow, 2021).

The most attractive host for recombinant Hb production has so far been *E. coli*, which comes with advantages such as ease of genetic manipulation and straightforward cultivation with cheap media components. However, this system also has drawbacks such as insufficient intrinsic heme supply for achieving high Hb expression, unsatisfactory methionine aminopeptidase activity, and endotoxin contamination. These concerns can for the most part be overcome, as heme supply in *E. coli* can be enhanced to improve the Hb yield (Weickert et al., 1999; Villarreal et al., 2008), methionine aminopeptidase can be co-expressed for efficient N-terminal Met removal (Shen et al., 1997), and endotoxin reduction can be carried out during downstream processing with commercial endotoxin-removal measures, or, alternatively, engineered *E. coli* strains with lower endotoxin levels may be considered (Mamat et al., 2015). As the limitations related to the heterologous host often can be managed, the area for improvement could be focused on the intrinsic properties of the protein. The α-subunit suffers from stability issues both in the red blood cells and during recombinant expression in *E. coli* (Hoffman et al., 1990). In the maturing red cell, the assembly of Hb is aided by the alpha-hemoglobin stabilizing protein (AHSP) acting as a chaperone (Weiss et al., 2005). This protein can also be co-expressed during Hb production in *E. coli* with favorable outcomes on the α-subunit yield (Vasseur-Godbillon et al., 2006), but protein engineering strategies to enhance the stability of the α-subunit during expression, as shown with the αG15A mutation (Graves et al., 2008), might, if explored more extensively, be similarly used to improve Hb production. The stability of the apoglobin has been shown to directly correlate with the expression yield of the monomeric model protein myoglobin (Samuel et al., 2015). Other strategies of increasing recombinant protein production have shown that adaptation of the protein surface to fit the cytosolic electrostatic environment of the host cell could significantly improve solubility (Mu et al., 2017). If also taking into account the correlation between increased surface net charge and myoglobin concentration in tissues of deep-diving mammals (Mirceta et al., 2013), the mutational plasticity of the Hb α-subunit, especially the exposed surface-located residues, is worthwhile to dissect further. As the subunits still must be able to readily combine with each other, as well as retain Hb functionality as an oxygen carrier, the choice of mutation sites for this strategy should focus on surface-exposed sites located far away from the subunit contact interfaces and key structures of the heme pocket. We have previously identified one HbF mutant that exhibited a significantly higher yield than recombinant wt HbF (wt rHbF) in *E. coli* cultures (Kettisen and Bulow, 2021). The present study aims to examine this particular HbF mutant in a more in-depth characterization study. The HbF mutant harbors substitutions of three positive lysine residues on the surface of the α-subunit into negatively charged glutamic acid, combined with an asparagine residue substituted for aspartate (Kettisen and Bulow, 2021). The mutation sites are spread out across the surface of the alpha chain at α11 (A9) Lys→Glu, α56 (E5) Lys→Glu [Hb Shaare Zedek (Abramov et al., 1980)], α78 (EF7) Asn→Asp [Hb J-Singa (Wong et al., 1984)], and α90 (FG2) Lys→Glu (Hb Sudbury). We analyze the consequences of introducing these negatively charged substitutions on the alpha chains of HbF in terms of oxygen binding, redox activity, heme loss, DNA cleavage, thermal stability and crystal structure. We have also included an initial study of plasma clearance in a simple mouse model.

2 Materials and methods

2.1 Production and purification of hemoglobin

Four mutations at surface-exposed locations on the α-subunit were previously selected for introducing negative charges on HbF (Kettisen and Bulow, 2021). The four mutations were as follows, α11 (A9) Lys→Glu, α56 Lys→Glu, α78 (EF7) Asn→Asp, and α90 (FG2) Lys→Glu, and this HbF variant will henceforth be called rHbFα4. The α- and γ-subunits were expressed in tandem using the HbF-pETDuet-1 vector as described previously (Ratanasopa et al., 2016).

The cells were grown in Terrific Broth supplemented with 0.1 mg/L carbenicillin for selective pressure, 0.1 mM IPTG for protein expression induction, and 1 mM δ-aminolevulinic acid to improve intracellular heme production. At the end of cultivation, the cultures were bubbled with carbon monoxide (CO) gas to stabilize the protein, and CO bubbling was repeated after each subsequent downstream processing step. The cultivation and purification procedures have been described in more detail elsewhere (Kettisen and Bulow, 2021). The purity of the Hb fractions was estimated with sodium dodecyl sulfate-polyacrylamide gel electrophoresis (SDS-PAGE) using densitometric analysis. Throughout the downstream procedures, the Hb concentration was estimated by scanning the spectra and calculating the target protein concentration based on the Hb-CO Soret peak at 419 nm. The purified samples were concentrated to 2 mM using Vivaspin® 20, 30 kDa MWCO (Sartorius) and then snap-frozen in liquid nitrogen and stored at −80°C until further analysis. Before subsequent characterization experiments, heme-based Hb concentrations were confirmed using the pyridine-hemochromogen method (Antonini and Brunori, 1971). Isoelectric focusing was also performed in a Novex® pH 3–10 IEF gel (Invitrogen) with IEF Standards (Bio-Rad), as well as under denaturing conditions in 8 M urea, using Immobiline DryStrip pH 3–10 (7 cm), run in an IPGphor Isoelectric Focusing System (Pharmacia) to verify the presence of two subunits.

2.2 Oxygen binding

Oxygen equilibrium curves were measured for the wt HbF and the HbFα4 mutant using a modified diffusion chamber (Weber, 1992) coupled to a gas mixing system (GMS500, Loligo Systems), as described previously (Jendroszek et al., 2018; Andersen et al., 2021). Briefly, pure oxygen (O_2) and pure nitrogen gas (N_2) were mixed to generate known pO_2 at 37°C. The gas mixtures were used to equilibrate the atmosphere in the diffusion chamber containing the Hb sample. The samples were prepared in a concentration of 0.3 mM heme in 0.1 M HEPES buffer pH 7.4 supplemented with 0.1 M KCl and measured with or without the addition of 0.75 mM DPG (10x tetramer excess). The corresponding absorption change was measured at 415 nm (Hb-O_2 Soret peak) and used to determine the fractional Hb-O_2 saturation induced by changes in pO relative to the endpoints at full oxygenation and full deoxygenation during equilibration with pure O_2 and N_2, respectively. The oxygen affinity (P50) and cooperativity coefficient (n50) was determined from at least four saturation steps within 20%–80% Hb-O_2 saturation range (Jendroszek et al., 2018).

2.3 Autoxidation

The spontaneous autoxidation reaction of ferrous Hb-O_2 (Fe^{2+}) to ferric Hb (Fe^{3+}) was monitored for 60 h at 37°C. The samples were kept at 20 μM heme, in 100 mM phosphate buffer pH 7.4, supplemented with 4.6 U/mL superoxide dismutase, 414 U/mL catalase, and 1 mM EDTA. The spectrum was recorded in a Cary 60 UV–vis spectrophotometer (Agilent Technologies) every 15 min. In the end, the reaction was forced to completion by the addition of 1.5x excess potassium ferricyanide (Sigma-Aldrich) and after incubation with the oxidant, the endpoint spectrum was acquired. The collected spectral series were processed with component analysis in the 450–700 nm range (Singh et al., 2020), and the ferrous decay time course was fitted to a single exponential equation.

2.4 H_2O_2 oxidation

The rate of ferryl Hb (Fe^{4+}) formation was examined by adding increasing concentrations of hydrogen peroxide to ferric Hb (Fe^{3+}). The reaction was initiated by rapid mixing in a stop-flow setup using the RX-2000 Rapid Mixing Stopped-Flow Accessory (Applied Photophysics) coupled to a Cary 60 UV–vis spectrophotometer (Agilent Technologies) as described previously (Ratanasopa et al., 2015). Briefly, 1:1 mixing of 20 μM Hb (heme) in 40 mM phosphate buffer pH 7.2 with increasing concentrations of H_2O_2 in H_2O, resulted in a final reaction concentration of 10 μM Hb (heme) with 100–500 μM H_2O_2 in 20 mM phosphate buffer. The ferric decay was monitored at 405 nm and fitted to a double exponential equation, and the fitted k_{obs} rates were plotted against the H_2O_2 concentration for determination of the second-order rate constant.

2.5 Ferryl reduction

The reverse reaction from the ferryl (Fe^{4+}) to the ferric (Fe^{3+}) state of Hb was studied by adding increasing concentrations of the reducing agent ascorbic acid at 25°C. The ferryl Hb sample was formed by incubating 5 μM ferric Hb in 40 mM phosphate buffer pH 7.2 with 20x H_2O_2 for 5 min and then removing the excess H_2O_2 by adding 12 U of catalase (Sigma-Aldrich) and waiting for 1 min. The reduction reaction was initiated by the addition of ascorbic acid at concentrations ranging from 0–500 μM. The spectral range between 450–700 nm was monitored during the time course for complete ferryl reduction to ferric Hb. The ferryl state of Hb is not stable and the protein will autoreduce to the ferric state spontaneously. The spontaneous reduction of the ferryl state was followed overnight and the obtained autoreduction rate was deducted from the time courses acquired with ascorbic acid. The time courses

TABLE 1 Summary of the redox reaction rates, heme loss, and DNA cleavage of the wt rHbF and the rHbFα4 mutant.

			wt rHbF	rHbFα4
Autoxidation rate (h^{-1})			0.0142 ± 0.0002	0.0154 ± 0.0009
Ferryl formation by H_2O_2 ($\mu M^{-1}s^{-1}$)		k_α	0.6 ± 0.01 10^{-4}	0.5 ± 0.01 10^{-4}
		k_γ	3.2 ± 0.01 10^{-4}	3.1 ± 0.01 10^{-4}
Ferryl reduction α-subunit	(min^{-1})	k_{max}	0.52 ± 0.02	0.63 ± 0.08
	(mM)	K_D	3.8 ± 0.2 10^{-3}	7.9 ± 3.1 10^{-3}
	($mM^{-1}min^{-1}$)	k_{max}/K_D	138 ± 6	80 ± 17
	(min^{-1})	k_{linear}	3.1 ± 0.2 10^{-4}	9.0 ± 2.0 10^{-4}
 γ-subunit	(min^{-1}) (min^{-1})	$k_{autored}$ k_{max}	0.07 ± 0.004 0.98 ± 0.11	0.14 ± 0.005 0.99 ± 0.30
	(μM)	K_D	1.3 ± 0.2	1.5 ± 0.6
	($mM^{-1}min^{-1}$)	k_{max}/K_D	0.73 ± 0.04	0.67 ± 0.08
	(min^{-1})	$k_{autored}$	0.010 ± 0.0015	0.016 ± 0.0022
Ferric reduction (h^{-1})			0.26 ± 0.02	0.21 ± 0.01
Heme loss rate (min^{-1})		k_α	5.3 ± 0.06 10^{-3}	6.1 ± 0.04 10^{-3}
		k_γ	57 ± 2 10^{-3}	60 ± 7 10^{-3}
DNA cleavage rate constant ($\mu M^{-1}h^{-1}$)			15.7 ± 0.5 10^{-3}	3.6 ± 0.02 10^{-3}

(545–630 nm) were fitted to double exponential equations, with the fast phase assigned to the α-subunit and the slow phase to the γ-subunit, as described before (Ratanasopa et al., 2015; Reeder et al., 2008; Cooper et al., 2019). The obtained rates were plotted against the ascorbic acid concentration and fitted with a rectangular hyperbola to find k_{max} and K_D, plus a linear equation for the α-subunit k_{obs}, while a single rectangular hyperbola was used to fit the γ-subunit k_{obs}, as described by Simons et al. (2018).

2.6 Ferric reduction

The oxidized ferric (Fe^{3+}) form can be reduced back to ferrous Hb (Fe^{2+}) with reducing agents. The ferric form was prepared with potassium ferricyanide (Sigma-Aldrich) and buffer exchanged in PD-10 Desalting Column (GE Healthcare) to remove excess oxidant. 10 μM Hb (heme) in 40 mM phosphate buffer pH 7.2 was incubated with 10 mM ascorbate at 25°C. The spectral changes were monitored in the range 450–700 nm for 18 h. The kinetics were resolved with component analysis of the spectral range and the ferric decay was fitted to a single exponential equation to determine the ferric reduction rate.

2.7 Heme loss

Heme loss was monitored by incubating the heme scavenging myoglobin mutant H64Y/V67F (gMb) (Hargrove et al., 1994) with ferric samples of Hb. The reaction of 2.5 μM Hb (heme) with 30 μM gMb was monitored in the spectral range 450–700 nm for 12 h at 25°C in 20 mM phosphate buffer pH 7.2, supplemented with 150 mM sucrose, according to procedures described previously (Kettisen et al., 2018). The kinetic spectral series were resolved with component analysis and the time course was fitted to a double exponential equation to obtain the heme loss rates from the α- and γ-subunits.

2.8 DNA cleavage

The tendency of Hb to cleave DNA was assessed by examining the deterioration of purified pUC18 plasmid in presence of varying concentrations of Hb, according to previously described procedures, with some modifications (Chakane et al., 2017). The experiments were performed in 20 mM phosphate buffer pH 7.2 at 37°C, with a plasmid DNA (pDNA) concentration of 3 ng/μL and Hb concentrations ranging from 0 μM to 300 μM (heme). The incubation was performed in thin-walled PCR tubes in a total volume of 55 μL. Samples were withdrawn every hour for 6 hours, and a final sample at 12 h. 11 μL loading dye was added and mixed immediately before freezing the samples at −20°C. The samples were examined with gel electrophoresis in 1% agarose gels and densitometric analysis was used to quantitate the separated DNA bands. The nicking of the supercoiled pDNA resulted in the formation of the open circular pDNA band, and subsequently the linear pDNA, which in turn also deteriorated during the experiment at the highest Hb concentrations. The relative quantity of the supercoiled DNA band was plotted against time and fitted to a single exponential equation. The obtained rates were plotted against

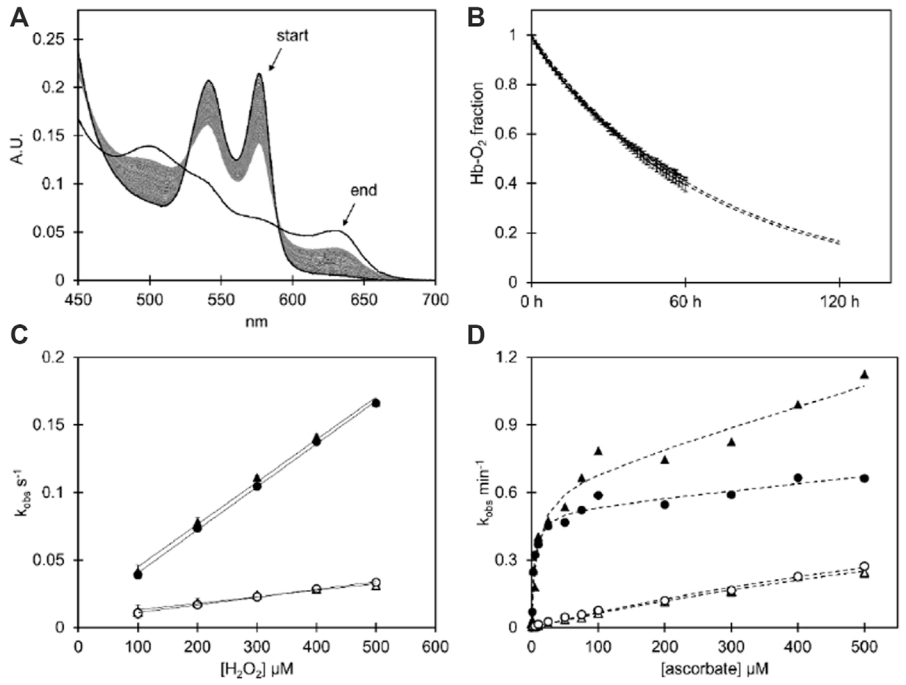

FIGURE 1
(A) Spectral series of the spontaneous autoxidation reaction of the HbFα4 mutant during 60 h at 37°C in 100 mM phosphate buffer pH 7.4 supplemented with 4.6 U/mL superoxide dismutase, 414 U/mL catalase, and 1 mM EDTA using Hb at 20 μM heme. The end spectrum shows the potassium ferricyanide-induced complete ferric state of the same sample. **(B)** The autoxidation decay of ferrous O_2-bound Hb as resolved by component analysis for wt HbF and the HbFα4 mutant. The data is shown with error bars representing the standard deviation (n = 3), and the fitted single exponential decay equation is depicted as dashed lines, which extend beyond 60 h to represent the extrapolated continued reaction. **(C)** The graph shows the k_{obs} plotted against the H_2O_2 concentration of the H_2O_2-induced ferryl formation experiment ($Fe^{3+} \rightarrow Fe^{4+}$), with a linear fitting of the second-order rate constant $\mu M^{-1}s^{-1}$. **(D)** The plot shows the k_{obs} plotted against ascorbate concentration during the induced reduction from the ferryl to the ferric state of Hb ($Fe^{4+} \rightarrow Fe^{3+}$). The data is fitted with a rectangular hyperbola plus a linear equation for the fast phase (α-subunit), and a single hyperbola for the slow phase (γ-subunit). For graphs **(C, D)**, the fast phase k_{obs} are shown with filled symbols and the slow k_{obs} have open symbols. Circles represent wt HbF and triangles represent HbFα4 mutant. For experimental details cf Material and Methods.

Hb concentration and a linear fitting to the data was used to determine the rate constant of the DNA decay.

2.9 Thermal denaturation

The thermal denaturation of Hb was monitored by differential scanning fluorimetry (DSF) in a Prometheus NT.48 instrument (NanoTemper Technologies). Ferrous Hb samples at 3 mg/mL (188 μM heme) in 100 mM phosphate buffer pH 7.4, either bound to O_2-bound or CO, were analyzed in standard grade capillaries (Prometheus NT.48 Series nanoDSF Grade Standard Capillaries). The intrinsic fluorescence intensity ratios between 350 and 330 nm were measured over a temperature ramp from 20°C to 95°C. The data were processed in the PR.therm Control v.2.04 program and the onset and inflection temperatures were determined for each sample.

2.10 Size exclusion chromatography

The Hb samples were analyzed on a Superdex® 75 10/300 GL column (GE Healthcare) in 50 mM sodium phosphate buffer pH 7.2, supplemented with 150 mM NaCl, at a flow rate of 0.5 mL/min. A standard curve containing conalbumin, carbonic anhydrase, ribonuclease, and aprotinin, was used to estimate protein size. Haptoglobin (Bio Products Laboratory) and ferric Hb were mixed in a 1:1 M ratio, incubated at 37°C for 30 min, and applied to the column in a total volume of 100 μL.

2.11 Animal study

The protocols used for the animal study were approved by the Institutional Animal Care and Use Committee at Malmö/Lund, Sweden (Kettisen et al., 2021). Briefly, endotoxin removal procedures were performed by passing the samples sequentially through two high-capacity *Proteus* NoEndo™ spin columns (Vivaproducts), according to the manufacturer's instructions. Female Balbc mice (Janvier, Le Genest-Saint-Isle, France) were supplied with a top addition of Hb, injecting 5 mg of Hb (volume ≤0.2 mL). At five time-points (5 min, 2 h, 6 h, 8 h, and 24 h, n = 5) plasma and urine samples were collected and frozen and stored at −80°C before analysis. Physical data such as weight and body temperature were recorded. With four time-point groups per

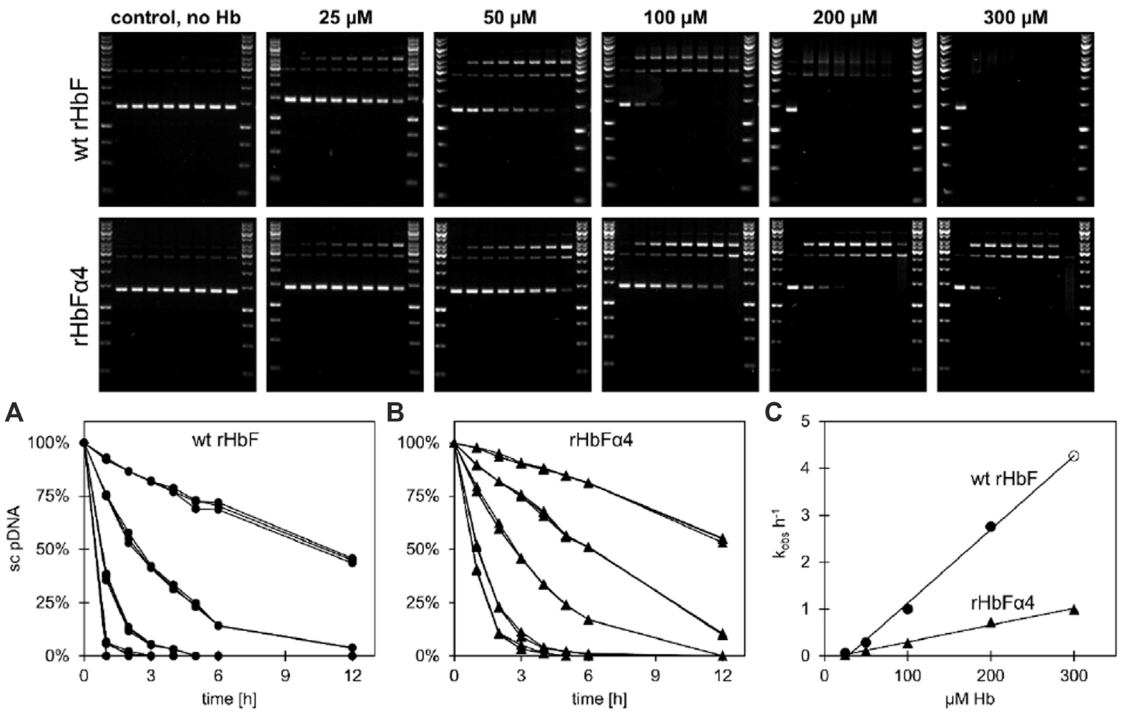

FIGURE 2
Plasmid DNA cleavage of wt HbF and the HbFα4 mutant was monitored for 12 h at 37°C in 20 mM phosphate buffer pH 7.2. Without the addition of Hb, no cleavage of the supercoiled (sc) pDNA was observed. In contrast, when Hb was included, the sc form deteriorated and open circular and linear pDNA bands emerged. By increasing the Hb concentrations from 0 μM to 25, 100, 200 and 300 μM (heme) the process was accelerated. The decay of sc pDNA over time was plotted and fitted to a single exponential equation and the data for wt HbF and HbFα4 mutant can be seen in graphs **(A)** and **(B)**, respectively. Circles represent wt HbF and triangles represent HbFα4 mutant. The obtained rates were then plotted against the Hb concentration and the linear relationship was used to determine the decay constants of pDNA cleavage [graph **(C)**]. The data point for wt HbF at 300 μM (open circle) in graph **(C)** is a product of the linear fitting to the other wt HbF data points, due to the lack of detection of the sc DNA band after 1 h of incubation.

TABLE 2 Thermal denaturation data of wt and mutant HbF as determined by nanoDSF in a Prometheus NT.48 instrument (NanoTemper Technologies).

	wt HbF		HbFα4	
	O_2	CO	O_2	CO
Onset	55.5°C ± 1.5°C	55.4°C ± 2.4°C	53.7°C ± 0.3°C	54.6°C ± 0.7°C
1st peak	62.9°C ± 1.3°C	65.1°C ± 1.3°C	62.6°C ± 0.8°C	62.2°C ± 0.5°C
2nd peak	N/A	76.7°C ± 0.9°C	N/A	75.8°C ± 0.7°C

Hb variant plus non-injected control group (n = 5) for both wildtype and mutant HbF series, a total of 50 mice were used in this study. The samples were frozen and stored at −80°C before pharmacokinetic evaluation.

We used enzyme-linked immunosorbent assay (ELISA) to quantify the HbF levels in the samples. Rabbit anti-HbF affinity-purified polyclonal antibody ("Bonita", Agrisera AB, Sweden), horseradish peroxidase-conjugated sheep anti-HbF polyclonal antibody (Bethyl Labs, TX, United States), and tetramethylbenzidine (TMB single solution, Invitrogen), were used to capture and detect the HbF protein in microtiter plates (NUNC, MaxiSorp, VWR). The absorbance was recorded at 650 nm using a SpectraMax® M2 Microplate Reader (Molecular Devices LLC). A single exponential decay equation was fitted to the data with a least-square fitting using the Solver function in Excel (Microsoft) to determine the half-life in plasma. The mouse albumin levels in the urine samples were quantified with a commercial kit (Mouse Albumin SimpleStep ELISA Kit, Abcam, United Kingdom) to evaluate the effect on kidney filtration function.

2.12 Crystallization of the HbF mutant

Crystallization conditions were screened using a PACT premier™ crystallization screen (Molecular Dimensions) and a Mosquito (TTP Labtech, Melbourn, United Kingdom) crystallization robot for automated droplet formation (Newman et al., 2005). Crystals were grown at 20°C and hits were obtained in several conditions. After 10 days the crystals were harvested and cryoprotected with reservoir solution containing 20% (v/v) glycerol briefly before immersing in liquid nitrogen for cryostorage during transit for X-ray experiments. No measures were taken to prevent autoxidation of the heme and the final Hb crystals were present in the Met form. Diffraction data for rHbFα4 were collected at the MAX IV Laboratory (Lund, Sweden) at the BioMAX beamline (Ursby et al., 2020). The best data set was collected for a large crystal 50 μm × 150 μm × 600 μm) formed in 0.1 M Bis-Tris propane

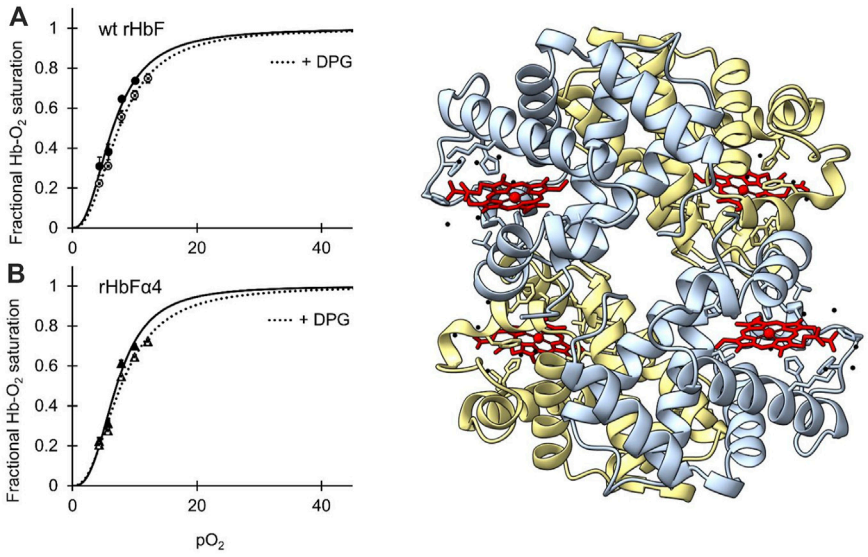

FIGURE 3
[IN COLOR] Oxygen binding curves of wt HbF **(A)** and HbFα4 mutant **(B)** at 37°C, at a Hb concentration of 0.3 mM heme in 0.1 M HEPES buffer pH 7.4 supplemented with 0.1 M KCl. Solid lines represent the oxygen-binding curve without the addition of DPG, while the dotted lines show the oxygen binding with 0.75 mM DPG present. To the right of the graphs, the 3D structure of mutant rHbFα4 obtained by X-ray crystallography is shown (PDB database entry code: 7QU4). The α-subunits are colored light blue and the γ-subunits are light yellow. The heme groups are shown in red while water molecules are colored black. The figure was created in the UCSF ChimeraX molecular visualization program (Goddard et al., 2018).

pH 6.5, 0.2 M sodium fluoride, 20% w/v PEG 3350 (Molecular Dimensions PACT premier screen MD1-29 condition F1) using a protein concentration of 10 mg/mL. The structure was solved by molecular replacement with PDB entries 1FDH (chain G for gamma chain) and 1BZ1 (chain A for alpha chain) as search models using PHASER of the PHENIX suite (Adams et al., 2010). Electron density and difference density maps were manually inspected, and the model was improved using Coot (Emsley et al., 2010) and several rounds of refinement using the Phenix.refine software (Adams et al., 2010). The calculation of R_{free} used 4.89% of the data.

2.13 Data and statistical analysis

All experimental reactions were performed in at least three repeats (n = 3) for each sample unless otherwise stated. The time courses were fitted with the Solver add-in in Microsoft Excel software using least square fitting. Statistical analysis was performed with independent t-tests ($p < 0.05$ was considered statistically significant) and the data are reported as mean ± SD.

3 Results

The recombinant HbF samples of wt rHbF and rHbFα4 were produced by expression in *E. coli* with shake flask cultures and successfully purified in two steps of liquid chromatography as described before (Ratanasopa et al., 2016; Kettisen et al., 2018; Kettisen and Bulow, 2021). The initial capture step was performed with a CaptoS resin (GE Healthcare) or a TREN resin (Bio-Works) for wt rHbF and rHbFα4, respectively. The final polishing step was performed on a Q HP resin for both protein variants. The yields of the final samples were similar to the values reported previously (Kettisen and Bulow, 2021), 30 mg/L and 69 mg/L for wt rHbF and mutant rHbFα4, respectively. Isoelectric focusing were used to determine the effects of the introduced surface charges. The obtained pI values for the mutant was 5.8 for compared to 7.1 for the wt HbF. The isoelectric focusing study clearly verifies that the mutations contribute to lowering the pI of the HbF mutant.

The redox behavior of the two HbF variants was monitored during spontaneous reactions and by examining the consequences of oxidant/reductant agent additions. A summary of the experimental results obtained can be found in Table 1. Overall, the introduction of negative charges appeared to have no or only limited effects on the redox properties. The autoxidation rates did not differ between the rHbFα4 mutant and the wt rHbF (Figures 1A, B). The same was concluded for the ferryl formation rates with H_2O_2, (Figure 1C), as the calculated minor difference in rates was not regarded as significant. The reduction rates from the ferryl and ferric state by ascorbic acid, however, did show some more prominent differences (Figure 1D). The autoreduction rate of the rHbFα4 mutant from the ferryl to the ferric state was doubled in the fast phase, and increased by 60% in the slow phase, compared to wt rHbF (Table 1). This indicated that the mutant more quickly reverted to the ferric state than wt rHbF when no reducing agent was present. However, when ascorbate was added, no significant differences were found in the slow phase of the reaction between the two HbF variants. The slow kinetic phase has previously been assigned to be governed by the γ-subunit (Reeder et al., 2008; Cooper et al., 2019). In contrast, the faster phase governed by the α-subunit showed that the mutant was less efficiently converted to the ferric state compared to wt rHbF, as

TABLE 3 X-ray crystallization data collection and refinement statistics of HbFα4 in the Fe^{3+} state.

Crystal data	
Space group	$C222_1$
Cell parameters (Å/°)	97.45 189.20 66.61/90.0 90.0 90.0
Wavelength (Å)	0.976
Resolution range (Å)	54.463–1.657 (1.685–1.657)[a]
R_{merge}	0.067 (1.337)[a]
No. of observations	989,780 (49,724)[a]
No. of unique observations	72,637 (3,568)[a]
Mean I/σ(I)	21.2 (2.2)[a]
Completeness	98.9 (98.3)[a]
Multiplicity	13.6 (13.9)[a]
CC(1/2)	0.999 (0.774)[a]
Refinement	
Resolution range (Å)	52.946–1.656
R_{work}/R_{free}	0.1821/0.2194
R_{free} test set, reflections (%)	4.89
No. of non H-atoms	5,098
Ligands	4 heme
R.m.s deviation from ideal geometry	
Bonds (Å)	0.008
Angles (°)	0.955
Average B, all atoms (Å^2)	30.6 (range 16.9–69.1)
Ramachandran plot	
Favored regions (%)	99.29
Allowed regions (%)	0.71
Outliers (%)	0.00
MolProbity clash score	1.56

[a]Outer resolution shell.

seen by the k_{max}/K_D value, which was only 60% of wt rHbF (Table 1). However, the low-affinity phase (direct heme reduction of the α-subunit) showed a significantly faster rate for the mutant HbF. The ferric reduction experiment (Fe^{3+} to Fe^{2+}) with ascorbate also showed that the mutant converted back to the ferrous state more slowly than the wt rHbF, further suggesting that the mutant utilized the reducing agent less efficiently. In summary, the oxidation rates towards the oxidized iron states ferric (Fe^{3+}) and ferryl (Fe^{4+}) did not differ between wt rHbF and the mutant. The reduction of the heme iron from both ferryl to ferric, and ferric to ferrous, indicated that the mutant less efficiently utilized the reducing power of ascorbate compared to wt rHbF. The observed differences appeared to be related to the kinetic phases directed by the α-subunit. Although, the mutant did show a faster autoreduction rate from the ferryl to the ferric state in absence of ascorbic acid, as well as a faster slow phase (direct heme reduction) rate in the α-subunit in presence of ascorbate.

The heme release from the ferric state of the HbF variants was monitored with the heme scavenging myoglobin mutant H64Y/V67F. The fast phase governed by the γ-subunit (k_γ) was found not to differ between the samples, while the slow phase (k_α) did show a minor significant difference, with a slightly faster heme release from the mutant compared to wt rHbF (Table 1).

Hb is prone to participate in oxidative side reactions causing modifications of other biomolecules like lipids, proteins, and nucleic acids. Hydrolytic cleavage of DNA caused by oxygen radicals formed by Hb is thus often observed (Chakane et al., 2017). The DNA cleavage activity can be analyzed by monitoring the decay of the supercoiled plasmid DNA in presence of increasing concentrations of Hb (Figure 2). Prominent differences were observed between the two Hb variants. When comparing the two HbF proteins, the rate constant for the mutant HbF was only 23% of the wt rHbF, indicating a much slower DNA degradation for the modified Hb (Figure 2C). This verified that the mutant HbF protein significantly reduced the degradation activity on the DNA backbone in comparison to wt rHbF. At the highest Hb concentration used in this study, 300 μM, the supercoiled DNA band completely disappeared after only 1 h when incubated with the wt rHbF. In contrast, at the same concentration of the mutant, 40% of the supercoiled DNA band remained after 1 h, and the signal could be detected up to 4 h before disappearing.

Thermal denaturation of the HbF proteins was measured using DSF by monitoring the ratio 350/330 nm. This technique measures the changes in fluorescent side-chain exposure of tryptophan and tyrosine during unfolding events. Three temperature ramps were used to assess the structural movements. We found that at slower temperature ramps, unfolding events were difficult to resolve for the wt rHbF due to 350/330 nm ratio measurements resulting in complicated first derivative plots (Supplementary Figure S1). This could be remedied with faster temperature ramps. Overall, we found that the amplitude of the 350/330 nm ratio change was markedly lower for the wt rHbF in comparison to the rHbFα4 samples. Nevertheless, the resolved thermal denaturation events showed no significant differences between the wt rHbF and the rHbFα4 mutant (Table 2). As for the results regarding the different ligand-bound samples, the CO-bound samples had two distinct transition temperatures, while O_2-bound samples only displayed a single well-defined transition temperature. The first transition of the CO-bound samples overlapped with the peak of the O_2-bound samples, and the corresponding scattering curves showed that this transition temperature was accompanied by a significant increase in scattering signal in the O_2-bound samples, probably signifying a tandem collapse of the protein structure and globin precipitation. This increase in scattering did not appear in the CO-bound samples at the first transition temperature but appeared later at the second transition temperature. This implied a delay of the collapse when CO was bound to the protein in comparison to when the Hb was carrying O_2. In the end, when comparing the calculated temperatures for both proteins no significant differences in neither onset nor transition temperatures were seen between the wild type and the mutant HbF samples.

Haptoglobin (Hp) is a plasma protein that captures cell-free Hb with high affinity. It has an important physiological role and by forming a Hp-HbF complex it inhibits toxic oxidative reactions linked to Hb (Alayash et al., 2013). To verify that the negative charges of the mutant HbF did not disrupt this binding reaction, the Hb samples were applied to a size exclusion column, with and without prior incubation with Hp (Supplementary Figure S2). The wt rHbF and the rHbFα4 mutant eluted at the same volumes, both

TABLE 4 Oxygen bidning characteristics of native and mutant HbF.

			wt HbF	HbFα4
P50	(*mm Hg*)	+ DPG	6.5 ± 0.3	7.1 ± 0.1
			7.5 ± 0.2	7.8 ± 0.1
n50		+ DPG	2.4 ± 0.3	2.8 ± 0.1
			2.4 ± 0.2	2.4 ± 0.05

when analyzed in their free forms as well as when complexed to Hp. The incubation with Hp demonstrated that there were no apparent changes to the dimer interface that participates in the binding of Hp for the rHbFα4 mutant.

The toxicity and plasma half-life of the HbF mutant was assessed in a top-load mouse model experiment. All test animals appeared healthy after injection of either wildtype or mutant HbF, and no significant differences in weight or body temperature were found compared to the untreated controls. The plasma samples were examined with sandwich ELISA to assess the Hb concentration in plasma and urine and showed decreasing concentrations throughout the experiment (Supplementary Figure S4). The proteins were relatively quickly removed from circulation and did not remain in the plasma at detectable levels after 24 h. Both proteins showed an identical behavior. To further characterize plasma clearances, Hb levels were also analyzed in urine samples. The Hb concentrations reached a peak after 2 h and then slowly dropped to background levels after 24 h. The calculated half-life was 36 min, indicating a fast clearance of the Hb protein from the plasma. The albumin analysis in the urine samples showed that albumin levels were elevated at 2, 6, and 8 h, while at 24 h the albumin was back to the level of the untreated control. The increased albumin level in urine indicated that the overall glomerular filtration was affected by the Hb proteins during the experiment. However, the albumin level decreased back to non-injected control levels at 24 h, showing that the effect was transient.

To examine if the mutations of rHbFα4 affected the 3D structure of HbF we performed X-ray crystallography experiments to determine the protein structure. The overall structure of the mutant HbF crystal was found to be very similar to the wt rHbF and the mutations did not appear to cause any apparent structural perturbations (Figure 3). The statistics and parameters of the crystallographic data processing are presented in Table 3. The 3D structure of this work also compares well to previously reported HbF PDB structures 1FDH (Frier and Perutz, 1977) and 4MQJ (Soman and Olson, 2013). The structure confirms that the mutation sites are located as expected from the initial design idea, and the negatively charged side-chains are positioned on the protein surface as intended. Figure 4 shows the electrostatic surface and the 3D alignment of the α-subunit of the rHbFα4 structure. A closer inspection of the electron densities of each of the residues in the α-subunit revealed that two residues in close proximities to the mutation sites differed between the wt rHbF and the mutant rHbFα4. The charged side-chains of αD75 (EF4) and αH89 (F10) had altered directions in the HbFα4 crystal structure compared to wt HbF. These residues are not in direct contact with heme nor any redox-active residues. This may indicate that any differences seen related to heme or redox rates would be difficult to pinpoint in this type of rigid crystal structure.

The oxygen binding study showed that the mutations in the rHbFα4 mutant did not affect the oxygen affinity or the cooperativity of the wt HbF protein (Figure 3; Table 4). It was also confirmed that DPG had a little effect on the oxygen binding curves of both the wildtype and the mutant protein, as known for native HbF. This indicated that Hb's main functionality trait as an oxygen carrier was not compromised by the modified design of the α-subunit.

4 Discussion

Insertion of charged residues has become an attractive strategy for decreasing the aggregation properties of proteins. It may involve single residues or can be more substantial and include so-called "supercharged" proteins to prevent tendencies for aggregation (Miklos et al., 2012). In a heterologous system, the possibilities of using this chaperone are limited and the control of globin chain concentrations can be difficult, if not impossible, to fully achieve. The introduction of negative charges on the less soluble α-subunit promotes the formation of the HbF tetramers and this strategy for increasing HbF expression in *E. coli* represents a simple way to enhance production by at least 2-fold (Kettisen and Bulow, 2021). However, to verify the feasibility of this strategy, the mutated protein must be extensively characterized to ensure that the modifications do not disrupt any critical functions of the protein. In this study, we compared the biochemical properties of a negatively charged and high-yielding HbF mutant with the wt HbF protein. Several characteristics were examined including oxygen binding properties, spontaneous and oxidant/reductant-induced redox reactions, heme release in presence of heme-scavenging myoglobin, DNA cleavage activity, thermal denaturation, and plasma clearance in mice in a top-load experiment. To verify that no structural perturbations occurred upon including more negative charges on the protein surface, we also examined the ability to bind to the Hb-scavenger Hp, as well as determined the 3D structure of the mutant HbF. The long-term aim is to use this HbF mutant for oxygen therapeutics applications by entrapping the protein in lipid vesicles (Buehler et al., 2010).

4.1 Redox reactions reveal differences in rates of reduction by the mutant HbF with ascorbate

The reaction rates towards higher oxidation states of the heme iron (Fe^{3+} and Fe^{4+}) did not differ between the wt rHbF and the mutant, but reducing the heme iron back to lower oxidation states with a reducing agent revealed that the mutant reacted in a slightly different way. Ferryl reduction is governed by different kinetic phases–a high and a low-affinity pathway, related to the different pathways of electron transfer, through-protein electron "hopping" and direct heme reduction, respectively (Reeder et al., 2008). Within the range of ascorbate concentrations applied in this study, we found that the kinetic phase governed by the α-subunit appeared to be less effective in utilizing the high-affinity pathway in the mutant, as revealed by the decreased k_{max}/K_D value compared to wt rHbF. As this pathway is assumed to be dependent on tyrosine residues in the vicinity of the heme group to act as an electron conduit, this could be

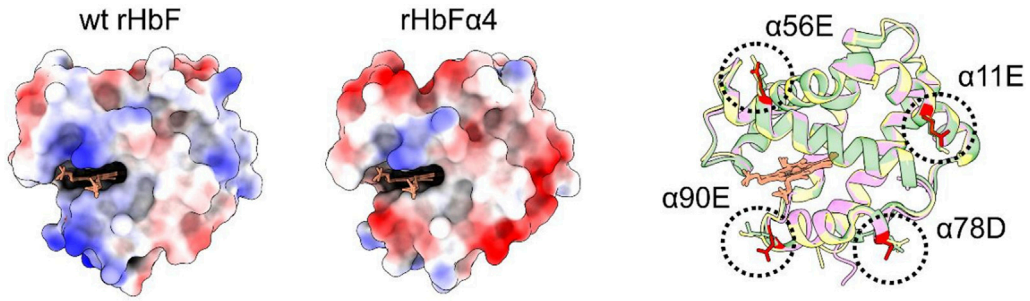

FIGURE 4
[IN COLOR] The α-subunits of the wt and mutant HbF structures are shown with electrostatic surface coloring. Blue color indicates positive charge and red color indicates negative charge. To the right, three different HbF α-subunit structures, one from this work (rHbFα4 purple) and two from the PDB database (1FDH (Soman and Olson, 2013) yellow, 4MQJ (Miklos et al., 2012) green), are three-dimensionally aligned with the peptide backbones shown as ribbons. The mutation sites of the rHbFα4 mutant are colored in red for clarification. All 3D structures of the α-subunit in HbF align and show that the four mutations introduced on the protein in this work do not disrupt the globin fold.

due to some structural change affecting the αY42 residue position originating from the selected mutations. Another difference seen in the ferryl reduction experiment related to the α-subunit was the increased low-affinity pathway reduction rate, which was increased 3-fold. As this pathway is believed to be governed by the direct reduction of the heme by the reductant, it could mean that there is increased access to the heme in the mutant protein. A further indication of possible rearrangement of residues able to affect the heme-related reactions was that the autoreduction of the ferryl state to the ferric state was increased in the mutant. Coupled with the heme loss study indicating a slightly increased heme loss from the α-subunit, small structural changes in the heme pocket vicinity may be considered to be responsible for the observed differences. However, the X-ray crystallographic analysis showed that the 3D structures of wt rHbF and rHbFα4 were almost identical and no apparent changes in the structural configuration of the peptide backbones could be observed. The difference in charge distribution coming from the mutation sites α78 and α90 may have had an impact on the charged residues of αD75 in the EF corner and αH89 at the end of helix F, as the side-chains of these residues appeared to be able to align differently in the rHbFα4 crystal structure. The modification of charge distribution on the Hb surface could very well affect the heme surroundings in a subtle way, which unfortunately appears to be hard to pinpoint from the crystal structure. The environment in which protein crystals are formed could be quite different from the native conditions of a protein, which might affect the exact configuration of the crystallized protein, and especially the more flexible parts. Evidently, from the differences seen in the redox studies in this work, the rHbFα4 appears to have some minor alterations that influence the reactions rates when the heme iron is reduced from a higher oxidation state compared to wt rHbF.

4.2 DNA cleavage activity was greatly reduced with the mutant HbF compared to wild type

Important biomolecules, such as nucleic acids, are often subjected to hydrolytic and oxidative side reactions (Simunkova et al., 2019). The oxidative activities of Hb have been shown to readily cleave supercoiled plasmid DNA (Chakane et al., 2017). In a previous study, we reported that the addition of 1-2 negative charges successfully decreased the DNA cleavage rate of HbF (Kettisen et al., 2021). Here, the cleavage rates of supercoiled plasmid DNA at increasing concentrations of Hb were analyzed and compared. The rate constant was four times faster with the wt rHbF compared to the mutant, which showed that the negatively charged surface-exposed residues on the mutant decidedly contributed to a reduced rate of degradation of the negatively charged backbone of plasmid DNA. This can be an advantage during the expression of the mutant compared to wt rHbF and could be an additional contributing factor to the increased yield seen in *E. coli* with this mutant. The expression plasmids coding for Hb in heterologous hosts may be affected by increasing concentrations of Hb, especially in high-yield fermentation, and decreasing the effect of such harmful reactions should be attractive to ensure efficient production levels. This study shows that the strategy of adding to the negative net charge on the surface of HbF considerably contributed to a slower rate of Hb-induced DNA damage.

4.3 Oxygen binding, thermal denaturation, haptoglobin binding, and plasma half-life are not affected by the mutations in the HbF mutant

Mutations in a multimeric and cooperative protein like Hb may cause an unintended impact on the protein functionality. Four mutations on the α-subunit result in eight positions in total on the complete assembled tetramer and will lead to a substantially changed electrostatic nature. Thermal denaturation profiles of the proteins were determined in a concentrated solution of Hb (188 μM heme) to ensure stable Hb tetramers. We could not observe any significant differences between the wt and the mutant in this work. However, the mutant showed much clearer transitions than wt rHbF. As the instrument measures the general signal of fluorescent residue side-chains, the increased ratio amplitude changes in the mutant HbF might indicate a difference in

exposure of these side chains. However, as discussed previously, the crystal structures solved in this work showed no indication of apparent structural differences, also regarding the aromatic side-chains of Phe, Tyr, and Trp in the mutant. Considering the locations of the mutations, the αD78 residue is close to αY140 and could perhaps influence the location of the C-terminal residues in solution, and the αE56 residue on the E-helix might be able to affect αE23 on the B-helix which is close to αY24. Nevertheless, even though the amplitude of the fluorescence ratio changes might suggest some difference in aromatic side-chain exposure between the HbF variants, the onset and transition temperatures were similar between wt rHbF and the mutant, and thus indicated no difference in overall thermal stability.

In the size-exclusion experiments with or without Hp, it was found that Hp efficiently could capture both the wt rHbF and the mutant. The mutations in the rHbFα4 thus did not affect the dimer interface responsible for Hp binding (Alayash et al., 2013; Ratanasopa et al., 2013). Similarly, the plasma half-life of the mutant HbF was comparable to previously reported values in mouse models (Kettisen et al., 2021; Bobofchak et al., 2003). Without other retention time-extending engineering strategies, for example, cross-linking, polymerization, or genetic fusion of subunits/functional polypeptide tags, the Hb will be removed rapidly from circulation. We previously observed a slightly extended half-life with another mutant of HbF where non-polar alanine residues were substituted for aspartate on the α-subunit (Kettisen et al., 2021). However, the mutant in this work where mainly positive charges were substituted into negative charges, the total number of surface charges were not changed. Although the increased negative charge of the rHbFα4 mutant in this work was hypothesized to possibly influence the interaction with the negatively charged fine mesh that makes up the selective filtration in the glomerular filtration barrier (Bunn et al., 1969; Schlöndorff et al., 2017), it is concluded that this strategy cannot be properly evaluated unless combined with a protein design where the tetrameric form of Hb is ensured. The strategy of switching or adding surface charges may thus still be worthwhile to explore further. The obtained results are promising, but to fully elucidate the influence of charged Hb proteins on the expression in heterologous host systems, redox properties, and *in vivo* physiological behaviors, more studies deserve to be carried out.

Data availability statement

The original contributions presented in the study are included in the article/Supplementary Material, further inquiries can be directed to the corresponding authors.

Ethics statement

The animal study was reviewed and approved by Institutional Animal Care and Use Committee at Malmö/Lund, Sweden.

Author contributions

LB and KK initiated the project. KK designed and performed all the experiments except for the protein crystallography (MN) and the animal handling (ES). KK, MN, AF, and ES analyzed the data. KK wrote the manuscript with contribution from MN and AF and editing by LB. All authors read, commented on, and approved the final manuscript.

Funding

This work was supported by the Swedish Research Council (VR 5607-2014, VR 2019-03996) and the Swedish Foundation for Strategic Research (RBP14-0055). The structural work was generously financed by BioCARE (a Strategic Research Area in Cancer performed at Lund University).

Acknowledgments

The authors would like to thank Dr. John S. Olson for providing the genetic material to enable the production of the heme scavenging myoglobin variant H64Y/V67F and thank Alfia Khairullina for producing and purifying the recombinant myoglobin. We also want to thank Elin Ellebæk Petersen for excellent technical assistance with the oxygen-binding experiment.

Conflict of interest

The authors declare that the research was conducted in the absence of any commercial or financial relationships that could be construed as a potential conflict of interest.

Publisher's note

Supplementary material

The Supplementary Material for this article can be found online at: https://www.frontiersin.org/articles/10.3389/fmolb.2023.1133985/full#supplementary-material

References

Abramov, A., Lehmann, H., and Robb, L. (1980). Hb Shaare Zedek (alpha 56 E5 Lys leads to glu). *FEBS Lett.* 113 (2), 235–237. doi:10.1016/0014-5793(80)80599-0

Adams, P. D., Afonine, P. V., Bunkóczi, G., Chen, V. B., Davis, I. W., Echols, N., et al. (2010). PHENIX: A comprehensive python-based system for macromolecular structure solution. *Acta Cryst. D.* 66 (2), 213–221. doi:10.1107/S0907444909052925

Alayash, A. I., Andersen, C. B. F., Moestrup, S. K., and Bulow, L. (2013). Haptoglobin: The hemoglobin detoxifier in plasma. *TIBTECH* 31 (1), 2–3. doi:10.1016/j.tibtech.2012.10.003

Alayash, A. I. (2014). Blood substitutes: Why haven't we been more successful? *Trends Biotechnol.* 32 (4), 177–185. doi:10.1016/j.tibtech.2014.02.006

Andersen, N. C. M., Fago, A., and Damsgaard, C. (2021). Evolution of hemoglobin function in tropical air-breathing catfishes. *J. Exp. Zool. A* 335 (9-10), 814–819. doi:10.1002/jez.2504

Antonini, E., and Brunori, M. (1971). *Hemoglobin and myoglobin in their reactions with ligands*. Amsterdam: North-Holland Publishing Company.

Ascenzi, P., Bocedi, A., Visca, P., Altruda, F., Tolosano, E., Beringhelli, T., et al. (2005). Hemoglobin and heme scavenging. *IUBMB life* 57 (11), 749–759. doi:10.1080/15216540500380871

Bauer, C., Ludwig, I., and Ludwig, M. (1968). Different effects of 2.3 diphosphoglycerate and adenosine triphosphate on the oxygen affinity of adult and foetal human haemoglobin. *Life Sci.* 7 (23), 1339–1343. doi:10.1016/0024-3205(68)90249-X

Bobofchak, K. M., Mito, T., Texel, S. J., Bellelli, A., Nemoto, M., Traystman, R. J., et al. (2003). A recombinant polymeric hemoglobin with conformational, functional, and physiological characteristics of an *in vivo* O2 transporter. *Am. J. Physiol.* 285, H549–H561. doi:10.1152/ajpheart.00037.2003

Bozza, M. T., and Jeney, V. (2020). Pro-inflammatory actions of heme and other hemoglobin-derived DAMPS. *Front. Immunol.* 11, 1323. doi:10.3389/fimmu.2020.01323

Buehler, P. W., D'Agnillo, F., and Schaer, D. J. (2010). Hemoglobin-based oxygen carriers: From mechanisms of toxicity and clearance to rational drug design. *Trends Mol. Med.* 16 (10), 447–457. doi:10.1016/j.molmed.2010.07.006

Bunn, H. F., and Briehl, R. W. (1970). The interaction of 2,3-diphosphoglycerate with various human hemoglobins. *J. Clin. Invest.* 49 (6), 1088–1095. doi:10.1172/JCI106324

Bunn, H. F., Esham, W. T., and Bull, R. W. (1969). The renal handling of hemoglobin I. Glomerular filtration. *J. Exp. Med.* 129 (5), 909–923. doi:10.1084/jem.129.5.909

Chakane, S., Matos, T., Kettisen, K., and Bulow, L. (2017). Fetal hemoglobin is much less prone to DNA cleavage compared to the adult protein. *Redox Biol.* 12, 114–120. doi:10.1016/j.redox.2017.02.008

Cooper, C. E., Silkstone, G. G., Simons, M., Rajagopal, B., Syrett, N., Shaik, S., et al. (2019). Engineering tyrosine residues into hemoglobin enhances heme reduction, decreases oxidative stress and increases vascular retention of a hemoglobin based blood substitute. *Free Rad. Biol. Med.* 134, 106–118. doi:10.1016/j.freeradbiomed.2018.12.030

Emsley, P., Lohkamp, B., Scott, W. G., and Cowtan, K. (2010). Features and development of Coot. *Acta Cryst. D.* 66 (4), 486–501. doi:10.1107/S0907444910007493

Frier, J. A., and Perutz, M. F. (1977). Structure of human foetal deoxyhaemoglobin. *J. Mol. Biol.* 112 (1), 97–112. doi:10.1016/S0022-2836(77)80158-7

Goddard, T. D., Huang, C. C., Meng, E. C., Pettersen, E. F., Couch, G. S., Morris, J. H., et al. (2018). UCSF ChimeraX: Meeting modern challenges in visualization and analysis. *Protein Sci.* 27 (1), 14–25. doi:10.1002/pro.3235

Graves, P. E., Henderson, D. P., Horstman, M. J., Solomon, B. J., and Olson, J. S. (2008). Enhancing stability and expression of recombinant human hemoglobin in *E. coli*: Progress in the development of a recombinant HBOC source. *Biochim. Biophys. Acta -Proteins Proteomics* 1784 (10), 1471–1479. doi:10.1016/j.bbapap.2008.04.012

Hargrove, M. S., Singleton, E. W., Quillin, M. L., Ortiz, L. A., PhillipsOlson, G. N. J. S., Jr, Mathews, A. J., et al. (1994). His64(E7) → Tyr apomyoglobin as a reagent for measuring rates of hemin dissociation. *J. Biol. Chem.* 269 (6), 4207–4214. doi:10.2210/pdb1mgn/pdb

Hoffman, S. J., Looker, D. L., Roehrich, J. M., Cozart, P. E., Durfee, S. L., Tedesco, J. L., et al. (1990). Expression of fully functional tetrameric human hemoglobin in *Escherichia coli*. *Proc. Natl. Acad. Sci. U.S.A.* 87 (21), 8521–8525. doi:10.1073/pnas.87.21.8521

Jendroszek, A., Malte, H., Overgaard, C. B., Beedholm, K., Natarajan, C., Weber, R. E., et al. (2018). Allosteric mechanisms underlying the adaptive increase in hemoglobin–oxygen affinity of the bar-headed goose. *J. Exp. Biol.* 221 (18), jeb185470. doi:10.1242/jeb.185470

Kettisen, K., and Bulow, L. (2021). Introducing negatively charged residues on the surface of fetal hemoglobin improves yields in *Escherichia coli*. *Front. Bioeng. Biotechnol.* 9 (798), 721794. doi:10.3389/fbioe.2021.721794

Kettisen, K., Strader, M. B., Wood, F., Alayash, A. I., and Bulow, L. (2018). Site-directed mutagenesis of cysteine residues alters oxidative stability of fetal hemoglobin. *Redox Biol.* 19, 218–225. doi:10.1016/j.redox.2018.08.010

Kettisen, K., Dicko, C., Smeds, E., and Bulow, L. (2021). Site-specific introduction of negative charges on the protein surface for improving global functions of recombinant fetal hemoglobin. *Front. Mol. Biosci.* 8, 649007. doi:10.3389/fmolb.2021.649007

MamatWilke, U. K., Bramhill, D., Schromm, A. B., Lindner, B., Kohl, T. A., Corchero, J. L., et al. (2015). Detoxifying *Escherichia coli* for endotoxin-free production of recombinant proteins. *Microb. Cell Fact.* 14, 57. doi:10.1186/s12934-015-0241-5

Miklos, A. E., Kluwe, C., Der, B. S., Pai, S., Sircar, A., Hughes, R. A., et al. (2012). Structure-based design of supercharged, highly thermoresistant antibodies. *Chem. Biol.* 19 (4), 449–455. doi:10.1016/j.chembiol.2012.01.018

Mirceta, S., Signore, A. V., Burns, J. M., Cossins, A. R., Campbell, K. L., and Berenbrink, M. (2013). Evolution of mammalian diving capacity traced by myoglobin net surface charge. *Science* 340 (6138), 1234192. doi:10.1126/science.1234192

Mu, X., Choi, S., Lang, L., Mowray, D., Dokholyan, N. V., Danielsson, J., et al. (2017). Physicochemical code for quinary protein interactions in *Escherichia coli*. *Proc. Natl. Acad. Sci. U.S.A.* 114 (23), E4556–E4563. doi:10.1073/pnas.1621227114

Newman, J., Egan, D., Walter, T. S., Meged, R., Berry, I., Ben Jelloul, M., et al. (2005). Towards rationalization of crystallization screening for small-to medium-sized academic laboratories: The PACT/JCSG+ strategy. *Acta Cryst. D.* 61 (10), 1426–1431. doi:10.1107/S0907444905024984

Olson, J. S. (2020). Lessons learned from 50 years of hemoglobin research: Unstirred and cell-free layers, electrostatics, baseball gloves, and molten globules. *Antioxid. Redox Signal.* 32 (4), 228–246. doi:10.1089/ars.2019.7876

Perutz, M. F. (1974). Mechanism of denaturation of haemoglobin by alkali. *Nature* 247 (5440), 341–344. doi:10.1038/247341a0

Ratanasopa, K., Chakane, S., Ilyas, M., Nantasenamat, C., and Bulow, L. (2013). Trapping of human hemoglobin by haptoglobin: Molecular mechanisms and clinical applications. *Antioxid. Redox Signal* 18 (17), 2364–2374. doi:10.1089/ars.2012.4878

Ratanasopa, K., Strader, M. B., Alayash, A. I., and Bulow, L. (2015). Dissection of the radical reactions linked to fetal hemoglobin reveals enhanced pseudoperoxidase activity. *Front. Physiol.* 6, 39. doi:10.3389/fphys.2015.00039

Ratanasopa, K., Cedervall, T., and Bulow, L. (2016) "Possibilities of using fetal hemoglobin as a platform for producing hemoglobin-based oxygen carriers (HBOCs)," in *Advances in experimental medicine and Biology: Oxygen transport to tissue XXXVII*. Editors T. S. Leung, C. E. Elwell, and D. K. Harrison (New York, NY, London, UK: Springer), 445–453.

Reeder, B. J., Grey, M., Silaghi-Dumitrescu, R.-L., Svistunenko, D. A., Bulow, L., Cooper, C. E., et al. (2008). Tyrosine residues as redox cofactors in human hemoglobin implications for engineering nontoxic blood substitutes. *J. Biol. Chem.* 283 (45), 30780–30787. doi:10.1074/jbc.M804709200

Samuel, P. P., Smith, L. P., Phillips, G. N., Jr, and Olson, J. S. (2015). Apoglobin stability is the major factor governing both cell-free and *in vivo* expression of holomyoglobin. *J. Biol. Chem.* 290 (39), 23479–23495. doi:10.1074/jbc.M115.672204

Schechter, A. N. (2008). Hemoglobin research and the origins of molecular medicine. *Blood* 112 (10), 3927–3938. doi:10.1182/blood-2008-04-078188

Schlöndorff, D., Wyatt, C. M., and Campbell, K. N. (2017). Revisiting the determinants of the glomerular filtration barrier: What goes round must come round. *Kidney Int.* 92 (3), 533–536. doi:10.1016/j.kint.2017.06.003

Shen, T.-J., Ho, N. T., Zou, M., Sun, D. P., Cottam, P. F., Simplaceanu, P. F., et al. (1997). Production of human normal adult and fetal hemoglobins in *Escherichia coli*. *Prot. Eng.* 10 (9), 1085–1097. doi:10.1093/protein/10.9.1085

Simons, M., Gretton, S., Silkstone, G. G. A., Rajagopal, B. S., Allen-Baume, V., Syrett, N., et al. (2018). Comparison of the oxidative reactivity of recombinant fetal and adult human hemoglobin: Implications for the design of hemoglobin-based oxygen carriers. *Biosci. Rep.* 38 (4). doi:10.1042/BSR20180370

Simunkova, M., Lauro, P., Jomova, K., Hudecova, L., Danko, M., Alwasel, S., et al. (2019). Redox-cycling and intercalating properties of novel mixed copper (II) complexes with non-steroidal anti-inflammatory drugs tolfenamic, mefenamic and flufenamic acids and phenanthroline functionality: Structure, SOD-mimetic activity, interaction with albumin, DNA damage study and anticancer activity. *J. Inorg. Biochem.* 194, 97–113. doi:10.1016/j.jinorgbio.2019.02.010

Singh, M., Bharadwaj, K., Dey, E. S., and Dicko, C. (2020). Sonication enhances the stability of MnO2 nanoparticles on silk film template for enzyme mimic application. *Ultrason. Sonochem.* 64, 105011. doi:10.1016/j.ultsonch.2020.105011

Soman, J., and Olson, J. S. (2013). *PDB ID: 4MQJ (structure of wild-type fetal human hemoglobin HbF)*. Houston, TX: Rice University.

Ursby, T., Åhnberg, K., Appio, R., Aurelius, O., Barczyk, A., Bartalesi, A., et al. (2020). BioMAX–the first macromolecular crystallography beamline at MAX IV Laboratory. *J. Syn. Rad.* 27 (5), 1415–1429. doi:10.1107/S1600577520008723

Varnado, C. L., Mollan, T. L., Birukou, I., Smith, B. J. Z., Henderson, D. P., and Olson, J. S. (2013). Development of recombinant hemoglobin-based oxygen carriers. *Antioxid. Redox Signal* 18 (17), 2314–2328. doi:10.1089/ars.2012.4917

Vasseur-Godbillon, C., Hamdane, D., Marden, M. C., and Baudin-Creuza, V. (2006). High-yield expression in *Escherichia coli* of soluble human α-hemoglobin complexed with its molecular chaperone. *Prot. Engin. Des. Sel.* 19 (3), 91–97. doi:10.1093/protein/gzj006

Villarreal, D., Phillips, C., Kelley, A., Villarreal, S., Villaloboz, A., Hernandez, P., et al. (2008). Enhancement of recombinant hemoglobin production in *Escherichia coli* BL21 (DE3) containing the Plesiomonas shigelloides heme transport system. *Appl. Environ. Microbiol.* 74 (18), 5854–5856. doi:10.1128/AEM.01291-08

Weber, R. (1992). Use of ionic and zwitterionic (Tris/BisTris and HEPES) buffers in studies on hemoglobin function. *J. Appl. Physiol.* 72 (4), 1611–1615. doi:10.1152/jappl.1992.72.4.1611

Weickert, M. J., Pagratis, M., Glascock, C. B., and Blackmore, R. (1999). A mutation that improves soluble recombinant hemoglobin accumulation in *Escherichia coli* in heme excess. *Appl. Environ. Microbiol.* 65 (2), 640–647. doi:10.1128/AEM.65.2.640-647.1999

Weiss, M. J., Zhou, S., Feng, L., Gell, D. A., Mackay, J. P., Shi, Y., et al. (2005). Role of alpha hemoglobin-stabilizing protein in normal erythropoiesis and β-thalassemia. *Ann. N. Y. Acad. Sci.* 1054 (1), 103–117. doi:10.1196/annals.1345.013

Wong, S., Ali, M., Pond, J., Rubin, S., Johnson, S., Wilson, J., et al. (1984). Hb J-Singa (alpha-78 Asn leads to Asp), a newly discovered hemoglobin variant with the same amino acid substitution as one of the two present in Hb J-Singapore (alpha-78 Asn leads to, alpha-79 Ala leads to Gly). *Biochim. Biophys. Acta -Protein Struct. Mol. Enzym.* 784 (2-3), 187–188. doi:10.1016/0167-4838(84)90126-2

Yagami, T., Ballard, B. T., Padovan, J. C., Chait, B. T., Popowicz, A. M., and Manning, J. M. (2002). N-terminal contributions of the γ-subunit of fetal hemoglobin to its tetramer strength: Remote effects at subunit contacts. *Protein Sci.* 11 (1), 27–35. doi:10.1110/ps.30602

frontiers | Frontiers in Bioengineering and Biotechnology

TYPE Mini Review
PUBLISHED 14 April 2023
DOI 10.3389/fbioe.2023.1188399

OPEN ACCESS

EDITED BY
Binglan Yu,
Massachusetts General Hospital, Harvard Medical School, United States

REVIEWED BY
Yupeng Wang,
Southern Medical University, China
Hongli Zhu,
Northwest University, China

*CORRESPONDENCE
Thomas Ming Swi Chang,
thomas.chang@mcgill.ca

RECEIVED 17 March 2023
ACCEPTED 06 April 2023
PUBLISHED 14 April 2023

CITATION
Bian Y and Chang TMS (2023), Nanobiotechnological basis of an oxygen carrier with enhanced carbonic anhydrase for CO_2 transport and enhanced catalase and superoxide dismutase for antioxidant function. *Front. Bioeng. Biotechnol.* 11:1188399. doi: 10.3389/fbioe.2023.1188399

Nanobiotechnological basis of an oxygen carrier with enhanced carbonic anhydrase for CO_2 transport and enhanced catalase and superoxide dismutase for antioxidant function

Yuzhu Bian and Thomas Ming Swi Chang*

Artificial Cells and Organs Research Centre, Departments of Physiology, Medicine and Biomedical Engineering, Faculty of Medicine, McGill University, Montreal, QC, Canada

This is a mini review on the biotechnological aspects of the most extensively developed hemoglobin-based oxygen carriers The emphasis is on the most recent Polyhemoglobin-catalase-superoxide dismutase-carbonic anhydrase (PolyHb-CAT-SOD-CA), which is a nanobiotechnological complex that is being investigated and scaled up with the potential for clinical use as nanobiotherapeutics. Hemoglobin, a tetramer, is an excellent oxygen carrier. However, in the body it is converted into toxic dimers. Diacid or glutaraldehyde can crosslink hemoglobin into polyhemoglobin (PolyHb) and prevent its breakdown into toxic dimers. This has been developed and tested in clinical trials. A bovine polyhemoglobin has been approved for routine clinical use for surgical procedures in South Africa and Russia. Clinical trials with human PolyHb in hemorrhagic shock were effective but with a very slight increase in non-fatal myocardial ischemia. This could be due to a number of reasons. For those conditions with ischemia-reperfusion, one would need an oxygen carrier with antioxidant properties. One approach to remedy this is with prepared polyhemoglobin-catalase-superoxide dismutase (PolyHb-CAT-SOD). Another reason is an increase in intracellular pCO_2. We therefore added an enhanced level of carbonic anhydrase to prepare a PolyHb-CAT-SOD-CA. The result is an oxygen carrier with enhanced Carbonic Anhydrase for CO_2 transport and enhanced Catalase and Superoxide Dismutase for antioxidant functions. Detailed efficacy and safety studies have led to the industrial scale up towards clinical trial. In the meantime, oxygen carriers are being investigated around the world for use in *ex vivo* biotechnological fluid for organ preservation for transplantation, with one already approved in France.

KEYWORDS

nanobiotherapeutic and nanobiotechnology, oxygen carriers, antioxidant, catalase, superoxide dismutase, oxygen radicals, carbonic anhydrase carbon dioxide carrier, organ preservation and transplantation

1 Introduction

Hemoglobin, a tetramer, is an excellent oxygen carrier. However, in the body it is converted into toxic dimers (α1β1 and α2β2) and monomers (α1, β1, α2, β2). A number of approaches have been used to prevent this. These include intermolecular crosslinking, intramolecular crosslinking, conjugation, nanoencapsulation, and recombinant methods. These are described elsewhere (Chang et al., 2021; Chang et al., 2007). This mini review concentrates on the most extensively developed approach to nanobiotechnologic intermolecular crosslinking in the form of 1) polyhemoglobin, an oxygen carrier, 2) polyhemoglobin-catalase-superoxide dismutase (PolyHb-CAT-SOD), an oxygen carrier with enhanced antioxidant enzymes, and 3) polyhemoglobin-catalase-superoxide dismutase-carbonic anhydrase (PolyHb-CAT-SOD-CA), an oxygen carrier with enhanced antioxidant enzymes and enhanced CO_2 carrier functions.

2 Polyhemoglobin

Polyhemoglobin: diacid (Chang, 1964) or glutaraldehyde (Chang, 1971) can crosslink hemoglobin into polyhemoglobin (PolyHb) and prevent its breakdown into dimers. There was no initial major interest in this until the HIV-contaminated donor blood crisis in the late 1980s led to urgent development and clinical trials. A bovine polyhemoglobin (Jahr, 2021) has been approved for routine clinical use for surgical procedures in South Africa and Russia. Clinical trials with a human PolyHb in hemorrhagic shock prehospital ambulance patients (Moore et al., 2009) were effective but with a very slight increase in non-fatal myocardial ischemia. This could be due to a number of reasons to be discussed later. PolyHb is only an oxygen carrier and could be used in conditions needing only an oxygen carrier in well-controlled surgical patients (Gould et al., 2002; Jahr, 2021). On the other hand, prehospital ambulance hemorrhagic shock patients could have different degrees of severity and may need more than just an oxygen carrier.

3 Oxygen carrier with antioxidant enzymes

PolyHb could act as an oxygen carrier but fails to deal with the problem of oxidative stress, including ischemia-reperfusion that produces damaging oxygen radicals (D'Agnillo & Chang, 1998). Hypoxanthine accumulates during the ischemia process. When perfused with oxygen again, xanthine oxidase converts hypoxanthine into superoxide resulting in the formation of oxygen radicals that can cause tissue injury. The antioxidant enzymes SOD converts superoxide into hydrogen peroxide which is then converted to H_2O and O_2 by CAT. However, in severe ischemia, even the enzymes' activities contained inside the RBCs are not enough to prevent the tissue from ischemia-reperfusion injuries. For conditions with ischemia-reperfusion one would need an oxygen carrier with enhanced levels of antioxidant properties. One approach is to use prepared polyhemoglobin-catalase-superoxide dismutase (PolyHb-CAT-SOD) (D'Agnillo & Chang, 1998). The results on ischemic reperfusion rat models showed that PolyHb-SOD-CAT could protect the brain against the damage induced by ischemic-reperfusion in hemorrhagic shock with brain ischemia (Powanda & Chang, 2002). This result and the repeated warning (Alayash, 2005) of the need for antioxidants in oxygen carriers have led many groups to work on oxygen carriers with antioxidant properties (for example, Ma & Hsia, 2013).

4 Oxygen carriers with enhanced carbonic anhydrase for CO_2 transport and catalase and superoxide dismutase as antioxidants

4.1 General

Clinical trials with human PolyHb in hemorrhagic shock (Moore et al., 2009) were effective but with a very slight increase in non-fatal myocardial ischemia. This could be due to a number of reasons, one of which is an increased intracelluar pCO_2 (Sims et al., 2001; Tronstad et al., 2010). We therefore added an enhanced level of carbonic anhydrase (CA) to prepare a PolyHb-CAT-SOD-CA. The result is an oxygen carrier with enhanced Carbonic Anhydrase for CO_2 transport and enhanced Catalase and Superoxide Dismutase for antioxidant functions. Our detailed efficacy and safety studies (Chang, 2015; Chang, 2019) have led to the industrial scale up towards clinical trial.

4.2 Details

In addition to the needs for enhanced antioxidant enzymes discussed above, some clinical conditions also require increased transport from the tissues to the lungs for excretion. Examples include severe hemorrhagic shock and severe COVID treated by oxygenator (Chang, 2022). Increased levels of intracellular pCO_2 are associated with myocardial ischemia as well as higher mortality rates in hemorrhagic shock (Tronstad, et al., 2010; Sims, et al., 2001). The enzyme carbonic anhydrase is the enzyme that converts CO_2 into H_2CO_3 for ease of transport to the lung (Geers and Gros, 2000). This accounts for the transport of 75% of intracellular carbon dioxide to the lung. We therefore construct a new generation of nanobiotherapeutics by crosslinking hemoglobin with enhanced amounts of antioxidant enzymes (catalase and superoxide dismutase) and CO_2 transport enzyme (carbonic anhydrase) into PolyHb-SOD-CAT-CA (Figure 1) (Bian & Chang, 2015).

The *in vivo* study was conducted with a severe hemorrhagic shock rat model by removing two-thirds of the whole blood and 60 min of sustained hemorrhagic shock at 30 mm Hg. This was followed by the reinfusion of polymerized stroma-free hemolysate (polySFHb), polySFHb-SOD-CAT-CA, whole blood, lactated Ringer's solution, and polyHb. The results demonstrated that the infusion with 3 volumes of lactated Ringer's solution only increased the blood pressure transiently and it then fell to 43.3 mmHg ± 2.8 mmHg. Blood (Hb 15 g/dL) maintained the MAP at 91.3 mmHg ± 3.6 mmHg while Poly-Hb-SOD-CAT-CA (Hb 10 g/dL) did so at 87.5 mmHg ± 5 mmHg, Poly-Hb-SOD-CAT at 86.0 mmHg ± 4.6 mmHg, PolySFHb at 85.0 mmHg ± 2.5 mmHg, and PolyHb at 82.6 mmHg ± 3.5 mmHg. There were no significant

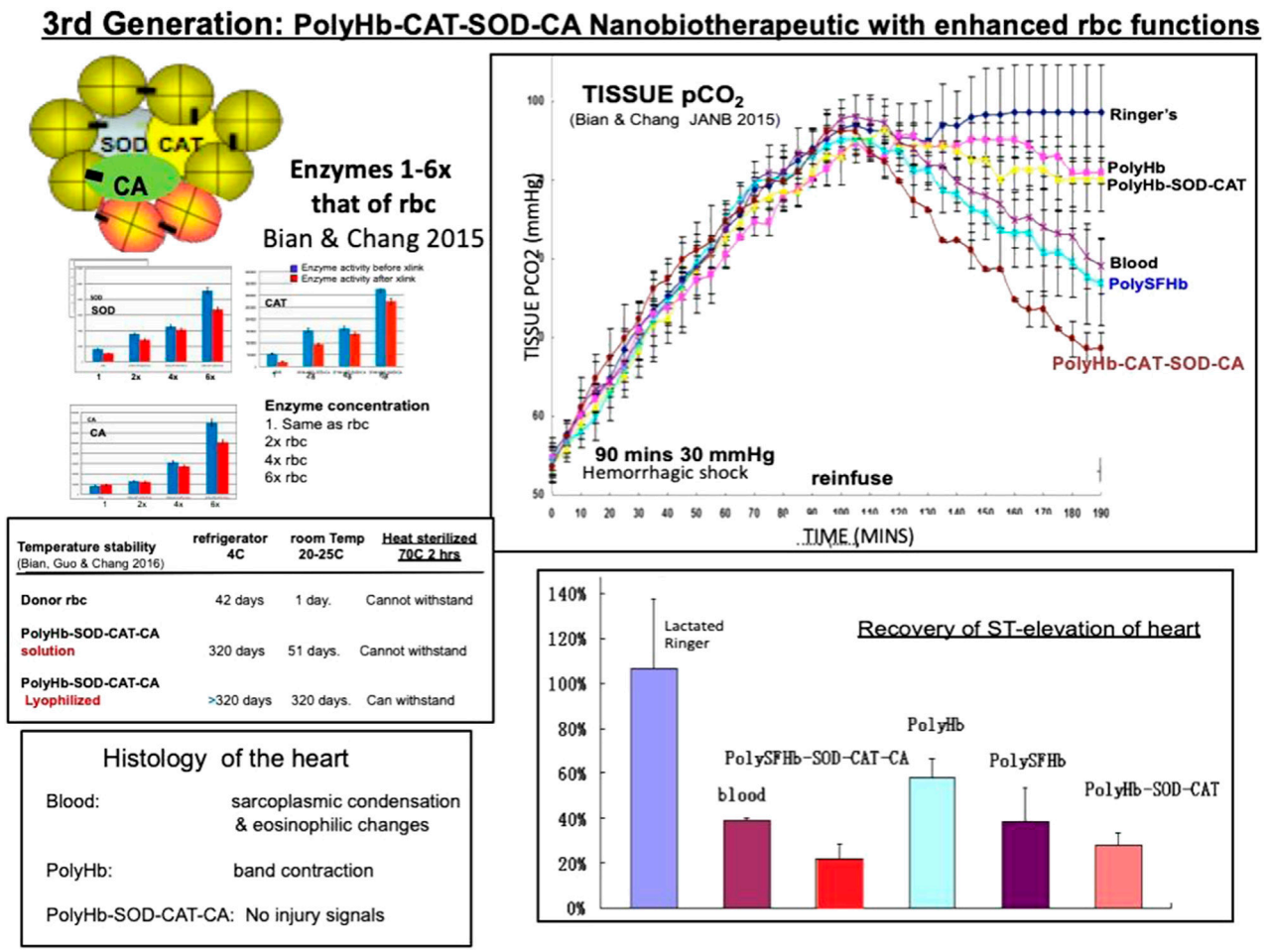

FIGURE 1
Left: PolyHb-CAT-SOD-CA with up to 6x enzyme enhancement and enzyme stability. Upper right: In a 90 min hemorrhagic shock animal model with 2/3 blood volume loss, it is superior to PolyHb and whole blood in the lowering of elevated intracellular pCO_2. Lower right: recovery of ST elevation. Lower left: histology of the heart (From Chang 2022 with written copyright permission to reproduce this figure from the publisher Taylor and Frances.).

differences in the MAP between the HBOCs groups and the whole blood group, suggesting that all the HBOCs could maintain the MAP effectively. However, these results did not show the details of intracellular pCO_2, recovery of heart ischemia, or histology of the heart.

Partial pressure of CO_2 (pCO_2) was measured upon applying the different resuscitation fluids. PolySFHb-SOD-CAT-CA was able to reduce tissue pCO_2 from 98.0 mmHg ± 4.5 mmHg to 68.6 mmHg ± 3.0 mmHg. It was significantly more effective than lactated Ringer's solution (ii, 98.0 mmHg ± 4.5 mmHg), blood (iii, 79.1 mmHg ± 4.7 mmHg), polyHb (iv, 90.1 mmHg ± 4.0 mmHg), polySFHb (v, 77.0 mmHg ± 5.0 mmHg), and polyHb-SOD-CAT (vi, 90.9 mmHg ± 1.4 mmHg) (Figure 1). ST elevation can be related to heart ischemia. The result of the recovery of ST elevation and the histology of the heart also shows that polyHb-SOD-CAT-CA is significantly better than blood and the other fluids in helping the cardiac tissues to recover from ischemia. (Figure 1) (Bian & Chang, 2015).

In vitro stability studies on polyHb-SOD-CAT-CA show that all three enzymes are stable even after 1 year of storage at 4°C or −80°C. Lyophilization makes the enzymes even more stable than the solution samples. After 1 year of storage, the freeze-dried PolyHb-SOD-CAT-CA still contain much of the original enzyme activities (Figure 1) (Bian & Chang, 2016).

The long-term safety and immunology studies of PolyHb-SOD-CAT-CA in rats (Guo & Chang, 2018) shows that the complex did not cause safety or immunological problems after 4 weekly 5% blood volume infusion followed by 30% volume exchange transfusion. Based on its efficacy and safety studies, the industrialization of PolyHb-SOD-CAT-CA is ongoing.

5 Discussions

5.1 General

We have reviewed the present status of 1) PolyHb, 2) PolyHb-SOD-CAT, and 3) PolyHb-SOD-CAT-CA. It would appear that each has its own area of use. For instance, PolyHb has been approved for clinical use in South Africa and Russia for surgical uses to avoid

the use of HIV-contaminated donor blood. It is also being used for the *ex vivo* preservation of organs for transplantation. PolyHb-SOD-CAT-CA shows efficacy, stability, and safety in in vitro and *in vivo* studies. The results show a promising nanobiotherapeutic application of the PolyHb-SOD-CAT-CA. The next step includes scaling up while maintaining batch-to-batch consistent quality and functional efficacy. In the meantime, it is an effective *ex vivo* preservation and regeneration method for organs for transplantation.

5.2 *Ex vivo* use for organ and cell preservation

Studies and methods to solve the potential toxicity of many HBOCs are being carried out with promising results. *Ex vivo* uses are also showing promising results in avoiding large volumes of nanobiotherapeutics being introduced into the body. Early research on the *ex vivo* use of PolyHb for preservation and regeneration of isolated small intestine for transplantation (Razack et al., 1997) is being extended with promising results. Recent exciting uses of different types of HBOCs for organ preservation and regeneration for transplantation include the heart, kidney, liver, lung, pancreas, and small bowel (Van Leeuwen et al., 2019; Cao, et al., 2021). HBOCs can be used together with traditional preservation solutions showing very good compatibility. Studies show that HBOCs could extend the preservation time and decrease ischemic and hypoxic damage to isolated organs to some extent. The safety and efficacy using a marine source of oxygen carrier with antioxidant properties for liver and kidney preservation has been demonstrated in recent clinical trials, leading to approval in France (Le Meur et al., 2020). Recently, Sestan's group demonstrated restored circulation and cellular activity hours post-mortem in isolated porcine brains using HBOCs as the resuscitation solution (Vrselja, et al., 2019). In the most recent exiting study published in Nature (Andrijevic, et al., 2022), they applied the OrganEx, an adaptation of the BrainEx extracorporeal pulsatile-perfusion system and cytoprotective perfusate containing HBOCs for porcine whole-body perfusion. Tissue integrity has been preserved and selected molecular and cellular processes have been restored across multiple vital organs after 1 h of warm ischemia. The most recent Polyhemoglobin-catalase-superoxide dismutase-carbonic anhydrase (PolyHb-CAT-SOD-CA) with enhanced enzyme activity could be even more effective in the preservation and regeneration of isolated organs.

Author contributions

This is part of YB's research for her PhD thesis. She carried out the laboratory research including literature search, establishing the methods, and preparing the draft of this manuscript. TS is the supervisor of her PhD and assisted with planning the research and discussing the results and how to solve problems with YB. He also carried out the detailed revision of her draft of this paper.

Funding

The funding of this research came from a grant from the Canadian Blood Agency/Canadian Institute of Health Research to TMSC.

Conflict of interest

The authors declare that the research was conducted in the absence of any commercial or financial relationships that could be construed as a potential conflict of interest.

Publisher's note

References

Alayash, A. I. (2005). Oxygen therapeutics: Can we tame haemoglobin? *Nat. Rev. Drug Discov.* 3, 152–159. doi:10.1038/nrd1307

Andrijevic, D., Vrselja, Z., Lysyy, T., Zhang, S., Skarica, M., Spajic, A., et al. (2022). Cellular recovery after prolonged warm ischaemia of the whole body. *Nature* 608 (7922), 405–412. doi:10.1038/s41586-022-05016-1

Bian, Y., and Chang, T. M. S. (2015). Effects on 90 min shock ischemic rat model of the novel nanobiotechnological complex with enhanced transport for oxygen and carbon dioxide and antioxidant properties: Polyhemoglobin-superoxide dismutase-catalase-carbonic anhydrase. *Artif. Cells Nanomedicine Biotechnol.* 43, 1–9. doi:10.3109/21691401.2014.964554

Bian, Y., and Chang, T. M. S. (2016). Temperature stability of Poly-[hemoglobin-superoxide dismutase-catalase-carbonic anhydrase] in the form of a solution or in the lyophilized form during storage at -80°C, 4°C, 25°C and 37°C or pasteurization at 70 °C. *Artif. Cells Nanomedicine Biotechnol.* 44 (1), 41–47. doi:10.3109/21691401.2015.1110871

Cao, M., Wang, G., Huang, X., Yue, R., Zhao, Y., Pan, L., et al. (2021). Hemoglobin-based oxygen carriers:potential applications in solid organ preservation. *Front. Pharmacol.* 12, 760215. doi:10.3389/fphar.2021.760215

Chang, T. M. S., Bulow, L., Jahr, S., and Yang, C. (2021). A multiauthor book on "Nanobiotheraeutic basis for blood substitutes. World Scientific Publisher/Imperial College 1042 pages. Available at: https://www.worldscientific.com/worldscibooks/10.1142/12054#t=toc.

Chang, T. M. S. (2022). The role of artificial cells in the fight against COVID-19: Deliver vaccine, hemoperfusion removes toxic cytokines, nanobiotherapeutics lower free radicals and pCO_2 and replenish blood supply. *Nanomedicine Biotechnol.* 50 (1), 240–251. doi:10.1080/21691401.2022.2126491

Chang, T. M. S. (2019). Artificial Cell evolves into nanomedicine, biotherapeutics, blood substitutes, drug delivery, enzyme/gene therapy, cancer therapy, cell/stem cell therapy, nanoparticles, liposomes, bioencapsulation, replicating synthetic cells, cell encapsulation/scaffold, biosorbent/immunosorbent haemoperfusion/plasmapheresis, regenerative medicine, encapsulated microbe, nanobiotechnology, nanotechnology. *Artif. Cells Nanomed Biotechnol.* 47 (1), 997–1013. doi:10.1080/21691401.2019.1577885

Chang, T. M. S. (2007). Monograph on "ARTIFICIAL CELLS: Biotechnology, nanotechnology, blood substitutes, regenerative medicine, bioencapsulation, cell/stem cell therapy". World Scientific Publisher/Imperial College Press, 435 pages. Available at: http://www.medicine.mcgill.ca/artcell/2007 ebook artcell web.pdf.

Chang, T. M. S. (1964). Semipermeable microcapsules. *Science* 146 (3643), 524–525. doi:10.1126/science.146.3643.524

Chang, T. M. S. (1971). Stablisation of enzymes by microencapsulation with a concentrated protein solution or by microencapsulation followed by cross-linking with glutaraldehyde. *Biochem. Biophys. Res. Com.* 44, 1531–1536. doi:10.1016/s0006-291x(71)80260-7

Chang, T. M. S. (2005). Therapeutic applications of polymeric artificial cells. *Nat. Rev. Drug Discov.* 4, 221–235. doi:10.1038/nrd1659

D'Agnillo, F., and Chang, T. M. S. (1998). Polyhemoglobin-superoxide dismutase-catalase as a blood substitute with antioxidant properties. *Nat. Biotechnol.* 16 (7), 667–671. doi:10.1038/nbt0798-667

Geers, C., and Gros, G. (2000). Carbon dioxide transport and carbonic anhydrase in blood and muscle. *Physiol. Rev.* 80, 681–715. doi:10.1152/physrev.2000.80.2.681

Gould, S. A., Moore, E. E., Hoyt, D. B., Ness, P. M., Norris, E. J., Carson, J. L., et al. (2002). The life-sustaining capacity of human polymerized hemoglobin when red cells might Be unavailable. *J. Am. Coll. Surg.* 195, 445–452. doi:10.1016/s1072-7515(02)01335-2

Guo, C., and Chang, T. M. S. (2018). Long term safety and immunological effects of a nanobiotherapeutic, bovine poly-[hemoglobin-catalase-superoxide dismutase-carbonic anhydrase], after four weekly 5% blood volume top-loading followed by a challenge of 30% exchange transfusion. *Artif. Cells Nanomed Biotechnol.* 46 (7), 1349–1363. doi:10.1080/21691401.2018.1476375

Jahr, J. S. (2021). "Hemoglobin-glutamer 250 (bovine) [HBOC-201, Hemopure®] clinical use in South Africa and comprehensive review of cardiac outcomes and risk/benefit in PeerReviewed, indexed studies in humans and animal models," in *Nanobiotherapeutic based blood substitutes*. Editors T. M. S. Chang, L. Bulow, J. S. Jahr, H. Sakai, and C. M. Yang (Singapore: World Science Publisher).

Le Meur, Y., Badet, L., Essig, M., Thierry, A., Büchler, M., Drouin, S., et al. (2020). First-in-human use of a marine oxygen carrier (M101) for organ preservation: A safety and proof-of-principle study. *Am. J. Transpl.* 20, 1729–1738. doi:10.1111/ajt.15798

Ma, L., and Hsia, C. J. C. (2013). "Polynitroxylated hemoglobin as a multifunctional therapeutic for critical care and transfusion medicine," in *Selected topics in nanomedicine*. Editor T. M. S. Chang (Singapore: World Science Publisher/Imperial College Press).

Moore, E. E., Moore, F. A., Fabian, T. C., Bernard, A. C., Fulda, G. J., Hoyt, D. B., et al. (2009). Human polymerized hemoglobin for the treatment of hemorrhagic shock when blood is unavailable: The USA multicenter trial. *J. Am. Coll. Surg.* 208, 1–13. doi:10.1016/j.jamcollsurg.2008.09.023

Powanda, D., and Chang, T. M. S. (2002). Cross-linked polyhemoglobin-superoxide dismutase -catalase supplies oxygen without causing blood brain barrier disruption or brain edema in a rat model of transient global brain ischemia-reperfusion. *Artif. Cells, Blood Substitutes, Biotechnol.* 30, 23–37. doi:10.1081/bio-120002725

Razack, S., D'Agnillo, F., and Chang, T. M. S. (1997). Crosslinked hemoglobin-superoxide dismutase-catalase scavenges free radicals in a rat model of intestinal ischemia-reperfusion injury. *Int. J.* 25, 181–192. doi:10.3109/10731199709118909

Sims, C., Seigne, P., Menconi, M., Monarca, J., Barlow, C., Pettit, J., et al. (2001). Skeletal muscle acidosis correlates with the severity of blood volume loss during shock and resuscitation. *J. Trauma Inj. Infect. Crit. Care* 51, 1137–1146. doi:10.1097/00005373-200112000-00020

Tronstad, C., Pischke, S. E., Holhjem, L., Tønnessen, T. I., Martinsen, Ø. G., and Grimnes, S. (2010). Early detection of cardiac ischemia using a conductometric pCO_2 sensor: Real-time drift correction and parameterization. *Physiol. Meas.* 31, 1241–1255. doi:10.1088/0967-3334/31/9/013

Van Leeuwen, O. B., de Vries, Y., Fujiyoshi, M., Nijsten, M. W. N., Ubbink, R., Pelgrim, G. J., et al. (2019). Transplantation of high-risk donor livers after *ex situ* resuscitation and assessment using combined hypo- and normothermic machine perfusion: A prospective clinical trial. *Ann. Surg.* 270 (5), 906–914. doi:10.1097/sla.0000000000003540

Vrselja, Z., Daniele, S. G., Silbereis, J., Talpo, F., Morozov, Y. M., Sousa, A. M. M., et al. (2019). Restoration of brain circulation and cellular functions hours post-mortem. *Nature* 568, 336–343. doi:10.1038/s41586-019-1099-1

frontiers | Frontiers in Oncology

TYPE Brief Research Report
PUBLISHED 03 May 2023
DOI 10.3389/fonc.2023.1129533

OPEN ACCESS

EDITED BY
Thomas Ming Swi Chang,
McGill University, Canada

REVIEWED BY
Pasqualino De Antonellis,
University of Toronto, Canada
Santosh Valvi,
Perth Children's Hospital, Australia

*CORRESPONDENCE
Bohdan J. Soltys
bohdan.soltys@antiradicaltherapeutics.com
Haotian Zhao
hzhao10@nyit.edu

†PRESENT ADDRESS
Katie B. Grausam,
Department of Regenerative Medicine Institute, Cedars Sinai Medical Center, Los Angeles, CA, United States

‡These authors have contributed equally to this work and share first authorship

RECEIVED 03 January 2023
ACCEPTED 04 April 2023
PUBLISHED 03 May 2023

CITATION
Soltys BJ, Grausam KB, Messerli SM, Hsia CJC and Zhao H (2023) Inhibition of metastatic brain cancer in Sonic Hedgehog medulloblastoma using caged nitric oxide albumin nanoparticles.
Front. Oncol. 13:1129533.
doi: 10.3389/fonc.2023.1129533

Inhibition of metastatic brain cancer in Sonic Hedgehog medulloblastoma using caged nitric oxide albumin nanoparticles

Bohdan J. Soltys[1*‡], Katie B. Grausam[2†‡], Shanta M. Messerli[2], Carleton J. C. Hsia[1] and Haotian Zhao[2,3,4*]

[1]AntiRadical Therapeutics LLC, Sioux Falls, SD, United States, [2]Cancer Biology and Immunotherapies, Sanford Research, Sioux Falls, SD, United States, [3]Department of Pediatrics, University of South Dakota, Vermillion, SD, United States, [4]Department of Biomedical Sciences, New York Institute of Technology, Old Westbury, NY, United States

Medulloblastoma is a tumor of the cerebellum that metastasizes to the leptomeninges of the central nervous system (CNS), including to forebrain and to spinal cord. The inhibitory effect of polynitroxylated albumin (PNA), a caged nitroxide nanoparticle, on leptomeningeal dissemination and metastatic tumor growth was studied in a Sonic Hedgehog transgenic mouse model. PNA treated mice showed an increased lifespan with a mean survival of 95 days (n = 6, $P<0.05$) compared with 71 days in controls. In primary tumors, proliferation was significantly reduced and differentiation was significantly increased ($P<0.001$) as shown by Ki-67$^+$ and NeuN$^+$ immunohistochemistry, while cells in spinal cord tumors appeared unaffected. Yet, histochemical analysis of metastatic tumor in spinal cord showed that the mean total number of cells in spinal cord was significantly reduced in mice treated with PNA compared to albumin vehicle ($P<0.05$). Examination of various levels of the spinal cord showed that PNA treated mice had significantly reduced metastatic cell density in the thoracic, lumbar and sacral spinal cord levels ($P<0.05$), while cell density in the cervical region was not significantly changed. The mechanism by which PNA may exert these effects on CNS tumors is discussed.

KEYWORDS

Sonic Hedgehog, medulloblastoma, metastasis, leptomeningeal dissemination, hematogenous dissemination, nitroxide, reactive oxygen species, reactive nitrogen species

Abbreviations: PNA, polynitroxylated albumin; MB, medulloblastoma; SHH, Sonic Hedgehog; WNT, Wingless; BBB, blood brain barrier; CSF, cerebrospinal fluid; CTC, circulating tumor cells; CNS, central nervous system; NP, nanoparticle; CNO, caged nitric oxide; ROS, reactive oxygen species; RNS, reactive nitrogen species; SOD, superoxide dismutase; NO, nitric oxide; TME, tumor microenvironment.

Introduction

Cancerous brain tumors such as medulloblastoma (MB) and glioblastoma begin as primary tumors with the brain and metastasize to secondary locations within the central nervous system (CNS) and possibly elsewhere. Owing to the blood brain barrier (BBB), pharmacological treatment of brain tumors is problematic due to lack of drug entry into the CNS (1, 2). Successful therapeutic intervention for malignant tumors could in principle be accomplished at primary tumors, on tumor cells in transit to secondary sites and/or at sites of secondary tumor formation. In the case of solid tumors that originate outside the brain the spread of metastatic tumor cells occurs primarily through the bloodstream (hematogenous dissemination) and in certain cases through the lymphatic system (3). In MB, the most common malignant pediatric brain cancer, primary tumors originate within the cerebellum and hindbrain, and metastasize to leptomeningeal membranes of the forebrain and spinal cord (4–7). Despite treatments, ~30% of patients with MB succumb, while survivors suffer from long-term side-effects due to treatments (4–7). Until recently, it was assumed that metastatic spread in MB occurred only through the cerebrospinal fluid (CSF). There is now evidence that MB may also spread by means of hematogenous dissemination (8, 9). This finding lays open the possibility that metastasis could in principle be inhibited by drugs that act within the vasculature without crossing the BBB.

Nanoparticles (NPs) are at the forefront in the development of anti-cancer treatments (10, 11). First generation NPs are exemplified by Abraxane, which has had broad clinical success and next generation NPs are being developed (11, 12). PolyNitroxylated Albumin (PNA) belongs to a class of caged nitric oxide NPs (CNO-NP) drugs developed by Dr. Carleton Hsia and associates. Another example is PolyNitroxylatedPEGylated Hemoglobin (PNPH). The actions of CNO-NPs is based firstly on the cyclic nitroxide moieties that are covalently linked to the macromolecule comprising the NP. The macromolecules themselves and any further chemical modifications may have ancillary activities. Low-molecular-weight nitroxides by themselves have a long history of studies showing beneficial effects in diverse diseases including cancer (13–15). Cyclic nitroxides can scavenge or dismutate reactive oxygen and reactive nitrogen species (ROS/RNS) which are overproduced in various diseases (16). The effectiveness of low-molecular-weight nitroxides is limited by a large volume of distribution and exchange between intracellular and extracellular spaces, rapid bioreduction and loss of activity, and toxicities. By covalent coupling of nitroxides to a macromolecule, NP-bound nitroxides do not normally cross membranes or enter cells, while the biologic half-life of the nitroxides is extended. The pharmacological action of CNO-NPs is expected to be confined mainly to within the vasculature. Using live animal imaging, PNA as the prototype example of this class of drugs has been directly shown in cancer studies to increase blood flow into peripheral solid tumors *in vivo* within minutes (17, 18). Furthermore, PNA has been shown to significantly increase animal survival and to reduce metastasis when used in combination with standard of care chemotherapeutics in a mouse model of breast cancer, attributable to effects within the vascular compartment (17). To date, both PNA and PNPH have been shown to have pharmacological efficacy in pre-clinical models of a wide variety of major medical conditions (17–38).

We previously developed a Sonic Hedgehog (SHH) MB transgenic murine model in which brain tumors arise spontaneously in the cerebellum at 6 weeks of age and metastasize to the forebrain and to spinal cord (39). SHH belongs to one of four main types of MB as defined by the primary developmental pathway activated: 1) SHH Pathway 2) wingless (WNT) 3) Group 3 4) Group 4 (5, 6, 8, 40). While SHH MB has an intact blood brain barrier (BBB) and apparently normal vasculature, WNT MB has an aberrant vasculature and lacks an intact BBB (40, 41). As a result, WNT MB has been found to be highly drug treatable while SHH MB is not (40, 41). The surprising finding we report is that PNA is highly effective in treating our SHH MB transgenic mouse model.

Methods

Transgenic mice and PNA treatment

Transgenic SHH MB mice (MAP mice) were generated as described previously (39). PNA is produced by the reaction of 4-(2-bromoacetamido)-2,2,6,6-tetramethyl-1-piperidinyloxy (BrAcTPO) (Sigma-Aldrich, St. Louis, MO) and human serum albumin, and manufactured as a 10% solution. PNA (Lot 032597, AntiRadical Therapeutics LLC, Sioux Falls, SD) or 25% USP grade human serum albumin (Baxter, Deerfield, IL) vehicle was injected intraperitoneally three times a week (n = 6 for PNA treatment; n = 3 for vehicle control), starting at six weeks of age. The final dosage in all animals was 10 ml kg-1. This dosing was based on that used previously in breast cancer mouse studies (17) and in other systems. The PNA dose administered was near maximum due to injection volume considerations and the size of mice.

Tissue processing

Animals were sacrificed and perfused at end-point with cold phosphate buffered saline (PBS) followed by cold 4% paraformaldehyde (PFA). Whole brain and spinal column were dissected and fixed in 4% PFA overnight at 4°C and processed for paraffin embedding and sectioning. Tissue sections were deparaffinized with CitriSolv (Decon Labs, King of Prussia, PA) and rehydrated through graded ethanol solutions. For frozen tissues, PFA fixed samples were further equilibrated in 20% sucrose for 24-48 hours at 4°C, embedded in TissueTek-Optimal Cutting Temperature (O.C.T.) compound (Sakura Finetek, Torrance, CA), and stored at -80°C. Frozen tissue blocks were sectioned at 15-20 μm thickness on a cryostat.

Immunohistochemistry

Immunostaining was carried out as described previously (39). Heat-induced epitope retrieval was performed for paraffin-embedded tissue sections using Rodent Decloaker (RD913 L,

Biocare Medical, Concord, CA). Endogenous peroxidase activities were quenched with 3% H_2O_2 for 10 minutes. Tissue sections were treated with 10% normal serum in PBS-0.1% Triton X-100 for 1 hour and incubated with primary antibodies for 1 hour at room temperature. After three washes of 5 minutes each with PBS, biotinylated secondary antibodies were applied for 1 hour at room temperature, after which avidin enzyme complex and substrate/chromogen were used for color development (Vector Laboratories, Burlingame, CA). Stained tissue sections were counterstained with hematoxylin and eosin (H&E). If suboptimal staining occurred due to suboptimal fixation or the staining was uninterpretable, the slides were not included in the analysis and sample size was reduced.

Cell quantitation

For cell proliferation analysis, the number of Ki-67$^+$ cells in 300 tumor cells was assessed from five distinct fields of each sample. For cell differentiation analysis, the number of NeuN$^+$ cells in 300 tumor cells was assessed from five distinct fields of sample. The percentage of Ki-67$^+$ or NeuN$^+$ cells in total tumor cell population was calculated by averaging the number of positively-stained cells per 100 tumor cells of all samples for each treatment.

Tumor cell number and density

To quantify spinal tumors, high magnification images were taken of cross sections at different spinal cord levels. Boxes of 600 μm in perimeter were placed in the tumor region and the number of tumor cells within each box was counted. The area encompassed by tumor mass was calculated to determine total number and density of tumor cells on each section using StereoInvestigator software (MBF Bioscience, Williston, VT). Total tumor cell number and density was determined by averaging results from four representative sections at each spinal cord level for each treated animal. If no tumor cells were found at a certain level, the density was scored as zero to demonstrate the effects of PNA.

Image acquisition

Light microscopic images were obtained using a Nikon SMZ1000 Stereomicroscope or a Nikon Eclipse 90i microscope system (Nikon Instruments, Melville, NY).

Statistics

The technician performing cell scoring and quantitation was blinded to the treatment condition. Other investigators were not blinded during experiments and outcome assessment. Statistical analyses were performed with GraphPad Prism 6.0 (GraphPad Software Inc., La Jolla, CA). All pooled data were expressed as the mean ± standard error of the mean (SEM). Differences between groups were compared using an unpaired two-tailed t test. Results were considered significant at $^*P < 0.05$; $^{**}P < 0.01$; $^{***}P < 0.001$; $^{****}P < 0.0001$. The significance of intergroup differences in the incidence of primary tumor, leptomeningeal disease, and metastasis was assessed using Fisher's exact test.

Animal welfare

Animals were housed in the AAALAC-accredited Laboratory Animal Research Facility at Sanford Research in accordance with NIH guidelines. All animal experimental procedures were approved by Sanford Research Institutional Animal Care and Use Committee (IACUC) and performed following national regulatory standards.

Results

Leptomeningeal dissemination and brain metastasis

SHH MB mice used in this study were generated as previously reported and are referred to as MAP mice (39). MAP mice were treated with PNA or albumin vehicle starting at six weeks of age, a time point at which primary tumors in cerebellum are present and small clumps of tumor cells are present in CSF, indicative of leptomeningeal disease (39). Animals received 3 treatments per week until endpoint (end of life). At endpoint, all vehicle control mice showed leptomeningeal dissemination and metastasis to both the forebrain and to spinal cord. In PNA treated mice only 1 of 6 mice exhibited leptomeningeal dissemination and metastasis to the forebrain and 4 of 6 exhibited metastasis to the spinal cord (Table 1, $P<0.05$). Thus, PNA prevented metastasis to the forebrain in ~83% of animals and prevented metastasis to the spinal cord in ~33% of animals.

Survival analysis

Kaplan-Meier survival analysis (Figure 1) showed MAP mice treated with albumin vehicle had a mean survival of 71 days (n = 3) while PNA treated MAP mice had a mean survival of 95 days (n = 6, $P < 0.05$, Figure 1). Thus, PNA increased lifespan by ~28%.

Cell proliferation and differentiation

Cell proliferation and differentiation in primary and secondary tumors were evaluated using quantitative Ki-67$^+$ and NeuN$^+$ immunohistochemistry (Figure 2) in animals at end point. Ki-67$^+$ and NeuN$^+$ are used as markers for mitotic cells and postmitotic cells, respectively (39). Ki-67$^+$ expression was significantly reduced by PNA in primary brain tumors (Figure 2B, $^{**}P<0.01$) but not in spinal cord tumors (Figure 2C). NeuN$^+$ expression as a measure of differentiation increased in primary tumors but was not significantly changed in secondary tumors (Figures 2B, C). Thus,

TABLE 1 PNA treatment and incidence of primary tumors in cerebellum, leptomeningeal disease (LMD), brain metastasis to forebrain and spinal cord metastasis.

Treatment	Tumor (#)incidence	LMD (#)incidence	Brain Met (#)incidence	S.C. Met (#)incidence	Average Age (days)
Polynitroxyl Albumin	100%(6/6)	17%(1/6)*	17%(1/6)*	67% (4/6)	95
Albumin Vehicle	100%(3/3)	100%(3/3)	100%(3/3)	100%(3/3)	71

p values were calculated using Fisher's Exact Test between treatment groups (*$P \leq 0.05$).

PNA treatment significantly affected cell proliferation and differentiation only in primary tumors.

Spinal cord tumor burden and cell density

The effects of PNA on tumor burden and cell densities in spinal cord was evaluated in animals at endpoint using H&E staining (Figure 3A). Tumor burden (mean total number of cells) for the entire spinal cord was significantly reduced in mice treated with PNA compared to albumin vehicle (Figure 3B, $P<0.05$). The density of cells (number of cells/μm2) in tumors at four levels of the spinal cord was quantified (Figure 3C). MAP mice treated with PNA were found to have significantly reduced metastatic cell density in the thoracic, lumbar and sacral regions ($P<0.05$), while cell density in the cervical region did not show significant change.

Discussion

Treatment of MAP mice with PNA completely prevented secondary tumor formation in the forebrain in 5/6 (83%) of animals and prevented secondary tumor formation in the spinal cord in 2/6 (33%) of animals, while all untreated animals had both. Concomitantly, lifespan was prolonged by nearly 30%. These effects are especially striking as the Sonic Hedgehog MB subtype is known to not be readily amenable to pharmacological intervention owing to an intact BBB (40, 41). The tumor microenvironment in all MB subtypes is also an immunosuppressive environment that prevents the recruitment and activity of endogenous immune cells (42).

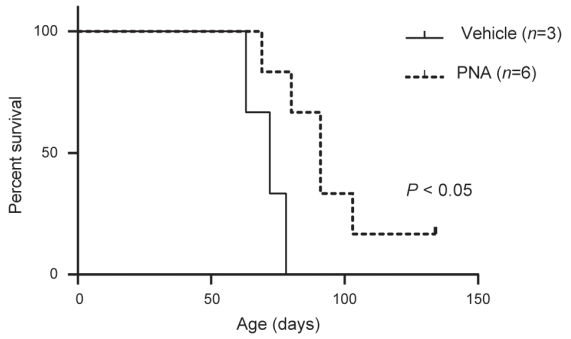

FIGURE 1
Kaplan-Meier curve. PNA treatment increased the survival of MAP mice.

PNA administration was started at 6 weeks of age when primary cerebellar tumors are first seen. However, our transgenic model has enhanced metastasis and small clumps of tumor cells are also already present in the CSF at 6 weeks (39). This protocol mimicked the clinical scenario where treatment is typically initiated only once tumors are present. Had treatment been started earlier, any inhibition of metastasis might result more from reducing tumor burden rather than from an effect on secondary tumor formation, causing false positives. Although the prevention of metastasis was most striking in forebrain brain cortex, due to the near absence of tumor lesions in forebrain we focused on primary and spinal cord tumors in further analyses.

Immunohistochemical analyses showed that PNA significantly reduced the proliferative index and increased differentiation in primary tumors but not in spinal cord tumors. Direct counting of the number of cells in spinal cord tumors, however, showed that the mean total number of cells was significantly reduced in mice treated with PNA. The results suggest that PNA causes a reduction in the ability of cancer cells to establish new tumors at distant sites but the lack of apparent change in proliferation and differentiation in spinal cord is puzzling. This may have been because PNA caused a shift in the balance between proliferation and cell death or PNA affected the tumor environment in a way that did not actually affect differentiation or proliferation.

For spinal cord tumors, we observed a significant decrease in metastatic cell density at the thoracic, lumbar and sacral regions but not in the cervical region. The lack of significant change at the cervical level could be due as one possibility to random variation because the number of mice used was low. Alternatively, there may be differences in the tumor microenvironment at different levels causing tumor cells to respond differently or pharmacokinetic properties may be different in different spinal regions. Different drug levels might result, for example, from differences in local blood flow or differences in the ability to cross the BBB and/or blood-spinal cord barrier.

Blood brain barrier and the pharmacological distribution of PNA

Numerous studies have shown that PNA is a vascular therapeutic in animal models of stroke, traumatic brain injury, sickle cell disease, myocardial infarction, and preventing lung capillary leak (27, 30–35, 37). The sustained therapeutic effects observed in all indications were thought to be derived from responses within the vasculature. In agreement, PNA's demonstrated vascular effects to date have included reversal of

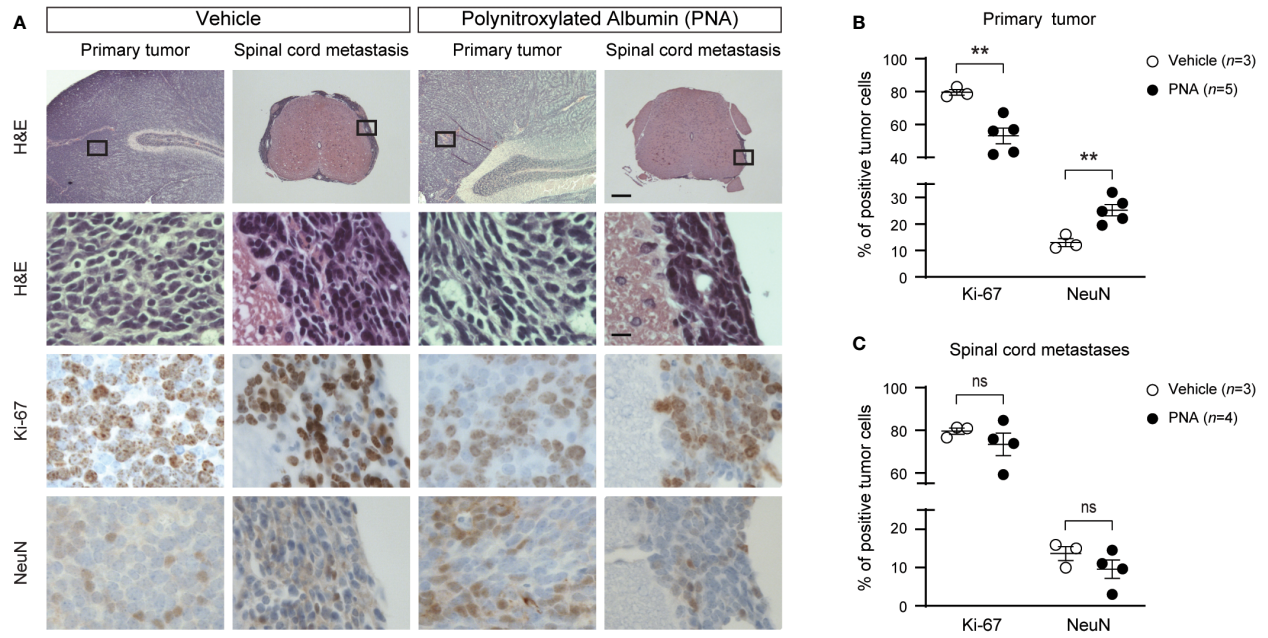

FIGURE 2
Effect of PNA treatment on proliferation and differentiation of tumors in MAP mice. **(A)** Representative results of hematoxylin and eosin (H&E) staining and immunohistochemical staining for Ki-67$^+$ and NeuN$^+$ are shown in primary and spinal metastatic tumor from MAP mice treated with PNA or vehicle. Boxed regions in top panel are magnified in lower panels. Scale bars, 250μm (top panel) and 12.5 μm (lower panels). **(B)** Quantitation of the percentage of Ki-67$^+$ or NeuN$^+$ tumor cells in primary tumor is shown (n = 3 for vehicle, n = 5 for PNA treatment; mean ± s.e.m., two-tailed unpaired t-test, $^{**}P<0.01$). **(C)** Quantitation of the percentage of Ki-67+ or NeuN$^+$ tumor cells in spinal metastatic tumor is shown (n = 3 for vehicle, n = 4 for PNA treatment; mean ± s.e.m., two-tailed unpaired t-test, ns, not significant).

hypoxia, blood flow enhancement, modulation of NO signaling, and alleviation of oxidative and nitrosative stress. It is unclear whether the effects of PNA on metastasis in MB requires crossing the BBB and entry into the CSF. The BBB is intact in SSH MB while in WNT MB it is leaky (40, 41). As a result, WNT MB is considered more treatable compared to SHH MB (40, 41). However, it is possible that highly local geographic variation in BBB leakiness could exist in SHH MB as suggested in glioma (43), despite overall integrity of the barrier in this MB subtype. Although data on the geographic variability of CNS drug penetration is quite sparse, we cannot rule out loss of BBB integrity in the specific vicinity of tumors in our model while the bulk of the BBB remains intact. On the other hand, given recent work by Taylor and colleagues on hematogenous dissemination of MB (9), it is also possible that PNA exerts its anti-tumor effects in MB without crossing the BBB.

Determining PNA's concentration in CSF in treated animals would help in addressing whether PNA is acting within the CSF, yet is made difficult by the small volume of CSF in mice as well as the risk of contamination from blood. The distribution of PNA is thought to be similar to the well-studied distribution of serum albumin (44, 45). The BBB and the blood-spinal cord barrier allow only very low levels of albumin in CSF. In contrast, BBB disruption or leakiness associated with pathological conditions leads to increased albumin levels in CSF (2, 44). Entry of albumin into the CNS normally is an active process involving receptor-mediated internalization into endothelial cells and transcytosis dependent on the albumin-binding protein SPARC (45). SPARC has been found to be over-expressed in glioma and provides a mechanism for albumin-based drug delivery to the CNS (46, 47). The expression of SPARC and its potential role in PNA transport into the CSF in SHH MB will need investigation.

Assuming an intact BBB and lack of enhancement in SPARC-mediated transport, the concentration of albumin in CSF is normally ~3 μM (48), a >200 fold lower concentration than in plasma (~640 μM). In the elderly or in chronic pathological conditions where the BBB is thought to be leaky, the CSF albumin concentration increases only ~2 fold (48, 49). Although CSF albumin levels in brain cancers such as MB and glioblastoma have not been directly measured, mass spectrometry data supports slightly increased albumin levels in glioblastoma (50).

In previous *in vitro* studies on DAOY medulloblastoma (21), U-87 glioblastoma cells (21) and in 4T1 breast cancer cells (17), the effective PNA concentration for inhibiting tumor cell proliferation was 30-120 μM. The amount of PNA administered in this study predicts a PNA concentration of ~49 μM in plasma (an ~8% increase in total serum albumin). If PNA distributes similarly to endogenous albumin and the BBB isn't appreciably leaky, then PNA within the CSF would be ~0.25 μM in our experiments, 100-480 fold lower than the concentrations effective in suppressing tumor cell proliferation (17, 21). Yet, PNA exerted significant effects on MB at primary and metastatic sites in our model. These observations argue that PNA is acting from within the vasculature. PNA's concentration in CSF would have to rise 100-480 fold to be effective. Although significant increases in CSF albumin levels have been seen to occur transiently in trauma situations (51), BBB disruption to the extent needed to reach effective PNA levels

10.3389/fonc.2023.1129533

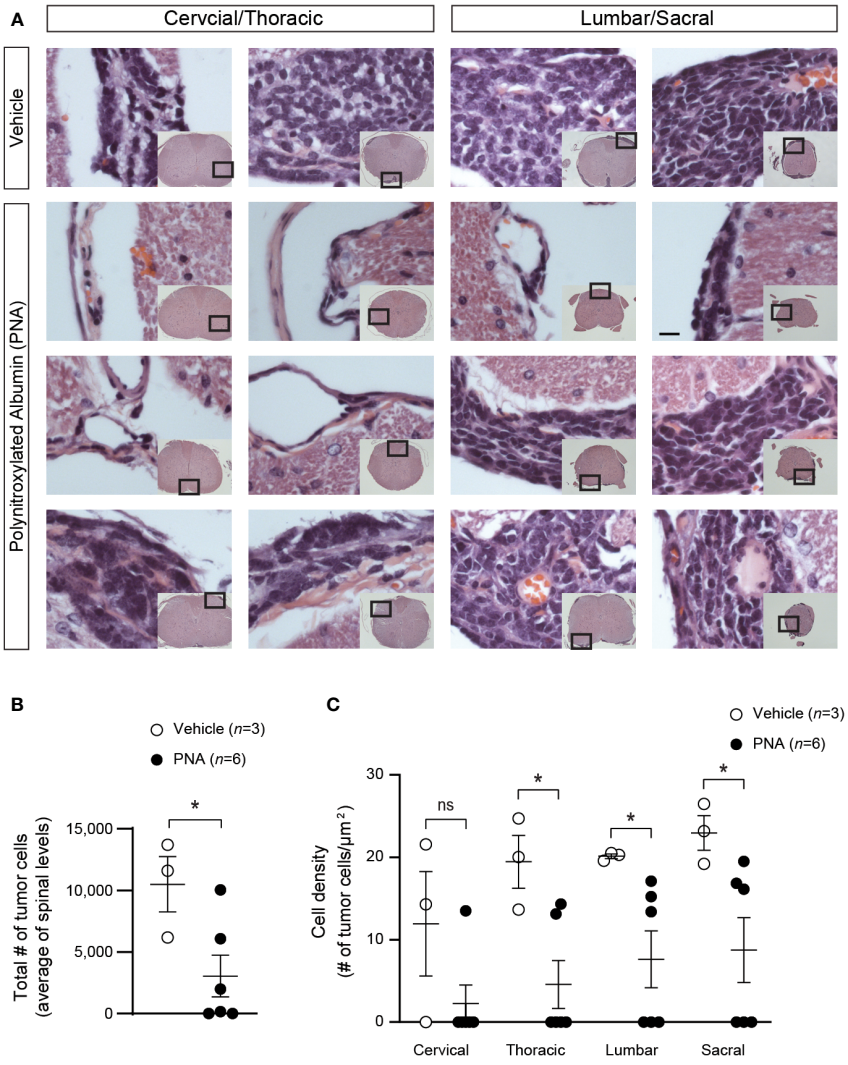

FIGURE 3
Effect of PNA treatment on spinal cord metastasis in MAP mice. **(A)** Representative results of H&E staining are shown in metastatic tumors at different spinal cord regions in MAP mice treated with PNA or vehicle. Boxed regions of the cross sections of the spinal cords in inset pictures are shown in higher magnification. Scale bar, 12.5 μm. **(B)** Quantitation of spinal metastatic tumor cell numbers is shown in MAP mice treated with PNA or vehicle. (n = 3 for vehicle, n = 6 for PNA treatment; mean ± s.e.m., two-tailed unpaired test *P<0.05). **(C)** Quantitation of metastatic tumor cell density is shown at different levels of the spinal cord (n = 3 for vehicle, n = 6 for PNA treatment; mean ± s.e.m., two-tailed unpaired t-test, *P<0.05; ns, not significant).

in CSF would have immediate life-threatening consequences and couldn't be sustained for long. Therefore, our results suggest that tumor suppression from PNA results from PNA's effects within the vasculature.

Mechanistic considerations

The anticancer effects of PNA mainly result from the covalently attached caged nitric oxide groups. While serum albumin on its own has anti-oxidative effects (52), total albumin in plasma (PNA + endogenous albumin) in our experiments increased only by ~8% after administration of PNA or control serum albumin (see above). Low molecular weight cyclic nitroxides are known to be superoxide dismutase (SOD)-mimetics, act as antioxidants by oxidizing cuprous and ferrous ions, and also react directly with a variety of free radicals to detoxify them e.g. lipid peroxidation (16). Numerous studies have shown the efficacy of low molecular nitroxides in animal models (13–15, 53). However, as they easily cross membranes, they are toxic and subject to rapid reduction intracellularly to the inactive hydroxylamine form. Covalent attachment of CNO groups to a macromolecule, as in PNA, addresses these issues by localizing activity extracellularly, prolonging pharmacological effects and preventing toxicity.

Imbalances in antioxidant defenses are one of the hallmarks of cancer (13, 15). There are 3 superoxide dismutases, two of which are intracellular (SOD1 and SOD3) and one is extracellular (SOD3/EcSOD) (15). Low molecular weight cyclic nitroxides on their own can act as SOD mimetics of all three enzymes (13, 15), but when coupled to PNA no longer cross membranes and can only act as an

SOD3 mimetic in the vasculature. Without PNA, nitric oxide (NO) reaction with elevated superoxide in the vasculature leads to depletion of NO levels and production of peroxynitrite. Peroxynitrite is where the oxidative and nitrosative stress pathways merge, and peroxynitrite is the major free radical in the pathogenesis of multiple diseases. Lowering of vascular superoxide with PNA would reduce peoxynitrite production and oxidative/nitrosative stress.

Hypoxia is well known in solid tumors and has been shown in glioblastoma to limit the effectiveness of chemotherapeutics (54). The CSF in MB is a hypoxic environment (55) while a derangement in ROS homeostasis promotes metastasis of SHH MB through stabilization of hypoxia-inducible factor 1α (HIF1α) (56). It has been shown using live animal imaging that PNA can increase blood flow within minutes in peripheral solid tumors (17, 18). Thus, in addition to reducing oxidative/nitrosative stress, the lowering of superoxide and elevation of NO levels with PNA would also increase blood flow to tumors, resulting in decreased hypoxia within tumors.

Anti-hypoxic effects are also seen with low molecular weight cyclic nitroxides that can cross membranes and act intracellularly. TEMPOL is one such example and has been shown to inhibit both hypoxia-inducible factor 1α (HIF-1α) and hypoxia-inducible factor 2 α(HIF-2α) in glioblastoma (54). Compared with PNA, these nitroxides do not show the vascular and therapeutic effects observed with PNA in diverse animal disease models. Nevertheless, comparison of the effects of these two classes of drugs in inhibiting dissemination and metastasis is warranted.

If hematogenous dissemination occurs in our transgenic model, the main candidate locations where PNA may be acting are:

1. The tumor microenvironment (TME) of primary cerebellar tumors.
2. Translocation of circulating tumor cells (CTCs) from CSF into the vasculature.
3. Translocation of CTCs from the vasculature into CSF.
4. The TME of secondary tumors

The TME of brain tumors is comprised of diverse cell types including malignant cells, astrocytes, macrophages/microglia, neurons, pericytes and endothelial cells (57–59). PNA may affect any of these cells as well as the dynamically changing extracellular matrix. The glycocolyx on the luminal site of endothelial cells may also be important owing to the central role of albumin in its properties (60). For peripheral solid tumors, it has been suggested that the vasculature can also adopt a hybrid structure that incorporates primary tumor cells (61), which if operative in MB would make tumor cells directly accessible to PNA from the luminal side of the vasculature.

The CCL2 pathway receptor is known to play an important role in the transit of leukocyte populations ito the CNS (62, 63). Recently, the CCL2 pathway has also been implicated to be involved in the reentry of CTCs into CSF in MB (9). In this respect, PNA might affect the CCL2 pathway in the entry of CTCs into the CSF.

Finally, all MB subtypes are characterized as having an immunosuppressive tumor environment and are considered not amenable to immunotherapy (42). As elevated NO levels after PNA treatment may help to create a favorable tumor environment for endogenous immune cell functions, this mechanism would not require the involvement of hematogenous dissemination of CTCs.

Conclusions

This is the first report to show that PNA, a representative of a new class of drugs referred to as caged nitric oxide nanoparticles, greatly inhibits metastasis in cancer. Inhibition of leptomeningeal dissemination and metastasis in MB is demonstrated. This finding extends a previous study in a triple negative breast cancer murine model where PNA was found to inhibit metastasis only when co-administered with standard of care chemotherapeutics and not if administered on its own (17). PNA is ideally suited for use as a conjunctive agent to be used in conjunction with other types of cancer therapies including chemotherapy, radiotherapy, surgery and immunotherapy. Future study of other MB subtypes, of xenograph models and of other brain cancers is warranted in order to further delineate the relevance of our findings to humans. Modulation of the immunosuppressive environment of tumors by PNA is also an exciting possibility.

Data availability statement

The original contributions presented in the study are included in the article/supplementary material. Further inquiries can be directed to the corresponding authors.

Ethics statement

The animal study was reviewed and approved by Sanford Research Institutional Animal Care and Use Committee (IACUC).

Author contributions

KG, BS, CH, and HZ conceptualized different aspects of the study. KG performed the experiments, analyzed results and prepared figures. BS analyzed data and wrote the manuscript. SM and CH reviewed results and the manuscript. HZ oversaw all research, performed data analysis and approved the final manuscript. All authors contributed to the article and approved the submitted version.

Funding

Research reported here was supported by Health Center of Biomedical Research Excellence CoBRE grants P20 GM103620 and

P20 GM103548 awarded by National Institutes of Health. SM is supported by US Department of the Army W81XWH2110023 (PI: WK Miskimins). HZ is supported by New York Institute of Technology College of Osteopathic Medicine, Matthew Larson Foundation, and NIH/NCI R01 CA220551. The content is solely the responsibility of the authors and does not necessarily represent the official views of the Department of the Army, the Matthew Lawson Foundation or National Institutes of Health.

Acknowledgments

The authors would like to thank Dr. Keith Miskimins at Sanford Research for his mentorship, guidance and support throughout the course of this study. We thank Ross Lanier for technical assistance. We also thank Jan Simoni, William Day, Andrew Lin, Jacek Kwiecien and Stephanie Dowhan-Soltys for comments on the manuscript.

Conflict of interest

AntiRadical Therapeutics LLC (ART) holds commercial rights to the use of PNA. BS and CH are employees of ART. ART did not provide any incentives or financial support for this study and was not involved in the execution of the experiments.

The remaining authors declare that the research was conducted in the absence of any commercial or financial relationships that could be construed as a potential conflict of interest.

Publisher's note

References

1. Arvanitis CD, Ferraro GB, Jain RK. The blood–brain barrier and blood–tumour barrier in brain tumours and metastases. *Nat Rev Cancer* (2020) 20:26–41. doi: 10.1038/s41568-019-0205-x

2. Pardridge WM. Blood-brain barrier and delivery of protein and gene therapeutics to brain. *Front Aging Neurosci* (2020) 11:373. doi: 10.3389/fnagi.2019.00373

3. Melissa C, von der Ohe J, Hass R. Breast carcinoma: from initial tumor cell detachment to settlement at secondary sites. *BioMed Res Int* (2017) 2017:8534371. doi: 10.1155/2017/8534371

4. Fults DW, Taylor MD, Garzia L. Leptomeningeal dissemination: a sinister pattern of medulloblastoma growth. *J Neurosurg Pediatr* (2019) 15:1–9. doi: 10.3171/2018.11.PEDS18506

5. Northcott PA, Robinson GW, Kratz CP, Mabbott DJ, Pomeroy SL, Clifford SC, et al. Medulloblastoma. *Nat Rev Dis Primers.* (2019) 5(1):11. doi: 10.1038/s41572-019-0063-6

6. Juraschka K, Taylor MD. Medulloblastoma in the age of molecular subgroups: a review. *J Neurosurg Pediatr* (2019) 24(4):353–63. doi: 10.3171/2019.5.PEDS18381

7. Ramaswamy V, Taylor MD. Medulloblastoma: from myth to molecular. *J Clin Oncol* (2017) 35(21):2355–63. doi: 10.1200/JCO.2017.72.7842

8. Van Ommeren R, Garzia L, Holgado BL, Ramaswamy V, Taylor MD. The molecular biology of medulloblastoma metastasis. *Brain Pathol* (2020) 30(3):691–702. doi: 10.1111/bpa.12811

9. Garzia L, Kijima N, Morrissy AS, De Antonellis P, Guerreiro-Stucklin A, Holgado BL, et al. A hematogenous route for medulloblastoma leptomeningeal metastases. *Cell* (2018) 172(5):1050–1062.e14. doi: 10.1016/j.cell.2018.01.038

10. Sharma N, Bietar K, Stochaj U. Targeting nanoparticles to malignant tumors. *Biochim Biophys Acta Rev Cancer*. (2022) 1877(3):188703. doi: 10.1016/j.bbcan.2022.188703

11. Jena L, McErlean E, McCarthy H. Delivery across the blood-brain barrier: nanomedicine for glioblastoma multiforme. *Drug Delivery Transl Res* (2020) 10 (2):304–18. doi: 10.1007/s13346-019-00679-2

12. Spada A, Emami J, Tuszynski JA, Lavasanifar A. The uniqueness of albumin as a carrier in nanodrug delivery. *Mol Pharm* (2021) 18(5):1862–94. doi: 10.1021/acs.molpharmaceut.1c00046

13. Lewandowski M, Gwozdzinski K. Nitroxides as antioxidants and anticancer drugs. *Int J Mol Sci* (2017) 18(11):2490. doi: 10.3390/ijms18112490

14. Bonetta R. Potential therapeutic applications of MnSODs and SOD-mimetics. *Chemistry* (2018) 24(20):5032–41. doi: 10.1002/chem.201704561

15. Wilcox CS. Effects of tempol and redox-cycling nitroxides in models of oxidative stress. *Pharmacol Ther* (2010) 126(2):119–45. doi: 10.1016/j.pharmthera.2010.01.003

16. Soule BP, Hyodo F, Matsumoto K, Simone NL, Cook JA, Krishna MC, et al. The chemistry and biology of nitroxide compounds. *Free Radic Biol Med* (2007) 42 (11):1632–50. doi: 10.1016/j.freeradbiomed.2007.02.030

17. Messerli SM, Schaefer AM, Zhuang Y, Soltys BJ, Keime N, Jin J, et al. Use of antimetastatic SOD3-mimetic albumin as a primer in triple negative breast cancer. *J Oncol* (2019) 2019:3253696. doi: 10.1155/2019/3253696

18. Hsia CJC, Miskimins WK. Can macromolecular nitroxide work as extracellular superoxide dismutase mimetic in cancer and stroke therapy? *Cell Biochem Biophys* (2018) 76(4):443–4. doi: 10.1007/s12013-018-0853-6

19. Day WG, Soltys BJ, Cole J, Simoni J, Hsia CJC, Lin AH. Potential value of polynitroxylated PEGylated hemoglobin (SanFlow) in pre-hospital medicine in austere environments including military deployments, disasters and remote emergencies. In: Liu H, Kaye AD, Jahr JS, editors. *Blood substitutes and oxygen biotherapeutics*. Cham: Springer (2022). doi: 10.1007/978-3-030-95975-3_23

20. Seno S, Wang J, Cao S, et al. Resuscitation with macromolecular superoxide dismutase/catalase mimetic polynitroxylated PEGylated hemoglobin offers neuroprotection in guinea pigs after traumatic brain injury combined with hemorrhage shock. *BMC Neurosci* (2020) 21(1):22. doi: 10.1186/s12868-020-00571-7

21. Hsia CJC, Messerli SM, Miskimins WK. Can anti-metastatic albumin-based superoxide dismutase mimetic serve as a "Moonshot" drug for treatment for brain tumors - from medulloblastoma to glioblastoma? *Cell Biochem Biophys* (2019) 77 (2):121–2. doi: 10.1007/s12013-019-00869-2

22. Cao S, Zhang J, Ma L, Hsia CJC, Koehler RC. Transfusion of polynitroxylated pegylated hemoglobin stabilizes pial arterial dilation and decreases infarct volume after transient middle cerebral artery occlusion. *J Am Heart Assoc* (2017) 6(9):e006505. doi: 10.1161/JAHA.117.006505

23. Brockman EC, Jackson TC, Dixon CE, Bayır H, Clark RS, Vagni V, et al. Polynitroxylated pegylated hemoglobin-a novel, small volume therapeutic for traumatic brain injury resuscitation: comparison to whole blood and dose response evaluation. *J Neurotrauma.* (2017) 34(7):1337–50. doi: 10.1089/neu.2016.4656

24. Byrd C, Wallisch J, Jha R, Vagni V, Wisniewski S, Ma L, et al. Polynitroxylated-pegylated hemoglobin as an ultra-small volume resuscitation therapy. *Crit Care Med* (2015) 43(12):3–4. doi: 10.1097/01.ccm.0000473840.00805.63

25. Hsia CJ, Ma L. A hemoglobin-based multifunctional therapeutic: polynitroxylated pegylated hemoglobin. *Artif Organs*. (2012) 36(2):215–20. doi: 10.1111/j.1525-1594.2011.01307.x

26. Brockman EC, Bayır H, Blasiole B, Shein SL, Fink EL, Dixon C, Clark RS, et al. Polynitroxylated-pegylated hemoglobin attenuates fluid requirements and brain edema in combined traumatic brain injury plus hemorrhagic shock in mice. *J Cereb Blood Flow Metab* (2013) 33(9):1457–64. doi: 10.1038/jcbfm.2013.104

27. Manole MD, Kochanek PM, Foley LM, Hitchens TK, Bayır H, Alexander H, et al. Polynitroxyl albumin and albumin therapy after pediatric asphyxial cardiac arrest: effects on cerebral blood flow and neurologic outcome. *J Cereb Blood Flow Metab* (2012) 32(3):560–9. doi: 10.1038/jcbfm.2011.165

28. Shellington DK, Du L, Wu X, Exo J, Vagni V, Ma L, et al. Polynitroxylated pegylated hemoglobin: a novel neuroprotective hemoglobin for acute volume-limited fluid resuscitation after combined traumatic brain injury and hemorrhagic hypotension in mice. *Crit Care Med* (2011) 39(3):494–505. doi: 10.1097/CCM.0b013e318206b1fa

29. Stoyanovsky DA, Kapralov A, Huang Z, Maeda A, Osipov A, Hsia CJ, et al. Unusual peroxidase activity of polynitroxylated pegylated hemoglobin: elimination of H(2)O(2) coupled with intramolecular oxidation of nitroxides. *Biochem Biophys Res Commun* (2010) 399(2):139–43. doi: 10.1016/j.bbrc.2010.07.030

30. Exo JL, Shellington DK, Bayir H, Vagni VA, Janesco-Feldman K, Ma L, et al. Resuscitation of traumatic brain injury and hemorrhagic shock with polynitroxylated albumin, hextend, hypertonic saline, and lactated ringer's: effects on acute hemodynamics, survival, and neuronal death in mice. *J Neurotrauma.* (2009) 26 (12):2403–8. doi: 10.1089/neu.2009.0980

31. Kaul DK, Liu XD, Zhang X, Ma L, Hsia CJ, Nagel RL. Inhibition of sickle red cell adhesion and vasoocclusion in the microcirculation by antioxidants. *Am J Physiol Heart Circ Physiol* (2006) 291(1):H167–75. doi: 10.1152/ajpheart.01096.2005

32. Mahaseth H, Vercellotti GM, Welch TE, Bowlin PR, Sonbol KM, Hsia CJ, Li M, et al. Polynitroxyl albumin inhibits inflammation and vasoocclusion in transgenic sickle mice. *J Lab Clin Med* (2005) 145(4):204–11. doi: 10.1016/j.lab.2005.02.008

33. Li H, Ma L, Hsia CJ, Zweier JL, Kuppusamy P. Polynitroxyl-albumin (PNA) enhances myocardial infarction therapeutic effect of tempol in rat hearts subjected to regional ischemia-reperfusion. *Free Radic Biol Med* (2002) 32(8):712–9. doi: 10.1016/s0891-5849(02)00762-1

34. Sugawara T, Yu F, Ma L, Hsia CJ, Chan PH. Delayed treatment with polynitroxyl albumin reduces infarct size after stroke in rats. *Neuroreport* (2001) 12 (16):3609–12. doi: 10.1097/00001756-200111160-00047

35. Blonder JM, McCalden TA, Hsia CJ, Billings RE. Polynitroxyl albumin plus tempol attenuates liver injury and inflammation after hepatic ischemia and reperfusion. *Life Sci* (2000) 67(26):3231–9. doi: 10.1016/s0024-3205(00)00907-3

36. Saetzler RK, Arfors KE, Tuma RF, Vasthare U, Ma L, Hsia CJ, et al. Polynitroxylated hemoglobin-based oxygen carrier: inhibition of free radical-induced microcirculatory dysfunction. *Free Radic Biol Med* (1999) 27(1-2):1–6. doi: 10.1016/s0891-5849(99)00037-4

37. Beaulieu C, Busch E, Rother J, de Crespigny A, Hsia CJ, Moseley ME. Polynitroxyl albumin reduces infarct size in transient focal cerebral ischemia in the rat: potential mechanisms studied by magnetic resonance imaging. *J Cereb Blood Flow Metab* (1998) 18(9):1022–31. doi: 10.1097/00004647-199809000-00012

38. Wang J, Shi Y, Cao S, Liu X, Martin LJ, Simoni J, et al. Polynitroxylated PEGylated hemoglobin protects pig brain neocortical gray and white matter after traumatic brain injury and hemorrhagic shock. *Front Med Technol* (2023) 5:1074643. doi: 10.3389/fmedt.2023.1074643

39. Grausam KB, Dooyema SDR, Bihannic L, Premathilake H, Morrissy AS, Forget A, et al. ATOH1 promotes leptomeningeal dissemination and metastasis of sonic hedgehog subgroup medulloblastomas. *Cancer Res* (2017) 77(14):3766–77. doi: 10.1158/0008-5472.CAN-16-1836

40. Phoenix TN, Patmore DM, Boop S, Boulos N, Jacus MO, Patel YT, et al. Medulloblastoma genotype dictates blood brain barrier phenotype. *Cancer Cell* (2016) 29(4):508–22. doi: 10.1016/j.ccell.2016.03.002

41. Alvarez JI, Dodelet-Devillers A, Kebir H, Ifergan I, Fabre PJ, Terouz S, et al. The hedgehog pathway promotes blood-brain barrier integrity and CNS immune quiescence. *Science* (2011) 334(6063):1727–31. doi: 10.1126/science.1206936

42. Eisemann T, Wechsler-Reya RJ. Coming in from the cold: overcoming the hostile immune microenvironment of medulloblastoma. *Genes Dev* (2022) 36(9-10):514–32. doi: 10.1101/gad.349538.122

43. Warren KE. Beyond the blood : brain barrier: the importance of central nervous system (CNS) pharmacokinetics for the treatment of CNS tumors, including diffuse intrinsic pontine glioma. *Front Oncol* (2018) 8:239. doi: 10.3389/fonc.2018.00239

44. Nicholson JP, Wolmarans MR, Park GR. The role of albumin in critical illness. *Br J Anaesth.* (2000) 85(4):599–610. doi: 10.1093/bja/85.4.599

45. Merlot AM, Kalinowski DS, Richardson DR. Unraveling the mysteries of serum albumin-more than just a serum protein. *Front Physiol* (2014) 5:299. doi: 10.3389/fphys.2014.00299

46. Guerit S, Liebner S. Blood-brain barrier breakdown determines differential therapeutic outcome in genetically diverse forms of medulloblastoma. *Cancer Cell* (2016) 29(4):427–9. doi: 10.1016/j.ccell.2016.03.024

47. Lin T, Zhao P, Jiang Y, Tang Y, Jin H, Pan Z, et al. Blood-Brain-Barrier-Penetrating albumin nanoparticles for biomimetic drug delivery via albumin-binding protein pathways for antiglioma therapy. *ACS Nano.* (2016) 10(11):9999–10012. doi: 10.1021/acsnano.6b04268

48. Castellazzi M, Morotti A, Tamborino C, Alessi F, Pilotto S, Baldi E, et al. Increased age and male sex are independently associated with higher frequency of blood-cerebrospinal fluid barrier dysfunction using the albumin quotient. *Fluids Barriers CNS.* (2020) 17(1):14. doi: 10.1186/s12987-020-0173-2

49. Seyfert S, Faulstich A, Marx P. What determines the CSF concentrations of albumin and plasma-derived IgG? *J Neurol Sci* (2004) 219(1-2):31–3. doi: 10.1016/j.jns.2003.12.002

50. Schmid D, Warnken U, Latzer P, Hoffmann DC, Roth J, Kutschmann S, et al. Diagnostic biomarkers from proteomic characterization of cerebrospinal fluid in patients with brain malignancies. *J Neurochem* (2021) 158(2):522–38. doi: 10.1111/jnc.15350

51. Blyth BJ, Farhavar A, Gee C, Hawthorn B, He H, Nayak A, et al. Validation of serum markers for blood-brain barrier disruption in traumatic brain injury. *J Neurotrauma.* (2009) 26(9):1497–507. doi: 10.1089/neu.2008.0738

52. Evans TW. Review article: albumin as a drug–biological effects of albumin unrelated to oncotic pressure. *Aliment Pharmacol Ther* (2002) 16(Suppl 5):6–11. doi: 10.1046/j.1365-2036.16.s5.2.x

53. Zarling JA, Brunt VE, Vallerga AK, Li W, Tao A, Zarling DA, et al. Nitroxide pharmaceutical development for age-related degeneration and disease. *Front Genet* (2015) 6:325. doi: 10.3389/fgene.2015.00325

54. Chen WL, Wang CC, Lin YJ, Wu CP, Hsieh CH. Cycling hypoxia induces chemoresistance through the activation of reactive oxygen species-mediated b-cell lymphoma extra-long pathway in glioblastoma multiforme. *J Transl Med* (2015) 13:389. doi: 10.1186/s12967-015-0758-8

55. Lee B, Mahmud I, Pokhrel R, Murad R, Yuan M, Stapleton S, et al. Medulloblastoma cerebrospinal fluid reveals metabolites and lipids indicative of hypoxia and cancer-specific RNAs. *Acta Neuropathol Commun* (2022) 10(1):25. doi: 10.1186/s40478-022-01326-7

56. Eyrich NW, Potts CR, Robinson MH, Maximov V, Kenney AM. Reactive oxygen species signaling promotes hypoxia-inducible factor 1α stabilization in sonic hedgehog-driven cerebellar progenitor cell proliferation. *Mol Cell Biol* (2019) 39(8): e00268–18. doi: 10.1128/MCB.00268-18

57. Bikfalvi A, da Costa CA, Avril T, Barnier JV, Bauchet L, Brisson L, et al. Challenges in glioblastoma research: focus on the tumor microenvironment. *Trends Cancer* (2023) 9(1):9–27. doi: 10.1016/j.trecan.2022.09.005. Epub 2022 Nov 16. Erratum in: Trends Cancer. 2023 Mar 28;: PMID: 36400694.

58. van Bree NFHN, Wilhelm M. The tumor microenvironment of medulloblastoma: an intricate multicellular network with therapeutic potential. *Cancers (Basel).* (2022) 14(20):5009. doi: 10.3390/cancers14205009

59. Faisal SM, Comba A, Varela ML, Argento AE, Brumley E, Abel C2nd, et al. The complex interactions between the cellular and non-cellular components of the brain tumor microenvironmental landscape and their therapeutic implications. *Front Oncol* (2022) 12:1005069. doi: 10.3389/fonc.2022.1005069

60. Aldecoa C, Llau JV, Nuvials X, Artigas A. Role of albumin in the preservation of endothelial glycocalyx integrity and the microcirculation: a review. *Ann Intensive Care* (2020) 10(1):85. doi: 10.1186/s13613-020-00697-1

61. Silvestri VL, Henriet E, Linville RM, Wong AD, Searson PC, Ewald AJ. A tissue-engineered 3D microvessel model reveals the dynamics of mosaic vessel formation in breast cancer. *Cancer Res* (2020) 80(19):4288–301. doi: 10.1158/0008-5472.CAN-19-1564

62. Semple BD, Kossmann T, Morganti-Kossmann MC. Role of chemokines in CNS health and pathology: a focus on the CCL2/CCR2 and CXCL8/CXCR2 networks. *J Cereb Blood Flow Metab* (2010) 30(3):459–73. doi: 10.1038/jcbfm.2009.240

63. Chu HX, Arumugam TV, Gelderblom M, Magnus T, Drummond GR, Sobey CG. Role of CCR2 in inflammatory conditions of the central nervous system. *J Cereb Blood Flow Metab* (2014) 34(9):1425–9. doi: 10.1038/jcbfm.2014.120

frontiers | Frontiers in Medicine

TYPE Original Research
PUBLISHED 13 June 2023
DOI 10.3389/fmed.2023.1158359

OPEN ACCESS

EDITED BY
Thomas Ming Swi Chang,
McGill University, Canada

REVIEWED BY
Thomas Ming Swi Chang,
McGill University, Canada
Hiromi Sakai,
Nara Medical University, Japan
Luciana Magalhães Rebelo Alencar,
Federal University of Maranhão, Brazil

*CORRESPONDENCE
Felice D'Agnillo
✉ felice.dagnillo@fda.hhs.gov

†These authors have contributed equally to this work

RECEIVED 07 February 2023
ACCEPTED 30 May 2023
PUBLISHED 13 June 2023

CITATION
Williams MC, Zhang X, Baek JH and D'Agnillo F (2023) Renal glomerular and tubular responses to glutaraldehyde- polymerized human hemoglobin.
Front. Med. 10:1158359.
doi: 10.3389/fmed.2023.1158359

Renal glomerular and tubular responses to glutaraldehyde-polymerized human hemoglobin

Matthew C. Williams†, Xiaoyuan Zhang†, Jin Hyen Baek and Felice D'Agnillo*

Laboratory of Biochemistry and Vascular Biology, Office of Blood Research and Review, Center for Biologics Evaluation and Research (CBER), U.S. Food and Drug Administration (FDA), Silver Spring, MD, United States

Hemoglobin-based oxygen carriers (HBOCs) are being developed as oxygen and volume replacement therapeutics, however, their molecular and cellular effects on the vasculature and different organ systems are not fully defined. Using a guinea pig transfusion model, we examined the renal glomerular and tubular responses to PolyHeme, a highly characterized glutaraldehyde-polymerized human hemoglobin with low tetrameric hemoglobin content. PolyHeme-infused animals showed no major changes in glomerular histology or loss of specific markers of glomerular podocytes (Wilms tumor 1 protein, podocin, and podocalyxin) or endothelial cells (ETS-related gene and claudin-5) after 4, 24, and 72 h. Relative to sham controls, PolyHeme-infused animals also showed similar expression and subcellular distribution of N-cadherin and E-cadherin, two key epithelial junctional proteins of proximal and distal tubules, respectively. In terms of heme catabolism and iron-handling responses, PolyHeme induced a moderate but transient expression of heme oxygenase-1 in proximal tubular epithelium and tubulointerstitial macrophages that was accompanied by increased iron deposition in tubular epithelium. Contrary to previous findings with other modified or acellular hemoglobins, the present data show that PolyHeme does not disrupt the junctional integrity of the renal glomerulus and tubular epithelium, and triggers moderate activation of heme catabolic and iron sequestration systems likely as part of a renal adaptive response.

KEYWORDS

hemoglobin oxygen therapeutics, heme oxygenase, tubular epithelium, glomerular podocyte, iron handling, endothelium, tubulointerstitial macrophage

Introduction

Chemically modified hemoglobin (Hb)-based oxygen carriers (HBOCs) are being developed as oxygen and volume replacement therapeutics for use as bridging agents when standard red blood cell (RBC) transfusions are not available, incompatible, or refused based on religious grounds (1, 2). HBOCs have also shown promise as oxygen-carrying perfusates in organ preservation settings (3, 4). Most HBOCs are manufactured from expired human or animal blood starting with the extraction and purification of Hb from RBCs, followed by

various protein modification strategies designed to stabilize the acellular Hb in circulation and/or maintain its oxygen transport properties (2, 5, 6). Despite significant progress over many years, unresolved safety issues continue to impede the development and licensure of these therapeutics in the United States. These safety concerns have been driven, in part, by reports of adverse clinical events including transient hypertension, stroke, and myocardial infarction observed with some HBOCs (2, 7–9). Some studies have proposed that the clinical benefits of these products may still outweigh their safety risks, especially in severe anemia settings when RBCs are not an option (10–12). While there are no HBOCs licensed for human use in the United States, a glutaraldehyde-polymerized bovine Hb (Hemopure®, HbO_2 Therapeutics, Souderton, PA, USA) was approved in South Africa for acute anemia settings (13).

Hemoglobin-based oxygen carrier-associated safety concerns have been difficult to resolve, partly because preclinical testing has not always been predictive of clinical safety outcomes for some HBOCs (7, 14). Moreover, there are important limitations related to the extrapolation of safety assessments in normal healthy animals to a heterogenous population of subjects with underlying comorbidities, endothelial dysfunction, and predisposition to various disease states (7, 14–16). This has prompted the search for preclinical approaches that may better predict HBOC safety in humans. Two areas of preclinical testing that have garnered some attention include the selection of relevant animal species and the use of sensitive biomarkers to help detect subtle safety signals (14, 17, 18). Previous studies from our laboratory indicate that the guinea pig may be a relevant small animal species to evaluate the unique pro-oxidative profiles of HBOCs (17, 19–23). This is based on the noted similarities between guinea pigs and humans in terms of their overall plasma and tissue antioxidant capabilities (14). Importantly, both species are unable to produce ascorbic acid (AA) due to an evolutionary loss of L-gluconolactone-oxidase, which is the rate limiting enzyme in AA synthesis. AA plays a key physiological role in limiting Hb oxidation, and thus the *in vivo* status of AA may be important in predicting the oxidation of HBOCs to methemoglobin and the effects of oxidized and/or degraded forms of Hb on tissues.

While the precise mechanisms underlying the reported adverse responses to HBOCs are not completely understood, the interaction of acellular Hb and/or its breakdown products with the vasculature of different organ systems is thought to be an important contributing factor (18, 24, 25). The kidney, for example, is recognized as being particularly susceptible to the adverse effects of high levels of circulating acellular Hb resulting from disease or drug-induced hemolysis, particularly when protective plasma protein defenses (e.g., haptoglobin) are overwhelmed (24, 26). This has been attributed to the glomerular filtration of dimerized Hb molecules, heme, and to a lesser extent native tetrameric Hb that can lead to acute tubular necrosis via oxidative and inflammatory mechanisms (26, 27). Renal failure and nephrotoxicity associated with early generation HBOCs were largely attributed to their high content of unmodified tetrameric Hb (28). Along these lines, we previously reported that chemically modified Hb and oxidized acellular Hb induced renal glomerular barrier dysfunction, downregulated the expression of key glomerular podocyte and endothelial intercellular junctional proteins, generated extensive renal iron deposition and oxidative stress in renal tubular epithelium, and suppressed the expression and activity of renal antioxidant enzymes (19, 21–23). Here, using a guinea pig transfusion model, we examine the renal glomerular and tubular responses to PolyHeme, a highly characterized glutaraldehyde-polymerized human Hb with low tetrameric Hb content. PolyHeme, manufactured by Northfield Laboratories (Evanston, IL, USA), was the subject of extensive clinical investigation but its production was discontinued following unsuccessful attempts to gain licensure in the United States (29, 30). Our study describes the renal responses to this highly characterized HBOC using a histological and immunohistological approach that may have useful implications for the preclinical assessment of other existing or emerging HBOC candidates.

Materials and methods

Polymerized Hb solution

PolyHeme is a chemically modified sterile Hb solution containing a heterogeneous mixture of glutaraldehyde-crosslinked and polymerized pyridoxylated human Hb at a concentration of 10 g/dl in an electrolyte solution. The product has a colloid oncotic pressure (COP) of 20–25 mmHg, a p50 of 26–32 mmHg, methemoglobin content of <5–8%, and an average molecular weight between 130 and 250 kDa with less than 1% tetramers. PolyHeme, originally manufactured by Northfield Laboratories (Evanston, IL, USA), was obtained via a Material Transfer Agreement from HbO_2 Therapeutics (Souderton, PA, USA). Upon receipt, PolyHeme stocks were aliquoted under sterile conditions and stored frozen at −80°C. Prior to use, biochemical characterization experiments were performed to verify the quality and stability of existing PolyHeme stocks, including the assessment of total Hb concentration and oxidation state, aggregation, impurities, COP, and molecular size distribution using SDS-PAGE (5).

Animal surgical preparation and experimental protocol

Male Hartley guinea pigs were purchased from Charles Rivers Laboratories (Wilmington, MA, USA) and acclimated for 1 week upon arrival at the FDA/CBER animal care facility. All animals were fed normal diets during the acclimation period and weighed 900–1,200 g at the time of the study. Animal study protocols were approved by the FDA/CBER Institutional Animal Care and Use Committee with all experimental procedures performed in accordance with the National Institutes of Health Guide for the Care and Use of Laboratory Animals (NIH Publications No. 8023, revised 1978). Surgical preparation and carotid catheter implantation were performed as previously described (17). Twenty-four hours after recovery from surgical catheter implantation, fully conscious and freely moving guinea pigs (n = 18 animals) underwent a 25% exchange transfusion (ET) (50 ml blood volume/kg body weight), replacing whole blood with PolyHeme at a rate of approximately 1 ml/min. Sham control animals underwent the surgical procedure and then recovered for 24 h. All animals

were caged and freely moving up until the indicated necropsy time. To harvest the kidneys, sham control and PolyHeme-infused animals were euthanized by intraperitoneal injection of Euthasol®, femoral veins were cut, and cold saline was perfused via the arterial catheter to remove blood. Kidneys were dissected, cut in half, and fixed in 10% formalin for 24 h.

Hb oxidation analysis

Spectral analysis of PolyHeme in plasma samples was performed using a rapid scanning diode array spectrophotometer (Model HP-8453, Agilent Technologies, Rockville, MD, USA). The concentration of total Hb and methemoglobin were determined using multi-component analysis (19).

Histological analyses

Formalin-fixed paraffin-embedded (FFPE) kidney sections 3 μm thick were dewaxed in Safeclear II (xylene substitute), rehydrated in graded alcohol (100, 95, and 50%) and deionized water, and stained by standard hematoxylin-eosin (H&E) procedures. Whole slide brightfield imaging was performed using a Hamamatsu NanoZoomer 2.0-RS whole-slide digital scanner equipped with a 20× objective. Analysis software NDP.view2 was used for image processing (Hamamatsu Photonics, Japan). H&E-stained sections were used for glomerular morphometry measurements, including glomerular density and glomerular tuft area. For glomerular density, the number of glomeruli were counted irrespective of size in the outer-to-mid cortex regions of each kidney section. Glomerular density values were derived by dividing the number of glomeruli by the measured cortical area of the region (minimum total cortical area analyzed was 20–30 mm^2 for each kidney section). Values for each animal per time interval were averaged and reported as the number of glomeruli per cortical area (n = 4–5 animals per group). For glomerular tuft area measurements, a total of 40–50 glomeruli per kidney were randomly selected from four different regions of the section. Tuft area values for each kidney section were measured using the NDP.view2 software and reported as the mean glomerular area in μm^2 for each group.

Immunofluorescence analyses

Formalin-fixed paraffin-embedded kidney sections 3 μm thick were dewaxed in Safeclear II (xylene substitute), rehydrated in graded alcohol (100, 95, and 50%) and deionized water, and heat-treated in a microwave oven for 15 min in 10 mM Tris/1 mM EDTA buffer (pH 9.0). After cooling for 30 min at room temperature (RT), heat-retrieved sections were blocked in phosphate-buffered saline containing 0.05% Tween-20 (PBST) and 2.5% bovine serum albumin (BSA) for 30 min at RT followed by overnight incubation at 4°C with primary antibodies in 1% BSA. Primary antibodies used included ETS-related gene (ERG, Biocare Medical, CM421), Wilms tumor protein (WT1, Abcam, ab89901), claudin-5 (CL5, Thermo Fisher Scientific, 35-2500), Iba1 (Abcam, ab5076), N-cadherin (NCAD, Cell Signaling, 13116S), E-cadherin (ECAD, Abcam, ab219332), podocin (Abcam, ab181143), podocalyxin (Abcam, ab203079), and heme oxygenase-1 (HO-1, Enzo Life Sciences, ADI-SPA-894). Sections were rinsed and incubated with Alexa Fluor 488 (A-21206) and Alexa Fluor 647-conjugated secondary antibodies (A-31571 and A-21447) for 1 h at RT (Thermo Fisher Scientific, Waltham, MA, USA). Nuclei were counterstained with Hoechst 33342. For double-labeling experiments, primary antibodies were mixed and incubated overnight at 4°C. For negative controls, sections were incubated without the primary antibody or mouse/rabbit isotype antibody controls. Sections stained with conjugated secondary antibodies alone showed no specific staining. Whole slide fluorescence imaging was performed using a Hamamatsu NanoZoomer 2.0-RS whole-slide digital scanner equipped with a 20× objective and a fluorescence module (#L11600). NDP.view2 software was used for image processing. Immunofluorescence and differential interference images were also captured using an Axio Observer Z1 inverted microscope (Carl Zeiss, Thornwood, NY, USA) equipped with an Axiocam 506 monochrome camera, an ApoTome.2 optical sectioning system, and a Plan-Apochromat 63×/1.4 NA oil immersion with WD = 0.19 and Plan-Apochromat 20×/0.8 objective lens. Digital image post-processing and analysis were performed using the ZEN 2 ver. 2.0 imaging software. Images were constructed from Z-stack slices collected at 0.48 μm intervals (5 μm thickness in total) and visualized as maximum intensity projections in orthogonal mode.

For WT1 or ERG semiquantitative analysis of podocytes or endothelial cells, respectively, a total of 20 glomeruli from randomly selected cortical areas per kidney section were acquired at 630× magnification and processed by Z-stack analysis using the ZEN 2 software. For each glomerulus, WT1 or ERG-positive nuclei were counted and divided by the glomerular tuft area. WT1 or ERG staining values for each section were averaged to derive a final score for each animal. The values were averaged to derive final scores for each group (n = 4 animals per group). For podocin, podocalyxin, and claudin-5 signal quantitation, relative fluorescence intensity values for a minimum of 10–15 randomly selected glomeruli per section were measured using the ZEN software. Average values per group were reported for each marker protein (n = 4 animals per group).

For semiquantitative analysis of proximal tubular HO-1 expression, a total of 40–50 randomly selected proximal tubular segments per kidney section were acquired at 630× magnification and processed by Z-stack analysis. Relative fluorescence intensity unit (RFU) values for each tubular segment were measured using the ZEN software, and average RFU values per group were calculated (n = 4 animals per group). Semiquantitative analysis of tubulointerstitial HO-1 expression was performed on whole-slide digital images of randomly selected cortical regions of each kidney section using the NDP.view2 software (6–10 images per section). For each image, threshold settings were applied to delineate HO-1-positive cells in the tubulointerstitium using ImageJ software ver.1.46 (National Institutes of Health, Bethesda, MD, USA). The percentage of HO-1-positive area for each image was measured, average values were derived for each section, and the mean percentage of HO-1 positive areas were calculated for each group (n = 4–6 animals per group).

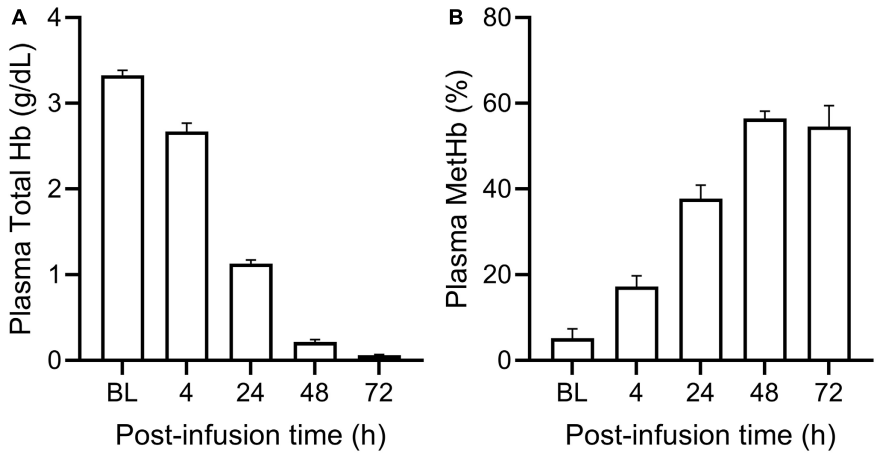

FIGURE 1
Total plasma Hb and methemoglobin levels in PolyHeme-infused guinea pigs. After a 25% exchange transfusion with PolyHeme (n = 18 total transfused animals), plasma samples were analyzed by spectrophotometry for the concentration of **(A)** total Hb and **(B)** methemoglobin. Serial samples were collected immediately after completion of infusion (baseline, BL) and at 4, 24, 48, and 72 h post-infusion.

Iron histochemistry

Ferric iron deposition primarily associated with hemosiderin was detected using the Perls method with diaminobenzidine (DAB) intensification as previously reported (19, 31). Semiquantitative analysis of Perls-DAB staining was performed on high resolution whole-slide digital images of each kidney section using the NDP.view2 software. For each kidney, the entire cortex region was divided into four areas and staining for each area was graded on the following scale: 0, no detectable brown staining; 1, detectable light staining in scattered cortical tubules; 2, brown deposits detected in <50% cortical tubules; and 3, brown deposits detected in >50% cortical tubules. The values were averaged to derive the staining score per animal and the final score for each time point was derived for all the animals combined (n = 5–6 animals per group).

TUNEL assay

Kidney sections were deparaffinized, hydrated, and pretreated with Proteinase K followed by EDTA, washed with distilled H_2O, and blocked with 2.5% BSA. Sections were then incubated in a reaction mixture (TdT, dUTP, and buffer), washed, and incubated with anti-digoxigenin antibody. Sections were then visualized with alkaline phosphatase-ImmPACT Vector Red and counterstained with hematoxylin.

Statistical analyses

Data values are expressed as mean ± SEM. Statistical comparisons were performed by a one-way ANOVA for planned comparisons and *post-hoc* Bonferroni's test for multiple comparisons between equal size groups or Dunnett's post-test when group comparisons involved unequal sizes (GraphPad Prism 5 software, La Jolla, CA, USA). In all analyses, $p < 0.05$ was taken as the level of statistical significance.

Results

Renal exposure to PolyHeme does not disrupt glomerular barrier integrity

PolyHeme administered as a 25% ET in guinea pigs produced a baseline or end-infusion maximum plasma Hb concentration of 3.3 ± 0.2 g/dl (n = 18 transfused animals) (**Figure 1A**). About 35% of this baseline concentration was still present in the circulation after 24 h but minimal levels remained 48 and 72-h post-infusion. In terms of the oxidative stability of PolyHeme, plasma methemoglobin levels rose from 5.2% at baseline to 17.2 and 37.8% at 4 and 24-h post-infusion, respectively (**Figure 1B**). Plasma methemoglobin measurements at 48 and 72-h are not considered meaningful given the minimal levels of circulating PolyHeme at these time points. Based on these initial data, renal tissues were collected at 4, 24, and 72 h post-infusion to investigate early, as well as late or persistent effects of PolyHeme on the kidney.

First, we sought to examine the effects of PolyHeme on the morphology and structural integrity of the renal glomerulus, as previous studies have reported that the glomerular filtration barrier is susceptible to Hb-induced damage (21, 23, 32). Routine H&E examination revealed no changes in the overall histology of glomeruli between sham controls or PolyHeme animals at 4, 24, and 72 h post-infusion (**Figure 2A**). TUNEL analyses also showed no major glomerular cell death following PolyHeme infusion (**Figure 2A**). Morphometric analyses showed no differences in glomerular density or average glomerular tuft area between sham controls and PolyHeme animals (**Figures 2B, C**).

Next, we examined the effect of PolyHeme on glomerular podocytes and endothelial cells that together form the glomerular filtration barrier. To specifically identify these glomerular cell types, we analyzed the expression of podocyte WT1 and endothelial ERG by immunofluorescence microscopy (33, 34). Podocytes and endothelial cells showed intense and distinct nuclear localization of WT1 and ERG, respectively, consistent with their role as key

10.3389/fmed.2023.1158359

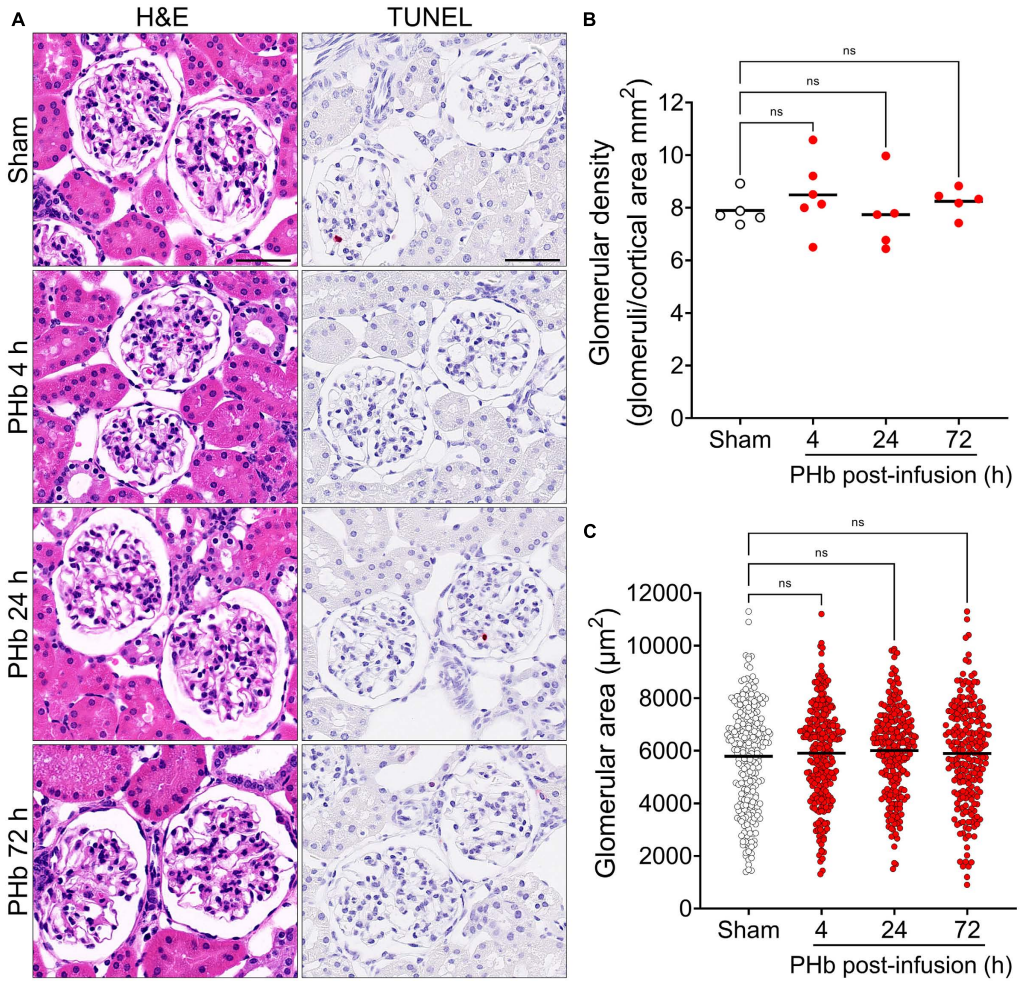

FIGURE 2
Glomerular histology and morphometric assessment in PolyHeme-infused guinea pigs. **(A)** Representative H&E and TUNEL staining of kidney sections from sham control animals or PolyHeme (PHb)-infused animals after 4, 24, and 72 h. Scale bars, 50 µm. **(B,C)** Measurement of glomerular density and glomerular tuft area using H&E-stained kidney sections from sham controls and PolyHeme-infused animals. **(B)** Glomerular density was determined by calculating the number of glomeruli per total renal cortical area (n = 5–6 animals per group). Glomerular density values for each animal and the means (black line) for each group are shown (n = 5–6 animals per group). **(C)** Glomerular tuft area was measured for 40–50 randomly selected glomeruli for each animal (n = 5–6 animals per group). The dots represent all the individual glomerular areas for each section and the means per group are shown (black line). ns, no statistical significance.

transcription factors in these cells (Figure 3A). Semiquantitative image analyses revealed no significant change in the number of WT1-positive podocytes (Figure 3B) or ERG-positive endothelial cells (Figure 3C) between sham controls and PolyHeme animals at 4, 24, or 72 h post-infusion.

We then analyzed the expression of podocin (a main constituent of slit diaphragm complexes between podocyte foot processes), podocalyxin (a major podocyte sialoglycoprotein that readily binds and stabilizes components of the glomerular glycocalyx), and claudin-5 (a key component of endothelial tight junctions) (34, 35). Figure 4A shows the linear and uniform staining pattern of podocin and podocalyxin along podocyte structures compared to the linear but more diffuse staining of claudin-5 in the glomerular capillaries. Semiquantitative analyses of podocalyxin and claudin-5 immunofluorescence showed no significant changes in expression of these proteins over the course of 72 h post-PolyHeme infusion (Figure 4B). In the case of podocin, there was an increase in relative staining intensity that reached statistical significance at 24 and 72 h (Figure 4B). In contrast to previous studies that reported that exposure to other types of acellular Hb alters the structural integrity of the glomerular filtration barrier, the present findings indicate that PolyHeme does not induce a loss of glomerular podocytes or endothelial cells or downregulate the expression of key proteins involved in barrier function regulation.

Effect of PolyHeme on the junctional integrity of renal tubular epithelium

Next, we examined the effect of PolyHeme on the renal tubular epithelium, which is a common site of damage in heme or iron overload settings and is also involved in mounting protective responses against these insults (24, 26). H&E staining of

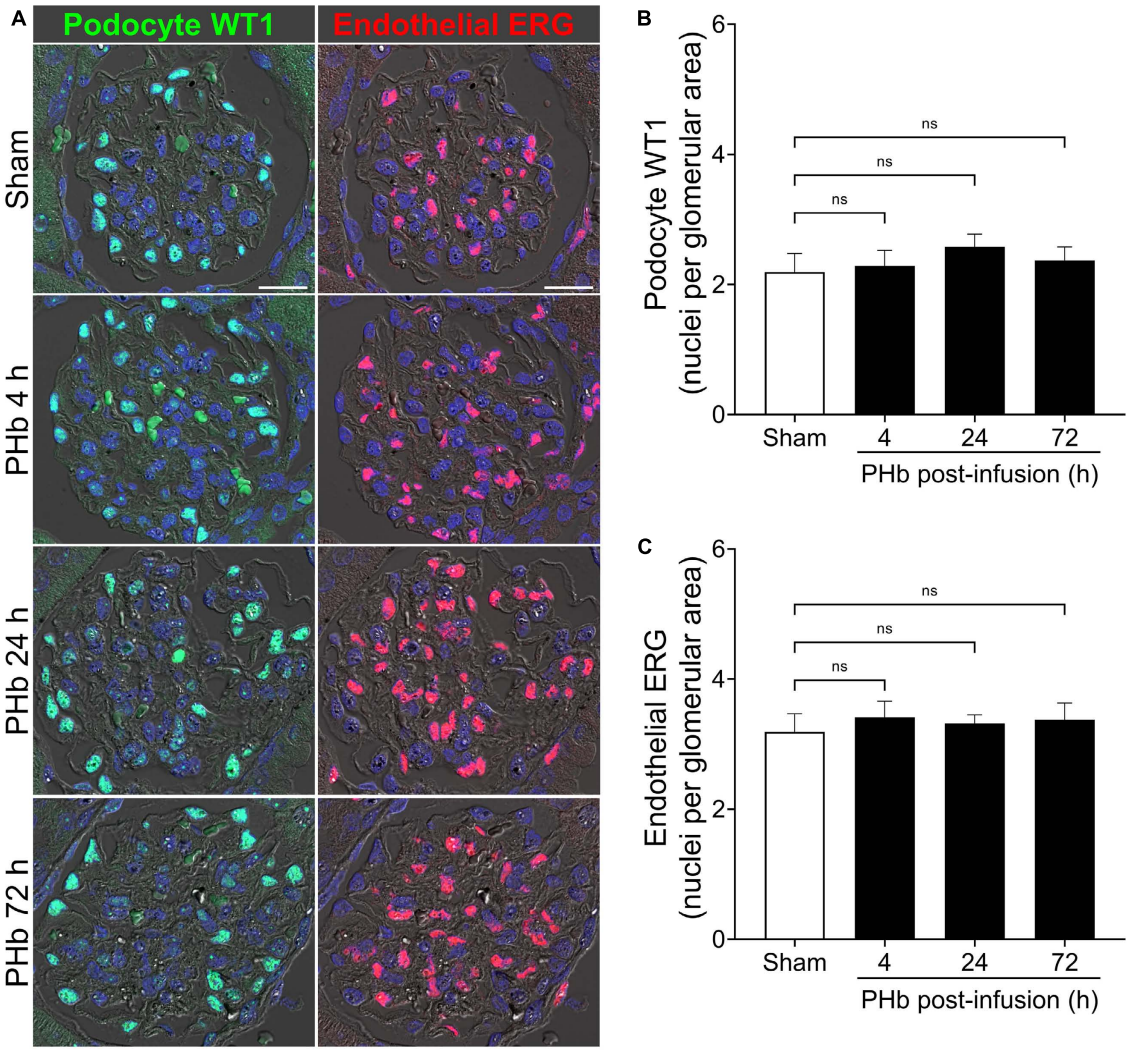

FIGURE 3
PolyHeme does not alter glomerular podocyte and endothelial density. **(A)** Representative immunofluorescence images combined with differential interference contrast of podocyte-expressed WT1 and endothelial-expressed ERG in serial kidney sections from sham control animals or PolyHeme (PHb)-infused animals after 4, 24, and 72 h. Nuclei were counterstained with Hoechst 33342 (blue). Scale bars, 20 μm. **(B,C)** Semiquantitative image analyses of podocyte WT1 and endothelial ERG. For each kidney section, the glomerular WT1 or ERG density values were derived by dividing the number of WT1 or ERG positive nuclei in each glomerulus by the glomerular tuft area (n = 15–20 randomly selected glomeruli per animal). The mean glomerular density values for each group are shown (n = 4 animals per group). ns, no statistical significance.

renal sections from PolyHeme-infused animals revealed minimal tubular brush border loss, tubular dilation, or sloughing of cellular debris in cortical nephron segments over the course of 72 h (Figure 5A). To investigate the possibility that PolyHeme induced more subtle changes to intercellular junctional complexes of the tubular epithelium, we analyzed the expression of N-cadherin and E-cadherin, two key epithelial transmembrane proteins that are highly expressed in proximal and distal tubules, respectively. Immunofluorescence analyses revealed minimal changes in the overall tubular expression of both N-cadherin and E-cadherin between PolyHeme-infused animals and sham controls (Figure 5B). N-cadherin and E-cadherin immunolabeling was not detected in glomeruli or the vasculature. High resolution confocal imaging showed that N-cadherin in proximal tubules was localized diffusely along the basolateral cell border and as thin, concentrated intercellular bands near the apical cell lining, while E-cadherin in distal tubules was mainly expressed at intercellular cell contacts (Figure 5C). No major differences were observed in the subcellular distribution patterns of these proteins between PolyHeme-infused and sham control animals (Figure 5C).

Renal HO-1 expression and iron deposition in PolyHeme-infused guinea pigs

Heme catabolism and iron sequestration systems play a critical protective role in the kidney and are highly activated by filtered heme, iron-bound transport proteins, or hemoprotein exposure (19, 24, 36, 37). To further evaluate the renal response to PolyHeme, we examined the expression of HO-1, an inducible rate-limiting

10.3389/fmed.2023.1158359

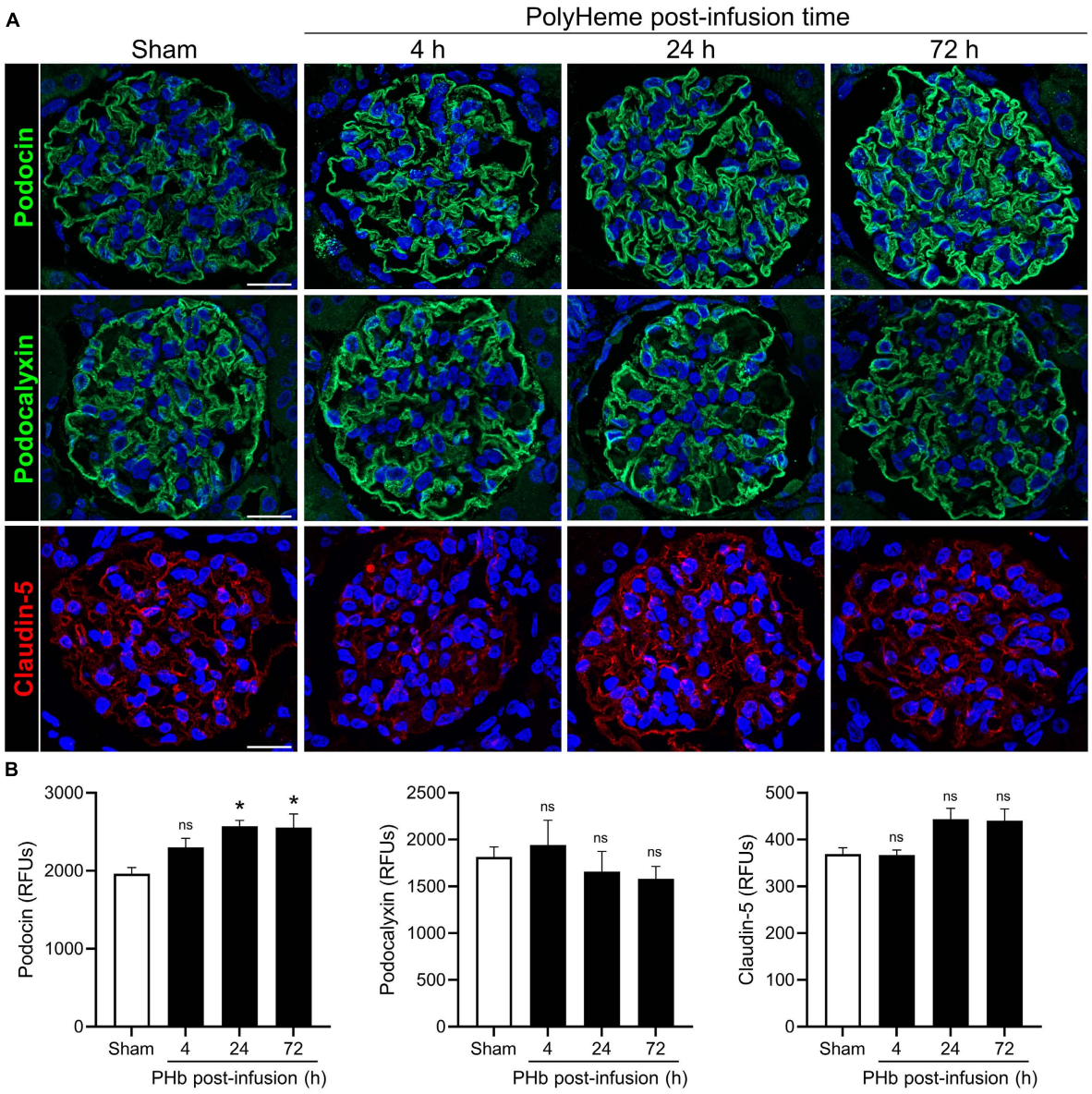

FIGURE 4
Effect of PolyHeme on podocyte and endothelial junctional and glycocalyx protein markers. **(A)** Representative immunofluorescence images of podocyte-expressed podocin and podocalyxin and endothelial-expressed claudin-5 in kidney sections from sham control animals or PolyHeme (PHb)-infused animals after 4, 24, and 72 h. Nuclei were counterstained with Hoechst 33342 (blue). Scale bars, 20 μm. **(B)** Semiquantitative image analyses of podocin, podocalyxin, and claudin-5. For each kidney section, the relative fluorescence intensity units (RFUs) of each respective protein were measured in 15–20 randomly selected glomeruli and the mean RFU values for each group were calculated (n = 4 animals per group). *$p \leq 0.05$; ns, no statistical significance.

enzyme of heme catabolism. Double-labeling experiments for HO-1 and E-cadherin expressed in distal tubules revealed increased HO-1 staining localized to cortical proximal tubular epithelium in PolyHeme-infused animals (Figure 6A). Semiquantitative image analysis of HO-1 expressed in proximal tubules confirmed a moderate but significant induction at 4 h but not at 24 and 72 h post-infusion (Figure 6B). No changes in glomerular HO-1 expression were detected between sham controls or PolyHeme-infused animals at any time interval. Further examination of these renal sections identified HO-1-positive cells in the cortical tubulointerstitium at 24 h post-infusion (Figure 6C). These HO-1 positive cells were identified as tubulointerstitial macrophages based on colocalization with macrophage marker Iba1. In sham controls, resident Iba1 positive tubulointerstitial macrophages showed no HO-1 expression (Figure 6C). Semiquantitative analyses revealed a significant increase in HO-1-positive cells in the cortical tubulointerstitium at 24 h, but not at 4 or 72 h post-infusion (Figure 6D).

Heme oxygenase-1 upregulation is often accompanied by the accumulation of ferritin and hemosiderin (a degradation product of excess ferritin stores) that helps trap iron generated by heme catabolism. To assess iron deposition, renal sections were stained using an enhanced Perls assay that mainly detects ferric iron in hemosiderin deposits. In the PolyHeme group, Perls-reactive

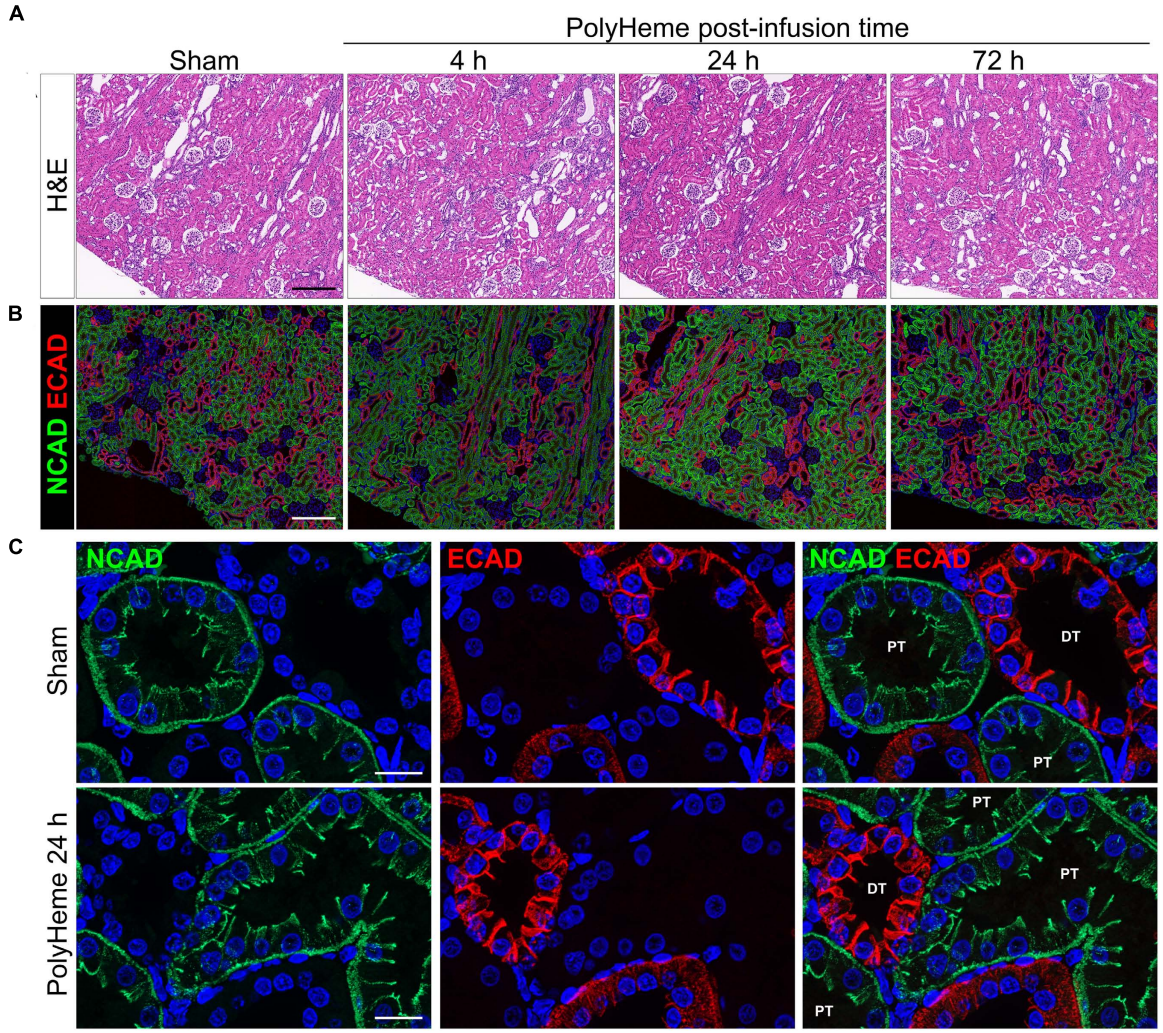

FIGURE 5
Effect of PolyHeme on epithelial junctional integrity of proximal and distal tubules. **(A,B)** Representative H&E and double-labeled immunofluorescence images of N-cadherin and E-cadherin in kidney sections from sham controls or PolyHeme-infused animals over the course of 72 h. **(C)** High resolution confocal imaging of the subcellular localization pattern of N-cadherin and E-cadherin in proximal and distal tubules, respectively. Scale bars, 250 μm **(A,B)**; 20 μm **(C)**. PT, proximal tubule; DT, distal tubule.

iron staining was detectable in proximal tubule segments, but not in the glomeruli, at every time point post-infusion (Figure 7A). Histological scoring identified significant increases in Perls-reactive iron staining at 4, 24, and 72 h post-infusion (Figure 7B). Together, these HO-1 and iron deposition observations suggest that exposure to PolyHeme and/or its breakdown products may be sufficient to trigger an adaptive response in the renal tubular and tubulointerstitial compartments.

Discussion

Our previous studies proposed the guinea pig as a physiologically relevant small animal species to evaluate the safety and efficacy of HBOCs, given the noted similarities in the overall plasma and tissue antioxidant profiles between guinea pigs and humans (17, 19, 22, 23). Many of these earlier studies were limited to the investigation of one well-characterized glutaraldehyde-polymerized bovine hemoglobin (Oxyglobin®, HbO_2 Therapeutics, Souderton, PA, USA) that was made available to our group at the time. In this study, we evaluated PolyHeme to further explore how the properties of different HBOCs may impact renal glomerular and tubular responses in this animal model. Although PolyHeme development has long been discontinued, there may be value in studying this highly characterized HBOC in the context of identifying different preclinical approaches and as a surrogate model for other similar types of products.

The present study shows that PolyHeme undergoes significant oxidation to methemoglobin in the circulation of guinea pigs. Uncontrolled oxidation of Hb in the circulation can be detrimental to the effectiveness of HBOCs because methemoglobin and other oxidized species no longer carry oxygen and have a greater propensity to release toxic heme or free iron into the circulation (14, 25). Plasma and tissue antioxidant systems play a critical role in controlling the oxidation and breakdown of

10.3389/fmed.2023.1158359

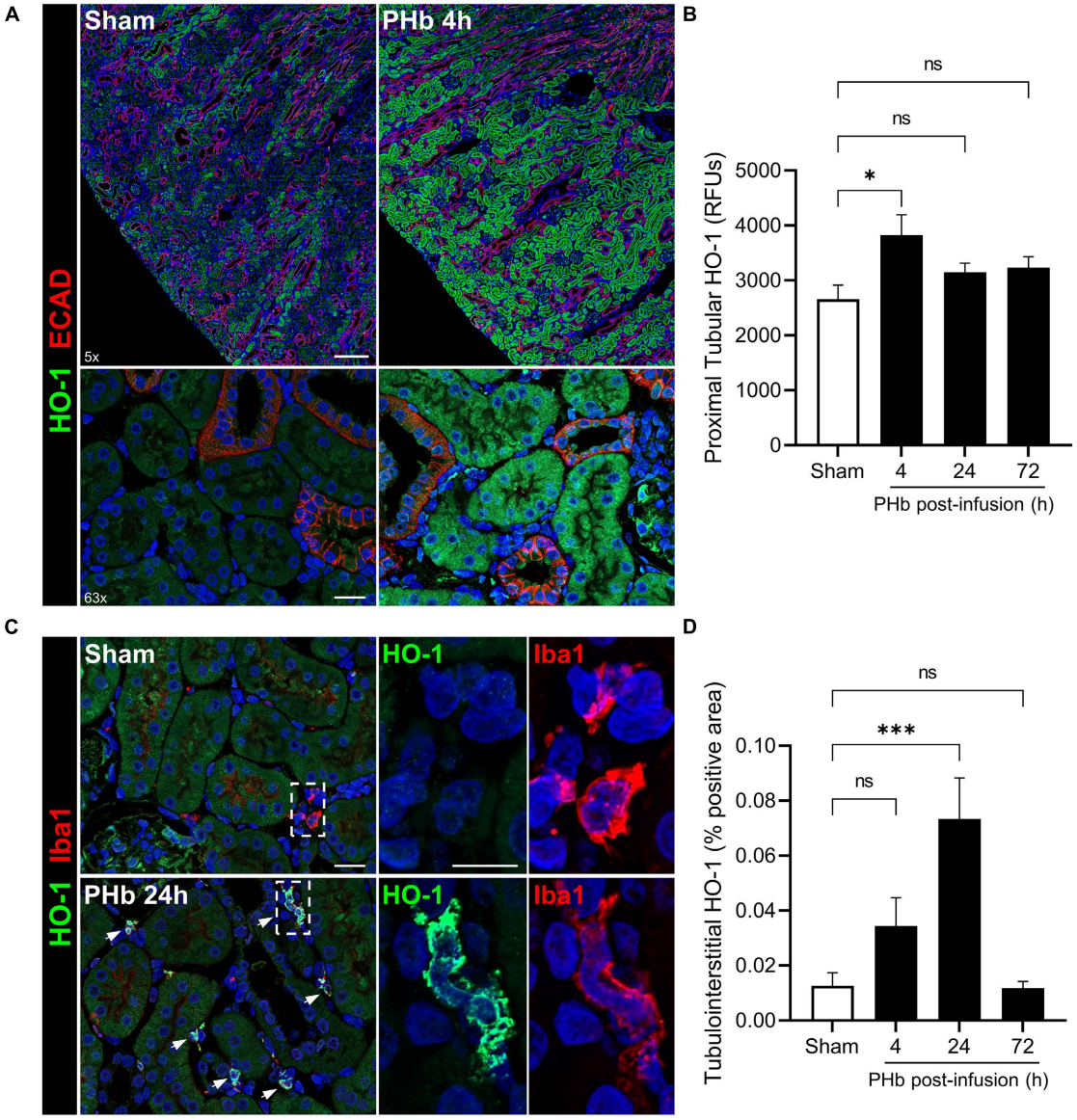

FIGURE 6
PolyHeme induces HO-1 in proximal tubular epithelium and tubulointerstitial macrophages. **(A)** Representative low and high magnification images of immunofluorescence staining for HO-1 and E-cadherin in cortical renal sections from sham controls or PolyHeme (PHb)-infused animals 4 h post-infusion. **(B)** Semiquantitative image analysis of HO-1 immunofluorescence intensity in proximal tubule segments. For each renal section, the RFU values of 40–50 randomly outlined proximal tubule profiles were measured, averaged, and the mean RFU values for each group were calculated (n = 4–5 animals per group). **(C)** Dual staining for HO-1 and macrophage marker Iba1 in sham controls or PHb-infused animals 24 h post-infusion. White arrows depict colocalized expression of HO-1 in Iba1-positive tubulointerstitial macrophages. **(D)** Semiquantitative analysis of tubulointerstitial areas positively labeled with HO-1-expressing tubulointerstitial macrophages. The mean area values for each group are shown (n = 4–5 animals per group). Scale bars, 250 μm (5× **A**); 20 μm (63× **A**); 20 μm **(C)**. *$p \leq 0.05$; ***$p \leq 0.001$; ns, no statistical significance.

HBOCs; and thus, the selection of animal species with similar antioxidant profiles to humans is important to accurately assess methemoglobin formation in preclinical studies. As evidence of this point, we previously showed that a glutaraldehyde-polymerized bovine Hb oxidized more readily in the circulation of guinea pigs (a non-ascorbate-producing species), compared to rats (an ascorbate-producing species with plasma and tissue antioxidant capacities different than that of humans) (17). The reductive capacity of ascorbate has also been used to mitigate methemoglobin formation in clinical settings with HBOCs such as Hemopure® (HbO_2 Therapeutics, Souderton, PA, USA) (13). Studying animal species that can accurately recapitulate the redox activity of HBOCs *in vivo* may also be important for the proper assessment of Hb-mediated nitric oxide (NO) scavenging reactions thought to underlie the reported hypertensive effects of HBOCs (14, 24, 25).

The present findings show that PolyHeme has minimal effects on the structural and junctional integrity of the renal glomerulus and the proximal/distal tubular epithelium in guinea pigs. These results differ from some of the previous renal findings we observed with the transfusion of other modified or acellular Hbs. For example, we previously reported that the infusion of glutaraldehyde-polymerized bovine Hb containing a high content

10.3389/fmed.2023.1158359

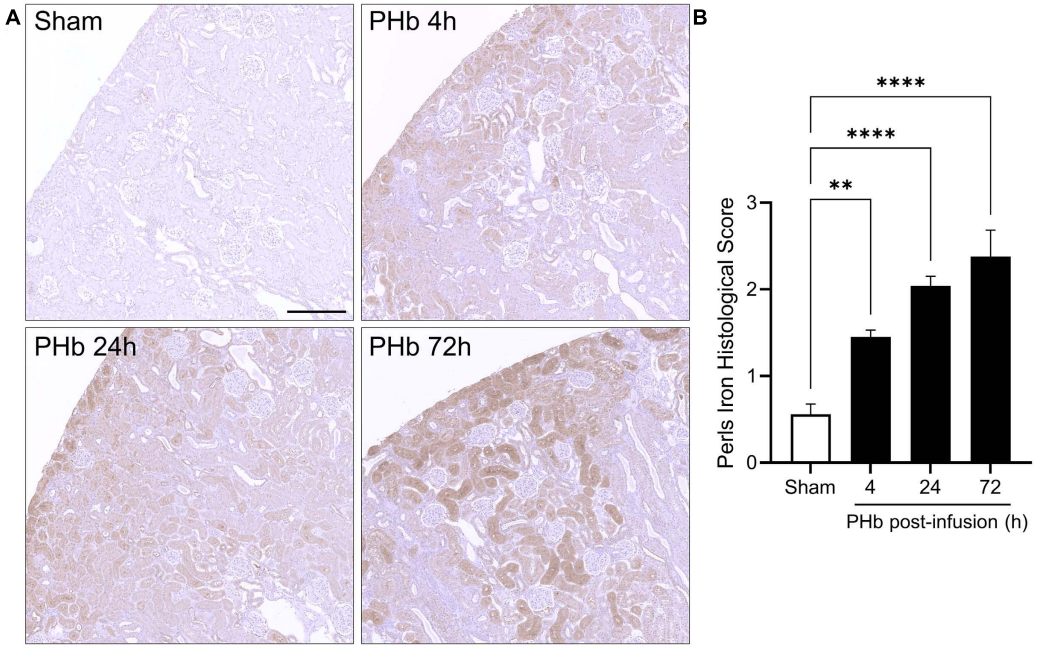

FIGURE 7
Renal iron deposition in PolyHeme-infused guinea pigs. **(A)** Non-heme iron staining using the Perls-DAB assay in sham control animals or at 4, 24, and 72 h after PolyHeme infusion. Perls-DAB reactivity (brown staining) is mainly observed in proximal tubules in PolyHeme-infused animals but not in glomeruli. Scale bars, 250 μm **(A)**. **(B)** Histological scoring of Perls iron deposition in sham control and PolyHeme-infused animals (n = 4–6 animals per group). $^{**}p \leq 0.005$; $^{****}p \leq 0.0001$.

of unmodified (<5%) and stabilized Hb tetramers (~35%) induced a transient disruption of renal glomerular barrier integrity and function that coincided with the reduced expression of glomerular podocyte and endothelial proteins (23). Guinea pigs infused with nitrite-oxidized human Hb also showed increased tubular and glomerular injury (21). Compared to these other solutions, PolyHeme contains a lower content of tetrameric Hb (<1%), which may partly explain the differences in glomerular and tubular responses. High molecular weight polymers of PolyHeme are less prone to glomerular filtration, thus limiting exposure of the tubular lumen to the product. Monitoring glomerular and tubular integrity using sensitive and specific biomarkers may allow for the assessment of subtle changes in the kidney nephron that may not otherwise be captured by traditional renal histological analyses. Intercellular junctional integrity and communication among podocytes, endothelial cells, and epithelial cells forming the glomerular filtration barrier and tubular segments of the nephron are particularly sensitive to changes in the microenvironment of the nephron (38–42). The loss or abnormal localization of these junctional adhesion molecules characterizes the pathogenesis of various renal injury or disease states (38, 43, 44).

Heme oxygenase (HO), the rate-limiting enzyme of heme catabolism, exists as two main isoforms: inducible HO-1 and constitutive HO-2. HO catalyzes the degradation of heme to biliverdin, carbon monoxide, and ferrous iron, which is rapidly exported from the cell via ferroportin or sequestered by ferritin for storage. HO-1 is up-regulated by exposure to Hb, heme, lipopolysaccharide, and several other pro-oxidant stimuli (36). In this study, PolyHeme induced a moderate and transient induction of HO-1 in the renal proximal tubular system. These observations suggest that there may be some level of exposure of these compartments to PolyHeme and/or its breakdown products. While an intact glomerular barrier may prevent the passage of high molecular weight forms of PolyHeme, we suspect that the filtration and tubular uptake of smaller degraded heme (bound/unbound) or iron-containing species derived from intravascular product breakdown or extravascular catabolism may have been sufficient to trigger the tubular HO-1 response. The increased oxidation of PolyHeme to methemoglobin would lend support to this hypothesis, as oxidized Hb is more easily degraded and prone to liberate heme. Consistent with this idea, we previously reported that differences in methemoglobin formation between rats and guinea pigs infused with Oxyglobin may differentially modulate the activation of heme catabolic and iron sequestration systems (19). Our present findings also revealed increased HO-1 expression in Iba1-positive tubulointerstitial macrophages, implying the possible exposure and cellular uptake of degraded heme or iron-containing species and possibly also intact PolyHeme polymers escaping the more permeable peritubular capillaries. Both sham controls and PolyHeme animals showed a similar degree of tubulointerstitial Iba1 staining with no clear histological evidence of tubulointerstitial damage, suggesting that this HO-1 induction occurs mainly in resident tubulointerstitial macrophages and not in cellular infiltrates attracted to this site by inflammatory or injury signals. Macrophage HO-1 induction is also observed in organs such as the liver and spleen, which likely serve as more prominent sites of PolyHeme degradation and removal than the kidney (**Supplementary Figure 1**). Previous studies in chimpanzees and guinea pigs with similar glutaraldehyde polymerized Hbs reported a shift from renal excretion to

reticuloendothelial elimination that correlated with the degree of Hb polymerization and/or the content of unmodified Hb (45, 46).

Many studies have provided evidence that HO-1 upregulation serves as an adaptive response that confers protection through anti-inflammatory and antioxidant mechanisms (36). HO-1 upregulation is often accompanied by the accumulation of ferritin and hemosiderin stores as a mechanism to trap liberated iron and limit toxicity (37). Conversely, under settings of excess heme exposure, HO-1 over-activation may promote iron or other byproduct toxicities (14, 27). In the case of this study, we speculate that the HO pathway may have provided some degree of protection to the kidney at these levels of PolyHeme exposure. It should also be noted that the iron deposition detected by the Perls method mainly represents the accumulation of hemosiderin, an iron storage complex with minimal free radical-generating potential. Thus, given the absence of renal damage in this study, the observed iron deposition may be interpreted as an indicator of exposure to PolyHeme or its degradation products rather than a marker of toxicity.

Protein modification strategies based on Hb polymerization have afforded nephroprotective benefits over early unmodified or intramolecularly cross-linked HBOC candidates (1, 28, 47). Although there is a lack of detailed published information on the renal toxicology of PolyHeme in animals, clinical studies have reported that PolyHeme does not cause overt renal toxicity (29, 30). There remains an important need to better understand and predict the renal effects of HBOCs in recipients that may be affected by pre-existing conditions including advanced age, diabetes, infection, ischemia, and chronic disease that render kidneys more susceptible to Hb or heme toxicity (26, 48–50). In this regard, the examination of HBOCs in relevant animal models of early or advanced endothelial dysfunction, inflammation, renal impairment, and traumatic shock should provide important information on safety and efficacy with potential implications for clinical trial design (14, 51).

Conclusion

The present study shows that the infusion of PolyHeme produces minimal damage to the junctional integrity of the renal glomerulus and tubular epithelium in this guinea pig model. The observed moderate activation of heme catabolic pathways and non-heme iron deposition likely reflects the induction of a renal protective response. Reported similarities in the clinical adverse event profiles of different HBOC formulations have led to suggestions of common mechanisms of toxicity with this class of products. However, it is important to recognize that not every HBOC is created equally. Differences in key physiochemical properties related to oxygen affinity, redox activity and stability, molecular size and shape, and extravasation potential can profoundly influence preclinical and clinical responses to these products (1, 5, 47). From a preclinical perspective, the application of relevant small animal models and sensitive biomarkers that take into consideration the unique pro-oxidative properties of HBOCs may provide important comparative information in future investigations of existing or emerging HBOC candidates.

Data availability statement

The raw data supporting the conclusions of this article will be made available by the authors, without undue reservation.

Ethics statement

The animal study was reviewed and approved by the FDA/CBER Institutional Animal Care and Use Committee.

Author contributions

FD conceived and designed the study, performed the statistical analysis, and wrote the first draft of the manuscript. FD, JHB, MCW, and XZ performed the animal studies and experimental analyses. XZ organized the animal database. FD and MCW revised the manuscript. All authors read and approved the submitted version.

Funding

This work was supported by the Intramural Research funding from the Center for Biologics Evaluation and Research, FDA (to FD).

Acknowledgments

We thank HbO_2 Therapeutics for kindly providing the PolyHeme used in these experiments.

Conflict of interest

The authors declare that the research was conducted in the absence of any commercial or financial relationships that could be construed as a potential conflict of interest.

Publisher's note

All claims expressed in this article are solely those of the authors and do not necessarily represent those of their affiliated organizations, or those of the publisher, the editors and the reviewers. Any product that may be evaluated in this article, or claim that may be made by its manufacturer, is not guaranteed or endorsed by the publisher.

Supplementary material

The Supplementary Material for this article can be found online at: https://www.frontiersin.org/articles/10.3389/fmed.2023.1158359/full#supplementary-material

References

1. Chang TMS, Bulow L, Jahr JS, Sakai H, Yang C. *Nanobiotherapeutic Based Blood Substitutes*. Singapore: World Scientific Publishing (2021). doi: 10.1142/12054

2. Jahr JS, Guinn NR, Lowery DR, Shore-Lesserson L, Shander A. Blood substitutes and oxygen therapeutics: a review. *Anesth Analg.* (2021) 132:119–29. doi: 10.1213/ANE.0000000000003957

3. Cao M, Wang G, He H, Yue R, Zhao Y, Pan L, et al. Hemoglobin-based oxygen carriers: potential applications in solid organ preservation. *Front Pharmacol.* (2021) 12:760215. doi: 10.3389/fphar.2021.760215

4. Lodhi S, Stone JP, Entwistle TR, Fildes JE. The use of hemoglobin-based oxygen carriers in *ex vivo* machine perfusion of donor organs for transplantation. *ASAIO J.* (2022) 68:461–70. doi: 10.1097/MAT.0000000000001597

5. Meng F, Kassa T, Jana S, Wood F, Zhang X, Jia Y, et al. Comprehensive biochemical and biophysical characterization of hemoglobin-based oxygen carrier therapeutics: All HBOCs Are Not Created Equally. *Bioconjug Chem.* (2018) 29:1560–75. doi: 10.1021/acs.bioconjchem.8b00093

6. Chen L, Yang Z, Liu H. Hemoglobin-based oxygen carriers: Where are we now in 2023? *Medicina.* (2023) 59:396. doi: 10.3390/medicina59020396

7. Silverman TA, Weiskopf RB. Hemoglobin-based oxygen carriers: current status and future directions. *Anesthesiology.* (2009) 111:946–63. doi: 10.1097/ALN.0b013e3181ba3c2c

8. Estep TN. Issues in the development of hemoglobin based oxygen carriers. *Semin Hematol.* (2019) 56:257–61. doi: 10.1053/j.seminhematol.2019.11.006

9. Mackenzie CF, Dubé GP, Pitman A, Zafirelis M. Users guide to pitfalls and lessons learned about HBOC-201 during clinical trials, expanded access, and clinical use in 1,701 Patients. *Shock.* (2017) 52(1S Suppl 1):92–9. doi: 10.1097/SHK.0000000000001038

10. Weiskopf RB, Beliaev AM, Shander A, Guinn NR, Cap AP, Ness PM, et al. Addressing the unmet need of life-threatening anemia with hemoglobin-based oxygen carriers. *Transfusion.* (2017) 57:207–14. doi: 10.1111/trf.13923

11. Weiskopf RB, Glassberg E, Guinn NR, James MFM, Ness PM, Pusateri AE. The need for an artificial oxygen carrier for disasters and pandemics, including COVID-19. *Transfusion.* (2020) 60:3039–45. doi: 10.1111/trf.16122

12. Jahr JS. Blood substitutes: Basic science, translational studies and clinical trials. *Front Med Technol.* (2022) 4:989829. doi: 10.3389/fmedt.2022.989829

13. Mer M, Hodgson E, Wallis L, Jacobson B, Levien L, Snyman J, et al. Hemoglobin glutamer-250 (bovine) in South Africa: consensus usage guidelines from clinician experts who have treated patients. *Transfusion.* (2016) 56:2631–6. doi: 10.1111/trf.13726

14. Buehler, PW, D'Agnillo, F. Preclinical evaluation of hemoglobin based oxygen carriers: Animal models and biomarkers. In: Kim H, Greenburg A, editors. *Hemoglobin-Based Oxygen Carriers as Red Cell Substitutes and Oxygen Therapeutics*. Berlin: Springer (2013). p. 299–313. doi: 10.1007/978-3-642-40717-8_26

15. Yu B, Shahid M, Egorina EM, Sovershaev MA, Raher MJ, Lei C, et al. Endothelial dysfunction enhances vasoconstriction due to scavenging of nitric oxide by a hemoglobin-based oxygen carrier. *Anesthesiology.* (2010) 112:586–94. doi: 10.1097/ALN.0b013e3181cd7838

16. Biro GP. Adverse HBOC-endothelial dysfunction synergism: a possible contributor to adverse clinical outcomes? *Curr Drug Discov Technol.* (2012) 9:194–203. doi: 10.2174/157016312802650733

17. Buehler PW, D'Agnillo F, Hoffman V, Alayash AI. Effects of endogenous ascorbate on oxidation, oxygenation, and toxicokinetics of cell-free modified hemoglobin after exchange transfusion in rat and guinea pig. *J Pharmacol Exp Ther.* (2007) 323:49–60. doi: 10.1124/jpet.107.126409

18. D'Agnillo F. Redox Activity of Cell-Free Hemoglobin: Implications for Vascular Oxidative Stress and Endothelial Dysfunction. In: Kim H, Greenburg A editors. *Hemoglobin-Based Oxygen Carriers as Red Cell Substitutes and Oxygen Therapeutics*. Berlin: Springer (2013). doi: 10.1007/978-3-642-40717-8_35

19. Butt OI, Buehler PW, D'Agnillo F. Differential induction of renal heme oxygenase and ferritin in ascorbate and nonascorbate producing species transfused with modified cell-free hemoglobin. *Antioxid Redox Signal.* (2010) 12:199–208. doi: 10.1089/ars.2009.2798

20. Butt OI, Buehler PW, D'Agnillo F. Blood-brain barrier disruption and oxidative stress in guinea pig after systemic exposure to modified cell-free hemoglobin. *Am J Pathol.* (2011) 178:1316–28. doi: 10.1016/j.ajpath.2010.12.006

21. Baek JH, Zhang X, Williams MC, Hicks W, Buehler PW, D'Agnillo F. Sodium nitrite potentiates renal oxidative stress and injury in hemoglobin exposed guinea pigs. *Toxicology.* (2015) 333:89–99. doi: 10.1016/j.tox.2015.04.007

22. Rentsendorj O, Zhang X, Williams MC, Buehler PW, D'Agnillo F. Transcriptional suppression of renal antioxidant enzyme systems in guinea pigs exposed to polymerized cell-free hemoglobin. *Toxics.* (2016) 4:6. doi: 10.3390/toxics4010006

23. Zhang X, Williams MC, Rentsendorj O, D'Agnillo F. Reversible renal glomerular dysfunction in guinea pigs exposed to glutaraldehyde-polymerized cell-free hemoglobin. *Toxicology.* (2018) 40:37–49. doi: 10.1016/j.tox.2018.04.005

24. Buehler PW, D'Agnillo F, Schaer DJ. Hemoglobin-based oxygen carriers: From mechanisms of toxicity and clearance to rational drug design. *Trends Mol Med.* (2010) 16:447–57. doi: 10.1016/j.molmed.2010.07.006

25. Alayash AI. Mechanisms of toxicity and modulation of hemoglobin-based oxygen carriers (HBOCs). *Shock.* (2017) 52(1S Suppl 1):41–9. doi: 10.1097/SHK.0000000000001044

26. Nath KA, Grande JP, Farrugia G, Croatt AJ, Belcher JD, Hebbel RP, et al. Age sensitizes the kidney to heme protein-induced acute kidney injury. *Am J Physiol Renal Physiol.* (2013) 304:F317–25. doi: 10.1152/ajprenal.00606.2012

27. Deuel JW, Schaer CA, Boretti FS, Opitz L, Garcia-Rubio I, Baek JH, et al. Hemoglobinuria-related acute kidney injury is driven by intrarenal oxidative reactions triggering a heme toxicity response. *Cell Death Dis.* (2016) 7:e2064. doi: 10.1038/cddis.2015.392

28. Savitsky JP, Doczi J, Black J, Arnold JD. A clinical safety trial of stroma-free hemoglobin. *Clin Pharmacol Ther.* (1978) 23:73–80. doi: 10.1002/cpt19782373

29. Moore EE, Johnson JL, Moore FA, Moore HB. The USA Multicenter Prehospital Hemoglobin-based Oxygen Carrier Resuscitation Trial: scientific rationale, study design, and results. *Crit Care Clin.* (2009) 25:325–56. doi: 10.1016/j.ccc.2009.01.002

30. Cralley A, Moore E. PolyHeme: History, clinical trials, and lessons learned. In: Liu H, Kaye AD, Jahr JS editors. *Blood Substitutes and Oxygen Biotherapeutics*. Berlin: Springer (2022). doi: 10.1007/978-3-030-95975-3_30

31. Meguro R, Asano Y, Odagiri S, Li C, Iwatsuki H, Shoumura K. Non-heme-iron histochemistry for light and electron microscopy: a historical, theoretical and technical review. *Arch Histol Cytol.* (2007) 70:1–19. doi: 10.1679/aohc.70.1

32. Rubio-Navarro A, Sanchez-Niño MD, Guerrero-Hue M, García-Caballero C, Gutiérrez E, Yuste C, et al. Podocytes are new cellular targets of haemoglobin-mediated renal damage. *J Pathol.* (2018) 244:296–310. doi: 10.1002/path.5011

33. Shah AV, Birdsey GM, Randi AM. Regulation of endothelial homeostasis, vascular development and angiogenesis by the transcription factor ERG. *Vascul Pharmacol.* (2016) 86:3–13. doi: 10.1016/j.vph.2016.05.003

34. Schlöndorff D, Wyatt CM, Campbell KN. Revisiting the determinants of the glomerular filtration barrier: what goes round must come round. *Kidney Int.* (2017) 92:533–6. doi: 10.1016/j.kint.2017.06.003

35. Scott RP, Quaggin SE. Review series: the cell biology of renal filtration. *J Cell Biol.* (2015) 209:199–210. doi: 10.1083/jcb.201410017

36. Nath KA. Heme oxygenase-1 and acute kidney injury. *Curr Opin Nephrol Hypertens.* (2014) 23:17–24. doi: 10.1097/01.mnh.0000437613.88158.d3

37. Balla J, Balla G, Zarjou A. Ferritin in kidney and vascular related diseases: novel roles for an old player. *Pharmaceuticals.* (2019) 12:96. doi: 10.3390/ph12020096

38. Prozialeck WC, Lamar PC, Appelt DM. Differential expression of E-cadherin, N-cadherin and beta-catenin in proximal and distal segments of the rat nephron. *BMC Physiol.* (2004) 17:10. doi: 10.1186/1472-6793-4-10

39. Kato T, Mizuno S, Kamimoto M. The decreases of nephrin and nuclear WT1 in podocytes may cause albuminuria during the experimental sepsis in mice. *Biomed Res.* (2010) 31:363–9. doi: 10.2220/biomedres.31.363

40. Haraldsson B, Nyström J. The glomerular endothelium: new insights on function and structure. *Curr Opin Nephrol Hypertens.* (2012) 21:258–63. doi: 10.1097/MNH.0b013e3283522e7a

41. Kriz W, Shirato I, Nagata M, LeHir M, Lemley KV. The podocyte's response to stress: the enigma of foot process effacement. *Am J Physiol Renal Physiol.* (2013) 304:F333–47. doi: 10.1152/ajprenal.00478.2012

42. Nagata M. Podocyte injury and its consequences. *Kidney Int.* (2016) 89:1221–30. doi: 10.1016/j.kint.2016.01.012

43. Prozialeck WC, Lamar PC, Lynch SM. Cadmium alters the localization of N-cadherin, E-cadherin, and beta-catenin in the proximal tubule epithelium. *Toxicol Appl Pharmacol.* (2003) 189:180–95. doi: 10.1016/s0041-008x(03)00130-3

44. Nürnberger J, Feldkamp T, Kavapurackal R, Opazo Saez A, Becker J, Hörbelt M, et al. N-cadherin is depleted from proximal tubules in experimental and human acute kidney injury. *Histochem Cell Biol.* (2010) 133:641–9. doi: 10.1007/s00418-010-0702-1

45. Lenz G, Junger H, Schneider M, Kothe N, Lissner R, Prince AM. Elimination of pyridoxylated polyhemoglobin after partial exchange transfusion in chimpanzees. *Biomater Artif Cells Immobil Biotechnol.* (1991) 19:699–708. doi: 10.3109/10731199109117848

46. Baek JH, Zhou Y, Harris DR, Schaer DJ, Palmer AF, Buehler PW. Down selection of polymerized bovine hemoglobins for use as oxygen releasing therapeutics in a guinea pig model. *Toxicol Sci.* (2012) 127:567–81. doi: 10.1093/toxsci/kfs109

47. Muller CR, Williams AT, Munoz CJ, Eaker AM, Breton AN, Palmer AF, et al. Safety profile of high molecular weight polymerized hemoglobins. *Transfusion.* (2021) 61:212–24. doi: 10.1111/trf.16157

48. Henao DE, Saleem MA, Cadavid AP. Glomerular disturbances in preeclampsia: disruption between glomerular endothelium and podocyte symbiosis. *Hypertens Pregnancy.* (2010) 29:10–20. doi: 10.3109/10641950802631036

49. Herrera MD, Mingorance C, Rodríguez-Rodríguez R, Alvarez de Sotomayor M. Endothelial dysfunction and aging: an update. *Ageing Res Rev.* (2010) 9:142–52. doi: 10.1016/j.arr.2009.07.002

50. Maxwell RA, Bell CM. Acute kidney injury in the critically ill. *Surg Clin North Am.* (2017) 97:1399–418. doi: 10.1016/j.suc.2017.07.004

51. Muller CR, Williams AT, Walser C, Eaker AM, Sandoval JL, Cuddington CT, et al. Safety and efficacy of human polymerized hemoglobin on guinea pig resuscitation from hemorrhagic shock. *Sci Rep.* (2022) 12:20480. doi: 10.1038/s41598-022-23926-y

frontiers | Frontiers in Bioengineering and Biotechnology

TYPE Brief Research Report
PUBLISHED 07 August 2023
DOI 10.3389/fbioe.2023.1231384

OPEN ACCESS

EDITED BY
Binglan Yu,
Harvard Medical School, United States

REVIEWED BY
Jonathan Jahr,
University of California, United States
Hongli Zhu,
Northwest University, China
Chen Guo,
Guangzhou Henovcom Bioscience Co. Ltd., China

*CORRESPONDENCE
T. M. S. Chang,
thomas.chang@mcgill.ca

RECEIVED 30 May 2023
ACCEPTED 24 July 2023
PUBLISHED 07 August 2023

CITATION
Hoq M and Chang TMS (2023), Preliminary feasibility study using a solution of synthetic enzymes to replace the natural enzymes in polyhemoglobin-catalase-superoxide dismutase-carbonic anhydrase: effect on warm ischemic hepatocyte cell culture.
Front. Bioeng. Biotechnol. 11:1231384.
doi: 10.3389/fbioe.2023.1231384

Preliminary feasibility study using a solution of synthetic enzymes to replace the natural enzymes in polyhemoglobin-catalase-superoxide dismutase-carbonic anhydrase: effect on warm ischemic hepatocyte cell culture

M. Hoq and T. M. S. Chang*

Artificial Cells and Organs Research Centre, Departments of Physiology, Medicine and Biomedical Engineering, Faculty of Medicine and Health Sciences, McGill University, Montreal, QC, Canada

This is a study on a simple solution of chemically prepared small chemical molecules of synthetic enzymes: catalase, superoxide dismutase, and carbonic anhydrase (CAT, SOD, and CA). We carried out a study to see if these synthetic enzymes can replace the natural enzymes (CAT, SOD, and CA) and avoid the need for the complicated cross-linking of natural enzymes to PolyHb to form PolyHb-CAT-SOD-CA. We compared the effect a solution of these three synthetic enzymes has on the viability of warm-ischemic hepatocytes that were exposed to nitrogen for 1 h at 37°C. PolyHb significantly increased the viability. The three synthetic enzymes themselves also significantly increased the viability. The use of both PolyHb and the three synthetic enzymes resulted in an additive effect in the recovery of viability. Increasing the concentration of the synthetic enzymes resulted in further increase in the effect due to the synthetic enzymes.

Implications: In addition to PolyHb, there are a number of other HBOC oxygen carriers. However, only Biopure's HBOC product has received regulatory approval, but only in Russia and South Africa. None of the HBOCs has received regulatory approval by other countries. If regulatory agencies require HBOCs to have antioxidant or CO_2 transport properties, all that is needed is to add or inject the solution of synthetic enzymes as a separate component.

KEYWORDS

regenerative medicine, artificial cell, polyhemoglobin, synthetic enzyme, warm ischemia, oxygen carrier, antioxidant, CO_2 carrier

Introduction

This study is a part of the Frontiers special series on artificial cells in novel medical applications. The study on artificial cells (Chang, 2019) is a very large area, and we could only include 12 articles. Six of the 12 articles in this series are devoted to nanobiotechnology-based blood substitutes. These include experiences on the routine clinical uses in South Africa by Jahr, a

bioengineering approach by Bulow, hemoglobin lipid vesicles by Sakai, use in preservation of transplant organs by Chan and Zhu, polyhemoglobin–catalase-superoxide dismutase–carbonic anhydrase (PolyHb-CAT-SOD-CA) by Bian and Chang, and the present article on the use of a solution of chemically prepared small enzyme molecules of CAT, SOD, and CA to replace the natural enzymes in PolyHb-CAT-SOD-CA. Since the other aspects have been discussed in detail in the other five articles, this paper will concentrate on the topic of synthetic enzymes.

Blood substitutes is a very broad area that has been reviewed in a recent open-access multiauthor book (Chang et al., 2022). One of the blood substitutes is polyhemoglobin, formed by the crosslinking of hemoglobin molecules. The use of gluteraldehyde to crosslink hemoglobin was first reported by Chang in 1971 (Chang, 1971). Since then, others have prepared a number of polyHbs using this basic glutaraldehyde method using bovine, human, pork, and cord blood Hb (Chang et al., 2022). Some of these have been developed and improved into products for clinical trials (Moore et al., 2009), and one has been approved for routine clinical use in South Africa and Russia (Mer et al., 2016; Chang, 2019). Laboratory research also includes the use of glutaraldehyde to prepare PolyHb-CAT-SOD-CA, which is an oxygen carrier with enhanced antioxidant function and CO2 transport function[5]. The last of the series is a brief research report on the use of synthetic CAT, SOD, and CA to replace the natural enzymes in PolyHb-CAT-SOD-CA. Thus, to have a valid comparison, we have selected our laboratory-made PolyHb and PolyHb-CAT-SOD-CA for comparison.

Natural enzymes have low stability, especially at body temperature. Nonhuman sources of natural enzymes are immunogenic and need complicated cross-linking with PolyHb to form PolyHb-CAT-SOD-CA. This study was performed to see if a simple solution of chemically prepared small chemical molecules of synthetic catalase, superoxide dismutase, and carbonic anhydrase (CAT, SOD, and CA) can replace the natural enzymes (CAT, SOD, and CA) in PolyHb-CAT-SOD-CA.

Synthetic enzymes are chemically prepared just to have the enzyme reaction sites of the large enzyme protein molecule (Bjerre et al., 2008). Zinc-based synthetic carbonic anhydrase is a novel approach (Liu et al., 2021). MnTmPyP is a commercially available manganese-containing metalloporphyrin synthetic superoxide dismutase (Zhu et al., 2016; Li et al., 2018; Gao et al., 2021). EUK-134 is a commercially available synthetic catalase (Dhanasekaran et al., 2018).

We perform this study to see if these synthetic enzymes can replace the natural enzymes we used for PolyHb-CAT-SOD-CA prepared and studied in this laboratory over the last 10 years. In order to compare the results, we have to use the same procedure of preparation for PolyHb-CAT-SOD-CA, including PolyHb (Table 1).

Organ and cell transplantation is dependent on the quality of donor organs and cells and their preservation before surgery. There have been promising results on the use of HBOCs for organ and cell pre-transplant preservation (Chang et al., 2021; Andrijevic et al., 2022; Chen et al., 2023). One of these has been approved in EU for organ preservation (Chen et al., 2023). Organs and cells vary greatly in their preservation requirements. The kidneys and limbs have lower requirements than the intestines or liver cells. Furthermore, the degree and duration of ischemia is also important. Again, for comparison, we have designed the present study based on our earlier studies of PolyHb and PolyHb-CAT-SOD-CA for hepatocytes in order to compare our results.

Results

Effects on regeneration of viability of warm ischemic human hepatocytes: Us

We compared the effect of these synthetic enzymes on the viability of warm-ischemic hepatocytes that were exposed to nitrogen for 1 h at 37°C. PolyHb significantly increased the viability. The three synthetic enzymes also significantly increased the viability. The use of both PolyHb and the three synthetic enzymes resulted in an additive effect in the recovery of viability. Increasing the concentration of the synthetic enzymes resulted in further increase in the effect due to the synthetic enzymes (Figure 1).

Stability analyses

The three synthetic enzymes showed good stability of close to 100% even when extrapolated to 260 days at both room temperature and at 37°C body temperature (Figure 2). The natural enzymes, even in the more stable crosslinked form of PolyHb-CAT-SOD-CA, are by far less stable (Bian et al., 2016) (Figure 2).

Enzyme activity assays

For carbonic anhydrase assay, the time taken to lower the pH of Tris-HCl from 8.3 to 6.3 is used to measure the W-A unit/ml of the solution. The CA activity for the PolyHb +three synthetic enzyme solution was significantly higher than for the control (no synthetic enzymes or PolyHb) and also significantly higher than for just PolyHb or just the three synthetic enzymes. For the control, it was 18.7 min; for the solution with neoenzymes, it was 4 min; for PolyHb alone, it was 1.1 min; and finally, for the novel solution containing PolyHb +three synthetic enzymes, it was 0.98 min. For the catalase assay, the time (in min) required to get a decrease of 0.05 absorbance unit was used to measure the activity in U/mL using the formula: U/mL = (3.45 x dilution factor)/(time x 0.1). The catalase activity of three synthetic enzymes in solution was 156,818 U/mL, while that of just PolyHb was 3450 U/mL, and that of PolyHb +three synthetic enzymes was 304,411 U/mL (Figure 3A). Lastly, for the superoxide dismutase assay, the enzyme activity was calculated in a coupled system, using xanthine and xanthine oxidase, where a unit of neoSOD that would inhibit the rate of reduction of cytochrome c by 50% is measured, and then, using the formula U/mL = (% inhibition) (DF)/(50%) (0.10), the activity was calculated. The SOD activity of PolyHb was 219.9 U/mL, that of just the three synthetic enzymes was 2,960.1 U/mL, and that of PolyHb +the three synthetic enzymes was 2,979.9 U/mL (Figure 3B). The enzyme activities of the synthetic enzymes in u/ml are shown in Table 2.

Discussion

We are not comparing PolyHb prepared in this laboratory with other PolyHb products. Instead, we are performing this study to see if synthetic enzymes can replace the natural enzymes we used for PolyHb-

TABLE 1 Test solutions: (i) PolyHb and (ii) synthetic enzyme solution.

P_{50}	Hb conc.	COP	Viscosity	MW	Hill coefficient, n50	MetHb content	K autoxidation (rate constant of autoxidation)	K NO (second-order rate constant of NO oxidation)
26.2 ± 0.2 mmHg	5 g/dL	20 mmHg	3 cP	>250 kDa	2.54 ± 0.03[19]	5.12% ± 1.67%	In the presence of superoxide and hydrogen peroxide, PolyHb shows oxidation of Hb (Fe2+) to metHb (Fe3+). This was prevented when PolyHb contains crosslinked antioxidant enzymes.	NO is important in maintaining the normal dilation of the microcirculation. Our present study studies the free suspension of hepatocytes. There is no microcirculation in the free suspension of hepatocytes, and thus, we did not follow this for the present study.

CAT-SOD-CA prepared and studied in this laboratory over the last 10 years. In order to compare the results, we have to use the same procedure of preparation for PolyHb-CAT-SOD-CA including PolyHb.

This study is performed to see if a simple solution of chemically prepared small chemical molecules of synthetic enzymes catalase, superoxide dismutase, and carbonic anhydrase (CAT, SOD, and CA) can replace the natural enzymes (CAT, SOD, and CA). Natural enzymes have low stability, especially at body temperature. Nonhuman sources of natural enzymes are immunogenic and need complicated cross-linking with PolyHb to form PolyHb-CAT-SOD-CA.

The present study shows that the three synthetic enzymes showed good stability of close to 100% even when extrapolated to 260 days at both room temperature and at 37°C body temperature (Figure 2). The natural enzymes, even in the more stable crosslinked form of PolyHb-CAT-SOD-CA, are by far less stable (Figure 2).

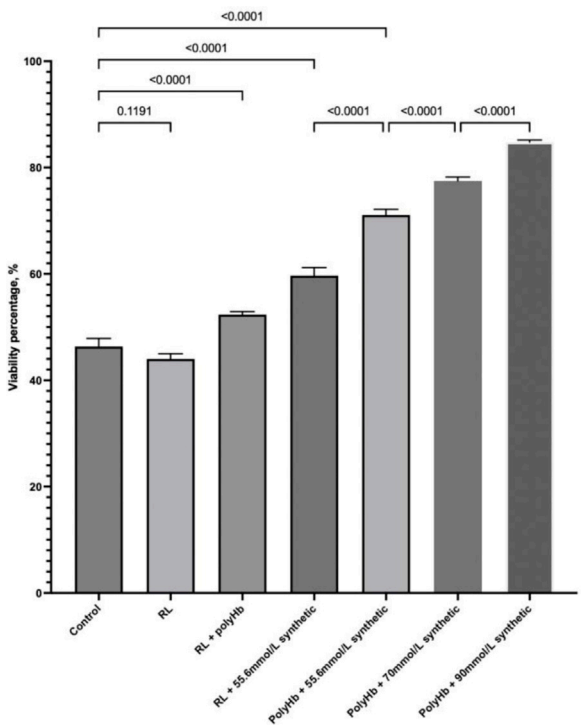

FIGURE 1
PolyHb significantly increased the viability. The three synthetic enzymes also significantly increased the viability. The use of both PolyHb and the three synthetic enzymes resulted in an additive effect in the recovery of viability. Increasing the concentration of the synthetic enzymes resulted in a further increase in the effect due to the synthetic enzymes.

We compared the effect of a solution of these three synthetic enzymes on the viability of warm-ischemic hepatocytes that were exposed to nitrogen for 1 hour at 37°C. PolyHb significantly increased the viability, most likely due to the supply of oxygen. The three synthetic enzymes also significantly increased the viability, most likely because of their antioxidant property and CO_2 transport property. The use of both PolyHb and the three synthetic enzymes resulted in an additive effect in the recovery of viability from the supply of oxygen, antioxidant effect, and CO_2 transport. Increasing the concentration of the synthetic enzymes (2x, 4x, and 6x) resulted in further increase in viability, most likely because of the severity of ischemic-reperfusion of the hepatocytes after 1 h in 37°C nitrogen incubation. This is similar to the use of natural enzymes, where increasing the enzyme by 2x, 4x, and 6x also increases the *in vivo* effect.

In summary, for this special case of hepatocytes after 1 h in 37°C nitrogen incubation, the simple solution of chemically prepared small chemical molecules of synthetic enzymes catalase, superoxide dismutase, and carbonic anhydrase (CAT, SOD, and CA) can replace the natural enzymes (CAT, SOD, and CA).

Future implications: There are a number of PolyHbs and HBOCs, including those that have been developed into products for clinical trials. However, only Biopure's PolyHb product has received regulatory approval but only in Russia and South Africa. None of the PolyHbs has received regulatory approval by other countries. If regulatory agencies require PolyHb to have antioxidant property and CO2 transport property, all that is needed is to add or inject the solution of synthetic enzymes as a separate component—after further safety and efficacy study of the synthetic enzymes. This could reactivate the many HBOCs developed by many researchers and companies over the years.

Methods

Reagents and cell line

All chemical reagents including neoSOD, MnTmPyP, (CAT# 475872) neoCAT, and EUK-134, (CAT# SML0743) were purchased from Sigma-Aldrich, Canada. The human hepatocyte cell line (CAT# HMCPMS) and the thawing media (CM7000) used in this study were purchased from Thermo Fisher Scientific.

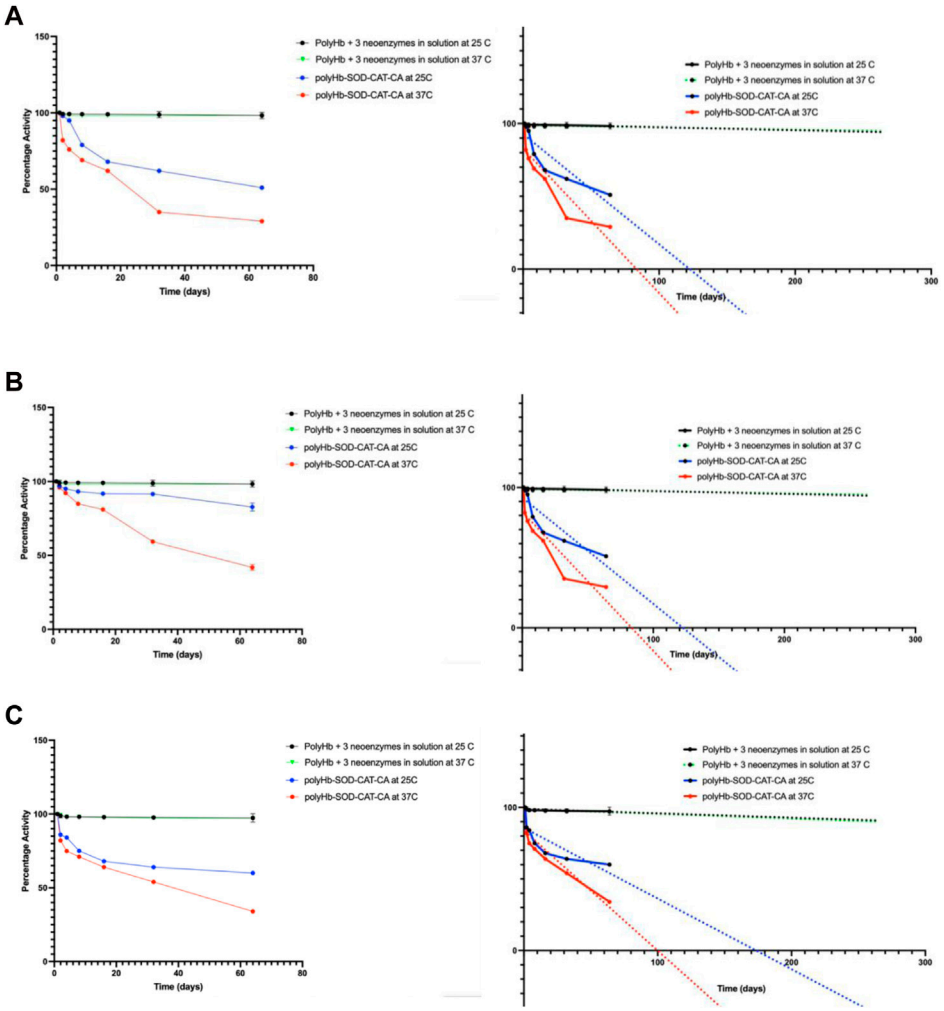

FIGURE 2
Comparing stability of neoenzymes and natural enzymes: **(A)** Carbonic anhydrase, **(B)** catalase, and **(C)** superoxide dismutase activities were analyzed over time at 25°C and 37°C for PolyHb + 3 synthetic enzymes in solution. These findings were then compared to our previous results on natural enzymes of PolyHb-SOD-CAT-CA (Bian et al., 2016). Copyright permission. The synthetic enzymes demonstrated significantly higher stability, nearly 100%, even when extrapolated to 260 days (see figures on the right). Results are presented as mean ± standard deviation (SD).

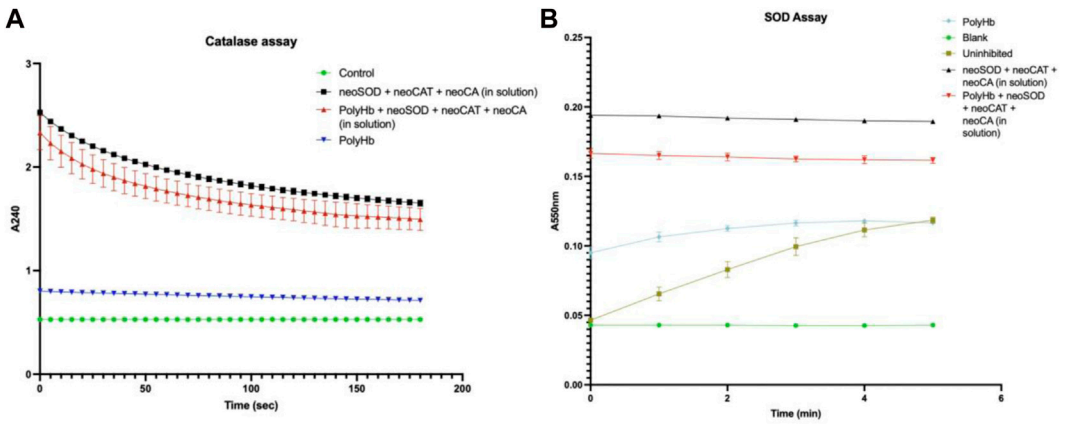

FIGURE 3
Enzyme activity assays of **(A)** neoCatalase and **(B)** neoSOD. The results are expressed as mean ± standard deviation (SD).

TABLE 2 Enzyme activities of the synthetic enzyme solution containing all the three synthetic enzymes in different concentrations.

Synthetic SOD activity U/mL	Synthetic CA activity W-A unit/mL	Synthetic CAT activity U/mL
1x (synthetic enzymes in the solution): 2,960	1x (synthetic enzymes in the solution): 360	1x (synthetic enzymes in the solution): 304,411
2x: 6,050	2x: 625	2x: 590,003
4x: 11,530	4x: 1,331	4x: 1,200,541
6x: 18,010	6x: 2,056	6x: 1,557,677

Neo-carbonic anhydrase (neoCA) synthesis

NeoCA was synthesized according to a previous report[8]. Briefly, 0.51 g of zinc chloride and 1.72 g of L-histidine were added into a beaker containing 4.8 mL of glycerol. This was then stirred at 70°C until a homogenous liquid phase was formed, which resulted in the mixture changing color to light yellow. Finally, the mixture was then dried in a vacuum oven at 60°C for 2 h, which resulted in the ZnHisGly, or neoCA.

Polyhemoglobin (PolyHb) preparation

PolyHb was prepared following the established protocol from this laboratory (Bian and Chang, 2015). Briefly, 4 mL of bovine hemoglobin was taken in a beaker (previously flushed with nitrogen gas and kept on ice throughout the process to prevent metHb formation). Then, 102 ul of 4 M sodium chloride along with 102 ul of 3 M potassium phosphate buffer were added to the beaker. Another 229 ul of 2 M lysine was added to it, and the mixture was shaken at 160 rpm at 4°C for 5 min. Without stopping the shaker, 162.4 ul of 0.5 M glutaraldehyde was added dropwise in four equal aliquots throughout a period of 15 min to start crosslinking. The beaker was kept shaking at 160 rpm overnight at 4°C. On the following day, 656 ul of 2 M lysine was added in two equal parts over 10 min and was shaken at 160 rpm for another hour at 4°C to stop crosslinking. The mixture was then centrifuged at 8,000 rpm at 4°C for 1 h to remove any precipitate. The supernatant was then purified using the Vivaspin 20 (CAT# GE28-9323–60) centrifugal filter at 2,500 g for 55 min at 4°C. This was exposed to vitamin C (0.05% w/v) for 24 h conc. Lastly, the retentate, containing just PolyHb, was collected and kept at −20°C for further use.

Preparation of a novel solution containing polyhemoglobin plus neoSOD, neoCAT, and neoCA

Four solutions were prepared starting at a ratio of the oxygen carrier, PolyHb to neoSOD, neoCAT, and neoCA 1 g: 18 mg: 18 mg: 18 mg. Then, the synthetic enzymes were increased to 2x, 4x, and 6x.

Enzymatic assays of the novel solution in comparison to PolyHb and a solution of just synthetic enzymes

The enzyme activities were measured following the procedures mentioned in a previous report (Mer et al., 2016). Briefly, carbonic anhydrase activity was determined by observing the time taken for the pH of 0.02 M Tris CO_2 buffer to decrease from pH 8.3 to 6.3. For measuring the catalase activity, the rate at which hydrogen peroxide disappeared at a wavelength of UV 240 nm was monitored. Lastly, for measuring the activity of superoxide dismutase, the reduction of cytochrome C was used. There were four technical replicates used for these assays (n = 4).

Stability analysis of the individual synthetic enzymes in the novel solution

The novel solution containing the synthetic enzymes and PolyHb was kept at both 37°C, body temperature, and at room temperature (RTP) for 2 months to check the stability of the synthetic enzymes. There were four technical replicates used for these stability analyses (n = 4).

Human hepatocyte culture

Hepatocytes were thawed in warm CHRM® medium, centrifuged at 100 x g for 10 min, and then mixed with plating medium (DMEM supplemented with 10% FBS and 1% penicillin/streptomycin) before being seeded (at a density of 2.4×10^5 cells/mL) onto collagen-coated plates and incubated for 6 h at 37°C. The medium was then replaced with warm DMEM and incubated for 24 h. There were six technical replicates used for this study (n = 6).

Regeneration of the viability of ischemic hepatocytes

The plates were transferred to a 37°C shaker with a constant flow of nitrogen gas to create an ischemic model. After 1 h, fresh DMEM was added, and the cells were treated with various combinations including the following:

1) Control hepatocytes treated with only fresh DMEM.
2) Hepatocytes treated with 20 ul Ringer's Lactate (RL) and fresh DMEM.
3) Hepatocytes treated with 20 ul RL + 55.6 mmol/L synthetic enzymes in solution (neoSOD + neoCAT + neoCA) and fresh DMEM.
4) Hepatocytes treated with 0.626 mmol/L PolyHb +55.6 mmol/L synthetic enzymes in solution and fresh DMEM.
5) Hepatocytes treated with 0.626 mmol/L PolyHb +70 mmol/L synthetic enzymes in solution and fresh DMEM.

6) Hepatocytes treated with 0.626 mmol/L PolyHb +90 mmol/L synthetic enzymes in solution and fresh DMEM.

The plates were then placed back in the incubator for 24 h.

Regenerative viability assay

Cells were washed twice with 2 mL PBS and treated with 4 mg/mL collagenase for 10 min. The reaction was stopped by adding 1.5 mL DMEM supplemented with FBS. The cells were then centrifuged at 1,500 rpm for 5 min and resuspended in 5 mL media. Cell count was determined by the trypan blue exclusion method, and cell viability was calculated using the following formula: percentage viability = (total no of cells - total no of cells in blue)/total no of cells x 100%

Data analysis

The data were presented as mean ± standard deviation (SD). The differences among the control, RL, PolyHb, synthetic enzymes, and PolyHb + synthetic enzymes were assessed using one-way ANOVA. The significance level for all tests was set at 95%.

Data availability statement

The original contributions presented in the study are included in the article/supplementary material; further inquiries can be directed to the corresponding author.

Author contributions

This research is part of MH ongoing research for his PhD thesis. He carried out the literature review, established the methods, and carried out the laboratory research. He analyzed the results obtained and prepared the drafts of the figures and the drafts of this paper. Professor TC is his research director. He suggested the research project, helped in his research, discussed the results obtained, including helping to solve problems, and helped revise this manuscript.

Acknowledgments

Professor TC acknowledges McGill University's Advancement Program for the unrestricted donation from Pro-Heme Biotech for TC's Laboratory.

Conflict of interest

The authors declare that the research was conducted in the absence of any commercial or financial relationships that could be construed as a potential conflict of interest.

Publisher's note

All claims expressed in this article are solely those of the authors and do not necessarily represent those of their affiliated organizations, or those of the publisher, the editors, and the reviewers. Any product that may be evaluated in this article, or claim that may be made by its manufacturer, is not guaranteed or endorsed by the publisher.

References

Andrijevic, D., Vrselja, Z., Lysyy, T., Zhang, S., Skarica, M., Spajic, A., et al. (2022). Cellular recovery after prolonged warm ischaemia of the whole body. *Nature* 608 (7922), 405–412. doi:10.1038/s41586-022-05016-1

Bian, Y., and Chang, T. M. S. (2015). A novel nanobiotherapeutic poly-[hemoglobin-superoxide dismutase-catalase-carbonic anhydrase] with no cardiac toxicity for the resuscitation of a rat model with 90 minutes of sustained severe hemorrhagic shock with loss of 2/3 blood volume. *Artif. Cells Nanomed Biotechnoly* 43 (1), 1–9. doi:10.3109/21691401.2014.964554

Bian, Y. Z., Guo, C., and Chang, T. M. (2016). Temperature stability of Poly-[hemoglobin-superoxide dismutase-catalase-carbonic anhydrase] in the form of a solution or in the lyophilized form during storage at -80 °C, 4 °C, 25 °C and 37 °C or pasteurization at 70 °C. *Artif. cells, nanomedicine, Biotechnol.* 44 (1), 41–47. doi:10.3109/21691401.2015.1110871

Bjerre, J., Rousseau, C., Marinescu, L., and Bols, M. (2008). Artificial enzymes, "Chemzymes": Current state and perspectives. *Appl. Microbiol. Biotechnol.* 81 (1), 1–11. doi:10.1007/s00253-008-1653-5

Chang, T. M. S., Jahr, J., Bulow, L., Sakai, H., and Yang, C. Y. (Editors) (2022). "Regenerative medicine, artificial cells and nanomedicine," *Nanobiotherapeutic basis of blood substitutes* (Singapore: World Science Publisher), 042. Available at: https://www.worldscientific.com/doi/epdf/10.1142/12054

Chang, T. M. S., Razack, S., Jiang, W., and D'Agnillo, F. (2021). "Nanobiotherapeutics as preservation fluids for organs and cells," in *Nanobiotherapeutic as blood substitutes* (Singapore: World Scientific Publishing Co. Pte. Ltd), 685–704. doi:10.1142/9789811228698_0044

Chang, T. M. S. (2019). ARTIFICIAL CELL evolves into nanomedicine, biotherapeutics, blood substitutes, drug delivery, enzyme/gene therapy, cancer therapy, cell/stem cell therapy, nanoparticles, liposomes, bioencapsulation, replicating synthetic cells, cell encapsulation/scaffold, biosorbent/immunosorbent haemoperfusion/plasmapheresis, regenerative medicine, encapsulated microbe, nanobiotechnology, nanotechnology. *Nanomedicine, Biotechnol.* 47 (1), 997–1013. doi:10.1080/21691401.2019.1577885

Chang, T. M. S. (1971). Stablisation of enzymes by microencapsulation with a concentrated protein solution or by microencapsulation followed by cross-linking with glutaraldehyde. *Biochem. Biophys. Res. Commun.* 44, 1531–1536. doi:10.1016/s0006-291x(71)80260-7

Dhanasekaran, A., Kotamraju, S., and Karunakaran, C. (2018). EUK-134: An investigational antioxidant for cardiovascular and neurological diseases. *J. Pharmacol. Exp. Ther.* 365 (3), 544–549. doi:10.1124/jpet.117.247460

Gao, Y., Wang, H., Cui, X., Dong, Y., Wang, Z., and Sun, D. (2021). MnTmPyP alleviates neuroinflammation and oxidative stress in a mouse model of Parkinson's disease. *J. Cell. Mol. Med.* 25 (14), 6822–6835. doi:10.1111/jcmm.16783

Li, X., Zhang, J., Li, Y., Li, Z., Hao, S., Lu, X., et al. (2018). Neuroprotective effects of MnTmPyP, a superoxide dismutase/catalase mimetic, in traumatic brain injury. *J. Drug Target.* 26 (7), 590–596. doi:10.1080/1061186X.2017.1410564

Liu, J., Li, X., Zhang, X., Zhu, H., Wei, H., and Fang, Y. (2021). Zinc-based deep eutectic solvent – an efficient carbonic anhydrase mimic for CO2 hydration and conversion. *Nat. Commun.* 12 (1), 1–11. doi:10.1038/s41467-021-23102-1

Mer, Mervyn, Hodgson, Eric, Lee, Wallis, Jacobson, Barry, Lewis, Levien, Snyman, Jacques, et al. (2016). Hemoglobin glutamer-250 (bovine) in SouthSouth Africa: Consensus usage guidelines from clinician experts who have treated patients. *Transfusion* 56 (10), 2631–2636. doi:10.1111/trf.13726

Moore, E. E., Moore, F. A., Fabian, T. C., Bernard, A. C., Fulda, G. J., Hoyt, D. B., et al. (2009). Human polymerized hemoglobin for the treatment of hemorrhagic shock when blood is unavailable: The USA multicenter trial. *J. Am. Coll. Surg.* 208, 1–13. doi:10.1016/j.jamcollsurg.2008.09.023

Chen, L., Yang, Z., and Liu, H. (2023). Hemoglobin-based oxygen carriers: where are we now in 2023?. *Medicina (Kaunas, Lithuania)* 59 (2), 396. doi:10.3390/medicina59020396

Zhu, Y., Yang, G. Y., Ahlemeyer, B., and Pang, L. (2016). Manganese superoxide dismutase as a drug target for the prevention and treatment of neurodegenerative diseases. *Drug Des. Dev. Ther.* 10, 343–353. doi:10.2147/DDDT.S93118

Frontiers in
Medical Technology

Explores innovative solutions to global healthcare challenges

An innovative journal that explores technologies which can maintain healthy lives and contribute to the global bioeconomy by addressing key medical and healthcare needs.

Discover the latest Research Topics

See more →

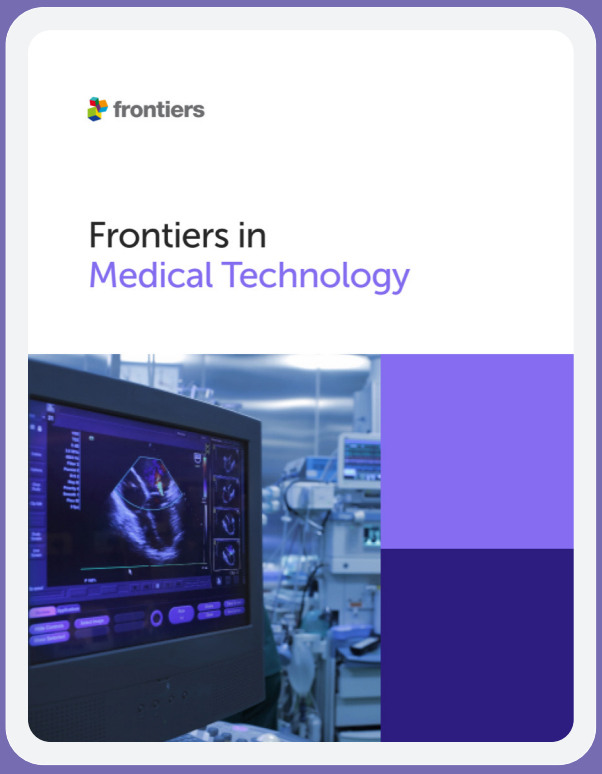

Frontiers

Avenue du Tribunal-Fédéral 34
1005 Lausanne, Switzerland
frontiersin.org

Contact us

+41 (0)21 510 17 00
frontiersin.org/about/contact